Improving sustainability of bascule bridge renewal projects

A STUDY ON THE IMPLEMENTATION OF AND OPTIMAZATION FOR SUSTAINABILITY IN BASCULE BRIDGE RENEWAL PROJECTS

C.T. COSIJN

(This page was left blank intentionally)

Improving sustainability of bascule bridge renewal projects

A study on the implementation of and optimazation for sustainability in bascule bridge renewal projects

By

C.T. Cosijn

5424844

In fulfilment of the requirements for the degree of:

Master of Science

In Civil Engineering

At the Delft University of Delft

With the master track Structural engineering

In cooperation with:

Royal HaskoningDHV

Master thesis committee

Dr. M. Pavlovic	TU Delft
Dr. O. Karpenko	TU Delft
DR. F. Di Maio	TU Delft
Ir. L. Tromp	RHDHV
Ir. T. Boeters	RHDHV

TU Delft

Royal HaskoningDHV
Enhancing Society Together

Abstract

Between the 1950's and 1970s, a large increase in bridge construction was realized accompanying a large increase in infrastructure. The increase in traffic intensity and weight results in that many of these bridges are now in need of reevaluation, possibly resulting in renovation or renewal. Meanwhile human-caused adverse environmental effects are increasingly impacting the world, of which the infrastructure sector is a large contributor.

This thesis provides a study into more sustainable renewal projects. The objective of this study is to provide a design which will increase the sustainability of renewing bascule bridges. The approach for this study is to:

- Literature review to set a scientific basis for this thesis project.
- Design study to explore the possibilities for bridge leaf design.
- Summary, conclusions, and recommendations to conclude the research project.

To design a more sustainable alternative the "Design for sustainable infrastructure" is followed. The ambitions identified following the "Ambition web" methodology highlights a great influence of a structural engineer in environmental sustainability. Key opportunities to increase environmental sustainability include reusing structural elements, maintaining or reducing the mass of the bridge leaf and designing the structure to fit inside the footprint of the current bridge.

The design process starts by applying "Circular design principles" to design a variant which reuses most of the available elements. Following variants increasingly differ from the current structure by removing elements, changing the materials from of the elements, or using free forming opportunities of FRP to come to new designs.

The sustainability performance is strongly dependent on the current state of the structure. Reusing the main structure and renewing only the deck can reduce the environmental impact of the bridge leaf by up to 53%, while not increasing the mass or requiring more space. Redesigning the entire structure with a full FRP structure can reduce the environmental impact by up to 48% and could reduce the mass of the bridge leaf by up to 33%. For both scenarios, the use of FRP, with a balsa core and partly recycled resins, was thus beneficial for the sustainability of a bascule bridge renewal project.

Preface

This thesis was written as the concluding project for the Master Civil Engineering with the track Structural Engineering. It was carried out in collaboration with Royal HaskoningDHV and with cooperation from Rijkswaterstaat.

I would like to thank everyone and anyone who was of help during my master's study and with great supervision during the thesis. In particular I would like to thank Liesbeth Tromp and Ton Boeters from Royal HaskoningDHV for their week-to-week supervision and guidance.

In addition, I would like to thank from the TU Delft the chair of my thesis, Dr. Marko Pavlovic for their insight, daily supervisor Dr. Olena Karpenko and Dr. Francesco Di Maio. The critical views provided by the TU Delft helped me and my thesis to reach higher quality.

A special thanks to Johan de Boon from Rijkswaterstaat for providing information and insight from governing body.

Then there is my gratitude for people close to me for their support during the process, thank you parents, girlfriend, and friends.

Coen Cosijn

Gouda, December 2024

Contents

Figures

Tables

Abbreviations

ADP	Abiotic depletion potential
AP	Acidification potential
CC2	Consequence class 2 (Can be CC1, CC2 or CC3)
CDW	Construction demolition waste
CF	Carbon footprint
C-glass	Corrosion glass fibers
CLT	Classical laminate theory
COVID	Coronavirus disease
CROW	Centrum voor Regelgeving en Onderzoek in de Grond-, Water- en Wegenbouw en de Verkeerstechniek (Center for norms and research in Soil-, Water-, and Roadconstruction, and Transport engineering)
CSR	Corporate social responsibility
CUR	Civieltechnisch centrum uitvoering, research en regelgeving (Civil engineering center for construction, research and norms)
D4S	Design for sustainability
ECI	Environmental costs indicator
EE	Embodies energy
E-glass	Electrical glass fibers
FCP	Foot- and cycle path
FRP	Fiber reinforced plastics
GFRP	Glass fiber reinforced plastics
GHG	Greenhouse gas
Glob.	Global
GWP	Global warming potential
HD	High density
IRI	Integrational roughness index
LCA	Life cycle analysis
LCC	Life cycle costs
Loc.	Local
MKI	Milieu kosten indicator (Dutch for ECI)
MS	Main structure
NB	Nationale bijlage (National annex)

NEN	Nederlandse norm (Dutch norms)
NMD	Nederlandse milieu databank (Dutch milieudatabase)
PET	Polyethylene terephthalate
PUR	Polyurethane
PVC	Polyvinyl chloride
R&D	Research and development
RD	Road deck
S-glass	Strength glass fibers
SROI	Social return on investment
u.c.	Unity check
UD	Unidirectional

Symbols

Latin symbols

A_{11}	Longitudinal tensile stiffness
A_{12}	Coupling tensile stiffness
A_{22}	Transverse tensile stiffness
A_{66}	Shear tensile stiffness
A_v	Area for resistance to shear force
D_0	Flexural stiffness per unit width of the face sheets of sandwich sections (about the neutral axis of the sandwich section)
D_c	Flexural stiffness per unit width of the core of a sandwich section (about its own neutral axis)
D_e	Costs of cumulate extra time spent traveling, due to road closure related to the project.
D_f	Flexural stiffness per unit width of each face sheet of a sandwich section (about its own neutral axis)
D_k	Characteristic value of the flexural stiffness per unit width of a sandwich beam
E_1	Combined in-axis Young's modulus, ply or laminate
E_2	Combined out-of-axis Young's modulus, ply or laminate
E_f	Young's modulus of E-glass fibers
E_r	Young's modulus of biobased polyester resin
$E_{x,c}$	Young's modulus balsa in compression
$E_{x,t}$	Young's modulus balsa in tension
E_z	Elastic bending modulus balsa
G_{12}	Combined shear modulus, ply or laminate
G_{balsa}	Shear modulus balsa
I_e	Cumulative extra time spent traveling, due to road closure related to the project.
P_c	Design value of the buckling load per unit width (of a sandwich panel)
P_{cb}	Design value of the buckling load component corresponding to pure bending (Euler buckling load)
P_{cs}	Design value of the buckling load component corresponding to transverse shear forces
V_f	Fiber volume fraction
X_{Ed}	Design value of X
X_{Rd}	Resistance value of X
f_e	Cost of extra time required per travel, due to road closure related to the project
l_{cr}	Critical buckling length
t_{extra}	Extra time required per travel, due to road closure related to the project.
A	Area
b	Width of element or between elements
CO_2	Carbon dioxide
CO_2 eq.	Carbon dioxide equivalent emission
EI	Cross section stiffness

$GtCO_2$	Giga tons of carbon dioxide
h	Height of cross section
k	Spring stiffness
M	Bending moments
N	Normal force
NO_2	Nitrogen dioxide
NO_x	Nitrogen oxides (Nitrogen oxide and nitrogen dioxide)
Q	Concentrated load
q	Distributed load
V	Shear force
w	Deflection
E_{st}	Young's modulus of steel
G_f	Shear modulus of E-glass fibers
G_r	Shear modulus of biobased polyester resin
T_g	Glass transition temperature
V_x	Variance coefficient
f_{st}	Tensile strength of steel
t	Thickness of element
w	Width of element or between elements

Greek symbols

γ_m	Partial factor for material property
γ_{max}	Maximal shear strain
γ_{rd}	Partial factor for resistance model
ε_{max}	Maximal linear strain
η_c	Combined conversion factor
η_{cm}	Moisture conversion factor
η_{ct}	Temperature conversion factor
ν_{12}	Combined Poisson's ratio, ply or laminate
ν_f	Poisson's ratio of E-glass fibers
ν_r	Poisson's ratio of biobased polyester resin
ρ_{balsa}	Density of balsa
ρ_f	Density of E-glass fibers
ρ_{ply}	Combined density, ply or laminate
ρ_r	Density of biobased polyester resin
ρ_{st}	Density of steel
$\sigma_{1,k}$	In-axis characteristic tensile stress limit
$\sigma_{2,k}$	Out-of-axis characteristic tensile stress limit
$\tau_{12,k}$	Characteristic shear stress limit
η_2	Young's modulus ratio between fibers and resin
η_G	Shear modulus ratio between fibers and resin
σ	Tensile stress
τ	Shear stress

1. Introduction

As more infrastructure is getting dated and climate change is increasingly affecting the modern world, sustainable renewal projects will have to become the norm.

1.1. Background

Bridges are an integral part of the Dutch landscape, society, and infrastructure. Bridges were built in The Netherlands as long ago as the Romans, but the oldest surviving bridge is not yet 1000 years old. A large part of the Dutch inventory of bridges were built between 1960 and 1980, to facilitate the emerging automotive transportation industry. In total, the Netherlands counts more than 90.000 bridges, of which it is estimated only around 8.500 are movable. Bridges built from the 60's onward are increasingly in need of revision [1].

Over the past decades, the intensity of vehicle traffic and subsequent loads on infrastructure has increased dramatically. This has consequences for said infrastructure, especially for the longevity of infrastructure. The amount of traffic, both passenger cars and commercial vehicles, has increased by +56% from the 90s to mid-10s [2].

At the same time, the Dutch government in combination with the administrators of civil engineering structures agreed to reduce environmental impact of civil engineering projects. The construction sector is responsible for a large fraction of greenhouse gas (GHG) emissions. Globally, the construction sector is responsible for 25% of the CO_2 emissions, of which almost 40% is non-residential construction. This totals to about 10 $GtCO_2$ equivalent emission. Next to this, the sector is expected to increase its productivity the oncoming decades, as it already has increased activities by +40% in 2021 since 2015. This leaves a need for more energy efficient building methods, which produce significantly less GHG's per m^2 [3].

To combat larger problem of climate change, we, as society, have stated the goal of reaching net zero emissions by 2050 and cutting emissions in half by 2030. This drastic change is needed to limit global temperature rise to 1.5 °C [4].

All civil engineering project must face this new reality, but certain projects are inherently more difficult to design more sustainable. Moveable bridges are one of the more challenging projects. They are only constructed where limited road elevation restricts boat traffic, restricting the freedom for engineers and emphasizes the need to reduce mass. As transportation has become an important part for Dutch society [5], an effective solution is required for moveable bridges.

Contrary to the need to reduce mass is the fact that the design standards have changed during the lifetime of the bridge to account for greater traffic intensity. This is expected to increase the weight of the bascule bridge with traditional steel orthotropic deck design. An increase in the weight of a bascule bridge will have consequences for the actuator, the counterweight and maybe the cellar. These consequences further reduce environmental sustainability.

A potential solution for moveable bridges is Fiber reinforced plastics (FRP), FRP is a combination of fibers, natural or synthetic, a bonding material and combinable with a core material to create a sandwich panel. The bonding agent has historically been a product of the petroleum industry, more recently alternatives have been thoroughly researched. The use of petroleum products is where the term plastic comes from. The product has been well adopted in the yachting- and the aviation industry [6].

The material has been studied for years and slowly implemented in civil engineering in the last 20 years. Earlier studies have concluded that the use of FRP may have a beneficial effect on sustainability of bascule bridges [7]. Next to this, the material, due to its lightweight nature and increased freedom of design, can result in structures with lower mass.

This thesis was brought forward by Royal HaskoningDHV, as Royal HaskoningDHV is interested in the sustainability of bascule bridge replacement. The use of FRP has been identified to potentially increase sustainability. This not only holds for moveable bridges, but moveable bridges potentially benefit more greatly from the use of FRP.

1.2. Problem definition

The main problem this thesis will address is the need for greater sustainability in moveable bridges renewal projects. As mentioned in the previous section, the government and we, as society, have set impactful goals for limiting the emissions of society. To reach this goal, innovations are needed in fields as material science and material use, energy use during construction and reduction of embodied carbon. Next to this, construction and structures optimized for sustainability can reduce emissions significantly [8]. But there is a need for a design methodology that can provide these sustainability improvements. Current design processes do not adequately consider the sustainability impact of their project.

For existing movable bridges the problem is more fundamental. They are generally built with full steel decks or with a wood deck and steel girders. Bridges designed in the 1960's typically had hardwood decks. This type fell out of favor as wood is more susceptible to weathering and steel became more readily available, allowing for larger bridge leaves. Steel orthotropic decks became popular in large span (moveable) bridges for its structural properties and economic design [9]. Wooden decks are vulnerable to aging, requiring many replacements. For steel decks fatigue is a growing problem [10].

Over the lifespan of the bridges, advancement in steel fatigue and an increase in vehicle weight altered the design of steel orthotropic decks to increase in thickness and weight. This has an adverse effect on movable bridges, as the requirement to move more mass will increase the required capacity of the actuators and the counterweight. In the worst-case scenario, the cellar housing these elements needs to be enlarged. [11]. An increase in weight and potential retrofitting of the surrounding components all decrease the sustainability of renewal projects.

1.3. Objective

The objective of this study is to provide a design which will increase the sustainability of renewing bascule bridges. The aim of this project is to achieve an improvement in sustainability by applying FRP and a design for sustainability process. The expectation is that a (hybrid) FRP bascule bridge will be able to reduce weight and reduce the environmental impact. This weight reduction is significant as it can potentially lead to reuse of other elements such as actuators counterweight and prevent redesign of surrounding infrastructure.

To reach this goal, subgoals are formulated. These goals will be translated into concise research questions in the next section.

- The first goal is to select a structured and substantiated method for measuring and quantifying sustainability. The first step in this process is identifying the key sustainability aspects which should be accounted for during the thesis. The next step would then be devising a method for quantifying these aspects.
- Next is identifying what materials and design alternatives can be selected which allow for an increase in sustainability. The goal is to include not only industry proven materials, but also investigate the use of more novel material layups. The uncertainty which comes with novel materials is also to be investigated.
- Next up is creating a list of requirements which will list all needs for the structure but will also include the goals concluded by the two prior subgoals. With this program, conceived design alternatives can be designed in more detail, entailing multiple iterations, to reach suitable design alternatives.

- The following goal is to conclude what alternative design will be best suited for further analysis. This conclusion must be substantiated, and a combination of design alternatives can also be found optimal.
- The final goal is to quantify the sustainability gains by applying innovative materials and design methods.

1.4. Research questions

To guide the research project, concise research questions are formulated. First, the main research question:

- To what extent does the use of FRP and optimizing for environmental and social sustainability reduce the impacts of a bascule bridge renewal project?

To help answer this question, a set of sub questions have been formulated:

- How should sustainability be considered to reduce the environmental and social impact of bascule bridge renewal projects?
- What materials and designs are traditionally used, and which innovative materials can be used for bascule renewal projects?
- What design variations can be made to increase the environmental and social sustainability of bascule renewal projects?

1.5. Approach

The approach of this thesis is three-fold:

- Literature review to set a scientific basis for this research.
- Design study to decide which parameters are most effective for bridge leaf design.
- Research outcome to conclude the study.

1.5.1. Literature review

The literature review of this project will aim to clarify key aspects of this innovation. These aspects are:

- Sustainability
- Dutch inventory of moveable bridges
- Fiber reinforced plastics

Research into sustainability will be twofold. First, the current application of sustainability within the field of civil engineering will be researched. This can provide valuable background, but also an insight into potential innovations. Second, the methodology of applying sustainability to a design study will be discussed. This segment will follow the after research of other literature, to be able to apply findings from the literature review into the methodology.

Research into the Dutch inventory of moveable bridges will have two aims. One of the aims is specifying the requirements for the case study. These requirements will provide a basis for selecting a case study. Another result of the research into the Dutch inventory of moveable bridges is to provide an estimate in the number of bridges for which this thesis could be relevant.

Studying fiber reinforced plastics is vital for applying the technology into the design. This section will aim to find what materials will be applied in the design phase.

1.5.2. Design

The process of designing an alternative bridge will be very similar to a standard design approach. The steps taken to design a valid alternative are:

- Iterative process to develop multiple variants.
- Variant study based on key sustainability factors outlined in the literature research.
- Applying the designs on potential replacements scenarios.

During the iterative process to design multiple variants, sustainability will be constantly accounted for. The reason for iterating through multiple designs is to learn from design alterations during the design process and implementing these lessons to further increase the sustainability of the final design. The environmental and social sustainability will be optimized for during this process. The initial design variants will all be analyzed based on hand calculations.

The replacements scenarios will provide better understanding and make this thesis more widely applicable. Although the theory will be applied to a specific case, the aim is to inspire methods for different cases.

1.5.3. Conclusions

This final design will be compared to a design for the structure with the use of conventional steel orthotropic deck. This comparison is the conclusion of the project, where a final quantification can be made on possible sustainability improvements.

1.6. Scope

For this thesis, the scope for the research into sustainability will include the aspects of sustainability, methods for assessing the sustainability of a project and methods of applying sustainability with models developed by the Dutch government. These methods and topics will provide the basis for the literature review. Additional sources for detailing of the methods and topics will be used.

The inventory of bridges will be compiled from publicly available data or data from a survey. Non-public data which other institution use as sources will be contacted, but the incorporation of their data will depend on their willingness to cooperate.

All materials included in the review of FRP will be sourced from the leading guidelines for designing with FRP. Any missing but obvious materials will also be noted.

The design phase will limit itself to the initial design of the structure. For the comparison to be more accurate all designs will follow comparable steps and be designed with similar levels of detail. Only the design of the bridge leaf will be considered. Thus, this will exclude the moving arm (detailed), counterweight, actuators, and basement. The bridge leaf will be designed with parameter constraints to approximately connect to the surrounding infrastructure.

The results of the design phase will be formulated in accordance with proposed renewal scenarios for the case study. This will be done to limit the data needed for the current state of the case study, but also create greater generality.

The research outcome will consist of key conclusion found in the design phase. Next to this, a discussion is held where the assumptions made during the thesis and their consequences will be discussed.

1.7. Graphic representation of project

For ease in understanding the project, a graphic representation of the research and design project is displayed below. This graphical representation will include all mayor parts of this project outlined in the previous sections. This graphic representation is displayed in Figure 1.1.

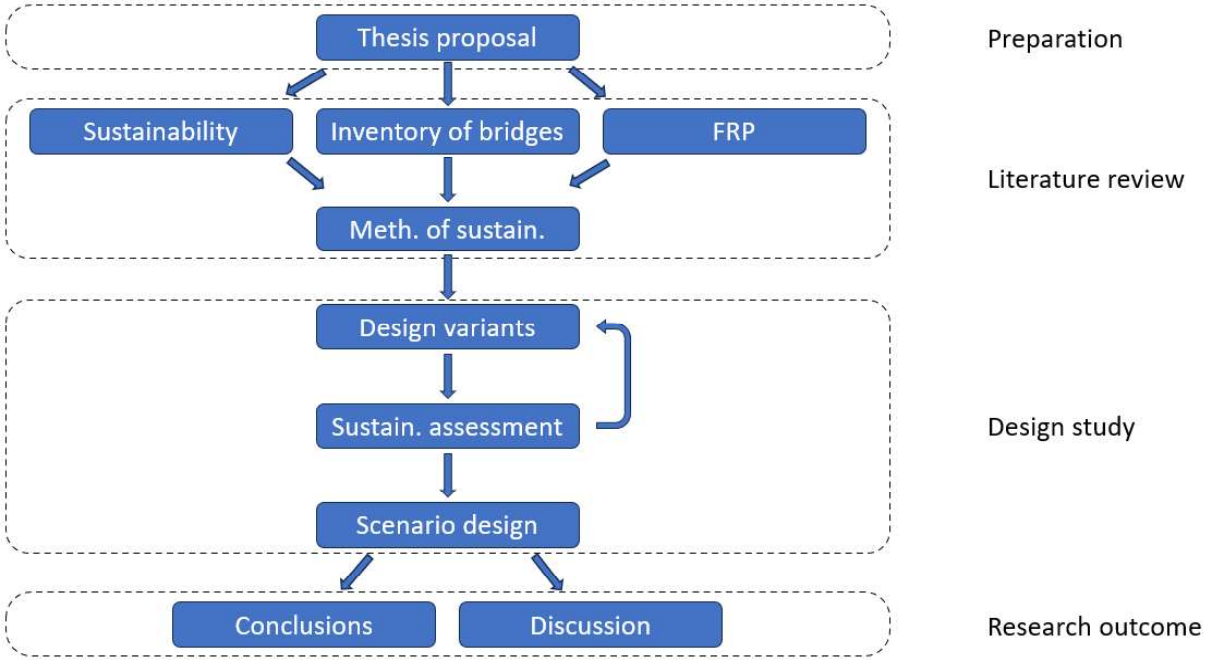

Figure 1.1, Graphic representation research and design project.

Part I. Literature review

2. Sustainability

2.1. Introduction

As introduced in the first section, the construction sector is a large contributor to climate change. A more sustainable construction sector is thus necessary if humans attempt to limit global warming [12]. The primary force behind climate change is global warming, which in turn is mainly caused by emitting large amount of greenhouse gasses (GHG) [13]. Limiting GHG emission is however not the only aspect of sustainability. Sustainability is defined as "the ability to continue at a particular level for a period of time without consequences for future generations" [14]. This leads immediately to the speculation that limiting emissions is not enough to be sustainable.

The application of sustainability has its origin in the mid 1980's. The concept of sustainability has greatly evolved since [15]. What started as a buzzword or ideal evolved to a galvanizing term which subsumes several other movements [16]. These movements can be categorized into three aspects:

- Economic sustainability.
- Environmental sustainability.
- Social sustainability.

These elements are described as co-equal, all equally important. [17].

Economic sustainability refers to the practices that support the long-term economic development of an entity [18]. It is the aspect society has been most interested in for a long time. Not because society has been optimizing for (economic) sustainability, but for an optimization in return of investment. For many years the appeal of economic sustainability was greater than the need for environmental or social sustainability. [19].

Environmental sustainability refers to the practices that support short- and long-term health for the environment [20]. This concept includes but is not limited to:

- greenhouse gas pollution,
- resource conservation
- natural ecosystem protection.

This aspect of sustainability gained less immediate focus since the Brundtland report, gaining traction in the mid 00's. Around this time research which was triggered because of the Brundtland reported clear conclusions about human induced climate change. Greenhouse gas pollution caused global warming, material use might cause depletion of finite resources and ever more natural ecosystems are declining in health [21]

Social sustainability refers to the "health" of a society, promoting wellbeing and accounting for the needs of individuals and groups [22]. Social sustainability includes the following non-exhaustive principles [23]:

- Equity/Equality ("Fair and impartial access to social or public services regardless of economic or social status")
- Responsibility ("Operating responsibly in the society in which they exist, by acting in an ethical and transparent way that contributed to health and welfare of society")
- Social justice ("Justice in terms of the distribution of wealth, opportunities and privileges within a society")
- Human capital ("Human beings are an asset in economical systems, partaking in labor and creating value by means of competence, knowledge, cognitive abilities, creativity and personal attributes")

- Social capital ("This concept is centered around social networks build on trust, reciprocity and common understandings")

2.2. Sustainability aspects

As introduced in the previous section, sustainability can be divided into three categories, environmental, social, and economic. Although this encompasses all aspects, it is too general to be effective. For a civil engineering project, it is useful to further divide these categories into aspects. Many aspects of ecological or economic sustainability can be effectively translated to civil engineering. For social sustainability, some aspects are difficult to be applied in an infrastructure project. All three categories of sustainability will be considered, as a fully sustainable solution must take all aspects into account [24]. The aspects that will be considered are subdivided by the three main categories, and are:

- Environmental
  - Energy and climate mitigation.
  - Materials and circularity.
  - Climate adaptation.
  - Nature effects.
  - Environmental effects.
  - Land use.
- Social
  - Social value.
  - Health and wellbeing.
  - Social relevance.
  - Accessibility.
- Economic
  - Financing.

These aspects are drafted by the Dutch governing bodies combined as CROW and detailed in what's called the ambition web, part of the "Approach to sustainable infrastructure". This ambition web consists of the above-mentioned aspects, as well as the ambition expectation per level of each aspect. The approach to sustainable infrastructure is detailed in section 5.

For the following sections, each aspect will be explained more thorough. For each aspect, the definition is first defined following the definition from ambition web [25]. This definition may be broadened with additional sources. Following the definition, the aspect is interpreted for circumstance specific to moveable bridge renewal projects. Finally, if relevant, more detail is given for an aspect for this thesis specific matters, such as, but not limited to, materials (FRP vs. steel), design.

2.2.1. Energy and climate mitigation

2.2.1.1. Detailed definition

As the name details, this aspect is about preventing energy use and the release of pollution. To measure this aspect, the emissions of the structure over its lifecycle are measured. The lifecycle emissions or environmental life cycle assessment (LCA) is comparable to the life cycle costs (LCC) of a structure, as it accumulates the costs of the structure over time. Instead of expenses, emissions are accumulated. The emissions can be grouped in the same phases as the LCC, however it is more insightful to list the main parameters that influence this score.

Like the lifecycle costs, performing a LCA will include all phases of the structure. This can be combined in environmental impact calculators such as the environmental costs indication ECI (MKI in Dutch) [26].

The main parameters are:

- Materials used for the structure.
- Installation of the structure.
- The protection treatment of these materials.
- Operation, repair, and maintenance activities.
- The end-of-life treatment.

The most significant contributors to emissions are the used materials for the structure and the energy used for operating the bridge. This influences the immediate environmental costs of the structure and dictate the repair, maintenance, and operating costs during the lifetime of the structure. The main contributing environmental aspects are, but not limited to [27]:

- Global warming potential (GWP).
- Acidification potential (AP).
- Abiotic depletion potential (ADP).

2.2.1.2. Aspect applied on movable bridge renewal projects

The method for assessing their performance will be a LCA, with the use of an ECI calculator. The ECI calculator uses lifecycle phases to assess the impact of a structure with different use cases. The life cycles are categorized from A to D, where [28]:

- A1 to A5: Production phase.
- B1 to B7: Use phase.
- C1 to C4: Removal phase.
- D: Environmental impact outside direct system influence (recycling / reuse).

2.2.2. Materials and circularity

2.2.2.1. Detailed definition

Raw material collection, processing and implementation account are one of the most energy intensive processing in civil engineering. This section will go into use of new raw material- and generation of waste prevention.

As mentioned, every lifecycle of the material will require energy to process it into a new required form. The total amount of CO_2 emitted during this lifecycle is called the carbon footprint (CF), and decisions on what material is more effective will increasingly take this figure into account. There is also a measure for energy used in its lifecycle, called embodied energy (EE). For the direct comparison between two materials an index considering both factors can be considered. An index for this is the SUB-RAW index, creating a logarithmic scale between embodied energy and CO_2 footprint. With which a consideration between the effect on CO_2 emissions and EE by switching materials can be made [29].

The problem with such indices is that not all aspects are considered. This means incorporating the index into a LCA is also problematic, as there will be uncertainty on what aspect are considered by which analytics. Effectively, the best way to incorporate raw material usage is in an LCA, so this is considered in the ECI calculations.

Waste is unwanted matter or material, especially what is left after useful substances or parts have been removed [30]. The construction sector in the Netherlands produced over 100 million metric tons of waste per year in 2018 (last year before the COVID pandemic measured). The construction demolition waste (CDW) was estimated at 24 million metric tons [31]. More alarmingly, before the COVID pandemic, this was an increasing metric. Reducing waste production is seen as an effective step in increasing material efficiency and therefore sustainability. EU ambitions are currently to recover 70% of solid nontoxic materials, with recycling [32].

On the other hand, the Netherlands has become very efficient in recovering materials from waste and prevent landfilling. Only 1% of the produced waste by weight from demolition was landfilled, most of the materials recovered were recycled, for non-energy purposes [32].

Materials that avoid these problems are renewable materials, or biobased materials. Biobased materials, such as wood, provided some requirements are met such as sustainable harvest, is considered renewable because it grows naturally, not depleting the worlds resources [33]. Implementing biobased materials is thus an effective measure to implement circularity.

Probably the most effective method for reducing material usage is the circularity principle with the value hill. The value hill has two mayor principles. First, assembling a product adds value, in the sense of work, to produce materials, systems, and the product. Disassembling or destroying these products then also destroys this added value. Retaining this value, or work, reduces waste and will allow for less work needed for future reuse of these materials, systems, or products. A schematic of the value hill is displayed in Figure 2.1 [34].

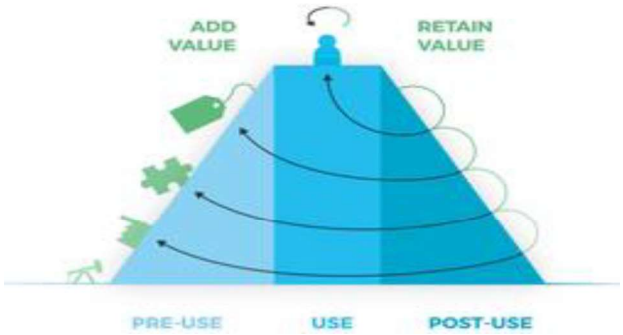

Figure 2.1, Value hill.

2.2.2.2. *Aspects applied on moveable bridge renewal projects*

Effective measures to apply the value hill is to design the structure such that elements are separable. This allows for easier reuse of elements at the end of life, easier separation of materials for recycling and provides easier repairability or allows for future changes.

To conclude, circularity will be accounted for qualitatively by adopting the value hill principles. Next to this, bio-based materials will be implemented were possible. During the performance assessment of the structures, the ability to retain value will be assessed and design revision can be made to improve this performance.

2.2.3. Climate adaptation

2.2.3.1. *Detailed definition*

The term climate adaptation is used to represent the ability of the structure to keep fulfilling its requirements in the future under a changing climate. The focus of this aspect is to prevent or reduce then negative effects from future climate effects on the project.

Effects identified which might affect a project in the long term include:

- Flooding
  - Prevention by ensuring storage capacity.
  - Protection against high water.
- Water shortage
  - Prevention of damage because of water shortage.
- Heat
  - Prevention of heat stress.
  - Prevention of nature fires which endangers users or nature.
- Extreme weather
  - Prevention of damage because of thunder, hail, storms, or strong wind.

2.2.3.2. *Project interpretation*

Many aspects listed above are not relevant for moveable bridges. Water storage capacity is not feasible, but high water might cause damage to structures. Water shortage is not relevant, as a moveable structure does not consume water. A bridge has little effect on heat stress, though expansion joints will need to be adequately designed. Finaly, change in strong winds affect the operational conditions of a moveable bridge.

For this project a qualitative assessment will be made if the bridge is climate resilient. Flooding, heat, and extreme weather can have effect on future operational requirements. It is important that during the design of the structures this aspect is thoughtfully considered. It is assumed that these aspects will be forestalled by applied norms.

2.2.3.3. *FRP specific considerations*

Temperature is a significant factor in the material properties of FRP. The reduction of material properties is amplified if the glass transition point is reached, where the material transitions from a glassy state to a rubbery state. Heat adaptation for FRP will include the considerations of temperature changes in the future, and what effect this temperature changes have on the material. For this project, it is assumed that the prescribed temperatures by the norms forestall the adverse effect of the temperature increase. Additional measures may be necessary for specific circumstance, or if the norms are found inadequate.

2.2.4. Nature effects

2.2.4.1. Detailed definition

Nature effects represents the influence a project has on the surrounding nature. This includes two principles, ecological structures, and biodiversity. For a thriving natural area, both the ecological structures and biodiversity are required.

Ecological structures represent the living area of the natural area. Factors influencing the ecological structures are:

- Maintaining living spaces and ecological connections.
- Improving ecological connections and prevention of fragmentation of natural areas.
- Limiting loss of natural areas.
- Make provisions for adaptability within the ecological structures.

Biodiversity represents the animals and plants living in each natural area. Important is not only that the number of animals and plants is numerous, but also that there is a diverse set of species. More biodiversity helps an area to be adaptable, creating more resilient nature. Factors influencing the biodiversity are:

- Building nature inclusive.
- Prevention of nuisance from lights, noises, and vibrations.
- Use of local flora to provide habitat for local fauna.

Methods of determining natural effects can be quantitative:

- Counting animals (species and amount), plants (species and amounts), trees (species and amount).
- Loss or gain of (fragmented) natural area.

Other qualitative methods are:

- Evaluation of ecosystems, with argumentation based on observations.

2.2.4.2. Aspects applied on moveable bridge renewal projects

For bridges the surrounding area dictates the function the bridge fulfills in ecosystems. Regardless of the case, a moveable bridge can have limited effects on some of the aspects listed above. Creating living spaces on moveable structures is undesirable for larger fauna, and for vertically rotating bridges this also applies to smaller fauna. Ecological connections are possible with bridges, but similarly to living spaces, for vertically rotating bridges this can be problematic. Limiting loss of natural areas is always desirable and making provisions for adaptability can only have an effect if ecological structures are utilized.

For biodiversity, creating an ecosystem, thus building nature inclusive or providing habitat for local flora and fauna is problematic on moveable bridges. Prevention of nuisance is however possible, lighting systems can be designed to minimize wasted light and there are numerous methods to reduce noise and vibrations [35]. A more detailed study into reducing nuisance is outside the scope of this project.

For this project, ecological structures are difficult to incorporate and is thus not accessed. Prevention of nuisance, a factor for biodiversity, should be assessed per bridge. Some elements, such as lighting systems, can be adopted such that it limits it nuisance. This is however outside the scope for this thesis.

2.2.5. Environmental effects

2.2.5.1. Detailed definition

Environmental effects are a collection of environmental influences a project has on its (local) surroundings. Many activities in civil projects affect the quality of the environment. The quality of the local environment is divided into three categories: water-, soil-, and air quality. To improve the quality of these environment a set of goals has been drafted, these are:

- Water
  - Prevention of ground and surface water contamination.
  - Methods of collecting, transporting, and cleaning (contaminated) water.
  - Prevention of polluting of water.
  - Decreasing use of toxic chemicals.
  - Prevention of leaching of materials.
- Soil
  - Prevention of soil contamination.
  - Remediation of contaminated ground.
  - Maintaining the balance in a soil system.
  - Stimulating soil life and achieving fertile soil.
- Air
  - Reducing NOx emissions.
  - Reducing of health damage due to construction equipment.
  - Preventing the use of high polluting (no particulate filter, high NO_2 emissions) machinery.
  - Limiting the emissions of particulate matter and NO_x during the use phase.

2.2.5.2. Aspects applied on moveable bridge renewal projects

Moveable bridges have very little influence on the soil quality, due to their being very little overlap. There will however be a construction site, for which soil quality needs to be considered. The construction phase is however not considered in this thesis.

Water quality is more relevant for moveable bridge replacements. Rainwater on bridges is deemed contaminated, thus it is important to take measures into preventing the seepage of rainwater into surface or groundwater [36]. Another risk is the use of toxic chemicals, both for the use of FRP and for the conservation of steel, toxic chemicals are used. It is important that during the use of these chemicals that measures are taken to prevent the contamination of the local water quality.

For air quality, a moveable bridge is powered solely by electricity, producing no particulate matter or NOx emissions. However, during the construction phase or during maintenance there will be production of pollution. Measures can be the use of (partly) electric equipment or even acquiring newer machinery with more effect pollutant filters [37]. These measures will be beneficial for the LCA as well, lowering emissions during construction phase.

For this project this aspect will not be considered, because of the identified factors above are outside of the scope. It is important that for a complete assessment of sustainability these factors must be considered, but they are not directly influenced by the design choices made during the initial design phase of the bridge leaf. The emissions of the construction phase are considered with base values provided by databases. Improvements over the base values are worth researching for every construction project.

2.2.6. Land use

2.2.6.1. Detailed definition

Land use or rather the allocation of (natural) area to structures or non-natural functions reduces the available area in which natural functions can be conducted. This not only consists of above ground land use, but also in ground land use. The goal is relatively simple, minimize the amount of land a project claims, to allow as much natural functions as possible.

For both above- as below ground the goals to accomplish this can be summarized to the following:

- Efficient use of land area both above and below ground.
- Minimize waste area and ground (both during construction and on the final design).
- Combine functions to increase efficiency.

Next to this, due to historic reasons, additional preventive measures may need to because of:

- Archeological value
  - Research may be necessary to determine the value.
  - Measures may be necessary to maintain the value and to be able to display and communicate this value.
- Explosives
  - Research may be necessary to determine the risks.
  - Measures may be necessary to minimize or eliminate the risks.

2.2.6.2. Aspects applied on moveable bridge renewal projects

For bridges crossing water, as stated previously, very little land area is used. This however does not eliminate the necessity to prevent wasteful land use. During the design-, construction- and maintenance phases attention must be paid to prevent wasteful land us.

For renewal projects of moveable bridges, maintaining as much of the surrounding infrastructure is beneficial for the land use aspect. If the possibility arises such that no work must be done on elements such as the connecting roads or the mechanism (cellar), then this reduces the land use of the final structure. During construction and with maintenance additional land use can be reduced to as little as possible.

Additional preventative measures may still be necessary because of archeological value or explosives. Case study specific circumstance might require additional research if historical data suggests that this was inadequately done previously.

For this project, the aim to fit a new structure into the footprint of the previous minimizes the effect of the structure on the aspect land use. The minimization of land use during construction or maintenance is outside the scope of this project. So is the evaluation of the possibility of archeological value or explosive risks.

2.2.7. Social value

2.2.7.1. Detailed definition

Social value, in Dutch "Ruimtelijke kwaliteit", is the aspect that aims to increase the value of any civil project for its user. It consists of the following categories:

- Future proof
- Relevance
- Social security

The future proofing principle is in essence self-explanatory, designing a structure such that it will be functional for its lifespan. Future proofing aims to ensure that a system will not be superseded by the need for future capabilities. The concept consists of multiple aspects to fulfill this need [38]:

- Analyze and anticipate what and when future needs might occur.
- Analyze the performance of the structure with these new needs.
- Adapt the structure to future needs if required.
- Repeat steps until a satisfactory result is acquired.

Relevance is a core principle of social value. Without relevance the value to its users is limited. Relevance can be categorized with the following goals:

- Ensure functionality meets demands and is of high (enough) quality.
- Ensure the accessibility for the relevant end users.

2.2.7.2. Aspects applied on moveable bridge renewal projects

For a renewal project, it is important to considered if the structure is- and will stay relevant before renewing it. Case specific circumstance might provide basis for additional requirements for the renewal project because of relevance. An example for bridges might be the inclusions of additional paths or lanes for road traffic, cycling, or walking.

Social security is about ensuring the creation of an environment within any user is comfortable. This can be created by creating an open space, ensuring enough lighting, or removing unpredictable street elements.

2.2.7.3. FRP specific considerations

For this project, a qualitative assessment will take place to ensure if the structure is future proof and relevant. Social security is an important factor for any bridge, as the bridge needs to feel safe to be used and is thus translated into requirements. This is more relevant for FRP bridges in comparison to steel bridges, as FRP bridges are more prone to deflections which might provoke an unsafe feeling.

2.2.8. Health and wellbeing

2.2.8.1. Detailed definition

Health and wellbeing focuses on the social responsibility an organization, company or governing body has on their employees or sub-contractors. It consists of the following criteria [39]:

- Employment stability
- Employment practices
- Health and safety
- Capacity development

Employment stability criteria reflects the creation / maintaining of labor, while employment practices reflect the equity of that labor. Both aspects are important for a company or organization to consider, as the workforce is an import asset. An important factor in this is the complexity of the work, for FRP, the work is relatively simple compared to steel and less physically taxing compared to concrete [40]. This creates jobs where workers can invest in their abilities and contribute meaningfully from an earlier stage in their development.

Health and safety are important topics in Civil engineering. In Europe, 753 construction workers lost their lives due work-related accidents. For every construction worker that lost it life, around 400 workers got injured. In total, approximately 1 in 60 workers get injured every year [41]. FRP can be beneficial, as heavy construction element are categorized as a health and safety hazard on construction sites [42]. Working with FRP has unique health concerns, as both the fibers as the bonding agent can cause health risks. However, studies show that with adequate protection, the risks of working with these materials can be significantly limited and to have low risk [43].

Capacity development criteria reflects the contribution of a project towards research and development (R&D) or career development. Both aspects are important consideration to increase social sustainability of a society, as R&D and career development increase the abilities of a society.

2.2.8.2. Aspects applied on moveable bridge renewal projects

For moveable bridges this aspect is as important as for any civil engineering project. Ensuring the health and wellbeing of all involved is the basis for a good working condition. In general, an engineer has little impact on this aspect, although the consequences from the use of FRP will be outlined in the following section.

2.2.8.3. FRP specific considerations

There is no evidence that the adoption of FRP in civil engineering has an impact on employment stability. Equally, there is no reason to suggest that an increase in FRP construction has consequences in the health and safety of the construction sector. Current research suggests that, while there are significant health hazards attributed to working with FRP, protection measures are sufficient in protecting the workers from these hazards [43]. A benefit of working with FRP can be the reduction of the mass of the structure. A lower mass of any structure could reduce the health and safety risks [44].

On the contrary there is a basis to suggest that the adoption of FRP can increase equity, for a larger share of the population is presumed to be able to work in the industry. However, the industry has always attributed a low score to this factor [45] [46]. Most indicators focused on scoring employment practices are post-initialization, measuring satisfaction during or after the project [46].

These factors are all relevant for bridge renewal projects but is mainly a consideration for management and not for engineers. Although FRP might improve certain elements of this aspects, this is difficult to outline in relation to design variants.

2.2.9. Social relevance

2.2.9.1. Detailed definition

Social relevance is associated with ensuring that the local influence in a project is included. It encompasses around the concepts of:

- Public support.
- Corporate social responsibility.
- Sustainable use of workers.

Public support or -involvement is important for any civil engineering project. It is to be included to prevent the misrepresentation of the local interests. With public support, a project is more likely to address the matters of the local inhabitants. A sub aspect of public support is local habitants' engagement, which aims to improve the understanding of the local interests. Another sub aspect is Social Return (SROI), which is a concept in the Netherlands that aim to incorporate disadvantaged workers with works related to any project. This can create opportunities for workers to increase the opportunities in the future.

Corporate social responsibility (CSR) is a business approach that aims to increase the understanding with companies to not only prioritize economic performance. This can have benefits for both their clients, stakeholders and thus for themselves. In the context of a civil engineering project, it is possible for the recruitment to take corporate social performance into account. This could improve work relations, efficiency from which the local habitants stand to benefit [47].

Sustainable use of workers is a sub concept of corporate social responsibility. It aims to improve to work conditions for all workers involved. The benefits are then also closely aligned with those of CSR.

2.2.9.2. Aspects applied on moveable bridge renewal projects

These factors are all relevant for bridge renewal projects but is a consideration for management and not for engineers. Therefore, this aspect is outside the scope of this project and thus will be given minimal consideration.

2.2.10. Accessibility

2.2.10.1. Detailed definition

Accessibility encompasses multiple aspects regarding how an object can be used. These are:

- Reachability.
- Efficient use of infrastructure.
- Traffic safety.

For reachability considerations are:

- Ensuring future proof traffic functionalities.
- Enabling usability for individuals with physical impairments.
- Reducing user delay from object down time.

For efficient use of infrastructure, it is important to prevent creating connections that are unnecessary. Next to this, a stimulus can be created for more sustainable forms of transport. In example, facilitating clean modes of transport by implementing charging spaces can be considered.

Traffic safety is also to be considered. The term encompasses quantitative aspects such as annual accidents, injuries, or casualties. A downside of using quantitative aspects for smaller roads can be the limited amount of data. More qualitative aspects can also be considered, such as users experience surveys.

2.2.10.2. Aspects applied on moveable bridge renewal projects

For this project, reachability will be considered, with a focus on a reduction of user delay. The following calculation can be made to quantify the effect of a bridge closure. The assumption has been made that a road closure has no effect on the number of travelers who want to travel from their origin to their destination who would normally use this connection.

For the calculations the first step is to quantify the amount of extra time a traveler would need to spend to travel. This will be defined as t_{extra} and can be calculated or assumed based on the connection. Next, the number of travelers who would use the connection. Multiplying these values will result in the cumulative amount of extra time spent traveling [48], defined as I_e, given in Formula 2.1.

$$I_e(t) = t_{extra} * f_t(t) \Leftrightarrow I_e = t_{extra} * \int f_t(t)dt \quad (2.1)$$

The total amount of delay costs can then be computed with Formula 2.2.

$$D_e = I_e * f_e \quad (2.2)$$

Where f_e represents the costs of the delay per person-hours.

Other sub aspects for this project will not be considered. It is outside the scope for this project to consider other options for the design of the structure that could either increase the efficiency of the structure or the safety of the road users.

2.2.10.3. FRP and design specific considerations

The use of FRP and the design for fast replacement or maintenance can have a significant influence on this aspect. Case specific circumstance, such as availability of detours, will be the determining factor for if this is relevant.

2.2.11. Financing

2.2.11.1. Detailed definition

Financing is another term for considering the economic consequences of the structure during its lifetime. This can be considered with the LCC [49]. The cost follows the phases of a project [50]:

- Planning/Construction phase, the costs associated with these phases are investment costs. These include research into unproven material / construction solutions.
- Operating phase, the cost associated with this phase is also called the operating costs or upkeep. This expense comes from inspection, maintenance and/or renewal of minor parts of the object.
- Discounted costs, these expenses are not directly tied to a phase of the object but is a representation of the current value to eliminate the effect of inflation.

These three costs combined are the life cycle costs of an object. Calculating the life cycle costs of an object is generally called a lifecycle assessment. A similar operation can also be performed for the emissions of an object during its lifecycle, this will be discussed in its relative section.

Vehicle operating costs can affect two aspects of sustainability, economic and environmental. For economic costs, the costs can be divided into fuel consumption and maintenance.

Fuel consumption is the dominant vehicle operating cost [51]. Fuel consumption varies with many environmental variables, the most governing are vehicle mass, engine efficiency and road conditions. Looking solely on road conditions, pavement roughness is used to define the road conditions, expressed in an integrational roughness index (IRI), measured in m/km. In general, an increase of 1 m/km will increase in 2% to 3% increase in fuel usage.

Maintenance for road vehicles is the other large operating cost. Like fuel consumption, the maintenance expenditure for road vehicles is dependent on many factors. Generalizing again for road condition, under a certain threshold, there is no dependency of road condition to maintenance expenditure. Only after this threshold, the expenditure is relative to road condition. This threshold is around 3 m/km, an increase from 3 to 4 m/km will increase expenditure by 10 %, from 3 to 5 m/km will increase expenditure by 40% [52]

Consuming fuel effects costs of operating a vehicle but also cause environmental damage. Over the last decade the average cost for fuel is € 1.69 in the Netherlands [53] and every liter emits approximately 2 Kg of CO_2 eq. [54]. On average, maintenance accounts for € 0.034 per km [55], but causes no significant environmental damage [54]. There is no evidence that the type of bridge or material used for the deck have an impact on the road durability and therefore fuel costs.

2.2.11.2. Aspects applied on moveable bridge renewal projects

Financing is an aspect of sustainability which is difficult to generalize, but almost always important. For an engineer, the design can be optimized to reduce the costs of a structure, either initially or over the lifespan of the structure.

2.2.11.3. FRP specific considerations

It is important to implement a LCC analysis for projects which consider FRP. The initial costs of producing an FRP structure are often more significant than for more traditional materials. These costs may be offset over the lifespan of the structure, with reduced upkeep or with a longer lifespan [56].

2.3. Application of sustainability

To conclude this section, the ambition web will be brought forward again. As this entire section, the ambitions are considered with respect to a structural engineer. The influence of an engineer is not equal in every aspect. This will be generally represented in this ambition web. The levels displayed in the section correspond to the level of applicability for this project, where:

1. This aspect will receive minimal consideration.
2. This aspect will receive thoughtful consideration.
3. It is aspired that this aspect will reach the highest achievable performance.

The ambition web, following the argumentations and consideration in the individual sections, is displayed in Figure 2.2. For how these aspects will be considered during the design process, a methodology is detailed in section 5.

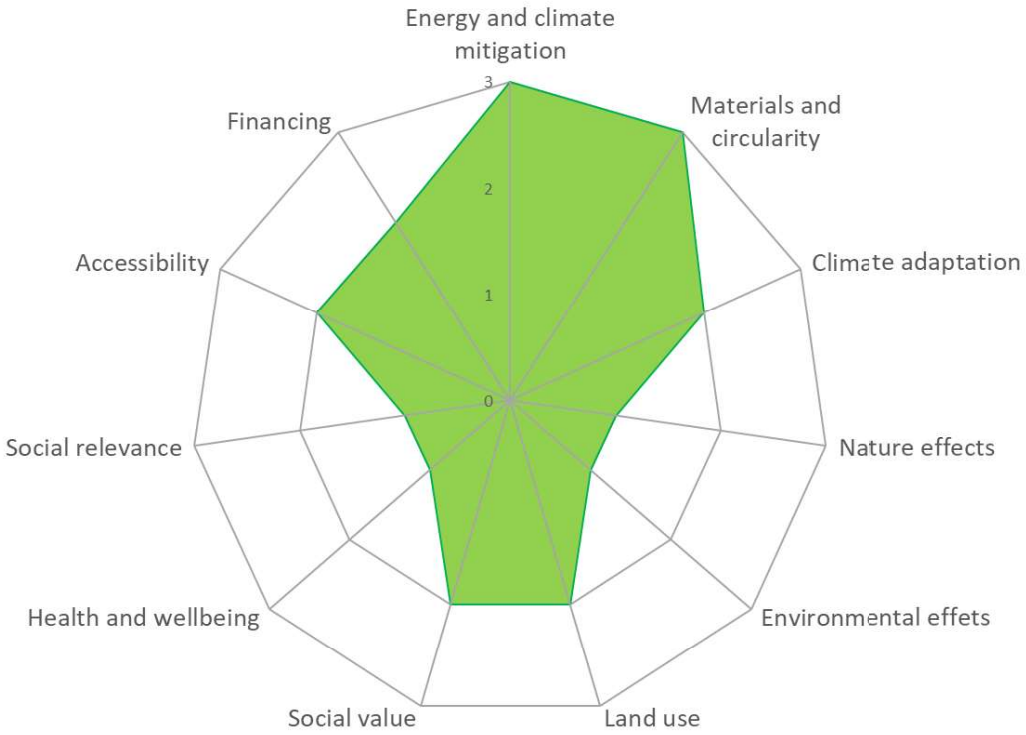

Figure 2.2, Ambition web.

3. Moveable bridges in The Netherlands

This section will go into the inventory of moveable bridges in The Netherlands. The goal of this section is to create an understanding of the moveable bridge renewal tasks that awaits the infrastructure sector. For this section data is collected in two ways, one is desk research by governmental bodies such as Rijkswaterstaat or research bureaus. Second, a survey has been conducted between municipalities and provinces.

3.1. Data collection

According to TNO The Netherlands has 8500 moveable bridges [57], of which, Rijkswaterstaat owns 167 [58]. Further research into the database from Rijkswaterstaat and waterkaart.nl shows a list of around 1500 bridges which span a waterway, cataloged into a database for waterway users. The data from Rijkswaterstaat and waterkaart.nl correlate strongly, indicating that waterkaart.nl might make use of the Rijkswaterstaat data. No other sources have provided information on the figure from TNO.

Looking into the waterway dataset from Rijkswaterstaat, each bridge location can be plotted onto a map Figure 3.1. Three main conclusions can be drawn from this map:

- Bridges are unevenly distributed through the Netherlands. The northern provinces and Holland account for more than 70% of all bridges in this dataset.
- The dataset does not contain all bridges, as mentioned previously. When comparing a more localized region of the map to a manual search of the area, the difference between the data becomes more apparent. The waterway data is focused on waterway users, and therefore only list public bridges which waterway users may encounter reasonably frequently.
- There is no reason to assume that some regions are overrepresented compared to other regions. Therefore, even though the total number of bridges maybe wrong, the distribution of them is assumed of to be correct.

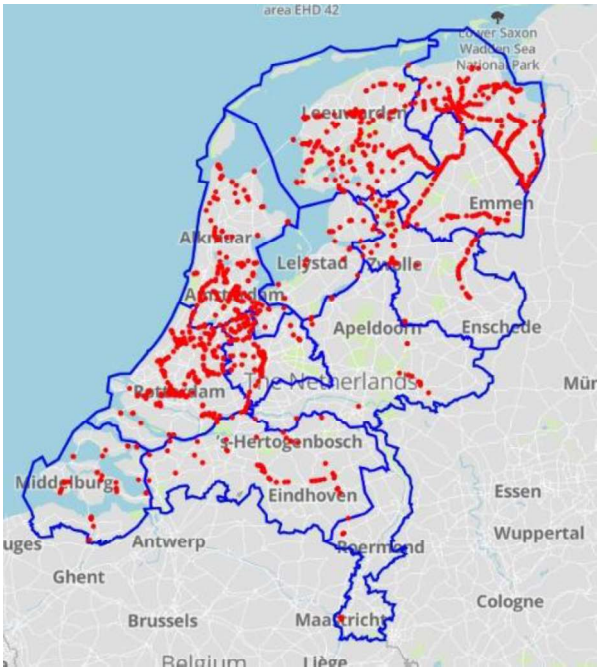

Figure 3.1, Map of movable bridges, from Rijkswaterstaat.

Comparing the bridges in the region of Gouda to the dataset gives an indication into what data is missing. The missing bridges can generally be placed into either or both of the following categories:

- Moveable bridges in regions where waterway traffic is (almost) nonexistence.
- Smaller bridges connection smaller roads to private property.

This gives reasonable expectation that the real bridge inventory of moveable bridges of interest is larger than the analyzed 1500 bridges. The discrepancy was however not significant enough to explain the 8500 estimates from TNO. The question remains if these structures will have the same moveability requirement if these are assessed for replacement.

Analyzing the location of the bridges indicates that moveable bridges are not evenly distributed through the Netherlands. As indicated above, the northern provinces and the Holland's combined inventory accounts for over 70% of the total for The Netherlands. This meets expectations as these regions are known for their waterways and is assumed to be not a statistical error. A pie chart with the distribution of the bridges in the Netherlands is shown in Figure 3.2.

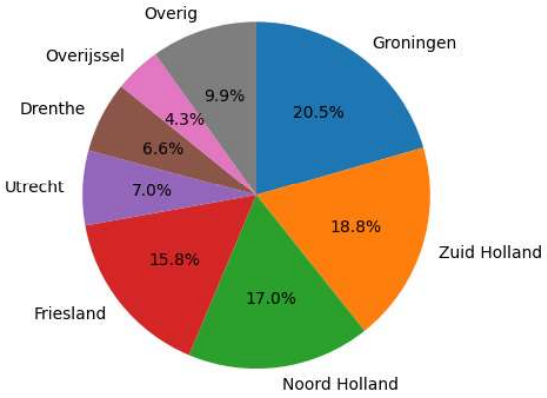

Figure 3.2, Distribution of bridges per province.

The next step in the analyses is the survey conducted by governing bodies, with both municipalities as with provinces. The goal of the survey was to determine the bridge systems and age of the bridges. In total, the responses account for 190 bridges, 12.5% of the waterway dataset or just 2% of the TNO estimate.

Looking at the bridge system, around 50% of all bridges are classified as draw bridges, with bascule bridges consisting of around 30%, see Figure 3.3. For this thesis the focus is on bascule bridges, but the technology might be able to be adopted for draw bridges as well due to their similarities.

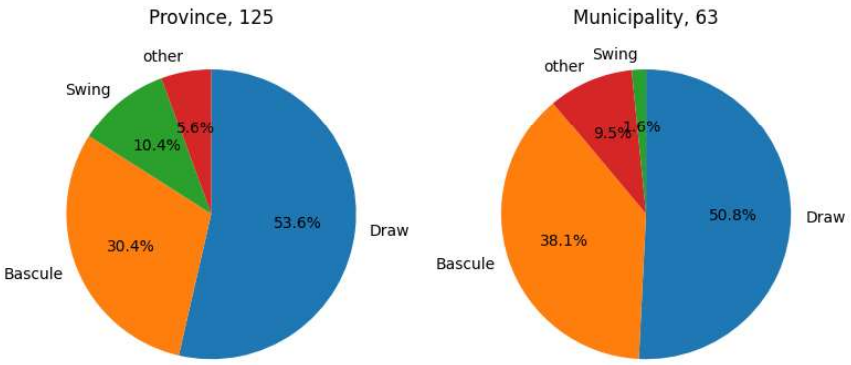

Figure 3.3, Moveable bridge type, separated by admin type.

Further analyzing the specifications of the bascule bridges, many bridges are very limited in length. The width of the waterway that must be unobstructed is specified based on the waterway classification. Most bridges are over waterways for which this width is no longer then 16m. This is visible in the data, with over 80% of all the bridges having a maximal length of 16, see Figure 3.4

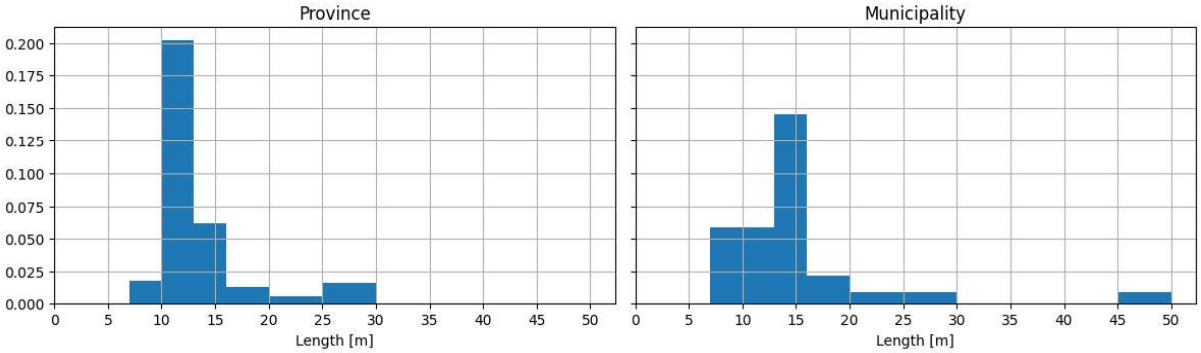

Figure 3.4, Length of bascule bridges, separated by admin type.

Analyzing the construction years of the structures, a notable peak around 1960 is visible. Considering the average lifespan of 60 to 70 years, the year of 1970 is chosen as the cutoff year to make an estimation of the coming assessment projects. 53% of provincial bridges and 77% of municipal bridges are constructed before 1970, see Figure 3.5.

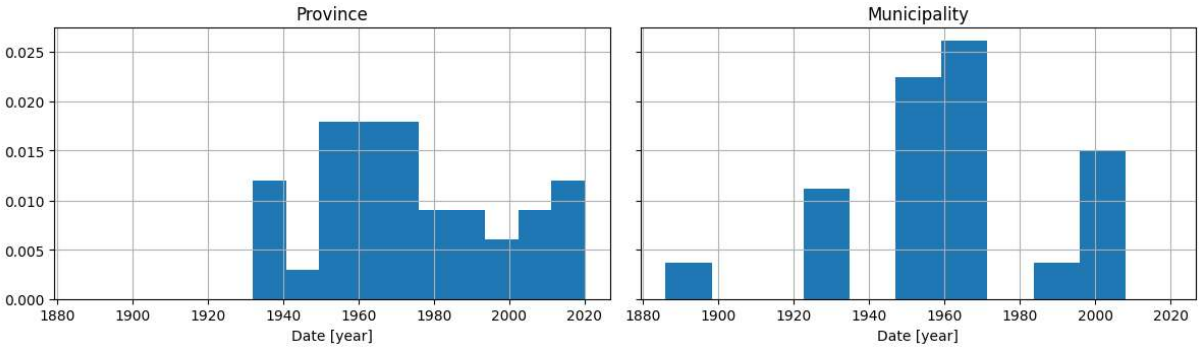

Figure 3.5, Construction year of bascule bridges, separated by admin type.

3.2. Extrapolating the data

This section will use the data above and produces an estimate for the moveable bridge inventory of The Netherlands. The initial question is: how many bridges of interest are there? The answer to this question remains ambiguous, as the data TNO used is not publicly assessable. For this thesis the answer will be assumed on 1500, as these structures can be accounted for.

An estimation on the distribution of ownership per government type is done as followed.

- The first step is to apply the known number of bridges managed by Rijkswaterstaat.
- The next step is to apply the distribution of bridges per province on the data acquired from the provinces.
- Finaly, what remains is assumed to be under management from the municipalities.

This estimation assumes that the distribution of owners remains constant throughout the Netherlands. The downside of the estimation is that this is most likely not the case, but merely a decent estimation. What is given is that the municipalities and the provinces own almost 90% of all “mayor” moveable bridges. A visual representation is given in Figure 3.6.

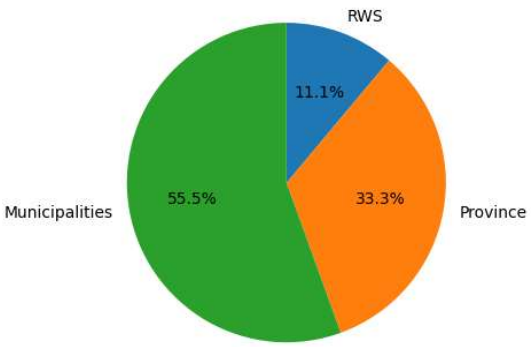

Figure 3.6, Distribution of bascule bridges over admin type.

Extrapolating the bridge type, dimensions, and age of the accounted 1500 bridges results in the following numbers, see Table 3.1.

Table 3.1, Summary of the relevant inventory of bascule bridges in the Netherlands.

Statistic	Bridges of interest
Bascule bridges	~ 500
Bascule bridges with length 16m or less	~ 400
Bascule bridges before 1970	~ 250

It is important to understand that these figures are a rough estimation based on a limited survey. That said, it does provide an insight into the challenge at hand. Given around 500 bascule bridges of which a potential 250 reach the point where reassessment becomes important, providing a more sustainable solution to renewal project is important.

Any savings provided in the conclusion of this research project, can potentially be applied to the 250 bridges with are reaching the point of reassessment. Even if these savings might not be possible due to case specific circumstance, the methodology discussed in this thesis can be applied.

3.3. Bascule bridges

The most common design of the main structure of moveable bridges has for a long time been steel. Steel designs allows for long spans with low weight, ideal for moveable bridges. Older bridges tend to be build using wooden decks. This has not always been the case, before steel as a building material was readily available, wood was the only material with which moveable bridges were conceivable.

In the previous section, the year of 1970 was used as a cutoff to determine the number of bridges that will start to require assessment in the coming years. This is not the only significance of this period. From the 1960's onward (though not instant), wooden decks fell out of use in favor for steel orthotropic decks. Initially, this was done to further reduce the mass of the bridge deck. To achieve this mass reduction, thin steel plates were used, down to 12 or even 10 mm [59]. It is assumed for this thesis, that the average cutoff was around 1970.

The downside of thin steel decks is that these structures are vulnerable to metal fatigue. This was at the time not a problem. Traffic weight and intensity meant that this was not the problem during the development of steel orthotropic decks. Next to this, the understanding on metal fatigue was not far enough advanced to allow for designs less susceptible to metal fatigue.

Studies into the actions of the steel orthotropic deck have changed the design of these decks. Modern steel decks, following the Dutch National annex EN 1993-2, are proposed to be 15 to 22 mm thick [59]. This is a significant increase in material use and therefore mass. Other improvements have been made in the detailing of the connections, making them more complicated to produce. Advancement in welding automating has diminished this problem and even allows for more complicated designs. Due to the increase in mass, modern steel decks no longer have the weight advantage because of the increased thickness.

Another downside of wooden decks is that wooden decks need to be replaced every 25 to 30 years [60]. Although a recent case, the Van Brienenoord bridge, had a wooden deck which reached a lifespan of 40 years [61]. Steel as well as wood requires regular maintenance, as steel without protection will corrode. Modern corrosion protection, in the form of a coating, must be renewed every 20 to 25 years [62]. Other options such as galvanization might increase the lifespan of the coating [63], but have far higher environmental impact [64].

4. Fiber reinforced plastics

Fiber reinforced plastics or fiber reinforced polymers is a composite material made of fiber reinforcement in a resin matrix. Fiber reinforced composites have been used since the Egyptian empire, where fiber reinforcement was usually added in the form of flax or straw. In the early 1900s, plastics were developed which would form the basis for the polymer resins used today. Development in the 1930s created the possibility to mass produce glass fibers, allowing for the industrial production of glass-fiber reinforced plastics (GFRP) [65]. Although the current material has gone through many advancements, the possibilities for end-of-life recyclability remains limited. [66]

Two material challenges of FRP result in a common application of FRP as a sandwich panel. The first is that, compared to materials such as steel, FRP is less stiff. Second, a shear force perpendicular to a laminate will result in interlaminar shear. This is a force which results in individual layers of fibers being separated from their matrix, called delamination. This is a matrix dominated failure mechanic, which is a significant problem for elements with high concentrated perpendicular loads, such as a road deck.

Sandwich panels counter these problems by creating height which provides stiffness instead of the material itself. For the second problem, the core is better suited for perpendicular concentrated forces. For softer core materials, which tend to be lighter, the core is not strong enough for these forces. Tho further increases the resistance to out-of-plane shear, webs can be constructed. This results in a balancing equation, using lighter materials will reduce the mass, but will requiring webs, which can have adverse effects on the environmental impact, costs, and production time.

This section will divide FRP into three subsections, fibers, the resin matrix, and its core.

The following fiber materials have been analyzed:

- Glass fibers
- Carbon fibers
- Aramid fibers
- Basalt fibers
- Natural fibers

The following resins are considered:

- Polyester
- Epoxy
- Biobased polyester

The following cores have been considered:

- Foam
- Balsa

The materials have been chosen because they are described within the norm with which the variants are designed or promise significant sustainability benefit.

4.1. Materials

4.1.1. Fibers

The main fibers used in engineering are glass-, carbon- and aramid fibers. Aramid fibers are synthetic polyamide molecules, where brands have commercialized copyrighted formulas such as Kevlar. Aramid fibers can potentially obtain high strength, although their compressive resistance is substantially lower than their tensile properties and brittle failures from impact [67].

Glass fibers is a group name for fibers from glass, where the composition of the glass can alter the properties of the fiber. Most common is E-Glass (electrical), but other types include C-Glass (corrosion) and S-Glass (strength) [68]. Glass fibers are the standard fibers used for civil applications, having a lower strength then carbon, but far less expensive [69] and lower environmentally impact [70].

Carbon fibers are a more specialized fiber for high performance low weight application. Their properties suit these application best, bust come at a more significant cost and environmental impact [71].

Basalt fibers are a relatively new product, which has great promises for civil application. The strength properties of basalt are comparable to glass and might have a better environmental performance then glass fibers [72], [73]. Studies have found comparative values to glass [74], but no environmental database data can be found for basalt.

Aramid fibers are a synthetic fiber defined by aromatic ring connections, where its name is also derived from (aromatic polyamide). Popular versions of aramid are branded variants, such as Kevlar. The tensile strength of aramid fibers is in between the strength of glass and carbon. The price of aramid fibers can be twice as high as carbon [75] with twice the carbon footprint compared to glass [76].

Natural fibers have the potential to provide the basis for an FRP with very little environmental impact. The drawback for natural fibers their low strength, poor bonding properties, and poor resistance to moisture and temperature. These properties currently prevent natural fibers from use in structural applications [77].

For comparison, the following Table 4.1 shows approximate characteristics used for material comparison.

Table 4.1, Approximate material characteristics of fibers.

Fiber material	Elastic modulus [MPa] [78]	Tensile strength [MPa] [78]	Density [kg/m^3] [78]	Costs [€/kg]	Carbon footprint [kg CO_2 eq./kg]
E-Glass	74-86	2500-3200	2500-2600	4.18 [79]	3.99 [80]
Carbon	230-450	4400-4900	1770-1800	41.86 [79]	83.29 [80]
Aramid	130	3600	1450	50-83.92[1] [75]	8.7 [76]
Basalt	90	3000	2700	4.74 [81]	2.23[2] [74]

For this research, aramid fibers will be excluded for their material properties provide little upside compared to its costs and environmental impact. For basalt fibers, the material will be excluded because of its omission from databases. Future research may provide enough data to include it into databases. Table 4.1 shows the potential of the material to further reduce the impact of FRP production.

[1] 50 €/kg is absolute value from [75], but 83.92 is scaled with relation found in [75] with data from [79].
[2] This value is calculated as 44% reduction compared to glass fibers.

Glass fibers will be used as primary fiber material, as the confirmed carbon footprint per strength will make this the optimal material for achieving a lower environmental impact. Carbon fibers will be utilized if the weight of the structure becomes governing.

4.1.2. Resin

Resin is the bonding material between fibers to create a matrix. Where fibers on their own offer great tensile properties, compressive strength is governed by the resin properties. For civil engineering applications, thermoset resins provide better material properties and resistance to moisture and temperature. The downside of thermoset resins is their poor end of life qualities, where the current best recycle method is the burn the resins to recover the fibers [82].

Polyester and epoxy have become the most applied resin material, because of their lower material costs [83]. Their molecule composition has a strong influence on the material properties, but in general, the material properties for polyester, epoxy and for resins such as vinyl ester or phenolic are comparable [78].

A proposed improved resin group are thermoplastic resins. Rather than creating an irreversible matrix, thermoplastic resins, provided with heat, soften, and can be removed from the matrix to separate the resin and fibers. Resins are however poor in high temperature environments. Thermoplastic resins have even poorer structural properties in high temperature environments [84]. The main specification for this characteristic is the glass transition temperature, T_g. The glass transition temperature is the temperature where the material transitions into a more viscous or "rubbery" state. Although this is not instant, but gradual, from this point a significant loss of mechanical properties is observed when temperature is increased. For polyester this is between 40 °C and 110 °C and epoxy can range from 40 °C to 300 °C [78].

Another improvement to resins is increasingly ecological material usage. Resins are predominantly oil-based product and therefor have significant environmental impact. Creating resins from (partly) from ecological friendly recourses significantly reduces their environmental impact. The best example for this is Polynt Ecopolyester, reducing their emissions by nearly 60% compared to conventional polyesters [85].

For this thesis the choice has been made for Eco polyester from Polynt. Although scarcely applied in civil engineering application, their significantly reduced environmental impact provide greater opportunity for FRP in renewal projects.

4.1.3. Core

For the core multiple materials are fabricated into a foam core, most conventional are PVC, PET, and PUR. These materials are oil-based foams, therefore having a significant impact per weight, although their specific density is low at around 100 kg/m^3. This can be improved by using recycled plastics, potentially reducing the environmental impact by 35% [86]. The advantage of these materials is their low density, reducing the mass of the structure. Their drawbacks are their low strength and lack of resistance to indentation, potentially reducing the strength of the sandwich panel and requiring webs in the sandwich panel [87].

Balsa is an option for the core material that is gaining prominence. Balsa is low density wood, which has the advantage of more strength and even a negative environmental impact. Next to this a balsa sandwich panel does not require webs to prevent core indentation. A drawback is that balsa has more self-weight and is more susceptible to moisture and temperature, requiring adequate shielding [88].

For this thesis balsa is chosen for preferred core material. This is because it allows for very low environmental impact sandwich panels. When weight becomes the governing constraint, then a (partial) substitution to foam cores can be considered.

4.2. End of life FRP

This section will outline current opportunities and challenges for the end-of-life processing of FRP. This area attracts much interest as this is currently a large environmental issue for FRP. FRP, consisting of at least two inseparable materials, is therefore inherently difficult to recycle. The at the time of writing most mature recycle process is generally called physical recycling. Current research is mainly being focused on thermal and chemical recycling [89].

4.2.1. Physical recycling

Physical recycling is an abstract term for what in essence is crushing, shredding, or grinding of FRP into smaller particles. Different processes will result in different size particles, chips, loose fibrous material, and very fine powder. The resulting fibrous material can be used in chopped fiber mats of microfiber reinforced concrete. Chips can be pressed into products such as artificial wood. Fine powder can be used as filler material for cement or asphalt. During this process the mechanical properties of the material deteriorates [90].

This results in a product that has lost most of it added value during the end-of-life process. The resulting market value is relatively low, creating limited incentives to process the material at the end of its lifecycle. An advantage of physical recycling is its relatively low energy demand, requiring 0.1-4.8 MJ/kg [91] to process.

4.2.2. Thermal recycling

Thermal recycling is the removal or separation of the constituent parts by (partially) thermal processing. There are three processes to thermally process the FRP, fluidized bed process, incineration, and pyrolysis.

The Fluidized bed process requires shredded parts and then heated between 450 °C and 110 °C on a silica sand bed. This separates the material into the fibers and a volatile compound. The short fibers can be reused in chopped fiber mats or microfiber reinforced concrete [92].

Incineration uses shredded parts in an energy plant, to recover the stored energy in the constituent parts. This recovers no material to be reused but does allow for the generation of energy [92].

Pyrolysis is the process of heating the material in an oxygen-deprived atmosphere, which results in thermal cracking of the matrix. This cracking separates the fibers from the resin, which flows out of the process as a volatile mix. This mix can be separated into a “pyrolysis oil” and fraction gas such as carbon dioxide. These byproducts can then be reused for the creation of fuel. A study from 2016 discuss that the recovered fibers retain only 50% to 20% of their tensile strength [93]. A newer study from 2021 discusses retaining the tensile strength up to 75% [94].

Heating by microwaving the material reduced the energy demand from 27 to 7.5 MJ/kg [91]. The resulting materials still lose substantially large portion of their added value.

4.2.3. Chemical recycling

There are two processes grouped under chemical processing, solvolysis and catalytic cracking. Solvolysis is the process of dissolving the polymer matric by a solution of acids. The resulting fibers retain the tensile strength, the original monomers and oligomers may be recovered from the resin and acid mix. The byproduct remains a chemical fluid with potentially significant environmental impact and must be post-processed [92].

Catalytic cracking is a process evolved from solvolysis, where catalytic agents are added to produce certain byproducts. The agents can be chosen to reduce the energy needed for the reaction or reduce the production of unwanted byproducts [95].

The energy needed for this process is highly dependent on which agents are included, ranging between 21 and 91 MJ/kg [91]. The fibers potentially retain their value, processing the byproducts will have significant environmental impact.

4.2.4. Future prospect

Many of the technologies discussed above have been developed over the last 20 years. The expectation is that the technologies will continue to be advanced and developed further. Recent advancements as using microwaves to heat the material reduced the energy consumption significantly but is still unable to keep the mechanical properties of the original materials. The significant pace of advancements causes optimistic views of the prospects of FRP recycling.

Possibly the best technology moving forward is chemical processing. The ability to recover fibers with original tensile strength retains significant value of the product. The possibility to include agents to refine the process provides opportunities for innovation. A notable mentioned for retaining original strength of the fibers is thermal recycling. As outlined in its own section, significant advances have been made in retaining the original strength.

The ceiling for FRP recycling remains uncertain, and at the time of writing, no technology has proven to be the benchmark technology for recycling FRP. For this thesis, the end-of-life environmental impact will not be discounted because of potential innovations, because these are difficult to quantify.

5. Methodology of sustainability

The section will detail the methodology that will be used to design for sustainability with the case study. This methodology begins with the "Aanpak Duurzaam GWW" [96], approach to sustainable infrastructure, developed by the ministry of infrastructure and environment to consider sustainability aspect into civil projects. A more detailed description will be displayed in the following section.

5.1.1. Approach to sustainable infrastructure

The approach to sustainable infrastructure was developed and released in 2016 and is an example of a design for sustainability (D4S) methodology. The document describes a government view on including sustainability in civil engineering projects. Important context for this methodology is that most engineers have little experience with sustainability. The approach is divided into six steps, these are:

1. Analysis of ambitions and goal.
2. Analyzing opportunities.
3. Describing ambitions and opportunities.
4. Defining specification and design.
5. Scoring on defined specifications and criteria.
6. Justify design choices.

The first step entails the analyzing the ambitions and goals of the participating parties. The ambitions and goals will differ per organizations, per project. It is important to determine and describe the ambitions and goals clearly at the start of the project, to prevent waste of resources. For the ambitions, an effective tool is the ambition web, which is described in section 2. This section also describes what aspects, from the perspective of an engineer, are most important. For the application of the ambitions and goals, case specific circumstance needs to be considered. Certain aspects will become less important due to these circumstances. This will be performed in section 6.2 for the case study.

The second step is to analyze the opportunities to increase the sustainability of the project. This step is very case specific, where every project will have differing opportunities. The identification of ambitions early into the project allows for greater increase in sustainability. For the case study this will be performed in section 6.3.

Step three is to describe the ambitions and opportunities. This step allows for the alignment of ambitions, goals, and opportunities between parties. This involves clear communication, preventing misaligned further down the process. It then also means that the parties are committing to a selection of goals and ambition. This step is less relevant for an engineer, as the description of the first two steps encompasses the work of an engineer for this step.

Step four is where most of the work for an engineer is performed. The specification defined in this step will lead into the design performed for this step. An engineer will have performed this step numerous times in their career, so for an engineer it may be difficult to then fully apply the sustainability methodology.

Step five allows for reflection of a project team on the design. The scoring will give insight into the sustainability performance of the structure. This insight can be used to further improve the designs.

Step six again is more focused on communicative aspects of the methodology. It gives the opportunity for the project team to reflect upon the design choices. This step is a continuation of step 4 and 5, and just like these steps, can be repeated to improve the designs.

The main benefits for this approach are that the approach is general and simple in principle. Generality is beneficial because it promotes the use of the methodology in contrasting projects and provides room for case specific adaptation. Simplicity (in principle) enables more people who can adopt this methodology and can thus start making simple improvements. Thus, both benefits increase the chances of implementation in a project.

There are however also drawbacks to simplicity and generality. For an engineer the methodology might be too vague, especially when applying them to specialist objects, such as movable bridges. Therefore, this methodology will be more refined in the following sections, from the perspective of an engineer working on renewal projects of bascule bridges.

5.1.2. Circular design principles

To provide context towards a design step in the approach, circular design principles are considered. Circular design principles can be interpreted in general, but as with the approach, the government has provided context to these principles. Therefore, this section will reflect on "Circulaire ontwerp principes" [97].

The circular design principles for Rijkswaterstaat are summarized in the following graphic Figure 5.1. It follows the same circular philosophy described in section 2, depicting a clear pyramid design where certain actions are conceived as more important. Using the circular design principles implicitly takes the ambition materials and circularity into account and thus climate mitigation.

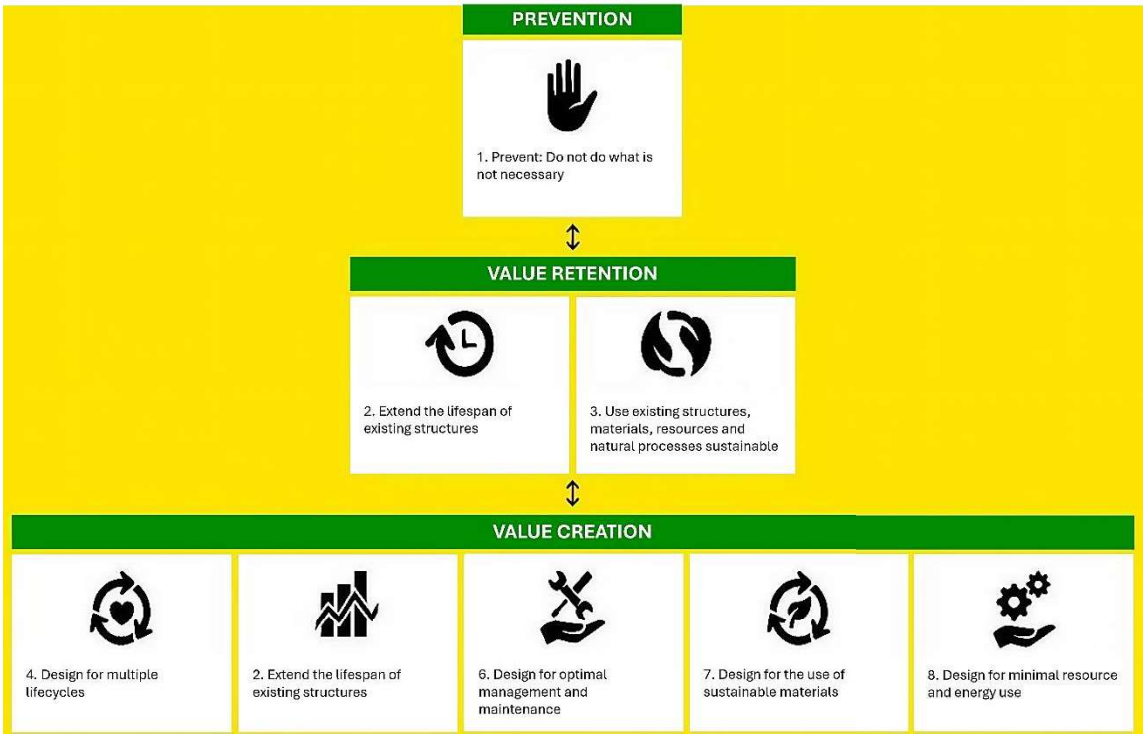

Figure 5.1, Circular design principles, by Rijkswaterstaat.

5.1.3. Sustainability methodology for bascule bridge renewal projects

In general, the approach provided by the government is the starting point for the methodology detailed below. For the perspective of a structural engineer, more context is given to steps four to six of this methodology. As a reminder these steps are:

4. Defining specification and work on design.
5. Scoring on defined specifications and criteria.
6. Justify design choices.

The context can be given by addressing certain considerations that should occur in a design process. These considerations follow from the ambition web, given in section 2. For remembrance, level two ambitions are:

- Climate adaptation.
- Environmental effects.
- Land use.
- Accessibility.

And level 3 ambitions are:

- Energy and climate mitigation
- Materials and circularity

For level 3 ambitions, a more implicit methodology will be used to fulfill these ambitions. In this case an implicit methodology is the use of a (design) principles use to fulfill the ambition, rather than solely translating the ambition into specifications. This has the advantage that an ambition is more thoroughly optimized compared to only complying to specifications. The drawback is that could allocate resources to ambitions which do not align with the ambition web. Therefore, for ambitions with a lower ambition level will not be implicitly optimized.

For materials and circularity, the circular design principles as detailed earlier will be applied. This will be an implicit method to improve to reduce the material waste of the design. As mentioned, these principles are also a tool to reduce the climate footprint of the structure. Other methods of implicitly reducing the climate footprint are the use of less polluting materials and the structural optimization of the structure.

From a circularity standpoint, it is favorable to prevent the construction or modification for as many elements of the bridge as possible. Next to this, the design with the use of separable elements provides opportunity for reuse of separate elements instead of the entire structure. This increases the chances that materials will be reused with more retained value.

Ideally, elements of the bridge leaf itself or surrounding infrastructure can be preserved. This can potentially result in a large sustainability improvement, in more areas than just circularity. Potential sustainability benefactors, called secondary benefits from circular design principles:

- Climate mitigation.
    - The prevention of work and use of materials could also lower the climate impact. The method of renovating the structure is however also a factor and more climate mitigating actions can or need to be performed.
- Environmental effects.
    - The prevention of having to demolish more of the old structure could result in lower environmental effects. Again, the method of renovation might require additional consideration.
- Land use.
    - Reusing most of the old structure could allow for less or no use of additional land for the final structure. During renovation there still need to be considerations for this ambition.

As mentioned above, not all sustainability benefactors are without risks. Therefore, specifications are required to further fulfill in the sustainability goals. Climate adaptation, environmental effects, land use and accessibility are all ambitions that could translate well into specifications. The required specifications differ strongly per case and might need more special attention then analyzed in section 2.

Finally, to fulfill in energy and climate mitigation, the primary criteria for measuring the performance of each design alternative will be the ECI. As mentioned, implicitly applying the circular principles will also provide climate mitigating effects.

All aspects and their application are summarized in Table 5.1.

Table 5.1, Relevant sustainability aspects and the method of application.

Level 3 ambition (Highest achievable performance)
Energy and climate mitigation • Secondary benefits from circular design principles. • Limiting use of polluting materials. • Structural optimization. • Primary criteria.
Materials and circularity • Circular design principles
Level 2 ambition (Thoughtful consideration)
Climate adaptation • Translation into specifications.
Environmental effect • Secondary benefits from circular design principles. • Translation into specifications.
Land use • Secondary benefits circular design principles. • Translation into specifications.
Social value • Provide requirements for future needs.
Accessibility • Translation into specifications.

Part II. Design study

6. Introduction to the design study

This section will go into case study for this thesis project. As mentioned, these are the Oostsluisbruggen in Terneuzen. These bridges are part of a lock complex in Terneuzen, where a canal connects Gent with the Western Scheldt.

A short introduction to the case study will provide context to the design study. Then the sustainability methodology for bascule bridge renewal project will be implemented during this and the following sections for the design process.

6.1. Case study introduction

The two bridges have identical structures, spanning just over 25 meters over the western lock. The greater lock area is known as the Terneuzen locks. The bridges and lock date from 1968. Recent inspections have marked the structure as faulty and its owner, Rijkswaterstaat, has marked the structure for repairs or replacement. Figure 6.1 to Figure 6.3 depict the structures. The exact dimensions will be discussed further in this section.

Figure 6.1, Oostsluisbruggen, deck view.

Figure 6.2, Oostsluisbruggen, structural system from below.

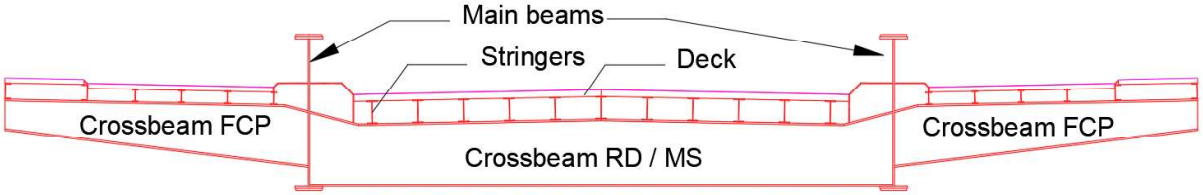

Figure 6.3, Oostsluisbruggen, cross section.

Points of interest for this structure are:

- The current structure's main beam extends above the deck, indicating a need to reduce height below deck.
- The structure is part of a lock complex. There are two bridges parallel to each other, where both structures have the same functionality. The lock complex consists of two locks and a third is under construction. This will have consequences for replacement and maintenance strategies.

The relevancy from this case study comes from its design and age. As analyzed in section 3, 50% of structures reviewed are constructed before 1970, like the Oostsluisbruggen. Many of these structures consist of a steel frame with wooden decks. Although the dimensions differ from the norm in The Netherlands, developing improvement for this case study is still relevant due to its typical structure for its time.

6.2. Sustainability ambitions for this case study

Following the method for sustainability, the ambitions must first be considered. This will follow the work in section 2. In section 2, the following aspects were identified which require adequate consideration:

- Climate adaptation.
- Environmental effects.
- Land use.
- Social value.
- Accessibility.
- Financing

The following ambitions are considered worth optimizing for:

- Energy and climate mitigation
- Materials and circularity

This was done after a broad consideration for each aspect with regards to bascule bridges, see section 2. The following section will consider what aspects are relevant for this case study.

6.2.1. Energy and climate mitigation

The environmental impact is a major consideration for this project. This is the most tangible aspect of environmental sustainability, and thus will be quantified with a MKI calculation. For this section two quantitative assessments will be performed.

- ECI, to indicate the environmental shadow costs associated with the use of materials for the structure.
- Mass, to indicate the need for additional materials in parts of the structure which are outside the scope for the parameters study.

6.2.2. Materials and circularity

Circularity is a major consideration for this project. This aspect is less tangible but will still be qualitatively evaluated. This evaluation will look at the following aspects:

- Ability to use reused materials and/or elements in the structure.
- Ability to reuse elements at the end of the lifecycle.
- Ability to recycle materials at the end of the lifecycle.

6.2.3. Climate adaptation

Climate adaptation is a key area for this case study. As analyzed in section 2, flooding, extreme heat, and extreme weather (strong winds) are key risks for moveable bridges.

Flooding is considered a small risk for this case study. With the renovation of the lock complex, the flood safety of the complex was accessed. The report finds that both bridges are on the inside of the primary dike ring and thus are protected from flooding from the sea. The dike ring is assessed for predicted water levels for over 100 years. The inland waterway water level is highly controlled and is only allowed to fluctuate with ±0.3m [98]. Thus, for this case flood safety will not be considered.

For extreme heat, it is important that enough dilatation is provided for both structural performance and operability. Next to this, with regards for FRP, the loss of structural performance is an important factor for the design resistance of the structure. It is assumed that the governing design codes account for this effect.

Extreme weather and specifically strong winds are important for the structure's operability. During the calculations it is important the operations envelope account for strong winds. It is assumed that the prescribed windspeeds in the NEN norms sufficiently account for the aspect.

For above mentioned reasoning, no sub aspect of climate adaptation will have an impact for the sustainability of the structure. This aspect is thus not considered for assessment.

6.2.4. Land use

Following section 2 and 5, land use is an aera in sustainability in which sustainability goals are possible. Following the discussion in section 5, land use already benefits greatly from the implementation of the circular design approach.

However, there is the possibility for elements of the structure which will not be able to be reused. If this is the case, the choice is made to design elements which can be placed in the already existing surrounding infrastructure. This results in a new structure which will not require extra space. If this is not possible, more consideration for this aspect is required, but this falls outside the scope for this project.

Because this project makes the choice of designing elements which fit in the space of the current elements, there is no comparison to be made between variants. Thus, this aspect is considered, but no comparison between variant will be made for this aspect.

6.2.5. Social value

For social value the future proof sub aspect will be similarly measured qualitatively as concluded in section 2. It is important to analyze the general surrounding when considering future needs. The structure is a part of the Terneuzen locks. A change in functionality of the structure requires a change in functionality of the locks. In addition, a main road has been constructed 4 km to the south of the locks to alleviate road intensity on the roads and bridges.

With the current design structure, the ability to change the layout of the bridge is limited. The main girders protruding from the deck hinders this. For possible future changes, the following scenarios are analyzed Table 6.1.

Table 6.1, Likelihood of future changes to the Oostsluisbruggen.

Scenario	Verdict	Reasoning
Road expansion	Unlikely	• Will require redesign entire complex. • Capacity is assessed by expansion of lock complex [99].
Foot and cycle path expansion	Unlikely	• Will require redesign entire complex. • Capacity is assessed by expansion of lock complex [99].
Fauna zone on bridge	Unlikely	• Will require redesign entire complex. • Fauna zones are undesirable on moveable bridges.
Loss of functionality	Neutral	• Capacity is assessed by expansion of lock complex [99]. • Future needs for the harbor for which this locks services might require further change.

For assessing the social value of the structure and thus the future needs of the structure, only the loss of functionality of the bridge is deemed not unlikely. Considering what effects this has on the structure, this scenario will also not be considered. To further improve the future proofness of the structure, the ability for the structure to facilitate free functional change for the entire area will be assessed.

6.2.6. Accessibility

Following section 2, only user delay is an aspect for accessibility. However, for this case study user delay is not considered. The considerations for this are:

- The bridges are part of the lock complex of Terneuzen. Every bridge is constructed twice, on either side of all locks. It is possible for any lock or bridge to be closed and alternatives to be available for traffic. I.E. if one of the two bridges is closed for maintenance, user delay for road users is minimal as another bridge will be opened for traffic. Similarly, for boat traffic another lock will be most likely available.
- If both bridges are closed to road traffic, a diversion route is available 4 km further south than the locks. This route, at most, adds 10 minutes to the travel. This scenario is less likely as this will have a larger impact on the users.

As mentioned above, the risk of mayor user delay due to maintenance or any other events that would render the structure inoperable are negligible. Thus, this aspect will not be a consideration in the comparisons between design variants.

6.2.7. Financing

Financing will remain important for any civil engineering project. However, financing can also constrain the possibilities of implementing environmental or social sustainability measures. For this thesis, financing will not be considered, as a method for eliminating the restraints on environmental or social sustainability. This result of the design choices will also not be translated into a financial gain or loss, to prevent the focus on this aspect instead of the other sustainability aspects.

6.2.8. Ambition web

For the case study the modified ambition web is displayed in Figure 6.4. The figure consists of two shades of green, where the light shade highlights the original assessment of the ambitions, and the darker shades display the ambitions for the case study.

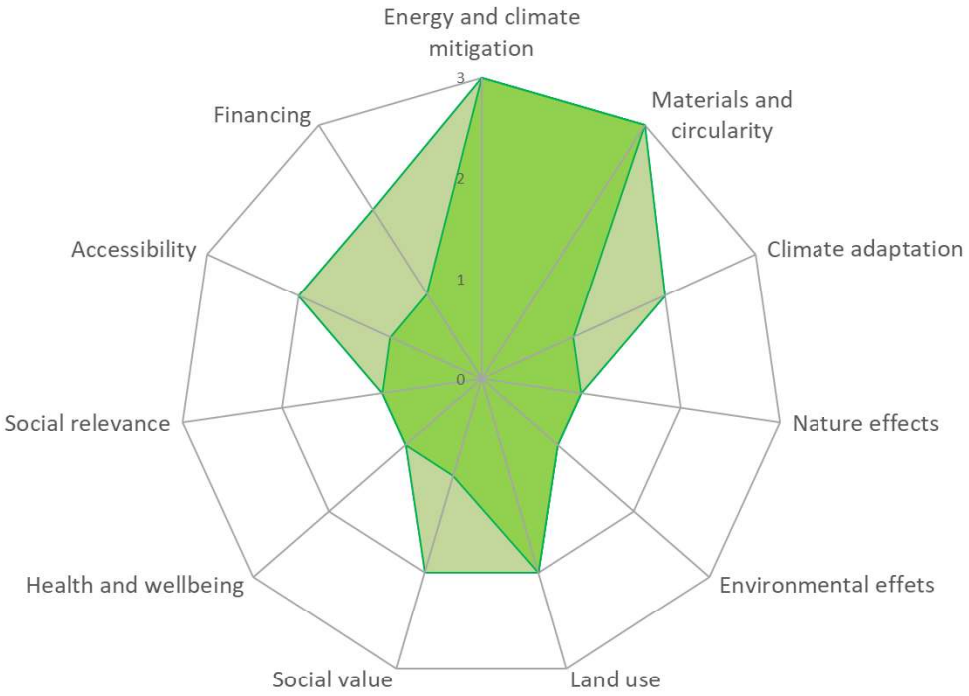

Figure 6.4, Ambition web adjusted to the Oostsluisbruggen.

6.3. Sustainability opportunities

Step two of the sustainability methodology is to analyze the opportunities for the renewal of the bascule bridge. By focusing on the ambitions selected in the first step, the following opportunities are identified:

- Elements of the current structure might be able to be reused. Since the lack of information on the state of the current structure, two scenarios are used to explore this opportunity.
    - Scenario 1 is that the deck needs replacement (wooden deck planks and supporting stringers)
    - Scenario 2 is that the entire structure needs replacement.
- Implementing simpler designs, such as consisted cross sections or standardized profiles reduces the costs of the structure and improves the chance of end-of-life reusability.
- Maintaining or reducing the mass of the structure, which can prevent the need for new or improved actuators or counterweight. A lower weight is also favorable for transport, reduces the risks of handling the structure and lowers the energy required for moving the structure.
- Designing the structure inside the current parameters (height between deck and supports, position of main beams, width of main beams), to prevent work on the basements or abutment.

6.4. Program of requirements

Following the methodology, this section is drafted to provide the basis for the design phase. The program of requirements starts with the design objective, followed by a description of the desired function and the ambitions. This is followed by more structural requirements, such as the dimensions, norms, material properties etc. Sustainability requirements are then included to guide the design process. Finally, some auxiliary requirements are imposed.

6.4.1. Function

The bridge will provide the crossing of the Buitenhaven road over the Oostsluis. This includes a two-way road, two cycle- and foot paths on either side of the roadway. Heavy traffic roadway loads must be included for the roadway and standard foot / cycle path loads must be considered for the paths on either side. In addition, a service vehicle must be considered on the foot / cycle path. The geometric profile of the decks must be maintained, as must the height of the bridge under the deck. The current structure features a protruding flange of the main beam, this can be a design option for the renewal structure. If this is the case, a kerb must be installed to avoid collision with the structural element.

6.4.2. Geometric requirements

The geometric requirements will be displayed in Figure 6.5 and Figure 6.6.

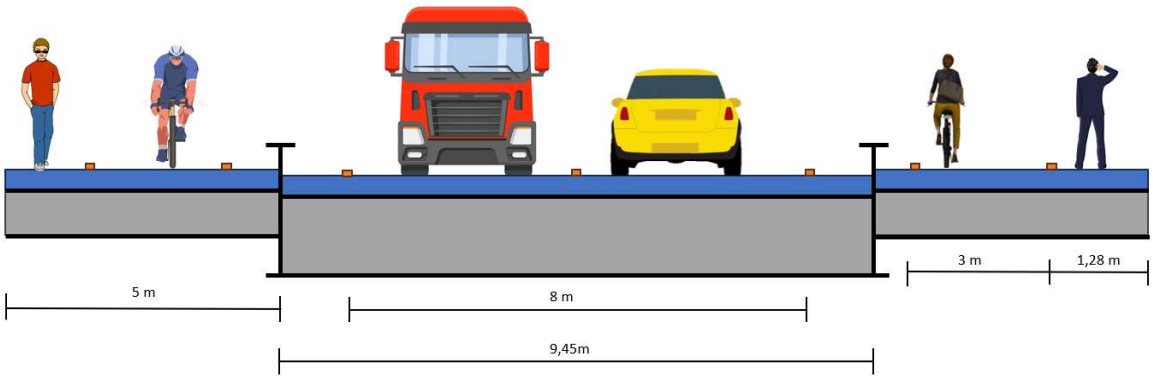

Figure 6.5, Cross section dimensions of the Oostsluisbruggen.

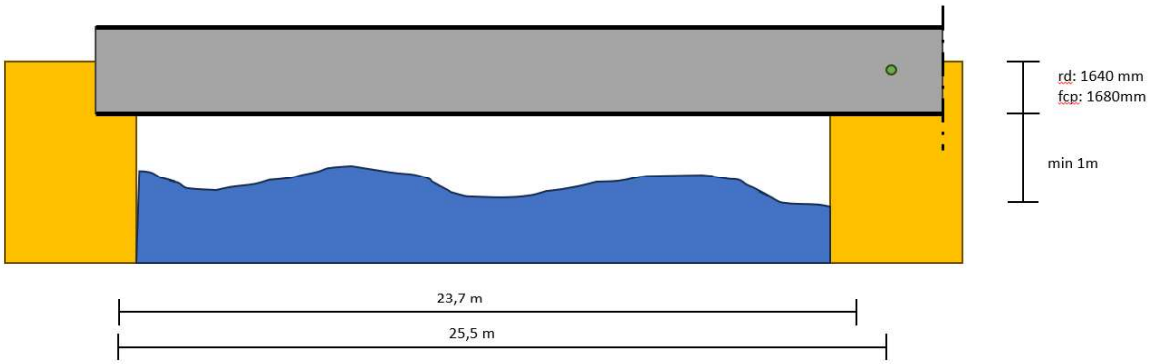

Figure 6.6, Longitudinal dimensions of the Oostsluisbruggen.

6.4.3. Norms and classification

The applicable norms for the basis of design, actions and verifications are Eurocodes [100]. For FRP material specific verifications UNI 19101 [78] is used.

The bridge will have sections dedicated to road traffic on the road deck (RD) and cycling and pedestrians on the foot and cycle path (FCP). For the designs, the section considering the road reck will be called the main structure (MS), as this includes crossbeam, if applicable, and the main beams The consequence class of the bridge is CC2. The waterway is category Va and part of the “hoofdstransportas”, the main transport waterways of the Netherlands. Finally, the bridge located in Zeeland, is in wind zone 2.

6.4.4. Load requirements

For all load cases self-weight must be considered (EN 1991-1-1 5.2) [101].

6.4.5. Vehicle loads

6.4.5.1. Road deck

For the road deck load case 1 (EN 1991-2 4.3.2) [102] and 2 (EN 1991-2 4.3.3) must be considered separately. In addition, brake forces must be considered, equal to 10% of the vertical distributed load of LC1 in addition to 60% of the concentrated load of LC2 (EN 1991-2 4.4.1).

6.4.5.2. Food and cycle path

For both the food and cycle paths a distributed load of 5 kN/m^2 (EN 1991-2 5.3.2.1) and a concentrated load representative of an emergency vehicle for resultant stresses (EN 1991-2 5.6.3) or service vehicle for deflections (EN 1991-2 5.3.2.3). All forces must be considered separately.

6.4.6. Wind load

In opened position, a continues force must be considered over the full length of the bridge (NEN 6786-1 2.3.2.3.1) to be calculated with (EN 1991-1-4 4.5). The length dimension of the bridge leaf in opened position is largely in a vertical direction.

6.4.7. Collision forces

Incidental loads perpendicular to the bridge must be considered on either the railing (EN 1991-2 4.7.3.3) or extruding structural elements (EN 1991 4.7.3.4). Assumed is that this is mitigated by implementing a kerb of minimal 200 mm for which the following loads must be considered separately (EN 1991-2 4.7.3.2).

Incidental loads because of a vessel colliding with the bridge must be considered on the width of 3 meters and a height of 0.25 meters (NEN 1991-1-7 4.6.2). The static equivalent force to be considered is 1 MN (NEN 1991-1-7 4.6.2).

6.4.8. Load combination

The weight of the structure, traffic and food/cycle path loads must be combined where both loads are maximized separately (EN 1991-2 4.5.1 NB.3).

6.4.9. Sustainability requirements

Following from the sustainability ambitions and -opportunities, sustainability requirements are imposed. These are displayed in Table 6.2.

Table 6.2, Sustainability requirements of the Oostsluisbruggen

Sustainability aspect	Requirements
Energy and climate mitigation	• The design must be optimized for ECI values. • The mass of the current structure must not exceed 150 metric tons, to prevent replacing the structure with a heavier structure.
Materials and circularity	• The design must be made with profiles with consistent cross-section to improve end-of-life reusability. This is an assumption, were more carefully design profiles might lower the environmental impact.
Land use	• The current height profile under the bridge must be maintained to comply with current assumed height clearance requirements. • The height profile of profiles for the moving arm must be maintained. • The deck must follow the geometry of the current deck to limit the addition work on the surroundings.

6.4.10. Auxiliary requirements

Auxiliary requirements are imposed to account for requirements imposed from different codes or allow for neglection of forces for the structural system Table 6.3.

Table 6.3, Auxiliary requirements for the Oostsluisbruggen.

Category	Requirements
Stiffness	• The maximal allowable deflection perpendicular to the driving direction at both abutments is 5 mm (EN 1993-2 7.8.2). • For midspan deflection of an FRP deck a limit is imposed of l/250 (CUR96 7.2).
Accessories	• Between the road deck and cycle path or structural element a kerb must be placed to prevent vehicles leaving the road surface. A guardrail must be included on both sides.
Lifespan	• The structure will be designed for a lifespan of 100 years.

6.5. Material properties

The following sections will contain the designs of the base and variants. This section will function as an overview of the materials used in the design calculations.

In general, two materials are used for the designs, steel and FRP. First, the material properties of steel will be displayed. For steel, the following material properties are used Table 6.4:

Table 6.4, Material properties of steel.

Quantity	Unit	Value	Unit
Tensile strength	f_{st}	355	MPa
Tensile modulus	E_{st}	210	GPa
Specific density	ρ_{st}	7800	kg/m^3

For FRP, a glass fiber bonded with polyester resin is used. The properties of the E-glass fibers and the biobased polyester are shown in Table 6.5 and Table 6.6 respectively. This is combined into a unidirectional (UD) ply, see Table 6.7, where a combination of plies will create the used laminate.

Table 6.5, Material properties of E-Glass.

Quantity	Unit	Value	Unit
Tensile modulus	E_f	74	GPa
Shear modulus	G_f	30	GPa
Poisson's ratio	ν_f	0.25	[-]
Specific density	ρ_f	7800	kg/m^3

Table 6.6, Material properties of biobased polyester

Quantity	Unit	Value	Unit
Tensile modulus	E_r	9.5	GPa
Shear modulus	G_r	1.4	GPa
Poisson's ratio	ν_r	0.4	[-]
Specific density	ρ_r	1200	kg/m^3

Table 6.7, Combined material properties of UD E-Glass with biobased polyester.

Quantity	Unit	Formula	Value	Unit
Fiber volume fraction	V_f	[-]	0.5	[-]
	ξ	[-]	1	[-]
	ξ_2	[-]	2	[-]
	ξ_G	[-]	1	[-]
	η_2	$\frac{E_f}{E_r} - 1 / \frac{E_f}{E_r} + \xi_2$	0.87	[-]
	η_G	$\frac{G_f}{G_r} - 1 / \frac{G_f}{G_r} + \xi_G$	0.91	[-]
In axis tensile modulus	E_1	$E_r + (E_f - E_r) * V_f$	38.75	GPa
Out of axis tensile modulus	E_2	$1 + \xi_2 * \eta_2 * V_f / 1 - \eta_2 * V_f * E_r$	11.59	GPa
Shear modulus	G_{12}	$1 + \xi_G * \eta_G * V_f / 1 - \eta_2 * V_f * G_r$	3.61	GPa
Poisson's ratio	ν_{12}	$\nu_r + (\nu_r - \nu_f) * V_f$	0.325	[-]
Specific density	ρ	$V_f * \rho_f + (1 - V_f) * \rho_r$	1900	kg/m^3
Variance coefficient [103]	V_x	[-]	0.05	[-]

The UD-plies are combined in layups to create the laminates. Three different layups have been used, the composition of the layups is given in Table 6.8. The three laminates have been chosen for different use cases. The flange layup is optimized for tension strength and the web layup is optimized for shear strength. The road layup is a combination between both layups, where more fibers are required to spread to load of the wheels.

Table 6.8, Layups used for the Oostsluisbruggen variants

Quantity	Road layup	Flange layup	Web layup
Layup	50%	62.5%	25%
	16.67%	12.5%	25%
	33.33%	25%	50%

To then calculate the laminate properties, classical laminate theory (CLT) is used. The values used during the calculations are scaled by the thickness of the laminate, the resulting combined characteristics only variable are the layups given in Table 6.8. The resulting material characteristics is given in Table 6.9, where for the intermediate results a laminate thickness of 16 mm is used.

It is important to highlight that not every laminate will be designed with a thickness of 16 mm. The minimal thickness of each laminate will be 12 mm, to prevent failure on non-tested failure mechanisms. More specifically, the following mechanism might require additional considerations:

- Face sheet wrinkling.
- Core indentation.
- Core punching failure.

Table 6.9, Application of CLT for the homogenized material properties for the Oostsluisbruggen variants.

Quantity	Unit	Formula	Road layup	Flange layup	Web layup	Unit
Thickness	t	[-]	16	16	16	mm
Normal force – strain matrix	A_{11}	$\sum_{i=1}^{n}(z_i - z_{i-1}) * E_i$	4.52E+05	4.99E+05	3.58E+05	N/mm
	A_{22}		3.02E+05	2.75E+05	3.58E+05	N/mm
	A_{12}		1.00E+05	0.91E+05	1.20E+05	N/mm
	A_{66}		1.00E+05	0.90E+05	1.20E+05	N/mm
Combined in axis tensile modulus	E_1	$\frac{1}{t} * \frac{A_{11} - A_{12}^2}{A_{22}}$	26.2	29.3	19.9	GPa
Combined of axis tensile modulus	E_2	$\frac{1}{t} * \frac{A_{11} - A_{12}^2}{A_{22}}$	17.5	16.2	19.9	GPa
Combined shear modulus	G_{12}	$\frac{1}{t} * A_{66}$	6.25	5.63	7.5	GPa
Maximum linear strain	ε_{max}	[-]	1.4%	1.4%	1.4%	[-]
Maximum shear strain	γ_{max}	[-]	2.4%	2.4%	2.4%	[-]
In axis characteristic stress limit	$\sigma_{1,k}$	$\varepsilon_{max} * E_1$	367	410	278	MPa
In axis characteristic stress limit	$\sigma_{2,k}$	$\varepsilon_{max} * E_2$	245	226	278	MPa
In axis characteristic stress limit	$\tau_{12,k}$	$\gamma_{max} * G_{12}$	150	135	180	MPa

When an FRP material is used in section where strong concentrated loads perpendicular to the laminate plane are expected, a sandwich panel is implemented. For more detail see section 4.1. Balsa is used for the core material. Notable for balsa is its high coefficient of variation, V_x. The result of a high variation are lower design structural characteristics. All material properties of balsa are given in Table 6.10.

Table 6.10, Material properties high density (HD) Balsa.

Quantity	Unit	Value	Unit
Specific density	ρ_{balsa}	285	kg/m^3
Tensile modulus in compression	$E_{x,c}$	4428	MPa
Tensile modulus in tension	$E_{x,t}$	6604	MPa
Elastic modulus in bending [104]	E_z	1800	MPa
Shear modulus	G	362	MPa
Tensile strength in compression	$f_{x,c}$	22	MPa
Tensile strength in tension	$f_{x,t}$	18.3	MPa
Shear strength	f_{xy}	5.2	MPa
Variation coefficient [105]	V_x	0.3	[-]

When applying FRP in designs, certain FRP specific partial factors need to be considered. In general, the partial factors are given for certain environments or design checks. A notable exception for this is the temperature conversion factor, which must be calculated with Formula 6.1 for a balsa core. For the laminate where the fibers or the matrix is the governing material property, Formula 6.2 or Formula 6.3 must be considered respectively. Finaly, the conversion factors are combined, as performed in Formula 6.4.

$$\eta_{ct,balsa} = \min\left(1.0 - \left(\frac{0.2}{\rho} + 0.004\right) * (T_s - 20); 1\right) \tag{6.1}$$

$$\eta_{ct,fiber} = \min\left(1.0 - 0.8 * \frac{T_s - 20}{T_g - 20}; 1\right) \tag{6.2}$$

$$\eta_{ct.matrix} = \min\left(1.0 - 0.25 * \frac{T_s - 20}{T_g - 20}; 1\right) \tag{6.3}$$

$$\eta_c = \eta_{ct} * \eta_{cm} \tag{6.4}$$

The material partial factors are given in Table 6.11.

Table 6.11, Partial factors for materials used in the Oostsluisbruggen variants.

Quantity	Unit	Balsa	GFRP			
Sun / shade	[-]	[-]	Shade	Shade	Sun	Sun
Material property dominant	[-]	[-]	fibers	matrix	fibers	matrix
Partial factor for material property	γ_m	1.51	1.07	1.07	1.07	1.07
Temperature conversion factor	η_{ct}	1	0.87	0.96	0.87	0.58
Moisture conversion factor	η_{cm}	1	0.6	0.6	0.6	0.6
Combined conversion factor	η_c	1	0.523	0.58	0.52	0.35

In addition to the material partial factors, a partial factor is introduced for uncertainty of the resistance model. This factor varies between resistance model, as the name implies. The partial factors are given in Table 6.12.

Table 6.12, Partial factors for resistance models used in the Oostsluisbruggen variants.

Quantity	Unit	Laminate material failure	Core material failure	Sandwich panel global buckling
Partial factor for resistance model	γ_{rd}	1.4	1.5	1.4

6.6. LCA data

For determining the environmental costs of the project, the following values will be used. The main database is the Dutch national milieu database (NMD). The drawback of the NMD is that FRP is not well established for civil engineering purposes in this database. Therefore, some values are appended from different sources, or specific manufacturers if available. A summary of the sources for the data is given in Table 6.13.

For the end of life for each material, the following assumption is made:

- For steel, the most efficient method is to recycle the material. Current steel processing methods already consist of at least 35% reused steel. Steel remelting also allows for the use of hydrogen furnaces, which produces far fewer emissions [106].
- For wood, the material is considered circular as the emissions embedded in the material are equally consumed when the trees grow, not adding, not diminishing the resources. The best method for recycling is to process the wood into pallets, which can be used to generate electricity.
- For GFRP, section 4.2. goes into more detail about recycling. The current applied method on a larger scale is thermal recycling. This allows for the reuse of the embedded energy and recovery of the fibers, albeit with lower tensile strength.

Table 6.13, Sources for the ECI values used for the Oostsluisbruggen evaluation.

Source	Material	Detailed description	End of life	Note
NMD [107]	Steel	Steel construction profiles (HEA/HEB/HEM/IPE/UNP).	Recycled (remelted)	
	GFRP laminate	FRP for lock gates, European origin.	Thermal recycling	Only for phase C and D
	Hard wood	Deck planks, South American origin.	Thermal recycling	Phase B envelops the renewal necessary, for the lifespan is not 100 years
	Paint	Paint systems for steel structures.	Discarded	Also used for FRP
	Galvanization	Galvanization of steel structures	Discarded	Assumed lifespan of 100 years, in combination with paint
Ecoinvent [108]	Glass fibers	Glass fibers.	Thermal recycling	
	Resin infusion	Vacuum assisted resin infusion of glass fibers.	Thermal recycling	
Manufacturer	Balsa [109]	Baltek SBC & SB balsa wood core material.	Thermal recycling	
	Biobased polyester resin [110]	Polynt 60% recycled polyester resin.	Thermal recycling	

Most of the values are directly derived from the source, depicted by no additional note in the table above. For GFRP laminate this is different, for the A1 to A5 values are calculated by combining the values for the fibers, resin and infusion scaled by weight. For C and D, these values do not account for the complete dismantlement of an FRP structure. Therefore, the values from an FRP lock gate are used to account for this absence. The drawback is that these values will be conservative due to the more difficult nature of removing a lock gate compared to a bridge.

For the emission during the construction phase for GFRP, the values for fibers and resin are scaled by weight fraction and combined. Glass fibers weight fraction is 68% and for the polyester is 32%.

For hardwood, the lifespan is increased from 30 to 100 years by increasing the environmental impact of maintenance and replacement (stage B) with twice the environmental impact of the entire lifecycle for 30 years.

All ECI values are displayed in Table 6.14.

Table 6.14, ECI values used in the Oostsluisbruggen variants evaluation.

Material	Unit	A1-A3	A4-A5	B	C	D	Sum	Lifespan [years]
Glass fibers	€/kg	€ 0.21	€ 0.028	€ 0	€ 0	€ 0	€ 0.244	100
Biobased polyester resin	€/kg	€ 0.37	€ 0.028	€ 0	€ 0	unknown	€ 0.4	100
Resin infusion	€/kg	€ 0.22	€ 0	€ 0	€ 0	€ 0	€ 0.22	100
GFRP laminate	€/kg	€ 0.33	€ 0.028	€ 0	€ 0.19	€ - 0.074	€ 0.446	100
Balsa	€/kg	€ -0.15	€ 0.028	€ 0	€ 0	€ 0.00	€ 0.129	100
Steel	€/kg	€ 0.116	€ 0.059	€ 0	€ 0.053	€ - 0.005	€ 0.223	100
Hardwood	€/kg	€ 0.099	€ 0	€ 0.198	€ 0.005	€ - 0.023	€ 0.297	100
Steel galvanization	€/m^2	€ 0.691	€ 0	€ 1.677	€ 0	€ 0	€ 2.367	100
Paint	€/m^2	€ 0.605	€ 0.206	€ 1.049	€ 1.42	€ 0	€ 3.28	100

7. Foot and cycle path design variations

Based on the program of requirements, 2 design variants for the foot and cycle path (FCP) developed. Next to these two variants, a base variant is included for reference. For each variant, the general considerations will be highlighted first, after which a design sketch will be displayed. From this, defining calculations will be highlighted including the following unity checks. All checks detailed in section 6 are performed and are included in Appendix II, Appendix III, and Appendix IV.

7.1. Design variants

7.1.1. Base variant

The base variant is a steel H-beam, support steel I-beams which support a wood deck. The deck structure, I-beam with the wood deck, is taken from the current bridge structure. These elements are not tested for structural performance. The steel H-beam is cantilevered from the side of the main beam. The connection between the two beams has not been designed.

To optimize the steel beam for sustainability, a standardized H-section has been used. This increases the chances of the use of a refurbished beam and the ability to reuse the beam after the lifespan of the bridge. The downside is that the beam is over dimensioned, as there is no ability to taper the section towards the edge. An overview of the cross section is given in Figure 7.1.

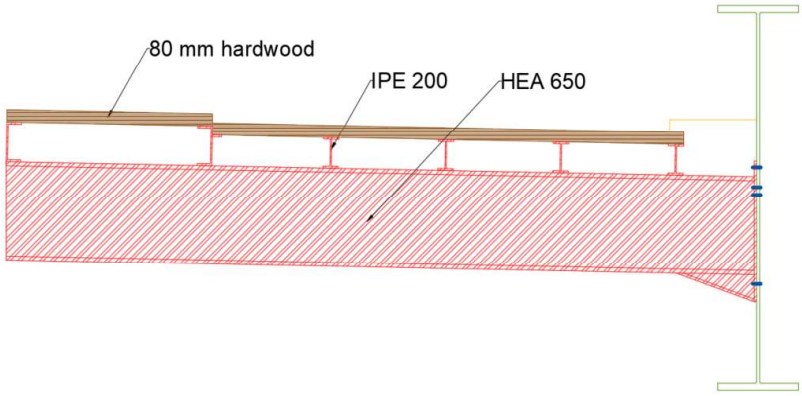

Figure 7.1, Cross section FCP base variant, steel crossbeam with wooden deck.

In case the crossbeam, or even the stringers can be reused, only the wooden deck will be replaced. In that case, the cross section of the crossbeam will differ from the provided cross section, as this current crossbeam does not have constant cross section.

7.1.1.1. Structural checks

Again, the deck of the base variant is not tested for structural performance. The crossbeam in the case of complete redesign is the same as for variant 1. See section 7.1.2.2. for the structural performance of the crossbeam.

7.1.1.2. ECI score

The materials and quantities used for the design of both sides of the FCP deck are given in Table 7.1.

Table 7.1, Materials and quantities of FCP base variant.

Material	Amount	Unit
Wood	21816	kg
Steel	15427	kg
Galvanization	376.6	m^2
Paint	376.6	m^2

The governing ECI component for the first variant is the wooden deck, the entire breakup is given in Figure 7.2.

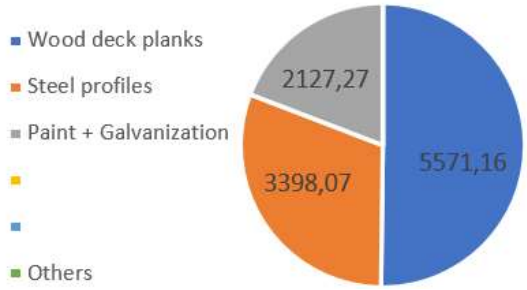

Figure 7.2, ECI Score FCP base variant, steel crossbeam with wooden deck.

7.1.2. Variant 1, steel crossbeam with FRP deck

The first design variant is highly inspired by the base or current design. This is done in accordance with the circular design principles, to explore the possibility of reusing elements of the current structure. The design is a steel H-beam with an FRP deck. The steel beam is cantilevered from the side of the main beam. The connection between the two beams has not been designed.

To optimize the steel beam for sustainability, a standardized I-section has been used. This increases the chances of the use of a refurbished beam and the ability to reuse the beam after the lifespan of the bridge. The downside is that the beam is over dimensioned, as there is no ability to taper the section towards the edge.

The FRP decks as simply supported between each crossbeam. This makes the design of the structure simple and enables the easy replaceability of each section. The FRP laminate will consist of 50% main direction fibers and 16.67% in every other direction, displayed in Table 7.2. This layup is chosen to ensure optimal use for main span resistance and provides resistance for local loads. The crossbeam is clamped to the main structure. An overview of the cross section is given in Figure 7.3.

Table 7.2, Layup FRP deck.

Orientation	Layup
0°	50%
90°	16.67%
±45°	33.33%

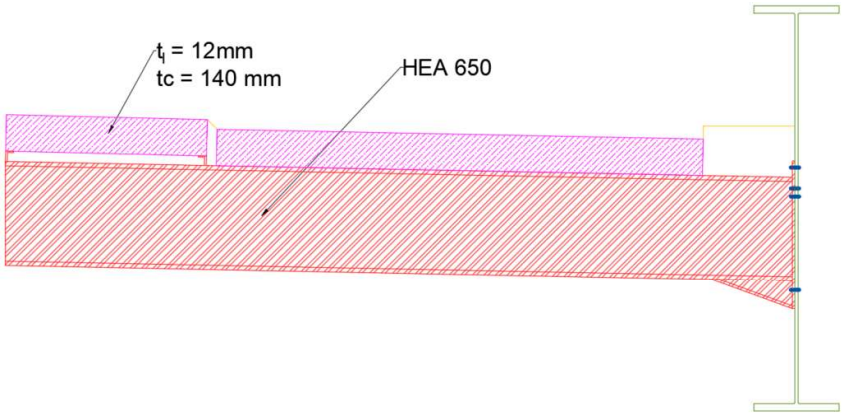

Figure 7.3, FCP variant 1, steel crossbeam with FRP deck.

7.1.2.1. Structural checks deck

For the deck of variant 1, the governing unity check is the shear capacity of the FRP sandwich panel. It is assumed that the panels will be simply supported between each crossbeam, with a span of 4.2 m. The governing load for the shear force and bending moments is the incidental vehicle. For the shear force, the heavier axle will be placed close to the crossbeam, where the other axle will contribute slightly to the total shear near the first axle. For the bending moments, the heavier axle is placed in the middle of the beam, the second axle will then not be placed on the same deck. The load case for the shear force and the bending moments are displayed in Figure 7.4 and Figure 7.5 respectively.

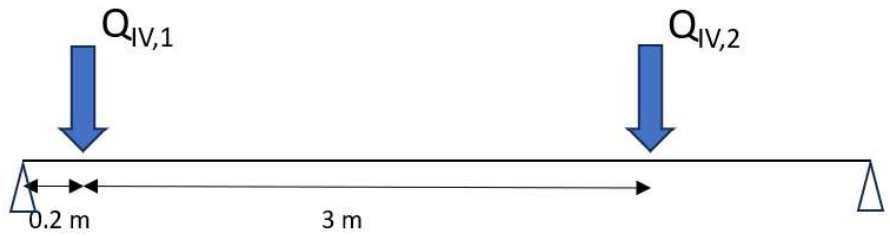

Figure 7.4, Load case for maximal shear in FCP deck.

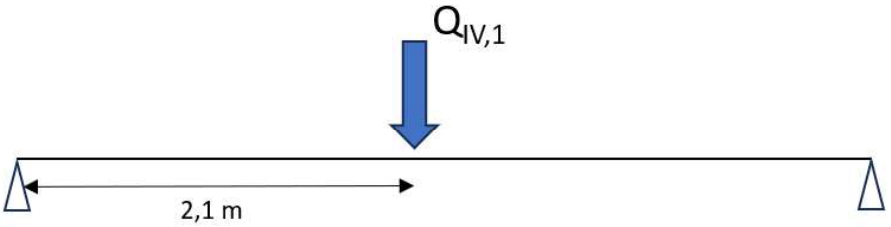

Figure 7.5, Load case for maximal bending moments in FCP deck.

The wheel load is distributed to a 20 by 20 cm square. The activated width of slab $w_{fcp} = 42.4$ cm, with the scheme shown in Figure 7.6.

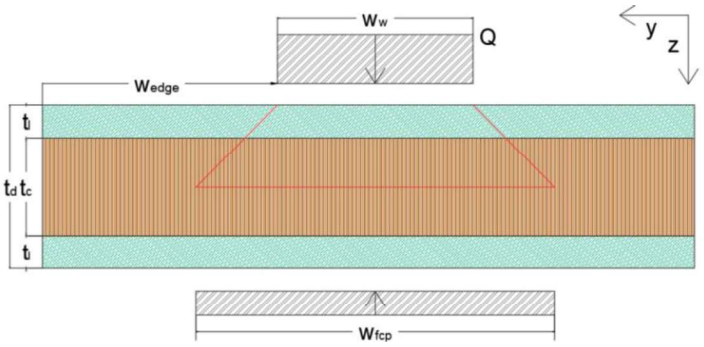

Figure 7.6, Concentrated load dispersion through deck.

The resulting shear force, $V_{IV} = 44.3$ kN, the resulting bending moments, $M_{IV} = 41.1$ kNm. The resulting shear and bending stresses are calculated with Formula 7.1 and Formula 7.2 respectively.

$$\tau_{Ed,deck} = \frac{V_{Ed,deck}}{A_{Core}} \quad (7.1)$$

$$\sigma_{Ed,cb,deck} = \frac{M_{Ed,deck}}{EI_{deck}} * E_{1,GFRP} * \frac{h_{deck}}{2} \quad (7.2)$$

Where:

$$V_{Ed,deck} = 1.2 * V_G + V_{deck} = 45.3\ kN$$

$$M_{Ed,deck} = 1.2 * M_G + M_{deck} = 42.2\ kNm$$

$$A_{Core} = 0.085 * m^2$$

$$EI_{deck} = 3.20 * 10^2\ kN * m^2$$

$$E_{1\_GFRP} = 26.2\ GPa$$

$$h_{deck} = 0.224\ m$$

The unity checks for the shear and bending stress is performed with Formula 7.3 and Formula 7.4 respectively.

$$u.c._{\tau,deck} = \frac{\tau_{Ed,\text{deck}}}{\frac{\eta_{c,balsa}}{\gamma_{m,balsa} * \gamma_{rd}}\tau_{c,k}} = 0.58 \quad (7.3)$$

$$u.c._{\sigma,deck} = \frac{\sigma_{Ed,\text{deck}}}{\frac{\eta_{c,GFRP}}{\gamma_{m,GFRP} * \gamma_{rd,GFRP}}\sigma_{1,k}} = 0.31 \quad (7.4)$$

For the partial factors used above, a fiber dominated failure criteria of a laminate in the sun was implemented. The partial factors for GFRP and the resistance model are given in Table 6.11 and Table 6.12 respectively. For the shear force, the thickness is increased to include more balsa, this is advantageous for the ECI score. For the bending moments, the limitation of the laminate thickness to 12 mm resulted in this unit check. The limitation to 12 mm is done to account for non-performed checks, see section 6.5. Considering the two unity checks, the possibility for further optimization is to increase the distance between the cross beams.

7.1.2.2. Structural checks crossbeam

For the crossbeam, the governing load is the incidental vehicle. For the resulting shear force and bending moments, the governing load case is displayed in Figure 7.7. Since the structural system is a cantilever beam, the position of the incidental vehicle is not relevant for the maximal shear force. For bending moments, the loads are placed as far from the hinge, to ensure maximum bending moments.

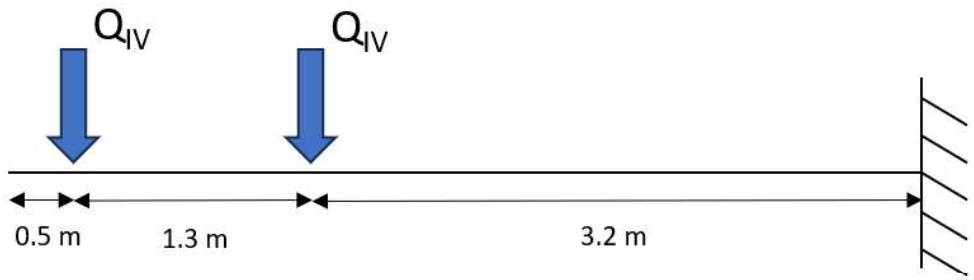

Figure 7.7, Load case for maximal shear and bending moments in crossbeam FCP.

The distance between crossbeam is 4.2 m, while the length of the vehicle is 3m, so the force Q_{IV} has been taken conservatively as the combined loads of the front and behind axle. The resulting bending moments are $M_{IV} = 450$ kNm. The resulting stresses are calculated with Formula 7.5.

$$\sigma_{Ed,cb,side} = \frac{M_{Ed,cb,side}}{EI_{cb,side}} * E_{steel} * \frac{h_{cb}}{2}$$

(7.5)

Where:

$$M_{Ed,cb,side} = 1.2 * M_G + M_{cb,side} = 545\ kNm$$

$$EI_{cb,side} = 3.62 * 10^5\ kN * m^2$$

$$E_{steel} = 210\ GPa$$

$$h_{cb} = 0.32\ m$$

To check the tensile strength of the crossbeam, the material properties of steel are reduced for lateral torsion instability, with $X_{lt} = 0.4$. The unity check is performed with Formula 7.6.

$$u.c._{cb,side} = \frac{\sigma_{Ed,cb,side}}{X_{lt} * f_{st}} = 0.71$$

(7.6)

7.1.2.3. Deflection

For the FCP deck plate, the deflection is checked. The same loading scheme is used as in section 7.1.2.1. The incidental vehicle is replaced by the service vehicle, with lower loads. The resulting deflection, $w_{midspan} = 6.1\ mm$. The deflection limit is $\frac{l}{250} = 16.8\ mm$. The unity check for deflection, $u.c._{deflecion} = 0.36$.

7.1.2.4. Unity checks

For variant 1, all unity checks are given in Table 7.3.

Table 7.3, Unity checks FCP variant 1, steel crossbeam with FRP deck.

Description	Abbreviation	Value
Displacement of crossbeam at abutment	$u.c._{w,threshold}$	0.07
Displacement of deck in between crossbeam, in middle of span	$u.c._{w,midspan}$	0.36
Shear force in deck core	$u.c._{deck,\tau}$	0.58
Tensile stress in deck laminate	$u.c._{deck,\sigma\_l}$	0.31
Tensile stress in deck core	$u.c._{deck,\sigma\_c}$	0.29
Shear force in cross beam	$u.c._{cb,\tau}$	0.06
Tensile stress in cross beam	$u.c._{cb\_\sigma}$	0.70

As mentioned previously, this variant can be further optimized. Since all unity checks for the deck are relatively low, the distance between crossbeam is can be increased. For the crossbeam this is not the case. The choice has been made to use standardized profiles. No smaller standardized profile passes all the structural checks. When the distance between crossbeam is increased, it is expected the load on the crossbeam will increase. Next to this, the further the crossbeams are apart, the less support the crossbeam receives for flexural buckling.

7.1.2.5. ECI score

The materials and quantities used for the design of both sides of the FCP deck are given in Table 7.4.

Table 7.4, Materials and quantities of FCP variant 1, steel crossbeam with FRP deck.

Material	Amount	Unit
GFRP laminate	11500	kg
Balsa	14393	Kg
Steel	8517	kg
Galvanization	144	m^2
Paint	528	m^2

The governing ECI component for the first variant is the fiberglass with biobased polyester, the entire breakup is given in Figure 7.8.

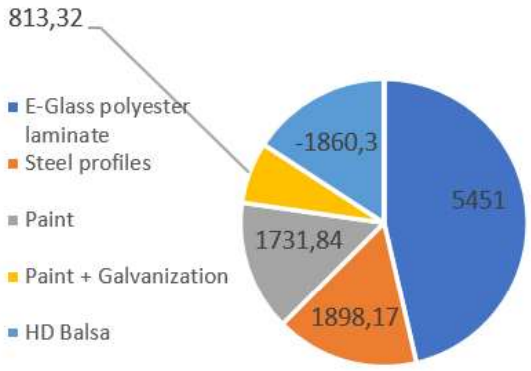

Figure 7.8, ECI score FCP variant 1, steel crossbeam with FRP deck.

7.1.3. Variant 2, FRP deck with FRP support

The second variant utilizes the free forming properties of FRP. The deck is also made of FRP, and the support structure is, unlike the first variant, also made of FRP. This also changes the main carrying direction of the deck. The support is placed at $3/10^{th}$ of the span. This has been done after an optimalisation analysis, which is provided in Appendix I. This parameter study limited the position of the support between $1/5^{th}$ and $2/5^{th}$ of the span. Compared to the most unfavorable situation, a reduction of 16% for the bending moments and 14% for the horizontal support load was achieved.

The supports are not continuous, with a support with the width of 0.5 meters every 1.58 meters. This results in a 2d load path, which is accounted for by considering bidirectional bending moments and deflection. This is a conservative estimate of the total bending moments, as it applies the full load in both directions, where the stiffness will determine the load path. The choice for this conservative approach has been made to simplify the calculations.

Another effect of this design is that in case of a ship collision, some of the energy of the ship will be dissipated. This effect will be considered on the main structure. When this happens, this element is expected to fail, but is an effective method of dissipating the energy of a collision due to the replaceable nature of the deck. The laminate layups are given for the deck and the support in Table 7.5 and Table 7.6 respectively. An overview of the cross section is given in Figure 7.9.

Table 7.5, Layup FRP deck.

Orientation	Layup
0°	50%
90°	16.67%
±45°	33.33%

Table 7.6, Layup FRP support.

Orientation	Layup
0°	56%
90°	22%
±45°	22%

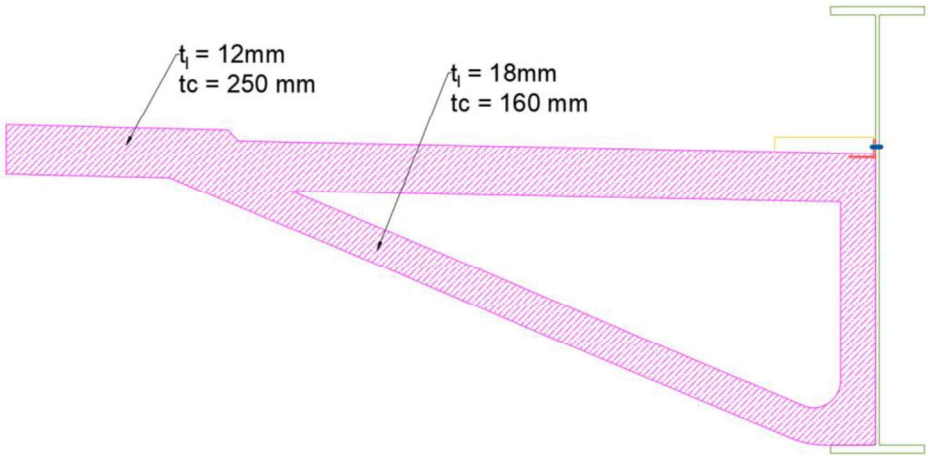

Figure 7.9, FCP variant 2, FRP deck and support (full FRP).

7.1.3.1. Structural checks deck

For this variant, two load cases are of note. The first load case is where both wheels of the vehicle is placed between the support and the main beams, as displayed in Figure 7.10. The maximal bending moments occurs at the main beam, as outlined in the parameter study in Annex I. For the shear, this load case is relevant. The calculations result in a low unity check, which is given further in this section. The calculations are like the first variant, see section 7.1.2.

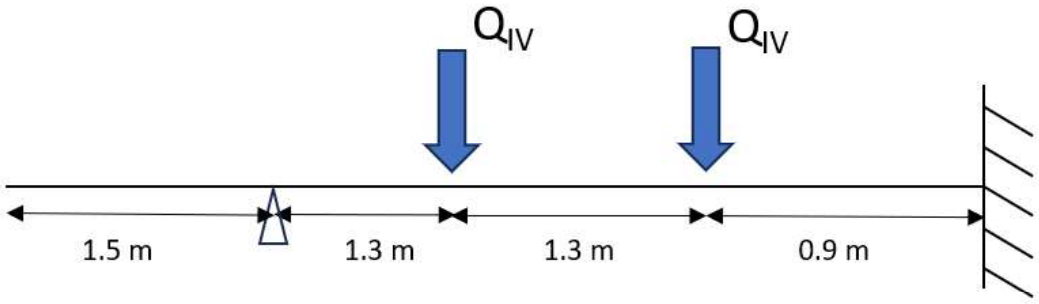

Figure 7.10, Load case for maximal shear and bending moments in deck FCP.

The second load case is introduced since the support are non-continuous, therefore a 2d load path is introduced. Both the directions of the load are considered. A schematic for this load path is given in Figure 7.11. The maximal bending moments stresses in the y direction do not have to be combined with the x direction, as these do not occur in the same point. For the combined stresses, the stresses in the middle of the span between the supports and the main beams is considered. For the bending moments, a simply supported cross section is considered. Similarly to the previous deck variant, the load is spread over a larger width, as shown in Figure 7.6. This load case is governing.

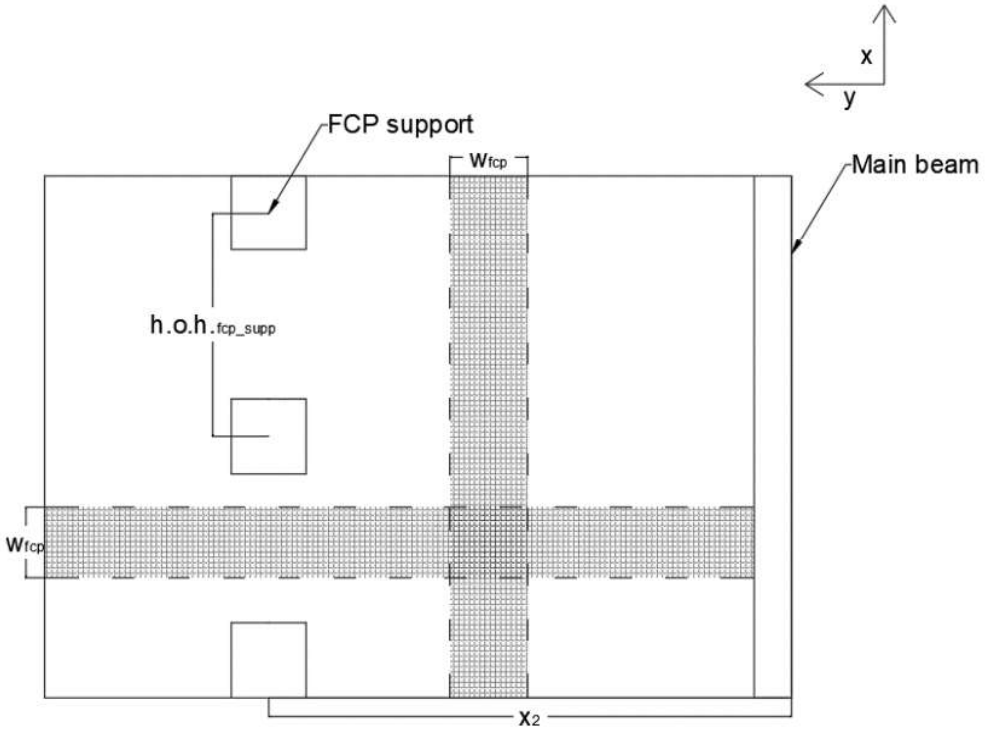

Figure 7.11, 2D load case FCP.

The resulting bending moments, $M_{AV,y} = 45.7$ kNm and $M_{AV,x} = 15.8$ kNm in y and x direction respectively. The resulting bending stresses in x and y direction are calculated with Formula 7.7 and Formula 7.8 respectively.

$$\sigma_{Ed,deck,x} = \frac{M_{Ed,deck,x}}{EI_{deck,x}} * E_{2,GFRP} * \frac{h_{deck}}{2} \quad (7.7)$$

$$\sigma_{Ed,deck,y} = \frac{M_{Ed,deck,y}}{EI_{deck,y}} * E_{1,GFRP} * \frac{h_{deck}}{2} \quad (7.8)$$

Where:

$$M_{Ed,deck,x} = 1.2 * M_G + M_{cb,side} = 46.7\ kNm$$

$$M_{Ed,deck,y} = 1.2 * M_G + M_{cb,side} = 16.0\ kNm$$

$$EI_{deck,x} = 5.56 * 10^3\ kN * m^2$$

$$EI_{deck,y} = 3.86 * 10^2\ kN * m^2$$

$$E_{1\_GFRP} = 26.2\ GPa$$

$$E_{2\_GFRP} = 17.5\ GPa$$

$$h_{deck} = 0.274\ m$$

The unity check for the shear, $u.c._{\tau,deck} = 0.35$, and for bending stress is calculated with Formula 7.9. An additional tension force is added to the unity check the tensile stress, as this introduced because of the inclination in the support.

$$u.c._{\sigma,deck} = \frac{\sigma_{Ed,deck,x}}{\frac{\eta_{c,GFRP}}{\gamma_{m,GFRP} * \gamma_{rd,GFRP}}\sigma_{2,k}} + \frac{\sigma_{Ed,deck,y}}{\frac{\eta_{c,GFRP}}{\gamma_{m,GFRP} * \gamma_{rd,GFRP}}\sigma_{1,k}} + \frac{\sigma_{Ed,deck,tension}}{\frac{\eta_{c,GFRP}}{\gamma_{m,GFRP} * \gamma_{rd,GFRP}}\sigma_{1,k}} = 0.74 \quad (7.9)$$

For the combined unity check shown above, the Tsai-Hill failure criteria have been implemented. For the partial factors used above, a fiber dominated failure criteria of a laminate in the sun was implemented. Next to this, the full wheel load is used to compute the stresses in transverse and longitudinal direction. Both assumptions are conservative, more detailed design will allow for further optimization.

The partial factors for GFRP and the resistance model are given in Table 6.11 and Table 6.12 respectively. The resulting unity check for the shear stress is relatively low. For the shear force, the thickness is increased to include more balsa, this is advantageous for the ECI score.

7.1.3.2. Structural checks deck support

For the supports of the deck, the maximal load case is where the reaction force is maximized in the scheme displayed in Figure 7.13. This occurs when the vehicle is centered around the support as displayed in Figure 7.12Figure 7.13. The position of the vehicle is determined in Appendix I.

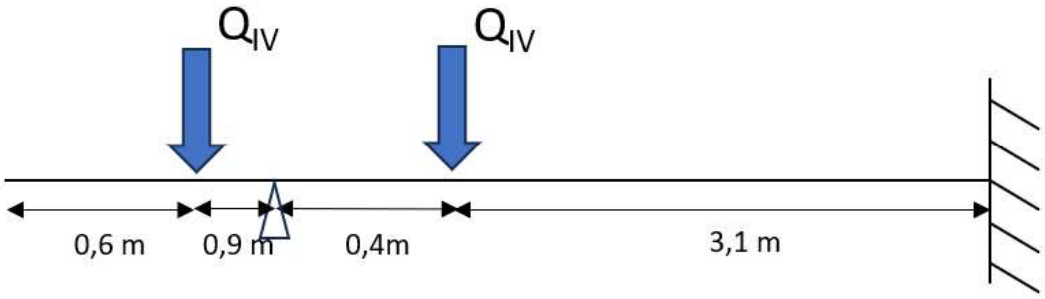

Figure 7.12, Load case for maximal normal force in FCP support.

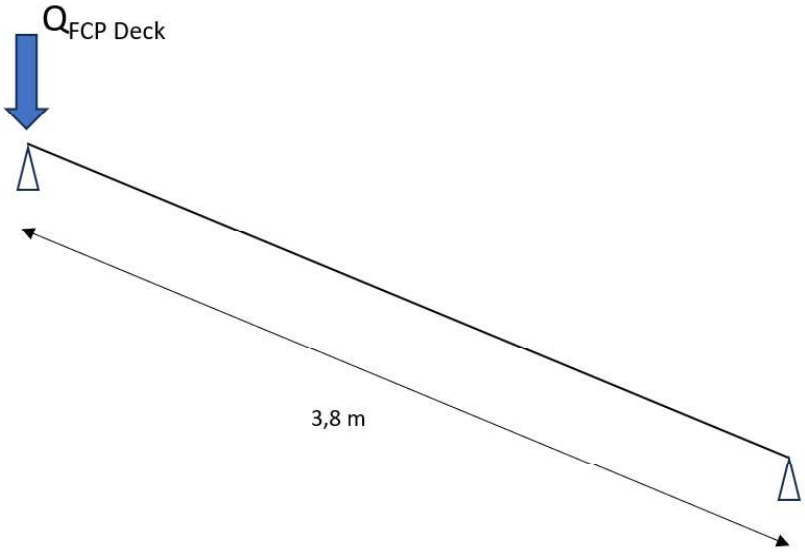

Figure 7.13, Load case for FCP support.

The support is tested for buckling. Where Formula 7.10 to 7.16 determine the buckling resistance of an FRP sandwich panel.

$$D_f = \frac{\eta_{c,GFRP} * E_{1,GFRP} * t_{l,GFRP}^3}{12}$$

(7.10)

$$D_0 = \frac{\eta_{c,GFRP} * E_{1,GFRP} * t_{l,GFRP} * \left(t_{core} + t_{l,GFRP}\right)^2}{2}$$

(7.11)

$$D_c = \frac{\eta_{c,balsa} * E_{balsa} * t_{core}^3}{12}$$

(7.12)

$$D_k = 2 * D_f + D_0 + D_c$$

(7.13)

$$P_{cb} = \frac{1}{\gamma_{m,GFRP} * \gamma_{rd}} * \frac{\pi^2 * D_k}{l_{cr}^2}$$

(7.14)

$$P_{cs} = \frac{\eta_{c,balsa}}{\gamma_{m,balsa} * \gamma_{rd}} * \frac{G_{balsa} * \left(t_{core} + t_{l,GFRP}\right)^2}{t_{core}}$$

(7.15)

$$P_c = \frac{P_{cb} * P_{cs}}{P_{cb} + P_{cs}}$$

(7.16)

Where:

$$E_{1,GFRP} = 27.5\ GPa$$

$$G_{balsa} = 0.15\ GPa$$

$$t_{l,GFRP} = 18\ mm$$

$$t_{core} = 160\ mm$$

$$l_{cr} = l_{supp} = 3.8\ m$$

For the partial factors used above, a matrix dominated failure criteria of a laminate in the shade was implemented. The final unity check is performed in Formula 7.17.

$$u.c._{supp} = \frac{N_{Ed}}{P_c * w_{supp}} = 0.33$$

(7.17)

7.1.3.3. Deflection

For the FCP deck plate, the deflection is checked. The same loading scheme is used as in section 7.1.3.1. The incidental vehicle is replaced by the service vehicle, with lower loads. The total deflection is computed by combining the deflection in longitudinal and transverse direction. The resulting deflection, $w_{midspan} = 2.3\ mm$. The deflection limit is $\frac{l}{250} = 6.3\ mm$. The unity check for deflection, $u.c._{deflecion} = 0.36$.

7.1.3.4. Unity checks

For variant 2, all unity checks are given in Table 7.7.

Table 7.7, Unity checks FCP variant 2, full FRP.

Description	Abbreviation	Value
Displacement of crossbeam at abutment	$u.c._{w,threshold}$	0.4
Displacement of deck in between supports, in middle of span	$u.c._{w,midspan}$	0.36
Shear force in deck core	$u.c._{deck,\tau}$	0.35
Combined tensile stress in deck laminate (both directions)	$u.c._{deck,\sigma}$	0.74
Combined buckling and tensile resistance support	$u.c._{supp,comb}$	0.37

As mentioned previously, the combined unity check for the deck is conservative. The loads are not distributed in the principal directions, and the combined stresses are combined with the Tsai-Hill failure criteria. More detailed design will allow for further optimization. For the support, and increased thickness resulted in lower unity checks then optimal. This is advantageous for the ECI score but may allow for fewer supports. Further optimizations need to account for increased stresses in the deck if fewer supports are used.

7.1.3.5. ECI score

The materials and quantities used for the design of both sides of the FCP deck are given in Table 7.8.

Table 7.8, Materials and quantities of FCP variant 2, full FRP.

Material	Amount	Unit
GFRP laminate	15900	kg
Balsa	20935	kg
Paint	889	m^2

The governing ECI component for the first variant is the fiberglass with biobased polyester, the entire breakup is given in Figure 7.14.

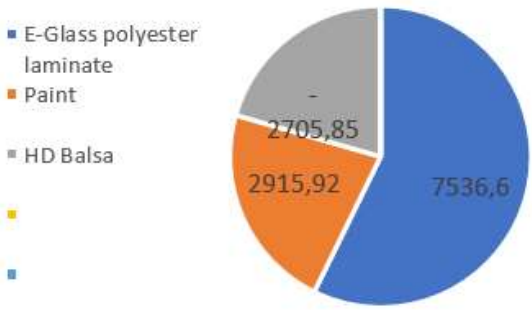

Figure 7.14, ECI score FCP variant 2, full FRP.

7.2. Comparison

For the comparison between the variants, the sustainability aspects mentioned in section 6 will be considered in addition to practicalities to the design.

7.2.1. Practicalities

The practicalities of each design are summarized in Table 7.9.

Table 7.9, Practicality comparison between FCP variants.

Variant	Positives	Negatives
1	+ Separated deck and support structure allow for easy replacement of element. + Design is comparable to current structure, giving insight into retrofitting options.	- Cantilever joint result in high forces, as for the large bending moments, but low joint height.
2	+ Support structure enables a large joint height, resulting in lower forces in the joint. + Support structure functions secondarily functions as ship collision barrier, dampening the forces for the main structure.	- Connected deck and support structure would not allow for separate element replacement.

7.2.2. Environmental impact

For the aspect environmental impact the ECI values are compared, in addition to the mass of each structure. The total ECI value of the variants are displayed in Figure 7.15, based on a 100-year lifespan.

The mass of each structure is given in Table 7.10. The reasons for including the mass are given in section 6.3, but to summarize:

- Prevent the need for renewing, or replacing the actuators, counterweight, moving arms.
    - This can have indirect influence on elements such as the actuator basement or foundation.
- Lower mass if favorable for transport and installation of the structure
- A lower mass structure requires less energy to rotate.
- A lower mass structure can rotate faster, given the moving arms can support the additional load.

Table 7.10, Mass comparison between FCP variants.

	Variant 1	Variant 2	Base variant
Mass [m. Ton]	34	37	37

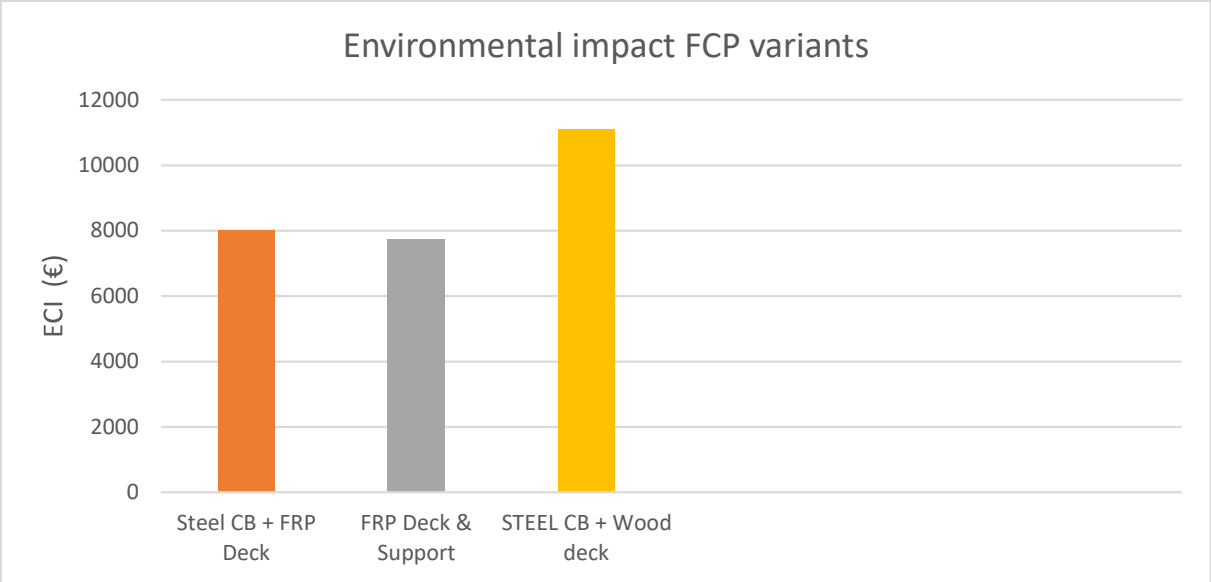

Figure 7.15, ECI comparison between FCP variants.

7.2.3. Circularity

For the aspect circularity the circular design principles were use during the design process. This section will go into each variants ability to incorporate circular design principles. The considerations are summarized in Table 7.11.

Table 7.11, Circularity comparison between FCP variants.

Variant	Positives	Negatives
1	+ Elements are easily separable, enabling end of life separation and reuse of individual elements. (FCP deck, and crossbeam) + Steel elements can be made by (mostly) recycled steel, can be recycled again at end of life. ++ Potential for reuse of steel elements, at start- and end of life. (Crossbeam) ++ Long lifespan of FRP enables reuse of elements after bridge lifespan.	- FRP is currently poorly recyclable. - Steel will require periodical maintenance
2	+ Elements are easily separable, enabling end of life separation and reuse of individual elements. (elements from main structure, and destructive deck from support removal) ++ Long lifespan of FRP enables reuse of elements after bridge lifespan.	- FRP is currently poorly recyclable. - The deck must be destructively removed from the support if only this element will be reused at end of life.

8. Road deck and main structure design variants

Four variants were conceived for the main structure (MS) in combination with the road deck. For each variant, the general considerations will be highlighted first, after which a design sketch will be displayed. From this, defining calculations will be highlighted including the following unity checks. All checks detailed in section 6 are performed and are included in Appendix V, Appendix VI, Appendix VII, Appendix VIII and Appendix XI.

8.1. Design variants

8.1.1. Base variant, modern adaptation on current structure

The base variant of the main structure is the exact same as the current structure, or the same deck system supported by the new crossbeams used in variant 1. It consists of a wooden deck on steel stringers, supported with steel crossbeams between steel main girders. The main steel girders keep the same cross section over the length of the structure. This is done so at the end of life of the structure, reuse of this profile is more likely.

The crossbeam is responsible for carrying the road deck and functions as a stiffener in case of a ship collision. For these functions, the beam has a constant cross section, with a stiffener at each main girder. A new cross section is depicted in Figure 8.1.

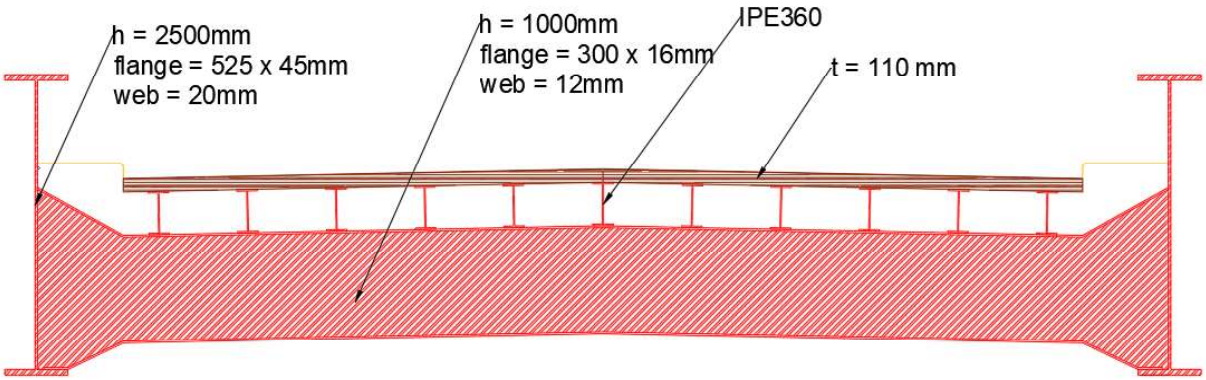

Figure 8.1, Cross section MS base variant, steel main- and crossbeam with wooden deck.

8.1.1.1. Structural checks

The design checks for this variant are based on variant 1, where the wooden deck is replaced by an FRP deck. Section 8.1.3. will detail the checks performed for both. The decks are not checked as this is a direct copy of the current deck. The mass of the deck is comparable to the FRP deck (0.5% mass difference compared to mass of the entire structure). The structural system will be the same as for the first variant. For these reasons, no additional checks are performed.

8.1.1.2. ECI score

The materials and quantities used in the design are given in Table 8.1.

Table 8.1, Materials and quantities of MS base variant, steel main- and crossbeams with wooden deck.

Material	Amount	Unit
Steel	103 000	kg
Galvanization	1 101	m^2
Paint	1 101	m^2

The main contributing factor for the ECI are the steel profiles, the entire breakdown is given in Figure 8.3.

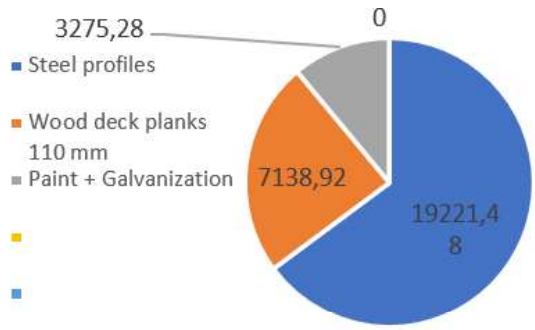

Figure 8.2, ECI score MS base variant, steel cross- and main beam with wooden deck.

8.1.2. Steel orthotropic deck variant, modern adaptation on current structure

The modern base variant of the main structure is a steel orthotropic deck, supported with steel crossbeams between steel main girders. The variant is a close resemblance to the current structure. The main steel girders keep the same cross section over the length of the structure. This is done so at the end of life of the structure, reuse of this profile is more likely.

The crossbeam is responsible for carrying the road deck and functions as a stiffener in case of a ship collision. For these functions, the beam has a constant cross section, with a stiffener at each main girder. A downside of an orthotropic deck is the complicated metalwork required for the troughs. This increases man hours, waste and reduces the likelihood of reuse at the end of life.

The road deck is the same design as from a different case study, the Amaliabrug in Gouda. This reduces the level of complexity for this study and ensures that the base variant can be used as comparison design for a modern bridge design. For this reason, the deck is not tested for structural performance. An overview of the cross section is given in Figure 8.3.

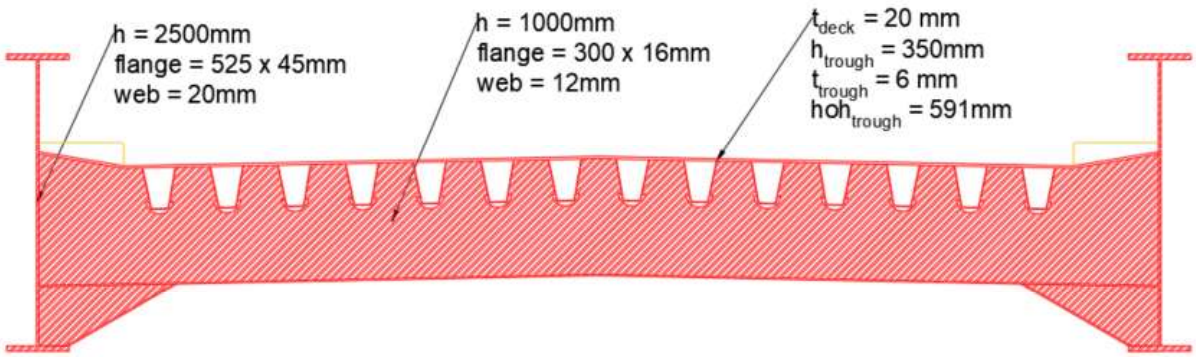

Figure 8.3, Cross section MS base variant, steel main- and crossbeam and orthotropic deck.

8.1.2.1. Structural checks

The design checks for this variant are based on variant 1, where the steel deck is replaced by an FRP deck. Section 8.1.3. will detail the checks performed for both. In summary, the steel orthotropic deck is not checked for structural performance. The unity checks for the crossbeam due to BM1 are $u.c._{\tau,cb} = 0.39$ and $u.c._{\sigma,cb} = 0.97$. For the main beam the unity checks due to BM1 are $u.c._{\tau,mb} = 0.44$ and $u.c._{\sigma,mb} = 0.84$. Auxiliary checks result in $u.c._{\sigma,sc,loc} = 0.75$ for local resistance to ship collision and $u.c._{\sigma,open} = 0.57$ for opened structure.

8.1.2.2. Unity checks

For the base variant with a steel orthotropic deck, all unity checks are given in Table 8.2.

Table 8.2, Unity checks MS base variant, steel main- and crossbeams and orthotropic deck.

Description	Abbreviation	Value
Shear force in crossbeam	$u.c._{cb,\tau}$	0.39
Tensile stress in crossbeam	$u.c._{cb,\sigma}$	0.97
Shear force in main beam	$u.c._{mb,\tau}$	0.44
Tensile stress in main beam	$u.c._{mb,\sigma}$	0.84
Shear force in main beam flange due to ship collision	$u.c._{mb,\tau,sc}$	0.10
Local tensile stress in main beam flange due to ship collision	$u.c._{mb,\sigma,sc,loc}$	0.75
Global tensile stress in main beam flange due to ship collision	$u.c._{mb,\sigma,sc,loc}$	0.06
Tensile stress in main beam in opened position	$u.c._{mb,\sigma,opened}$	0.57

From the unity checks it can be concluded that the tested elements are optimized. Both the crossbeam as the main beam highest unity checks is above 0.84. The only element not checked is the deck, it is possible this element can be further optimized.

8.1.2.3. ECI score

Due to the entire structure consisting of steel, the ECI breakdown does not reveal much new information. The materials and quantities used in the design are given in Table 8.3.

Table 8.3, Materials and quantities of MS base variant, steel main- and crossbeams and orthotropic deck.

Material	Amount	Unit
Steel	103 000	kg
Galvanization	1 101	m^2
Paint	1 101	m^2

The most steel is used for the main beams, the entire breakup is given in Figure 8.4.

Figure 8.4, ECI score MS base variant, steel cross- and main beam and orthotropic deck.

8.1.3. Variant 1, steel main- and crossbeams, FRP deck

The first variant is a close resemblance to the current structure. Following the circular design principles the structure is designed such that the variant can be adopted to the current structure. The structure consists of two steel main girders, bridged by steel crossbeams, on which the deck rests. The main steel girders keep the same cross section over the length of the structure. This is done so at the end of life of the structure, reuse of this profile is more likely.

The crossbeam is responsible for carrying the road deck and functions as a stiffener in case of a ship collision. For these functions, the beam has a constant cross section, with a stiffener at each main girder. The constant cross section increases the likelihood of reusability at the end of life of the structure.

The road deck is a simple design for this variant, being simply supported between two crossbeams. This results in the main load carrying direction being the same direction as the traffic flow, resulting in a slimmer deck. The laminate layup is given in Table 8.4, an overview of the cross section is given in Figure 8.5.

Table 8.4, Layup FRP deck.

Orientation	Layup
0°	50%
90°	16.67%
±45°	33.33%

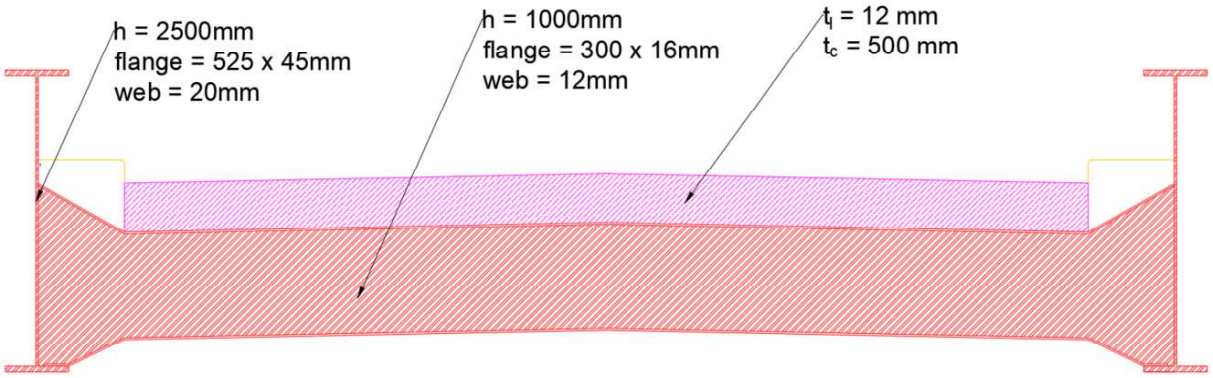

Figure 8.5, Cross section MS variant 1, steel main- and crossbeam with FRP deck.

8.1.3.1. Structural checks deck

The deck is an FRP sandwich panel simply supported between crossbeams. The load case applied to the deck is BM1. A single wheel width is considered, following the scheme displayed in Figure 8.6.

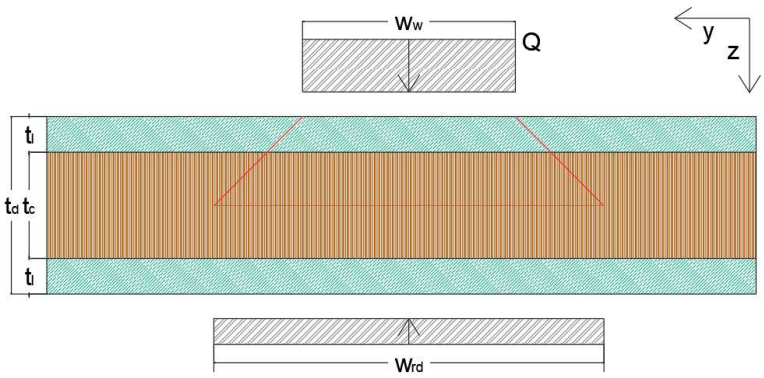

Figure 8.6, Concentrated load dispersion through deck.

The BM1 load case is applied twice, for the maximization of the shear force and bending moments. The load cases for the shear force and the bending moments are displayed in Figure 8.7 and Figure 8.8 respectively.

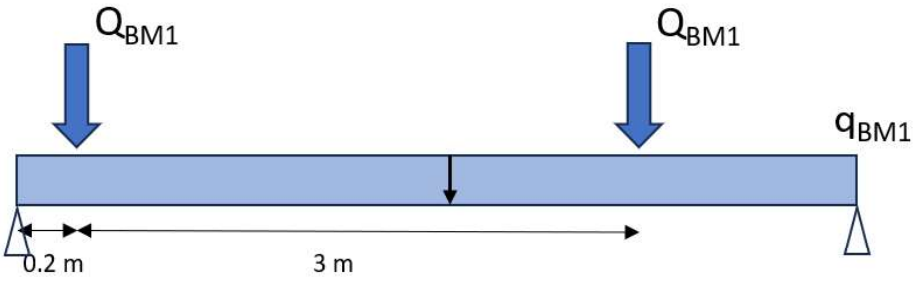

Figure 8.7, Load case for maximal shear in deck MS.

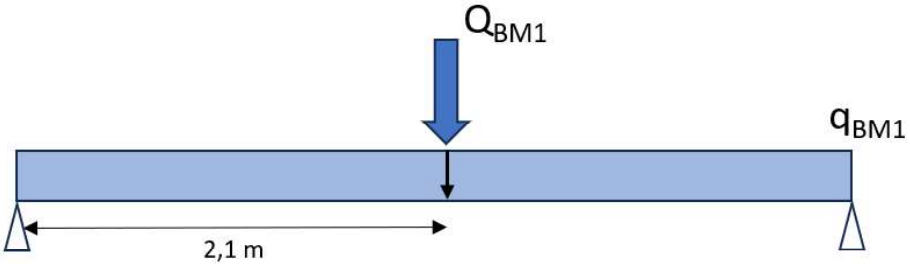

Figure 8.8, Load case for maximal bending moments in deck MS.

The resulting shear force, $V_{BM1} = 260\ kN$ and bending moments, $M_{BM1} = 244\ kNm$. For combining brakeforces with the bending moments, a normal force $N_{BM1} = 181\ kN$ in the load path direction is included. The resulting shear- and tensile stresses are calculated with Formula 8.1 and Formula 8.2 respectively.

$$\tau_{Ed,deck} = \frac{V_{Ed,deck}}{A_{Core}} \tag{8.1}$$

$$\sigma_{Ed,deck} = \frac{M_{Ed,deck}}{EI_{deck}} * E_{1,GFRP} * \frac{h_{deck}}{2} + \frac{N_{Ed,deck} * (2 * t_{c,deck} - t_{l,deck})}{2 * t_{l,deck} * w_{rd} * (t_{c,deck} - t_{l,deck})} \tag{8.2}$$

Where:

$$V_{Ed,deck} = 1.2 * V_G + 1.5 * V_{deck} = 395\ kN$$

$$M_{Ed,deck} = 1.2 * M_G + 1.5 * M_{deck} = 3\,775\ kNm$$

$$N_{Ed,deck} = 1.5 * N_{deck} = 271\ kNm$$

$$A_{Core} = 0.462 * m^2$$

$$EI_{deck} = 4.5 * 10^5\ kN * m^2$$

$$E_{1\_GFRP} = 26.2\ GPa$$

$$h_{deck} = 0.524\ m$$

The unity checks for the shear and bending stress is performed with Formula 8.3 and Formula 8.4 respectively. The deck is relatively optimized for the high unity checks.

$$u.c._{\tau,deck} = \frac{\tau_{Ed,\text{deck}}}{\frac{\eta_{c,balsa}}{\gamma_{m,balsa} * \gamma_{rd}}\tau_{c,k}} = 0.93$$

(8.3)

$$u.c._{\sigma,deck} = \frac{\sigma_{Ed,\text{deck}}}{\frac{\eta_{c,GFRP}}{\gamma_{m,GFRP} * \gamma_{rd,GFRP}}\sigma_{1,k}} = 0.89$$

(8.4)

8.1.3.2. Structural checks crossbeam

The crossbeam is tested to the load case BM1, a combination of multiple concentrated loads in combination of a distributed load. The crossbeam is simply supported between the main girders. The deck consists of two lanes, both lanes are to be loaded simultaneously. The resulting load case for shear and bending moments in are displayed in Figure 8.9 and Figure 8.10 respectively.

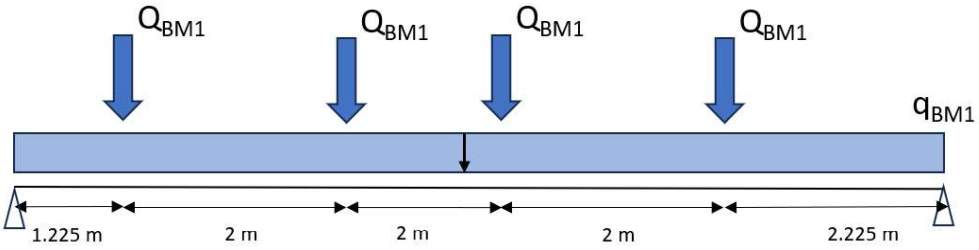

Figure 8.9, Load case for maximal shear in crossbeam MS.

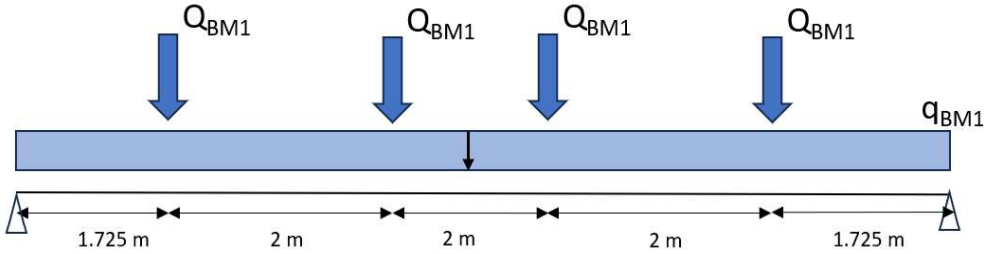

Figure 8.10, Load case for maximal bending moments in crossbeam MS.

The resulting shear force, $V_{BM1} = 499\ kN$ and resulting bending moments, $M_{BM1} = 1\,380\ kNm$. The resulting shear- and tensile stresses are calculated with Formula 8.5 and Formula 8.6 respectively.

$$\sigma_{Ed,cb} = \frac{M_{Ed,cb}}{EI_{cb}} * E_{steel} * \frac{h_{cb}}{2}$$

(8.5)

$$\tau_{Ed,cb} = \frac{V_{Ed,cb}}{A_{v,cb}}$$

(8.6)

Where:

$$V_{Ed,cb} = 1.2 * V_G + 1.5 * V_{cb} = 802\ kNm$$

$$M_{Ed,cb} = 1.2 * M_G + 1.5 * M_{cb} = 2\ 193\ kNm$$

$$A_v = 0.012\ m^2$$

$$EI_{cb} = 6.79 * 10^5\ kN * m^2$$

$$E_{steel} = 210\ GPa$$

$$h_{cb} = 1\ m$$

The unity checks for shear- and tensile stress are performed with Formula 8.7 and Formula 8.8 respectively.

$$u.c._{\tau,cb} = \frac{\sqrt{3} * \tau_{Ed,cb}}{f_{st}} = 0.33 \qquad (8.7)$$

$$u.c._{\sigma,cb} = \frac{\sigma_{Ed,cb}}{f_{st}} = 0.87 \qquad (8.8)$$

8.1.3.3. Structural checks main beam

For the main beams, the load case, BM1, is again applied twice to maximize shear force and bending moments. The individual axles of the vehicle are combined, the distributed load of a single FCP is combined with the distributed load on the road deck. The resulting in the load cases for shear force and bending moments displayed in Figure 8.11 and Figure 8.12 respectively.

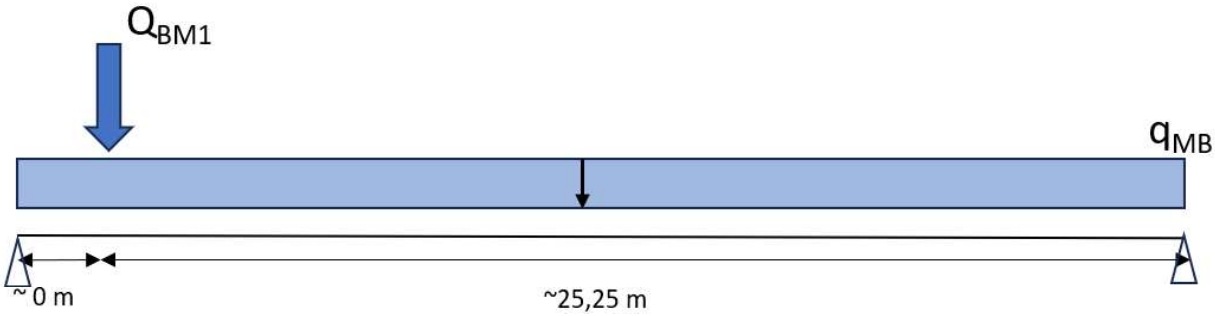

Figure 8.11, Load case for maximal shear force in main beam MS.

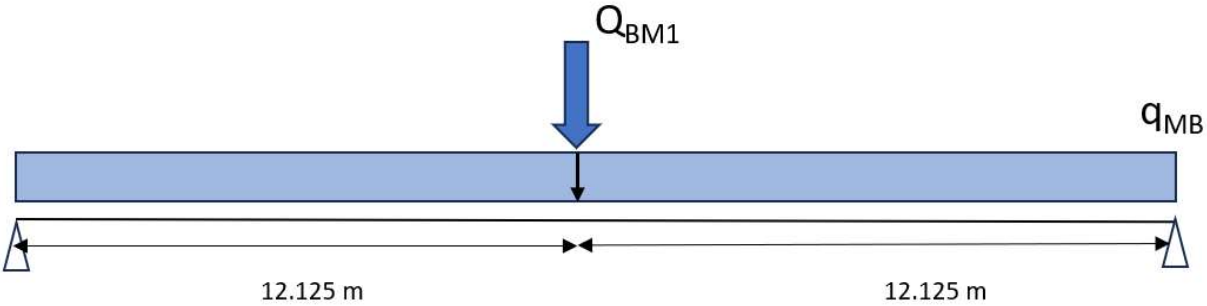

Figure 8.12, Load case for maximal bending moments in main beam MS.

The resulting shear force, $V_{BM1} = 2.6 * 10^3\ kN$, and the bending moments, $M_{BM1} = 1.22 * 10^4\ kNm$. The resulting shear- and tensile stresses are calculated with Formula 8.9 and Formula 8.10 respectively.

$$\sigma_{Ed,mb} = \frac{M_{Ed,mb}}{EI_{mb}} * E_{steel} * \frac{h_{mb}}{2}$$

(8.9)

$$\tau_{Ed,mb} = \frac{V_{Ed,mb}}{A_{v,mb}}$$

(8.10)

Where:

$$V_{Ed,mb} = 1.2 * V_G + 1.5 * V_{mb} = 4\ 682\ kNm$$

$$M_{Ed,mb} = 1.2 * M_G + 1.5 * M_{mb} = 23\ 270\ kNm$$

$$A_v = 0.462\ m^2$$

$$EI_{mb} = 1.97 * 10^7\ kN * m^2$$

$$E_{steel} = 210\ GPa$$

$$h_{mb} = 2.5\ m$$

The unity checks for shear- and tensile stress are performed with Formula 8.11 and Formula 8.12 respectively.

$$u.c._{\tau,mb} = \frac{\sqrt{3} * \tau_{Ed,mb}}{f_{st}} = 0.46$$

(8.11)

$$u.c._{\sigma,mb} = \frac{\sigma_{Ed,mb}}{f_{st}} = 0.87$$

(8.12)

8.1.3.4. Auxiliary structural checks

Auxiliary checks performed are checks against ship collision and for an opened structure. For a ship collision, the governing load case is the local strength of the main beam, in between crossbeams. The corresponding unity check, $u.c._{mb,\sigma,sc,loc} = 0.75$. For an opened structure, the load case for combined wind loads result in a unity check, $u.c._{mb,\sigma,opened} = 0.60$.

Displacement checks are performed at threshold, with a maximal allowable displacement of 5 mm. The resulting occurring displacement is 4.84mm, resulting in a unity check, $u.c._{w,threshold}$ 0.97.

8.1.3.5. Unity checks

For the MS variant 1 all unity checks are given in Table 8.5.

Table 8.5, Unity checks MS variant 1, steel main- and crossbeams with FRP deck.

Description	Abbreviation	Value
Deflection of the crossbeam at the threshold	$u.c._{w,threshold}$	0.97
Shear force in deck core	$u.c._{deck,\tau}$	0.93
Tensile stress in deck laminate	$u.c._{deck,\sigma,l}$	0.89
Tensile stress in deck core	$u.c._{deck,\sigma,c}$	0.46
Shear force in crossbeam	$u.c._{cb,\tau}$	0.33
Tensile stress in crossbeam	$u.c._{cb,\sigma}$	0.96
Shear force in main beam	$u.c._{mb,\tau}$	0.46
Tensile stress in main beam	$u.c._{mb,\sigma}$	0.87
Shear force in main beam flange due to ship collision	$u.c._{mb,\tau,sc}$	0.10
Local tensile stress in main beam flange due to ship collision	$u.c._{mb,\sigma,sc,loc}$	0.75
Global tensile stress in main beam flange due to ship collision	$u.c._{mb,\sigma,sc,glob}$	0.06
Tensile stress in main beam in opened position	$u.c._{mb,\sigma,opened}$	0.60

From the unity checks it can be concluded that the tested elements are optimized. The unity checks of the deck, the crossbeam and main beam highest are above 0.71.

8.1.3.6. ECI score

The materials and the quantities used in the design are given in Table 8.6.

Table 8.6, Materials and quantities of MS variant 1, steel main- and crossbeams with FRP deck.

Material	Amount	Unit
GFRP laminate	10 900	kg
Balsa	34 002	kg
Steel	48 500	kg
Galvanization	580	m^2
Paint	1 084	m^2

The governing ECI components for the first variant are the steel profiles, the entire breakup is given in Figure 8.13.

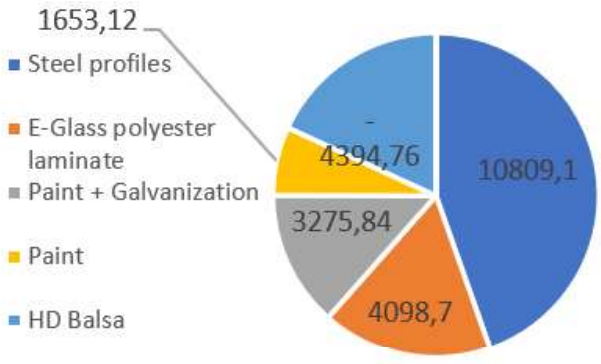

Figure 8.13, ECI score MS variant 1, steel cross- and main beam with FRP deck.

8.1.4. Variant 2, steel main beam, FRP deck

The second variant consists of two steel main girders, but with the deck spanning between them. The main girders also remain constant over the length of the structure, so to also enable end of life reusability.

The deck of the structure now carries the load perpendicular to the traffic direction. This complicates the design of the deck. Next to this, the span between the girders is almost ten meters, and thus the deck is relatively large compared to the first variant. The connection between the deck and the main beams is to be made so these elements are separable. The laminate layup is given in Table 8.7, where the plies are orientated in the direction of the main load carrying direction, perpendicular to the vehicle travel direction.

Table 8.7, Layup FRP deck.

Orientation	Layup
0°	50%
90°	16.67%
±45°	33.33%

Due to ship collision, stiffeners are used at the bottom of the structure to both resist the direct normal force of the collision and to also activate the whole structure against horizontal load. The stiffeners are designed from steel for this variant. An overview of the cross section is given in Figure 8.14.

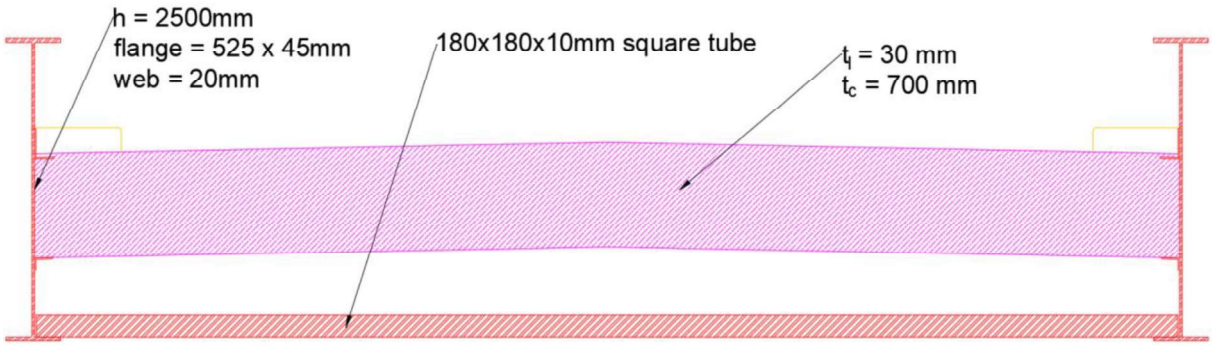

Figure 8.14, Cross section MS variant 2, steel main beam with FRP deck, without crossbeam.

8.1.4.1. Structural checks deck

The principal load carrying direction for this deck system is perpendicular to the traffic direction. This results in significant shear loads in the laminates in combination with bending loads. The BM1 load results is again applied twice to maximize and shear in the core the bending moments. These load cases are displayed in Figure 8.15 and Figure 8.16 respectively.

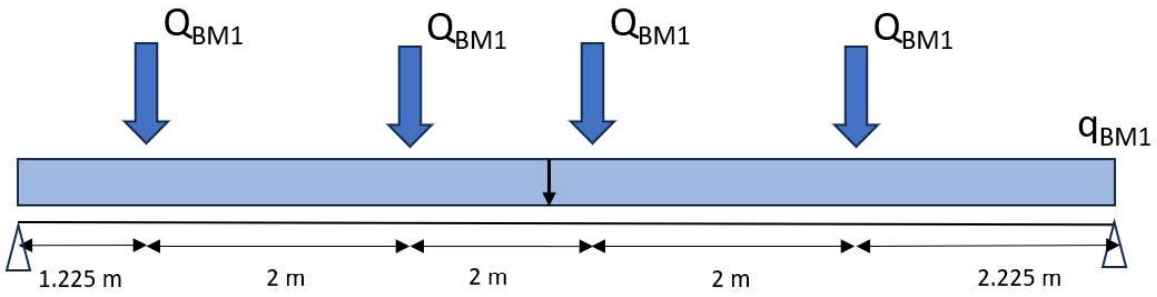

Figure 8.15, Load case for maximal shear force in deck MS.

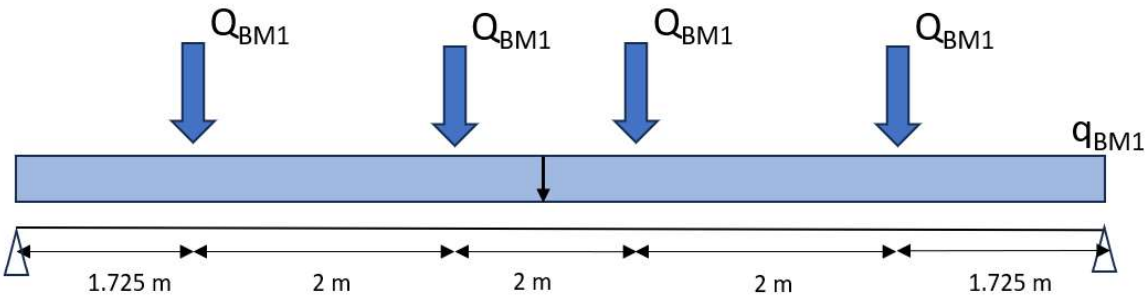

Figure 8.16, Load case for maximal bending moments in deck MS.

The resulting shear force in the core, $V_{deck,c} = 373\ kN$, the bending moments, $M_{deck} = 1\,081\ kNm$, and the shear force in the laminate $V_{deck,l} = 363\ kN$. The resulting shear- and tensile stresses are calculated with Formula 8.13, Formula 8.14, and Formula 8.15 respectively.

$$\tau_{Ed,deck,c} = \frac{V_{Ed,deck,c}}{A_{v,core}} \quad (8.13)$$

$$\tau_{Ed,deck,l} = \frac{V_{Ed,deck,l}}{A_{v,core}} \quad (8.14)$$

$$\sigma_{Ed,mb} = \frac{M_{Ed,deck}}{EI_{core}} * E_{1,GFRP} * \frac{h_{deck}}{2} \quad (8.15)$$

Where:

$$V_{Ed,deck,c} = 1.2 * V_g + 1.5 * V_{deck} = 580\ kNm$$

$$V_{Ed,mb,l} = 1.5 * V_{mb,l} = 544\ kNm$$

$$M_{Ed,deck} = 1.2 * M_G + 1.5 * M_{mb} = 1\,670\ kNm$$

$$A_v = 0.812\ m^2$$

$$EI_{mb} = 2.67 * 10^5\ kN * m^2$$

$$E_{1\_GFRP} = 26.2\ GPa$$

$$h_{deck} = 0.76\ m$$

The unity checks for shear stress in the core and laminate are performed with Formula 8.16 and Formula 8.17 respectively. The unity check for tensile stress in the laminate is performed with Formula 8.17. For the laminate, the checks are combined using Tsai-Hill failure criteria, using Formula 8.19.

$$u.c._{\tau,deck,c} = \frac{\tau_{Ed,\text{deck}}}{\frac{\eta_{c,balsa}}{\gamma_{m,balsa} * \gamma_{rd}}\tau_{c,k}} = 0.78$$

(8.16)

$$u.c._{\tau,deck,l} = \frac{\tau_{Ed,\text{deck}}}{\frac{\eta_{c,balsa}}{\gamma_{m,balsa} * \gamma_{rd}}\tau_{c,k}} = 0.51$$

(8.17)

$$u.c._{\sigma,deck} = \frac{\sigma_{Ed,\text{deck}}}{\frac{\eta_{c,GFRP}}{\gamma_{m,GFRP} * \gamma_{rd,GFRP}}\sigma_{1,k}} = 0.29$$

(8.18)

$$u.c._{deck,laminate} = u.c._{\tau,deck,l} + u.c._{\sigma,deck} = 0.81$$

(8.19)

8.1.4.2. Structural checks main beam

The structural checks for the main beam are identical to variant 1. This loads due to self-weight will be different because this variant is heavier. The resulting unity checks for the shear, $u.c._{\tau,mb} = 0.36$ and for the bending moments, $\sigma_{Ed,mb} = 0.88$.

8.1.4.3. Auxiliary structural checks

Auxiliary checks performed are checks for ship collision and for an opened structure. For a ship collision, the governing load case is the buckling strength of the stiffeners. The unity check for buckling, $u.c._{stiff,buck} = 1.00$. The unity check for an opened structure, $u.c._{opened} = 0.61$

Displacement checks are performed at threshold, with a maximal allowable displacement of 5 mm. The resulting occurring displacement is 4.8mm, resulting in a unity check, $u.c._{w,threshold} = 0.96$.

8.1.4.4. Unity checks

For the variant 2 all unity checks are given in Table 8.8.

Table 8.8, Unity checks MS variant 2, steel main beam with FRP deck, without crossbeam.

Description	Abbreviation	Value
Deflection of the crossbeam at the threshold	$u.c._{w,threshold}$	0.96
Shear force in deck core	$u.c._{deck,\tau}$	0.78
Tensile stress in deck laminate	$u.c._{deck,\sigma,l}$	0.81
Tensile stress in deck core	$u.c._{deck,\sigma,c}$	0.49
Shear force in main beam	$u.c._{mb,\tau}$	0.36
Tensile stress in main beam	$u.c._{mb,\sigma}$	0.88
Shear force in main beam flange due to ship collision	$u.c._{mb,\tau,sc}$	0.02
Local tensile stress in main beam flange due to ship collision	$u.c._{mb,\sigma,sc,loc}$	0.10
Global tensile stress in main beam flange due to ship collision	$u.c._{mb,\sigma,sc,loc}$	0.06
Buckling resistance of the main beam stiffener	$u.c._{stiff,buck}$	1.00
Tensile stress in main beam in opened position	$u.c._{mb,\sigma,opened}$	0.60

From the unity checks it can be concluded that the tested elements are optimized. The unity checks of the deck and main beam highest are above 0.81. For the ship collision, the structural system chosen results in a high utilization rate of the stiffener, while the main beams are barely loaded to capacity. This is inefficient and allows for optimization. A potential optimization is to increase the size of- and apply fewer stiffeners.

8.1.4.5. ECI score

The materials and the quantities used in the design are given in Table 8.9.

Table 8.9, Materials and quantities of MS variant 2, steel main beam with FRP deck, without crossbeam.

Material	Amount	Unit
Steel	46 200	kg
GFRP laminate	27 200	kg
Balsa	47 600	kg
Galvanization	366	m^2
Paint	882	m^2

The governing ECI component for the first variant is the glass fiber with polyester laminate, followed closely by the steel profiles. The entire breakup is given in Figure 8.17.

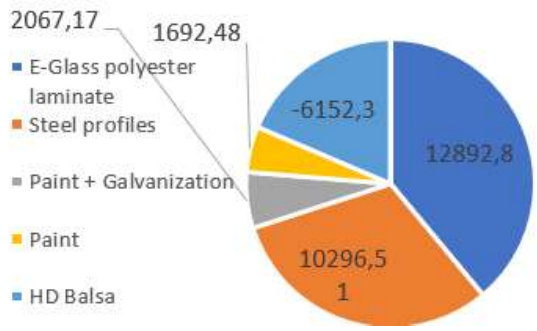

Figure 8.17, ECI score MS variant 2, steel main beam with FRP deck, without crossbeam.

8.1.5. Variant 3, FRP main beam and deck

The third design is highly inspired by the second variant. The main beam is replaced by an FRP main beam, and the stiffeners are designed with FRP. This results in the first of two full FRP designs. With the change from steel to FRP, the entire structure become more resilient to environmental effects. The downside of this change is that the structure becomes more prone to deflection. To prevent the deflection, higher main girders must be used. The height of the main girders must taper off towards the abutments, to ensure the structure can be retrofitted into the current surrounding infrastructure. The laminate layup for the main girders is given in Table 8.10.

Table 8.10, Layup FRP main beams.

Orientation	Layup Flange	Layup Web
0°	62.5%	25%
90°	12.25%	25%
±45°	25%	50%

The deck system is precisely the same as in the second variant. The connection is again made to be separable, for end-of-life reuse. The laminate layup is given in Table 8.11, where the plies are again orientated in the direction of the main load carrying direction, perpendicular to the vehicle travel direction.

Table 8.11, Layup FRP deck.

Orientation	Layup
0°	50%
90°	16.67%
±45°	33.33%

The stiffeners at the bottom of the structure are made with multiple FRP sandwich panels with gaps between them. The stiffeners are again needed for strengthening the main girders in case of a ship collision. The laminate layup for the stiffeners is given in Table 8.12, an overview of the cross section is given in Figure 8.18.

Table 8.12, Layup FRP stiffeners.

Orientation	Layup
0°	62.5%
90°	12.25%
±45°	25%

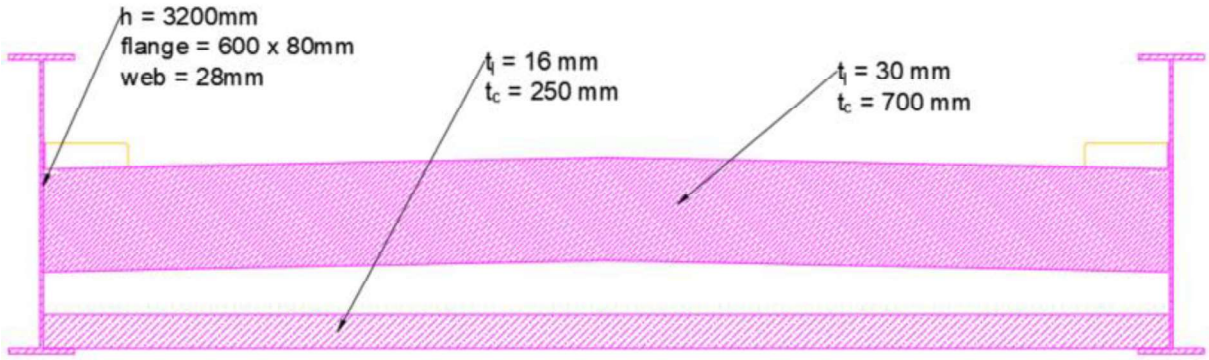

Figure 8.18, Cross section MS variant 3, FRP main beam and deck, without crossbeam.

8.1.5.1. Structural checks

The deck system of this variant is identical to the deck system of the previous variant. For the relevant calculations, see section 8.1.4.1.

For the calculations of the main beams of this variant, the calculations are identical to those performed for the previous variant. The major difference for is this change from a steel main beam to an FRP main beam. Because FRP is a less stiff material compared to steel, additional stiffness must be created with the main beam profile. The choice has been made to increase the height of the main beams, to reduce the amount of material needed. This is only necessary for the main beam between the spans and therefore has minimal impact on land use. The resulting unity check for shear, $u.c._{\tau,mb} = 0.69$ and for the bending moments, $\sigma_{Ed,mb} = 0.98$.

Auxiliary checks performed are checks for ship collision and for an opened structure. For a ship collision, the governing load case is the buckling strength of the stiffeners. The unity check for buckling, $u.c._{glob,buck} = 1.00$. The unity check for an opened structure, $u.c._{opened} = 0.97$

Displacement checks are performed at threshold, with a maximal allowable displacement of 5 mm. The resulting occurring displacement is 4.8mm, resulting in a unity check, $u.c._{w,threshold} = 0.93$.

8.1.5.2. Unity checks

For the variant 3 all unity checks are given in Table 8.13.

Table 8.13, Unity checks MS variant 3, FRP main beam and deck, without crossbeam.

Description	Abbreviation	Value
Deflection of the crossbeam at the threshold	$u.c._{w,threshold}$	0.93
Shear force in deck core	$u.c._{deck,\tau}$	0.84
Tensile stress in deck laminate	$u.c._{deck,\sigma,l}$	0.81
Tensile stress in deck core	$u.c._{deck,\sigma,c}$	0.49
Shear force in main beam	$u.c._{mb,\tau}$	0.69
Tensile stress in main beam	$u.c._{mb,\sigma}$	0.98
Global tensile stress in main beam flange due to ship collision	$u.c._{mb,\sigma,sc,loc}$	0.08
Buckling resistance of the main beam stiffener	$u.c._{stiff,buck}$	1.00
Tensile stress in main beam in opened position	$u.c._{mb,\sigma,opened}$	0.97

From the unity checks it can be concluded that the tested elements are optimized. Compared to the previous variant, the unity checks local effects due to the ship collision have been removed, as these were very low. The unity checks of the deck and main beam highest are above 0.81. For the ship collision, the structural system chosen results in a high utilization rate of the stiffener, while the main beams are barely loaded to capacity. This is inefficient and allows for optimization. A potential optimization is to increase the size of- and apply fewer stiffeners.

8.1.5.3. ECI score

The materials and the quantities used in the design are given in Table 8.14.

Table 8.14, Materials and quantities of MS variant 3, FRP main beam and deck, without crossbeam.

Material	Amount	Unit
GFRP laminate	44 600	kg
Balsa	47 600	kg
Paint	957	m^2

Due to the entire structure consisting of FRP, the ECI breakdown does not reveal much new information. The most FRP is used for the deck, the entire breakup is given in Figure 8.19.

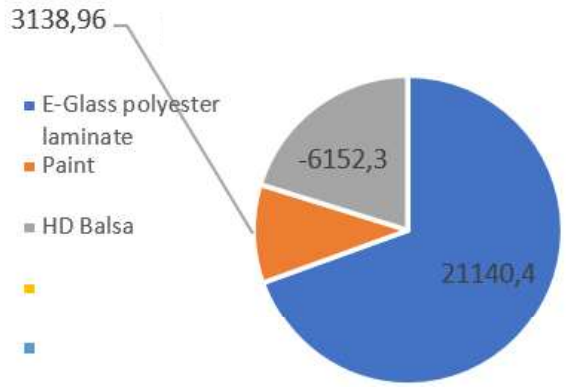

Figure 8.19, ECI score MS variant 3, FRP main beam and deck, without crossbeam.

8.1.5.4. Variant 4, FRP box girder and deck

The fourth and last variant is a closed FRP box girder. The design consists of a similar deck panel which is supported by a continuous plate girder on the bottom with multiple webs connecting these elements. The main structure thus becomes incorporated with the road deck. The laminate layup for the main bottom flange and webs are given in Table 8.15. The edge webs, including a small part of the flange is stronger to account loads during the opening cycle.

Table 8.15, Layup FRP main beams.

Orientation	Layup Flange	Layup Web
0°	62.5%	25%
90°	12.25%	25%
±45°	25%	50%

The design of this deck structure limits the stresses caused by local traffic loads, resulting in a slimmer deck. On the other hand, since the main structure lacks a top flange, the deck will also function as main flange. This will increase the longitudinal stresses, requiring more fibers directed in the same direction as the traffic. The laminate layup is given in Table 8.16, where the plies are again orientated in the direction of the traffic.

Table 8.16, Layup FRP deck.

Orientation	Layup
0°	50%
90°	16.67%
±45°	33.33%

This design will, because of the bottom flange, have no need for horizontal stiffeners. In case of a ship collision on the side of the bride, the first flange section from the most outer web to the next web is expected to break. An overview of the cross section is given in Figure 8.20.

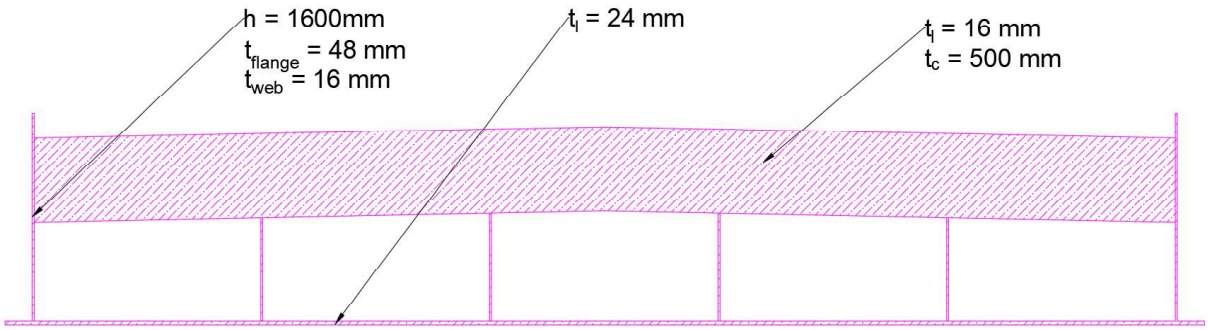

Figure 8.20, Cross section MS variant 4, FRP box structure (full FRP).

8.1.5.5. Structural checks

The design of this variant makes the structural checks more challenging. Deck cannot be checked without taken the main structure into account. To simplify the support of the deck, each web is replaced by a representative spring, see Figure 8.21.

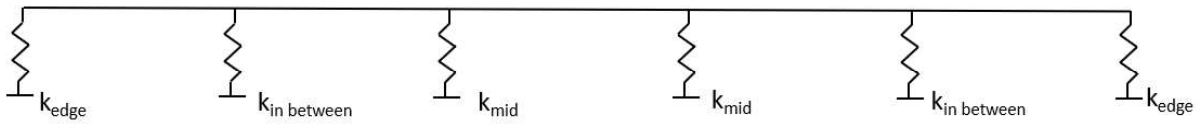

Figure 8.21, Structural system MS variant 4, FRP box structure (full FRP).

The edge webs are directly supported at each abutment and therefore only bend in the span. For the webs in between, the head board also bends, therefore these springs are calculated by taking the bending of the beam itself as the headboard into account. The deck is assumed to function in resisting the bending as well. The cross sections of the fictional edge beam and the fictional beams in between are displayed in Figure 8.22 and Figure 8.23 respectively.

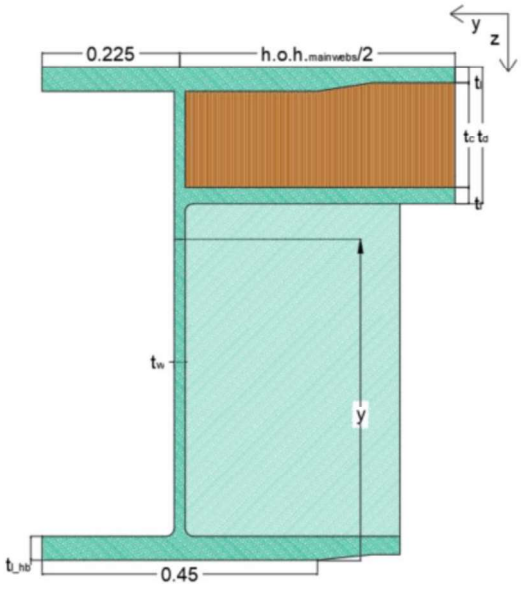

Figure 8.22, Outside fictional beam MS variant 4, FRP box structure (full FRP).

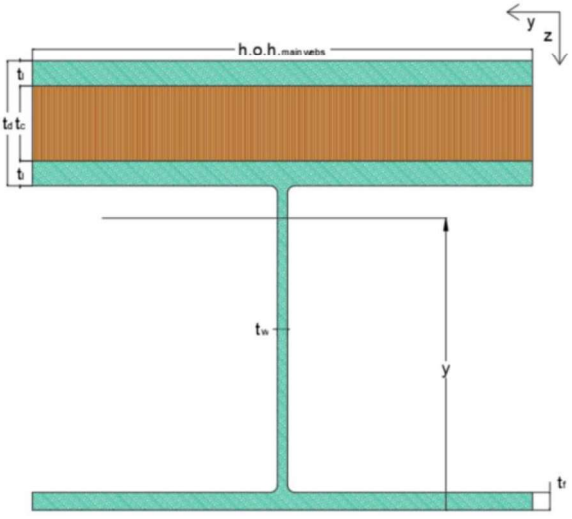

Figure 8.23, Inside fictional beam MS variant 4, FRP box structure (full FRP).

The springs are calculated by taking a fictional concentrated load into account. Rewriting the formula for bending of a simply supported beam due to a concentrated load results in Formula 8.20, used for determining the stiffness of each beam.

$$k_i = \frac{48 * EI_i}{l^3}$$

(8.20)

The structure is symmetric, therefore three distinct spring stiffnesses are determined. The spring stiffness of the in between beam, an average of the edge and middle beams is taken. The spring stiffnesses are given in Table 8.17. The $k_{headboard}$ for the in between beam is the value that would result in the combined stiffness.

Table 8.17, Spring stiffnesses fictional beams MS variant 4, FRP box structure (full FRP).

Spring	k_{span}	$k_{headboard}$	$k_{resultant}$	Unit
Edge	3215	[-]	3215	kN/m
In between	4469	6845	2704	kN/m
Middle	4469	4305	2193	kN/m

8.1.5.6. Structural checks deck

With the spring values, the deck can be tested for structural performance. With the use of Matrix Frame, it was found that the global stresses due to the shear force and bending moments are significantly more governing than the local stressed. Therefore, the load case is optimized to maximize the global stresses. The load case displayed in Figure 8.24 is used to determine the maximal shear force and bending moments.

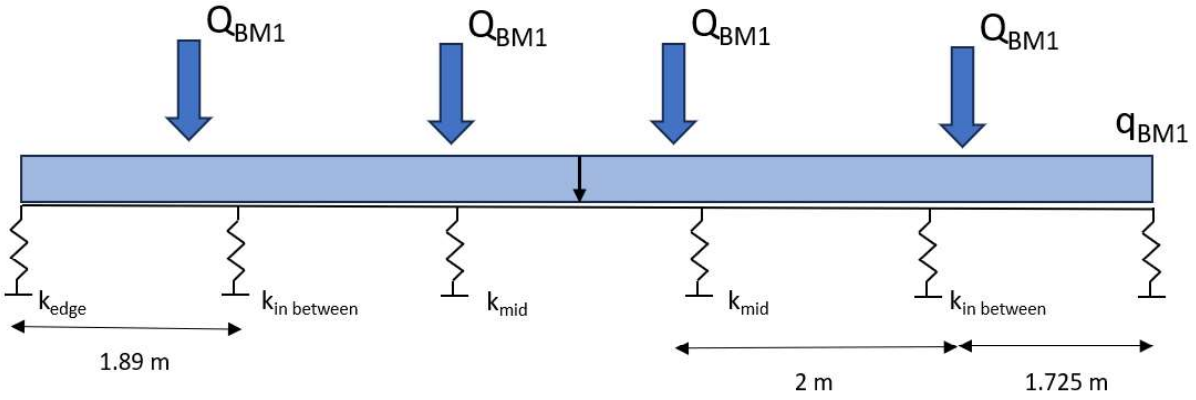

Figure 8.24, Load case for maximal shear and bending moments in deck MS.

The resulting shear force in the core, $V_{deck,c} = 191\ kN$, the bending moments, $M_{deck} = 310\ kNm$, and the shear force in the laminate $V_{deck,l} = 363\ kN$. Interesting to note is that the addition of the longitudinal webs reduced the transverse shear force by 49% and the transverse bending moments by 71% compared to variant 2 or 3 (similar transverse deck, without webs). The resulting unity checks are $u.c._{\tau,deck,c} = 0.67$ and $u.c._{deck,laminate\_loc} = u.c._{\tau,deck,l} + u.c._{\sigma,deck} = 0.372$. The laminates (in particular the top laminate) will also function in the main structure. For this reason, the unity check for the transverse part is relatively low.

8.1.5.7. Structural checks main structure

The structure consisting of multiple webs will be combined using the individual stiffnesses of each web. The combined stiffness of the structure will be calculated with Formula 8.21.

$$EI_{main\ structure} = \sum_{i=1}^{6} EI_i * \frac{k_i}{k_{edge}} \quad (8.21)$$

The load case for determining the maximal stress of the structure will assume a structure which is fully loaded. This includes the distributed load for the FCP path. The load case for maximizing the shear force and bending moments are displayed in Figure 8.25 and Figure 8.26 respectively.

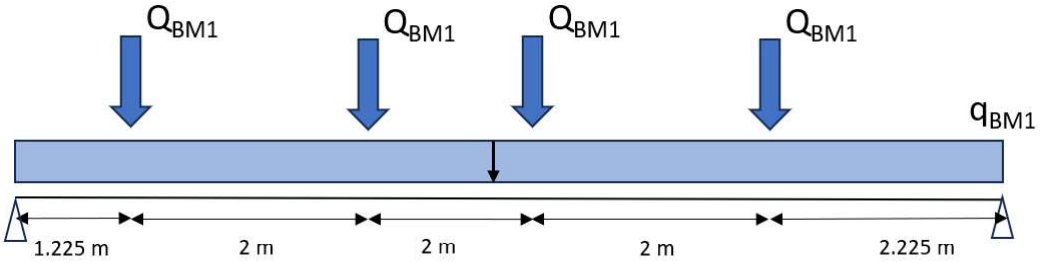

Figure 8.25, Load case for maximal shear force in deck MS.

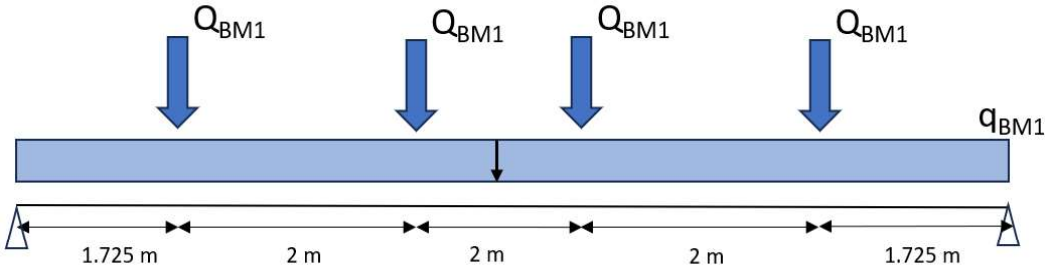

Figure 8.26, Load case for maximal bending moments in deck MS.

The resulting shear force in the core, $V_{ms} = 642\ kN$, and the bending moments, $M_{ms} = 4\,050\ kNm$. The shear force is distributed over the combined area of the webs. Similarly to the stiffness, the area is scaled by the spring stiffness compared to the edge beam. The resulting unity check for shear is $u.c._{\tau,deck,c} = 0.44$. For the bending moments, the global tensile stress in longitudinal direction is added unto the unity check of the transverse stress, $u.c._{deck,laminate\_total} = u.c._{deck,laminate\_loc} + u.c._{deck,global} = 0.58$. For the addition the conservative Tsai-Hill failure criteria has been used.

8.1.5.8. Auxiliary structural checks

Auxiliary checks performed are checks for ship collision and for an opened structure. For a ship collision, the governing load case is the buckling strength of the lower flange in combination with transverse stiffeners. The unity check for buckling, $u.c._{glob,buck} = 1.18$. The unity check is slightly higher then 1, this is by design, as for this variant it is acceptable for a part of the structure to fail. The whole structure will not collapse due to the loss of a part of the main beam, under self-weight. The unity check for an opened structure, $u.c._{opened} = 0.65$, this is tested for only the edge beam, the part that connects the leaf to the axle.

Displacement checks are performed at threshold, with a maximal allowable displacement of 5 mm. The resulting occurring displacement is 4.25 mm, resulting in a unity check, $u.c._{w,threshold} = 0.85$.

8.1.5.9. Unity checks

For the variant 4 all unity checks are given in Table 8.18.

Table 8.18, Unity checks MS variant 4, FRP box structure (full FRP).

Description	Abbreviation	Value
Deflection of the crossbeam at the threshold	$u.c._{w,threshold}$	0.85
Shear force in deck core	$u.c._{deck,\tau}$	0.67
Tensile stress in deck laminate	$u.c._{deck,\sigma,l}$	0.58
Shear force in main beam webs	$u.c._{mb,\tau}$	0.44
Tensile stress in main beam bottom flange	$u.c._{mb,\sigma}$	0.19
Global tensile stress in main beam flange due to ship collision	$u.c._{mb,\sigma,sc,loc}$	1.14
Tensile stress in main beam in opened position	$u.c._{mb,\sigma,opened}$	0.65

From the unity checks it can be concluded that the tested elements can be further optimized. The unity check for the deflection at the threshold mean that this area of the design is relatively well optimized. The unity checks for main structure in the midspan allow for further optimization. An optimization is to decrease the thickness of the laminates in midspan compared to at the abutments. Important with this optimization is the decrease of stiffness of the middle fictional beams. This means the stresses in the deck will also increase in the transverse direction.

The deck laminate can also be further optimized, as the unity check is relatively low, and the stresses are combined with a conservative estimation of the failure criteria. Again, it is important to include the effect of the loss of stiffness of the fictional beams when reducing the laminate thickness. This also holds if the thickness of the deck is decreased.

The unity check for the ship collision is higher than 1, but acceptable. The loss of a part of the main beam does not result in the loss of the structure, as argued in section 8.1.6.4.

8.1.5.10. ECI score

The materials and the quantities used in the design are given in Table 8.19.

Table 8.19, Materials and quantities of MS variant 4, FRP box structure (full FRP).

Material	Amount	Unit
GFRP laminate	32 400	kg
Balsa	34 000	kg
Paint	1 063	m^2

Due to the entire structure consisting of FRP, the ECI breakdown does not reveal much new information. The most FRP is used for the deck, the entire breakup is given in Figure 8.27.

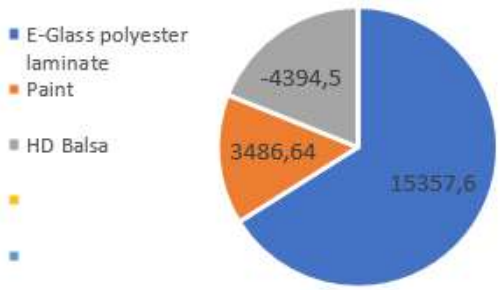

Figure 8.27, ECI score MS variant 4, FRP box structure (full FRP).

8.2. Comparison

For the comparison between the variants, the sustainability aspects mentioned in section 6 will be considered in addition to practicalities to the design.

8.2.1. Practicalities

The practicalities of each design are summarized in Table 8.20.

Table 8.20, Practicality comparison between MS variants.

Variant	Positives	Negatives
1	+ Separated deck and support structure allow for easy replacement of element. + Main beam structure can easily be connected to the hinge and counterweight.	
2	+ Separated deck and support structure allow for easy replacement of element. + Main beam structure can easily be connected to hinge and counterweight.	
3	+ Separated deck and support structure allow for easy replacement of element. + Main beam structure can easily be connected to the hinge and counterweight.	
4		- Connected deck and support structure would not allow for separate element replacement.

8.2.2. Environmental impact

For the aspect environmental impact the ECI values are compared, in addition to the mass of each structure. The total ECI value of the variants are displayed in Figure 8.28, based on a 100-year lifespan. The mass of each variant is given in Table 8.21.

Table 8.21, Mass comparison between FCP variants.

	Variant 1	Variant 2	Variant 3	Variant 4	Base variant
Mass [m. Ton]	93	121	92	66	103

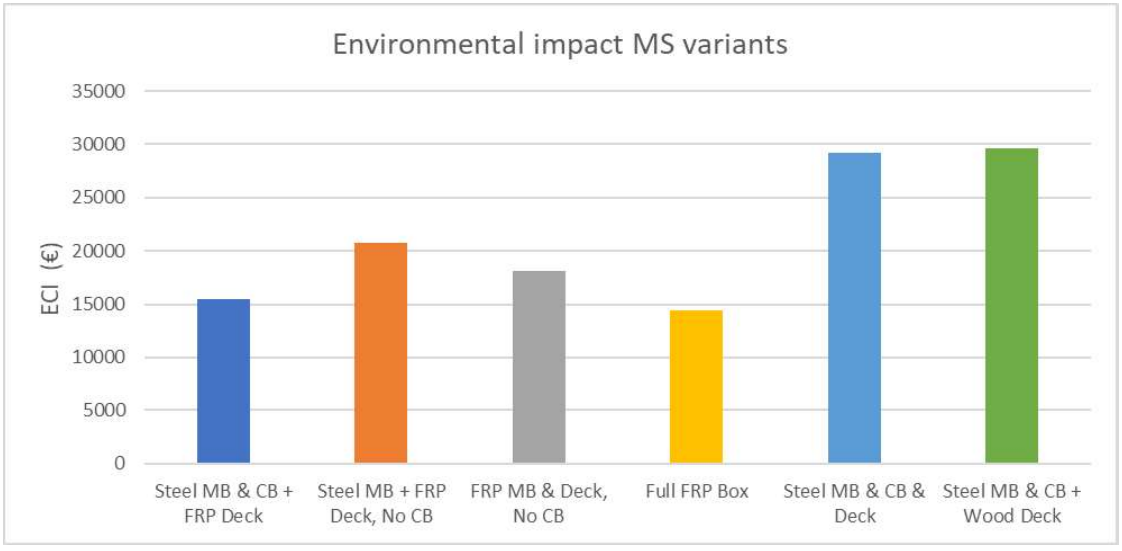

Figure 8.28, ECI comparison between FCP variants.

8.2.3. Circularity

For the aspect circularity the circular design principles were use during the design process. This section will go into each variants ability to incorporate circular design principles. The considerations are summarized in Table 8.22.

Table 8.22, Circularity comparison between FCP variants.

Variant	Positives	Negatives
1	+ Elements are easily separable, enabling end of life separation and reuse of individual elements. (Road deck) + Steel elements can be made by (mostly) recycled steel, can be recycled again at end of life. ++ Potential for reuse of steel elements. (Main beam) ++ Long lifespan of FRP enables reuse of elements after bridge lifespan.	- FRP is currently poorly recyclable. - Steel will require periodical maintenance
2	+ Elements are easily separable, enabling end of life separation and reuse of individual elements. (Road deck) + Steel elements can be made by (mostly) recycled steel, can be recycled again at end of life. ++ Potential for reuse of steel elements. ++ Long lifespan of FRP enables reuse of elements after bridge lifespan.	- FRP is currently poorly recyclable. - Steel will require periodical maintenance
3	+ Elements are easily separable, enabling end of life separation and reuse of individual elements. (Road deck) ++ Long lifespan of FRP enables reuse of elements after bridge lifespan.	- FRP is currently poorly recyclable. - The design of the main girders decreases to likelihood for end-of-life reuse.
4	+ Some elements are easily separable, enabling end of life separation and reuse of individual elements. (Road deck) ++ Long lifespan of FRP enables reuse of some elements after bridge lifespan. + Lower utilization of bottom flange will enable repairability of this element.	- FRP is currently poorly recyclable. - The deck must be destructively removed from the support if only this element will be reused at end of life. - In case of damage to the road deck, the road deck is not replaceable.

9. Comparison of renewal scenarios

For this thesis, there is no final design that can be build and applied directly to the case study. The reasons for this are:

- The design level is not in depth enough for a final design which can be constructed.
- The goal for this section is to indicate what designs can be applied to possible application scenarios.

As mentioned previously, the choice has been made to not design a single final design but propose combination of variants for different scenarios. For this exercise, the foot- and cycle path and the main structure are designed separate, except for mass load on the main structure. The results of this approach may differ from a final structure, as the complete structure may behave differently under certain load combination not considered by this approach.

As previously mentioned, the scenarios for the replacement of the Oostsluisbruggen are in order of increasing consequence. The scenarios are:

- The current structure is for the most part in good health and does not need replacement, except for the deck. A sub variant where the stringers are still in good health is also explored.
- The entire structure needs replacement.

The variants in the scenario are compared on 2 parameters, mass and ECI. These are the only factors that are influenced by the scenarios. The comparisons for practicalities and circularities are given in section 7 and 8. ECI is a direct parameter following from the ambition: environmental impact. Mass is included as this has a strong impact on multiple ambitions:

- Direct influence on environmental impact and financing through not included elements such as counterweight and actuator.
- Indirect influence on land use, though only when exceeding critical mass.
- Direct influence on health and safety of the workers.
- Direct influence on environmental impact and financing by increased costs-, complexity of-, and emissions as a result of transport.
- Increase in likelihood of reuse of actuators and/or counterweight.

9.1. Scenario 1, deck replacement

9.1.1. Scenario 1, deck replacement of Foot- and cycle path

Adopting variants to fit this scenario is of different difficulty to impossible for each design. The following Table 9.1 summarizes the work needed for different designs for the foot- and cycle path.

Table 9.1, Work required per FCP variant, for scenario 1, deck replacement.

Variant	Actions
Base variant Steel crossbeam with wooden deck	For the base variant a one-on-one replacement is possible for the deck. The variant is based on the current design of the FCP structure, with the same wooden deck. The crossbeam can be maintained but require maintenance. Two sub scenarios are considered, one where the stringers are maintained and one where the stringers must be replaced as well.
Variant 1 Steel crossbeam, FRP deck	For variant 1 a one-on-one replacement is possible for the deck. The deck does increase by 84 mm, but stringers with a height of 200 mm are removed. The crossbeam can be maintained but require maintenance.
Variant 2 Full FRP variant	The modifications to allow for this variant will include removing the crossbeam as well as the deck. This ensures that the structure can be placed and will result in no conflict between the structure and the surrounding infra structure.

The ECI calculations have been performed for each variant for the work summarized above. It includes the removal of the stringers and/or crossbeams for variants where this is needed. The costs (or gains) for removing the wooden deck are neglected as this is the same for all variants. It is assumed that the entire structure needs to be replaced after 100 years, thus increasing the ECI significantly at the end of the lifecycle. The initial costs for the base variant are relatively low, as little work needs to be done and there is no polluting FRP. But over the lifespan of the structure, the costs of a wooden deck that needs replacement is comparable to an FRP deck. Removing the current elements to make room for the full FRP variant will increase the costs of this variant significantly. If the stringers need replacement, replacing it with a replica of the current elements increases the environmental impact significantly. Figure 9.1 depicts the ECI for the complete scope of the product lifecycle (A, B, C & D), for a lifespan of 100 years.

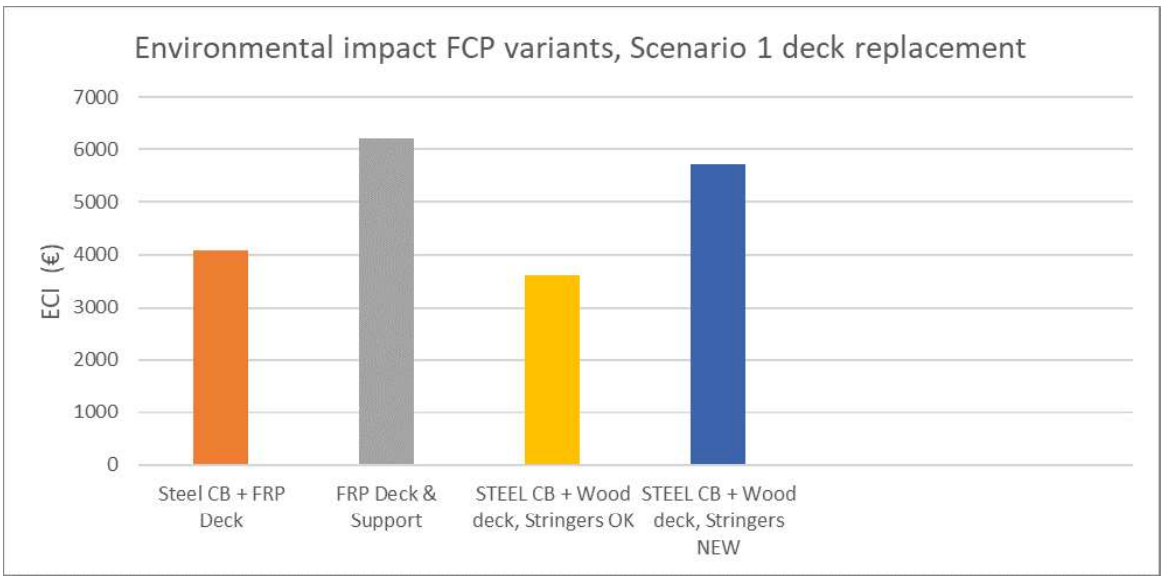

Figure 9.1, ECI comparison between FCP variants, for scenario 1, deck replacement.

The mass of each variant is given in Table 9.2. Both variants reduce the mass of the combined elements. Where replacing the current structure with a full FRP variant the mass is comparable. Replacing the wooden deck with the stringers for an FRP panel, the mass is reduced by 19% compared to the current FCP structure.

Table 9.2, Mass comparison between FCP variants, for scenario 1, deck replacement.

FCP	Wood deck	Steel CB + FRP deck	Full FRP
Reduction	21.8 ton	28.5 ton	37 ton
Addition	21.8 ton	21.6 ton	36.9 ton
Result	0 ton	- 6.9 ton	-0.1 ton

9.1.2. Scenario 1, deck replacement of main structure.

For the main structure, again certain variants require more modifications than others. The following Table 9.3 summarizes the work needed for the different variants.

Table 9.3, Work required per MS variant, for scenario 1, deck replacement.

Variant	Actions
Base variant Current design	For the base variant, two sub scenarios are used. The first sub scenario reuses the current stringers supporting the wooden deck, the second sub scenario has these elements replaced.
Steel variant Steel orthotropic deck	For the steel variant a significant modification is required for the crossbeams, to provide room for the troughs. To account for this, it is calculated as if the complete crossbeams are replaced.
Variant 1 Steel crossbeams + FRP deck	For variant 1 a one-on-one replacement might be possible for the deck. The deck height increases by 414 mm, but stringers with a height of 400 mm are removed. This results in an increase in height of 14mm. It is assumed that this difference in height can be resolved. No extra modifications will be considered.
Variant 2 Single span FRP Deck with Steel Main Beams	The modifications to allow for this variant will including removing the crossbeam as well as the deck. This ensures that the structure can be placed and will result in no conflict between the structure and the surrounding infra structure.
Variant 3 Single span FRP Deck with FRP Main Beams	Variant 3 and the current structure are too different that modifications to the main structure to allow for an adaptation of variant 3. The main beams need to be replaced to make significant difference between variant 3 and 2, but the main beams are maintained for this scenario. This variant will not be included into the comparison.
Variant 4 Full FRP Box	Variant 4 and the current structure are too different that modifications to the main structure to allow for an adaptation of variant 4. This variant will not be included into the comparison.

The ECI calculations have again been performed for 100 years. It includes the removal of stringers an/or crossbeams, where necessary. It does not include the removal of the wooden deck itself, as this is the same for each variant. The initial costs for the steel orthotropic deck variant are so significant, that it towers above the other variants when comparing the costs. Replacing the wooden deck with an FRP deck has a negative environmental after replacement, this will not be the case at the end of the life cycle. Completely removing the crossbeam increases the environmental impact of renewal significantly. If the stringers need replacement, replacing it with a replica of the current element increases the environmental impact significantly. Figure 9.2 depicts the ECI for the complete scope of the product lifecycle (A, B, C & D), for a lifespan of 100 years.

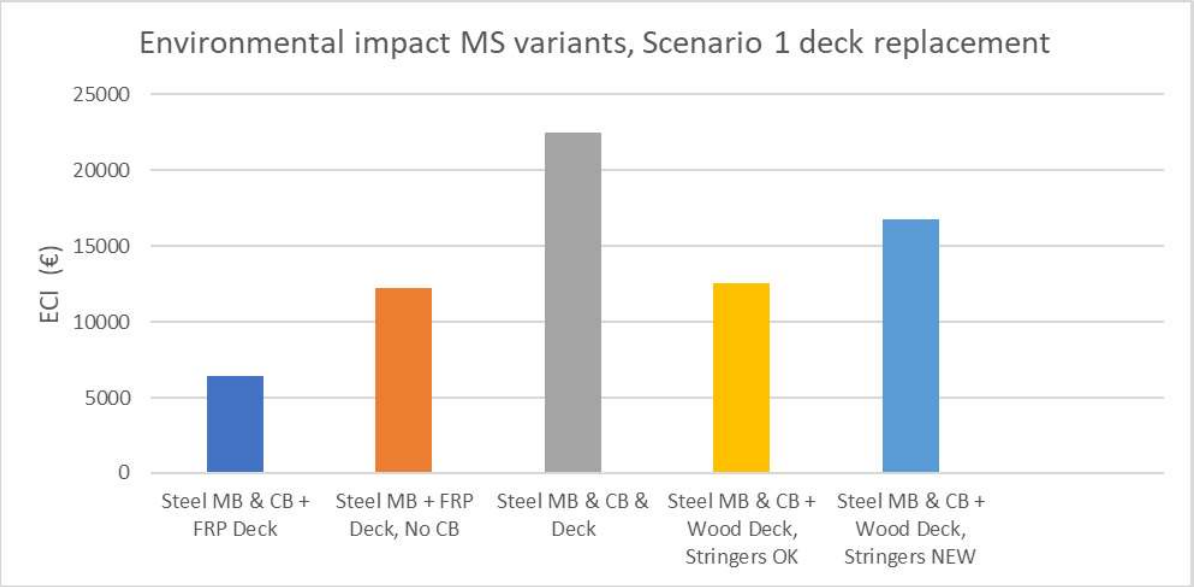

Figure 9.2, ECI comparison between MS variants, for scenario 1, deck replacement.

The mass of each variant is given in Table 9.4. All variants increase the mass of the final combinations. Replacing the wooden deck the FRP panel only increases the mass with 0.8% compared to the complete main structure. The Orthotropic steel deck or FRP deck without crossbeam increases the mass by 2.4% and 12.0%.

Table 9.4, Mass comparison between MS variants, for scenario 1, deck replacement.

MS	Wood deck	Steel orth. deck	Steel CB + FRP deck	No CB, FRP Deck
Reduction	44.1 ton	62.7 ton	44.1 ton	62.7 ton
Addition	44.1 ton	65.2 ton	44.9 ton	75.0 ton
Result	0.0 ton	+ 2.5 ton	+ 0.8 ton	+ 12.3 ton

9.2. Scenario 2, entire structure replacement

Adopting variants to fit this scenario is relatively simple. All scores are calculated for this scenario in the variant analysis. The actions required to fit each variant is thus the same.

- Current structure will need to be removed and recycled where possible.
- New structure will need to be produced, placed, and will have to be removed and recycled at the end of life.

9.2.1. Scenario 2, full replacement of foot- and cycle path

The ECI calculations have been performed for each variant and are again graphed over the lifecycle of the structure. Although removing the current structure is part of the environmental costs, for comparisons, this has been excluded, as this is the same for each variant. It is assumed that the entire structure needs to be replaced after 100 years, thus increasing the ECI significantly at the end of the lifecycle. Figure 9.3, ECI comparison between FCP variants, for scenario 2, full replacement. depict the entire ECI over the lifespan of the structure, including the entire scope of the product lifecycle (A, B, C & D).

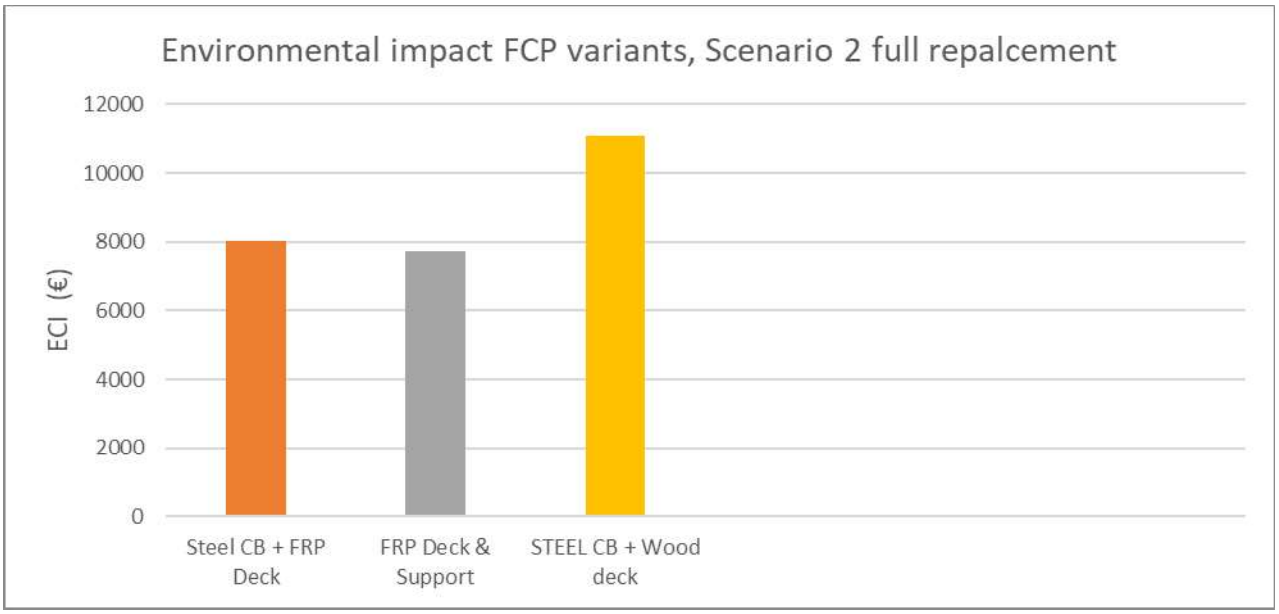

Figure 9.3, ECI comparison between FCP variants, for scenario 2, full replacement.

The mass of each variant is given in Table 9.5. The mass of each variant is reduced compared to the current structure, where the FRP deck with crossbeams or diagonal supports reduce the mass with 26.6% and 20.3% respectively.

Table 9.5, Mass comparison between FCP variants, for scenario 2, full replacement.

FCP	Base variant	Variant 1	Variant 2
Reduction	46.3 ton	46.3 ton	46.3 ton
Addition	37 ton	34 ton	36.9 ton
Result	- 9.3 ton	- 12.3 ton	- 9.4 ton

9.2.2. Scenario 2, full replacement of main structure

For the main structure the ECI calculations have again been performed for 100 years. The first variant has a negative ECI starting value, but this will not be the cast at the end of the life cycle. All variants perform significantly better than the base variant. The full FRP variants, variant 3 and 4 perform better initially, but the cost of recycling FRP diminishes their lead at the end-of-life cycle. Figure 9.4 depicts the entire ECI over the lifespan of the structure, including the entire scope of the product lifecycle (A, B, C & D).

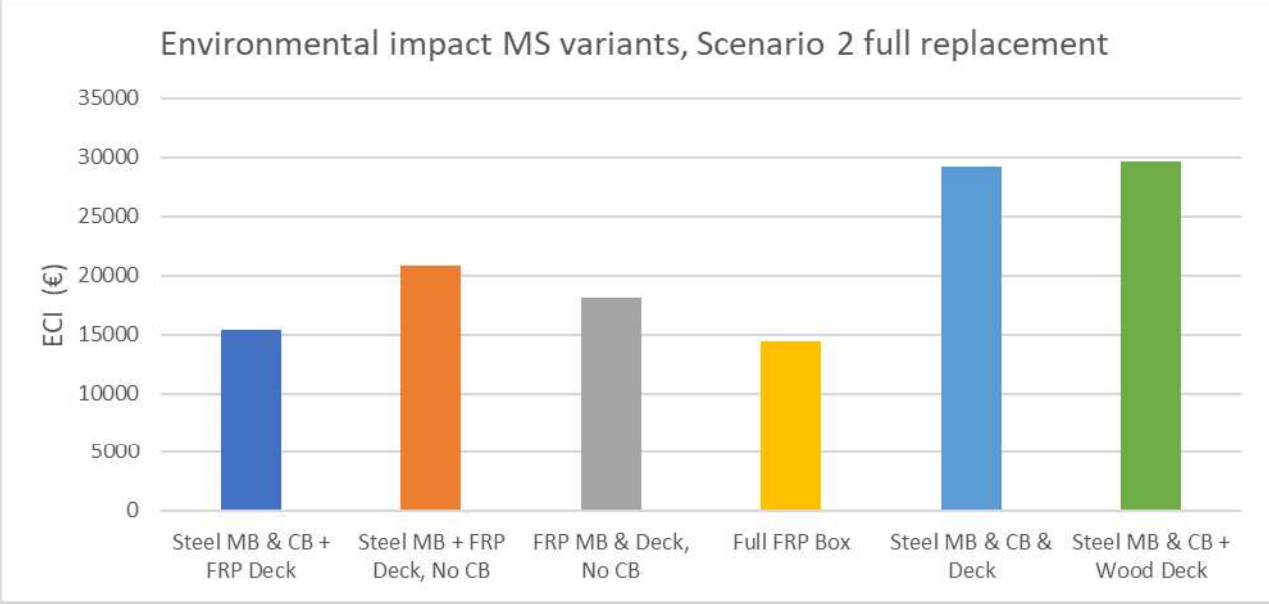

Figure 9.4, ECI comparison between MS variants, for scenario 2, full replacement.

The mass of each variant is given in Table 9.6. The masses differ strongly between different variants. Where a steel orthotropic deck results in the same mass, removing the crossbeam and replacing the deck structure with just an FRP sandwich panel will increase the mass by 11.9%. Replacing a wooden deck supported by stringers reduces the mass by 8.9%. Redesigning the main beams for FRP main beams with a single span FRP sandwich panel or FRP box structure reduces the mass by 10.3% and 35.8%.

Table 9.6, Mass comparison between MS variants, for scenario 2, full replacement.

MS	Wood deck	Steel orth. deck	Steel CB + FRP deck	No CB, Steel MB + FRP Deck	No CB, FRP MB + Deck	FRP Box
Reduction	102.8 ton	102.8 ton	102.8 ton	102.8 ton	102.8 ton	102.8 ton
Addition	102.8 ton	103.0 ton	93.0 ton	121.0 ton	92.4 ton	66.0 ton
Result	0.0 ton	+ 0.2 ton	- 9.2 ton	+ 12.2 ton	- 10.6 ton	- 36.8 ton

Part III. Conclusions

10. Summary, conclusions, and recommendations

This section will summarize and conclude all sections of this thesis. The summary consists of a concise answer to the sub questions with some extra context to highlight the findings. The conclusions consist of a concise answer to the main question.

10.1. Summary

10.1.1. Sub question 1: How should sustainability be considered to reduce the environmental and social impact of bascule bridge renewal projects?

Sustainability can be considered by applying methodologies developed by the Dutch government ("Aanpak duurzaam GWW" [96] and "Ambitieweb duurzaamheid" [25]). The methodology provided by the Dutch government ("Aanpak duurzaam GWW", translated as Approach to sustainable infrastructure) is adequate but lacks guidance for structural engineers. A structural engineer would benefit from understanding additional methodologies during the design work, to apply the goals and opportunities. The approach to sustainable infrastructure including additional guidance is explained in the following six steps.

Step 1 is to analyze the ambitions and goals. In general, for the renewal of bascule bridges, from the perspective of an engineer, important aspects are[3]:

- Energy and climate mitigation.
- Materials and circularity.
- Climate adaptation.
- Land use.
- Social value.
- Accessibility.
- Financing.

Step 2 is to analyze the opportunities of the renewal project. Opportunities for any bascule bridge may include:

- The reuse of structural elements of the current structure if the quality of the element is sufficient.
- Designing the replacement structure such that this fits inside the footprint of the current structure.
- Use of low maintenance materials.
- The reuse (or parts) of the moving mechanism. For this an analysis is necessary to determine the remaining capacity of the mechanism and its current state. For this thesis it is assumed that the mechanism is (almost) at capacity, which constraints the mass of replacement structure.

Step 3 is to describe the opportunities and ambitions. This step involves communicating found ambitions and opportunities with relevant parties to ensure that ambitions can be met, and opportunities can be applied to improve sustainability.

Step 4 is defined as: "Defining specifications and work on designs". This step is the focus for an engineer, and where more guidance is required to adequately apply the sustainability methodology. The step becomes less vague by applying methodologies such as the circular design principles. Circular design principles not only help in achieving circularity but can also be used to reduce the climate impact of renewal projects or can prevent the use of additional land.

[3] The aspects identified by this thesis will differ for different projects or organizations. Ambitions will have to be evaluated for each specific case.

Step 5 is scoring the designs on defined specifications and criteria. The step is implemented to ensure that sustainability goals and ambitions are met. This step is self-explanatory.

Step 6 is justifying the design choices. In essence, this is a continuation of the steps 4 and 5, where the best justification are the scores accumulated by step 5. This step, like step 3, focuses more on the communication aspects of the methodology.

10.1.2. Sub question 2: What materials and designs are traditionally used, and which innovative materials can be used for bascule renewal projects?

The starting point for understanding what materials were traditionally used, is an estimation in the Dutch inventory of bridges. The Netherlands has around 8500 moveable bridges, from which at least 1500 bridge large waterways. With a survey, it is estimated that around 30% to 40% of these 1500 bridges are bascule bridges, of which 50% are constructed before 1970. This date is significant because this provides insight into the age of the bridge inventory of the Netherlands and can be used to estimate the design of the structures. Many bridges constructed for Dutch roadways are relatively short, 80% have a length of at most 16 meters.

For roadway applications, by far the most common material for the main structure is steel. Steel allows for long spans with low weight, ideal for moveable bridges. Older bridges tend to be build using wooden decks. From the 1960's onward (though not instant), wooden decks fell out of use in favor for steel orthotropic decks. Initially, this was done to further reduce the mass of the bridge deck. To achieve this mass reduction, thin steel plates were used, down to 12 or even 10 mm [59].

The downside of thin steel decks is that these structures are vulnerable to metal fatigue, especially with ever increasing traffic weight and intensity. Modern steel decks, following the Dutch National annex EN 1993-2, are proposed to be 15 to 22 mm thick [59]. Modern steel decks no longer have the weight advantage because of the increased thickness.

Another downside of wooden decks is that wooden decks need to be replaced every 25 to 30 years [60]. Although a recent case, the Van Brienenoord bridge, had a wooden deck which reached a lifespan of 40 years [61]. Steel, as well as wood, requires regular maintenance, as steel without protection will corrode. Modern corrosion protection, in the form of a coating, must be renewed every 20 to 25 years [62]. Other options, such as galvanization, might increase the lifespan of the coating [63], but have much higher environmental impact [64].

A material that can provide a solution for both downsides is fiber reinforced plastics (FRP). FRP is a composite material, where fibers are bonded with a resin. The fibers have a high tensile strength but cannot be loaded in compression or shear. The combination of fibers in different direction and the bonding with resin will then provide these resistances and is called a laminate.

Fiber materials that are most used in civil engineering are glass and carbon. Glass fibers are the most common fibers in civil engineering for their low cost and environmental impact to weight ratio [69]. Carbon fibers are generally for more specialized applications, with superior strength to weight ratio [69]. The downside of carbon fibers are their higher costs [69] and environmental impact [70] next to their brittleness [69]. A relatively new fiber material is basalt, with similar structural properties to glass and possibly a lower environmental impact [73]. However, at the time of writing, basalt fibers have not been researched enough to be included in an environmental database, therefore this material has been excluded from this thesis.

Resins for engineering purposes are almost exclusively oil-based polymer products. Epoxy- and polyester resin are the most used resins. Polyester resin is usually cheaper than epoxy [83] and both resins have similar structural properties [78]. A new development is acquiring the polymers (partially) from recycled sources, also called bio resins. An example is Polynt Ecopolyester, with similar structural performance, but a 60% reduction in environmental impact [85].

An application for FRP is a composite sandwich panel, where the FRP laminates are separated by a core material. The core material creates height between the laminates to increase strength to perpendicular shear forces and stiffness. Most common core materials are oil-based foams, where foam produced from recycled plastic have a 35% reduction in environmental impact [86]. An alternative with lower environmental impact is balsa wood, as balsa has a negative environmental impact. Balsa also provides better shear and compression resistance but has 2.5 times higher density [78].

10.1.3. Sub question 3: What design variations can be made to increase the environmental and social sustainability of bascule renewal projects?

To arrive to the design variants, the methodology of sustainable design is followed. The first step is to re-evaluate the ambitions. For the case study the Oostsluisbruggen are selected because of their age and structural system. The cross section is provided in Figure 10.1.

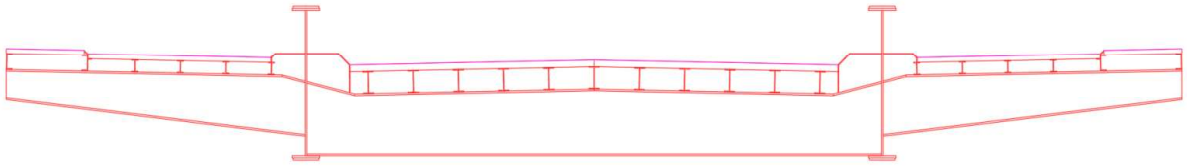

Figure 10.1, Cross section current Oostsluisbruggen.

The case study required a more refined ambition web, where the focus of the design will be on:

- Energy and climate mitigation.
- Materials and circularity.

Additionally, land use will receive thoughtful consideration.

Step two is to analyze the opportunities for the renewal of the bascule bridge. By focusing on ambitions selected in the first step, the following opportunities are identified:

- Elements of the current structure might be able to be reused. Since the lack of information on the state of the current structure, two scenarios are used to explore this opportunity.
    - Scenario 1 is that the deck needs replacement (wooden deck planks and supporting stringers)
    - Scenario 2 is that the entire structure needs replacement.
- Implementing simpler designs, such as consisted cross sections or standardized profiles reduces the costs of the structure and improves the likelihood of end-of-life reusability.
- Maintaining or reducing the mass of the structure, which can prevent the need for new or improved actuators or counterweight. A lower weight is also favorable for transport, reduces the risks of handling the structure and lowers the energy required for moving the structure.
- Designing the structure inside the current parameters (height between deck and supports, position of main beams, width of main beams), to prevent work on the basements or abutment.

Since step 3 is a communication step, for the purpose of this design study, this step is skipped and the next step to consider is step 4. To transition into the design phase, the circular design principles are applied first. The best option for reuse is the reuse of the main structure (main- and crossbeams). The current structure consists of steel main beams, crossbeams, stringers, and a wooden deck. This is displayed in Figure 10.1. The case study is compared with a bascule bridge with a steel main structure, and a steel orthotropic deck or wooden deck for the mains structure. For the FCP structure will consist of steel crossbeams and a wooden deck, shown in Figure 10.2.

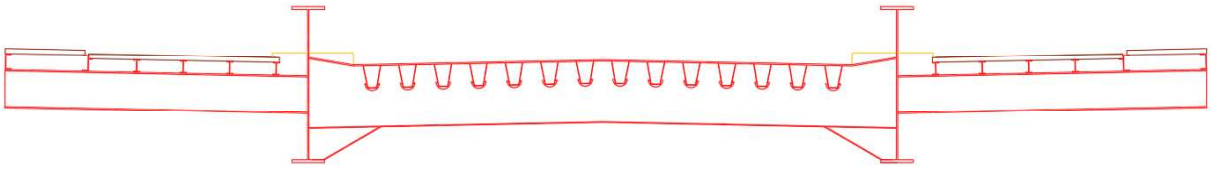

Figure 10.2, Cross section base variant, with a steel orthotropic RD and wooden FCP.

The first variant then uses these elements and replaces the deck with a composite sandwich panel. This variant can also be constructed with new main- and crossbeams. In this case the variant is slightly redesigned. Elements such as the crossbeams are simplified to increase the chance of end-of-life reuse. Completely replacing the current structure will result in the cross section presented in Figure 10.3. This is the first variant for both the main structure (main beams, including area in between main beams) and the foot- and cycle path (area outside the main beams).

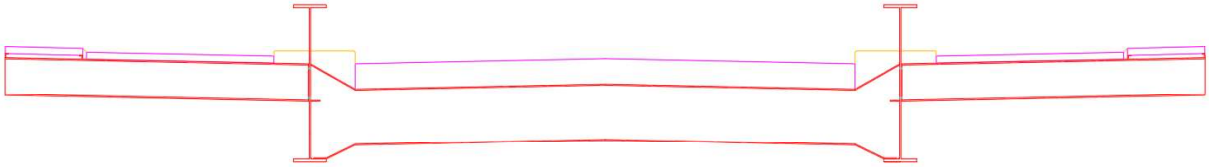

Figure 10.3, Cross section variant 1, FCP decks with steel MS.

The next variant is inspired less by the initial design. The idea for this variant is to remove the crossbeam entirely to determine if this will be beneficial for the structure. For the main structure, this results in an FRP sandwich panel that spans the main beams, where the main load path is rotated perpendicular to the main span. For the FCP structure, the crossbeam is also removed. The FRP panel will be supported by a diagonal support, which ends at the foot of the main beam. The position of the support is optimized to be placed around $3/10^{th}$ of the width from the edge, as shown in Annex 1. This results in the following cross section, displayed in Figure 10.4. Point of note is that with minor adaptations, the crossbeam with FRP deck FCP structure could also be used.

Figure 10.4, Cross section variant 2, FCP decks, no crossbeams and steel main beams.

The following variant is to explore the possibility of replacing the steel main beams with FRP main beams. The change from steel to FRP results in the need for larger main beams to maintain the same strength. The choice has been made to increase the height of the main beams between the spans, to reduce the material needed for the main beams. Again, for the FCP decks both designs are possible to apply. This results in the following cross section, displayed in Figure 10.5.

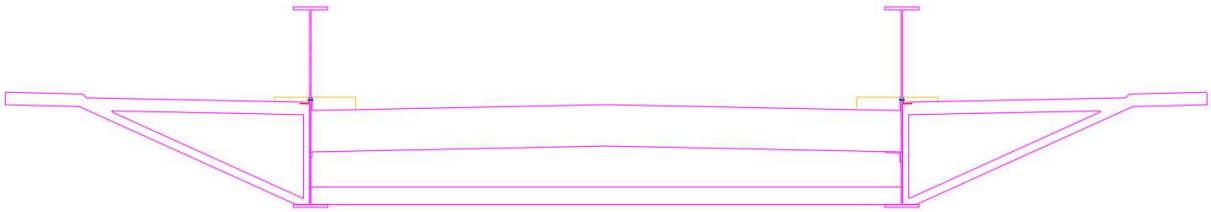

Figure 10.5, Cross section variant 3, FCP decks and main beams, no crossbeams.

For the final variant, the free form possibilities of FRP are further considered. The top flanges of the main beams are removed, and this functionality is transferred to the top laminate of the deck. To enable the deck to participate in the main span, multiple webs are placed between the deck and a bottom flange, which spans the width between the main beams. A transverse beam at the joint is required to enable these webs to participate, and cross webs are required for stability. The outer webs and a part of the flange around these webs are stronger to function as arms for opening the structure. Again, for the FCP decks both designs are possible to apply. This results in the following cross section, displayed in Figure 10.6.

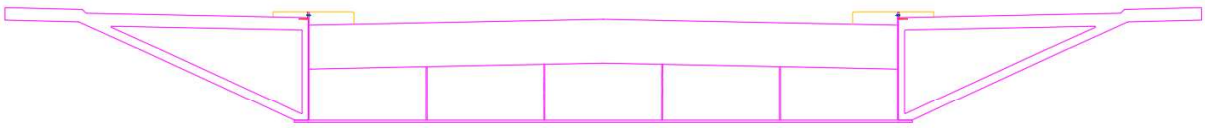

Figure 10.6, Cross section variant 4, FCP decks and box MS.

Step 5 of the methodology is to assess the design based on parameters set during the ambition study. Analyses performed in sections 7 to 9 shows that, given a scenario, optimizations are possible for all ambitions. Following the scenarios discussed in step two, possible optimizations are summarized in Table 10.1.

Table 10.1, Possible optimizations based on variant comparisons and scenarios.

Ambition	Scenario 1: Renewal of the deck	Scenario 2: Replacement of full structure
Environmental impact	Reduction of 37 % to 53% of ECI based on the state of the stringers. The current structure can be maintained, and the deck elements are replaced for FRP sandwich panels.	Reduction of 48% of ECI. The entire structure is replaced by an FRP box structure where the FCP paths are designed as FRP sandwich panels with diagonal FRP supports.
Materials and circularity	The structure can be designed such that at the end of lifespan each element can be separated and possible reused. The chances of reuse are maximized by standardized designs and constant cross sections. FRP on is currently poorly recyclable, but significant research into this field is taking place.	
Land use	Almost all structures can be fit within the current form factor or mass constraints (see next row). The exception for this is the FRP main beam variant, with the single span FRP deck. This variant requires stronger main beams, and the choice for higher beams have been made to reduce the materials used. This is only necessary in the span, thus for the moving arms the variant fits in the constraints, and thus has no influence on the surrounding infrastructure.	
Mass (not a direct ambition, but interesting due to influence on different ambitions)	Mass is not a defining factor for any of the variants, where the variant without crossbeam for the main structure does not satisfy the mass constraints. Significant mass reductions are not possible.	Mass is not a defining factor for any of the variants, where the combination of FCP and main structure always satisfy the mass constraints. Significant mass reductions are possible, up to 33%, in the case of an FRP box main structure and crossbeam with FRP sandwich panel FCP structure.

10.2. Conclusions

This section will provide an answer to the main research question, which is:

To what extent does the use of FRP and optimizing for environmental and social sustainability reduce the impacts of a bascule bridge renewal project?

To answer the main question, context is provided on how sustainability has been included into the design process. Adopting the design for sustainability methodology from the Dutch government provides the basis for optimizing for sustainability. On a step-by-step basis, goals and ambitions are defined, opportunities are analyzed and included in the design process. The traditional design process is modified to include sustainability requirements and follow the circular design principles.

The ambition for the design study was to optimize for a reduction of environmental impact and circularity, while also considering land use, or rather preventing additional work to surrounding infrastructure. The analysis of the opportunities highlighted aspects which are well suited to the material properties of fiber reinforced plastics (FRP). FRP can be used to decrease the mass of the structure, while requiring less maintenance. Using bio-based materials has resulted in the use of balsa and partly circular resin, with recycled PET ingredients. Simplifying designs and optimizing for reuse of elements have resulted in constant cross section elements, which are demountable. Preliminary traditional designs, in steel and steel with wooden decks, have been compared with preliminary designs with the use of FRP, for both the main structure as the foot- and cycle path (FCP). Designs have been exclusively made for the bridge leaf.

The environmental impact has been assessed using the environmental costs indicator (ECI). For the ECI, the entire lifecycle is considered, including recycling at the end of the lifecycle. Two scenarios have been assessed, one where only the deck needs replacement, and one where the entire bridge leaf is replaced. When only the bridge deck needs replacement, the consequences over a 100-year lifespan for the bridge leaf are: A reduction in ECI by 37%, by constructing an FRP deck, compared to replacing the wooden deck, when the stringers are reusable.

- A reduction in ECI by 53%, by constructing an FRP deck, compared to replacing the wooden deck, when the stringers are not reusable.
- No reduction of weight can be realized when just replacing the deck.

When the entire structure needs replacement, the consequences over a 100-year lifespan for the bridge leaf are:

- Neither a reduction nor an increase in ECI, by constructing a steel main structure with a steel orthotropic deck, compared to a wooden deck.
- A reduction in ECI by 48%, by constructing a full FRP bridge leaf, compared to constructing a steel main structure, with either a wooden or steel orthotropic deck.
- A reduction of 33% of the weight of the structure compared to the current bridge leaf.

Another result of the design study is that fully circular designs are not possible for FRP, as FRP is currently not recyclable. It is possible to optimize the design for likelihood of reuse, by simplifying the design and making the individual elements separable. Finally, it is possible to design a renewal structure, without having to make modifications to the surrounding infrastructure.

The reduction in impacts stated above only consider the bridge leaf itself. Considering the bascule bridge, the weight of the bridge leaf can lead to the reuse of- or allow for less environmental impact compared to the current actuators and counterweight.

As a final conclusion, FRP is a promising material for bascule bridge renewal projects, although challenges remain for the circularity of FRP. A significant reduction in environmental impact can be reached by applying the right methodology, using materials with favorable ECI scores, such as balsa

and low impact resin, optimizing the design for material usage, and finally, constraining the design to the dimensions of the current bascule bridge.

10.3. Recommendations for future research

Sustainable design processes and renewal projects are ever evolving subjects. The importance of these topics is also becoming increasingly apparent. This thesis aimed to incorporate a sustainable methodology in renewal projects. The following recommendations will aim to inspire future research projects in this field.

10.3.1. Sustainability

While working on this thesis some sustainability questions remained but were out of the scope of this study or are not relevant for an engineer. For future research, the logical first research project is the application of the design for sustainability methodology on other case studies. This case study allowed for the eliminations of sustainability aspects, such as nuisance, future proofing, or climate adaptation, that are very relevant for civil engineering projects. Therefore, it is important to reconsider each aspect for each case study.

10.3.2. FRP

One improvement with high potential for reducing the environmental impact of bascule bridges is basalt. Highlighted in the literature review, this material promises a serious reduction in environmental impact of FRP, while having better structural performance. The material, as stated previously, was emitted from the project because of the lacking information on climate mitigation. If enough research on basalt fibers allows basalt to be included in environmental databases, the design of FRP bridges with basalt might reduce the total impact of bascule bridge renewal projects further.

Another innovation that can lead to lower environmental impact of FRP in bascule bridges is recyclability. Currently, as highlighted in the literature review, methods for recycling are limited. Improvements in this field rapid, as the wind energy industry has very large incentives for this innovation. The civil engineering field can benefit from the efforts of the wind energy industry. If FRP is separable in its constituent parts, infinite lifecycles might be feasible, requiring minimal new materials. Current technology can recover the fibers, potentially at their original mechanical properties. Innovation is required to also allow for the recovery of the resin at their original material properties. However, the technology is currently not readily available on an industrial scale. These combined innovations will allow for FRP bascule bridges with a lower environmental impact.

10.3.3. Designs

The designs in this study were based on analytical models, for which simplifications were made. Due to the limited time available, no finite element analyses were performed. The use of FEM will allow for more optimized designs. Next to this, more concepts such as an FRP deck with FRP supports for the main structure (like the FCP deck) might provide further optimizations. Finally, not all loads were analyzed such as fatigue, local failures for the FRP sandwich panel, or local failures for the steel plates. Definitive designs are required to fully assess the impact of FRP in bascule bridge renewal projects.

Next to this, the scope of this thesis was limited to the bridge leaf. While surrounding infrastructure and the actuators were accounted for with additional checks, including these elements into the designs will provide a more complete overview of the impact of FRP in bascule bridge renewal projects.

11. Bibliography

[1] Haasnoot, "Aantal bruggen in Nederland," 22 02 2024. [Online]. Available: https://haasnootbruggen.nl/hoeveel-bruggen-telt-nederland.

[2] CBS, "Trends in the Netherlands," 2018. [Online]. Available: https://longreads.cbs.nl/trends18-eng/society/figures/traffic/.

[3] UN environment programme, "2022 global status report for buildings and construction," globalabc, 2022.

[4] IEA, "Pathway to critical and formidable goal of net-zero emissions by 2050 is narrow but brings huge benefits, according to IEA special report," 18 05 2021. [Online]. Available: https://www.iea.org/news/pathway-to-critical-and-formidable-goal-of-net-zero-emissions-by-2050-is-narrow-but-brings-huge-benefits.

[5] M. Amelink, "Betrouwbare bruggen voor een bereikbaar Nederland," RWS, Utrecht, 2015.

[6] G. Marsh, "50 years of reinforced plastic boats," 08 10 2006. [Online]. Available: http://www.reinforcedplastics.com/view/1461/50-years-of-reinforced-plastic-boats-.

[7] J. C. Moen, "Feasibility study on heavy-traffic fiber reinforced polymer (FRP) bascule bridges," TU Delft, Delft, 2014.

[8] D. Agenda, "This is the next hurdle in the construction industry's race to net-zero," 20 09 2022. [Online]. Available: https://www.weforum.org/agenda/2022/09/construction-industry-zero-emissions/.

[9] S. R. Duwadi and M. A. Ritter, "Timber Bridges In The United," Public Roads, 33, 1997.

[10] K. Geissler, "Assessment of old steel bridges, germany," *Structural engineering international,* vol. 12, no. 4, pp. 258-263, 2002.

[11] D. Mouroulis, "A Feasibility Study on Weight Saving in Bascule Bridge Design by Implementing an FRP-deck," Movares/Tu Delft, Delft, 2018.

[12] K. Abbass, M. Z. Qasim, H. Song, M. Murshed, H. Mahmood and I. Younis, "A review of the global climate change impacts, adaptation,," *Environmental Science and Pollution Research, Volume 29,* pp. 42539-42559, 2022.

[13] L. Berrang-Ford, J. D. Ford and J. Paterson, "Are we adapting to climate change?," *Global Environmental Change 21,* pp. 25-33, 2011.

[14] Cambridge Dictionary, Sustainability, Cambridge: Cambridge Dictionart, 2024.

[15] K. E. Portney, Sustainability, Cambridge, Massachusetts: The MIT Press, 2015.

[16] J. L. Caradonna, Sustainability, A history, Oxford: Oxford university Press, 2022.

[17] Brundtland Report, "Our Common Future," United Nations, 1987.

[18] M. Joseph J. Bish, "ECONOMIC SUSTAINABILITY EXAMPLES THAT INSPIRE CHANGE," 04 02 2021. [Online]. Available: https://www.populationmedia.org/the-latest/what-is-economic-sustainability.

[19] D. Doana and A. MacGillivray, "Economic Sustainability, The business of staying in business," New Economics Foundation, The Sigma project, 2001.

[20] S. E. Place, "4 - Animal welfare and environmental issues," *Woodhead Publishing Series in Food Science, Technology and Nutrition,* pp. 69-89, 2018.

[21] B. Elleuch, F. Bouhamed, M. Elloussaief and M. Jaghbir, "Environmental sustainability and pollution prevention," Environ Sci Pollut Res, Sfax, Tunisia, 2017.

[22] ADEC, "ESG," 26 02 2024. [Online]. Available: https://www.adecesg.com/resources/faq/what-is-social-sustainability/.

[23] C. Berlin and C. Adams, " Social Sustainablity," in *Production Ergonomics: Designing Work Systems to Support Optimal Human*, London, Ubiquity Press, 2017, pp. 241-258.

[24] M. T. Tiza, E. I. Ogunleye, V. Jiya, C. Onuzulike, E. Akande and T. Sesugh, "Integrating Sustainability into Civil Engineering and the Construction Industry," *Journal of Cement Based Composites 4,* p. 5756', February 2023.

[25] CROW, "Ambitie web," Dutch Government, 28 January 2024. [Online]. Available: https://www.duurzaamgww.nl/documenten/58-ambitieweb. [Accessed 17 September 2024].

[26] L. Kok and M. Gijp, "Tools voor Maatschappelijk Verantwoord Inkopen," Rijkswaterstaat, Utrecht, Nederland, 2016.

[27] J. Hammervold, M. Reenaas and H. Brattebø, "Environmental Life Cycle Assessment of Bridges," *Bridge Eng. 18(2),* pp. 153-161, 2013.

[28] Nationale Milieu Database, "Bepalingsmethode Milieuprestatie Bouwwerken / versie 1.1," Stichting nationale milieudatabase, Rijswijk, 2022.

[29] E. Bontempti, Raw Materials Subitution Sustainability, Cham, Switzerland: Springer, 2017.

[30] Camebridge Dictionairy, Camebridge Dictionairt, Camebridge: University of Camebridge, 2024.

[31] Eurostat, "Generation of waste by economic activity," 29 02 2024. [Online]. Available: https://ec.europa.eu/eurostat/databrowser/view/ten00106/default/table?lang=en&category=t_env.t_env_was.t_env_wasgt.

[32] P. V. Sáez, "A diagnosis of construction and demolition waste generation and recovery practice in the European Union," *Journal of Cleaner Production, Volume 241,* 2019.

[33] Woodbeaver, "Wood: A Renewable Resource or a Nonrenewable Commodity?," Woodbeaver, [Online]. Available: https://woodbeaver.net/wood-a-renewable-resource-or-a-nonrenewable-commodity/. [Accessed 18 11 2024].

[34] E. H. J. &. B. N. (. Achterberg, "Master circular business models with the Value Hill.," Circle Economy, Utrecht, 2016.

[35] M. Dittrich, "Acoustic characteristics and noise control measures for steel road bridges," in *Euronoise* , Crete, 2018.

[36] S. Taylor, M. Barret, G. Ward, M. Leisenring, M. Venner and R. Kilgore, "Bridge Stormwater Runoff Analysis and Treatment Options," Transportation Research Board, Washington D.C., 2014.

[37] Z. Culter, T. Dayton, M. Grant, S. Mahomed and J. Ojetayo, "Reducing embodied carbon in new construction," 17 11 2022. [Online]. Available: https://www.mckinsey.com/industries/travel-logistics-and-infrastructure/how-we-help-clients/global-infrastructure-initiative/voices/reducing-embodied-carbon-in-new-construction. [Accessed 24 09 2027].

[38] O. U. Rehman and M. J. Ryan, "A framework for design for sustainable future-proofing," *Journal of Cleaner Production,* vol. 170, pp. 715-726, 2018.

[39] C. Labuschange and A. C. Brent, "Assessing the sustainability performances of industries," *Journal of Cleaner Production Volume 13, Issue 4,* pp. 373-385, 2005.

[40] Y. J. Kim, "State of the practice of FRP composites in highway bridges," *Engineering Structures, Volume 179,* pp. 1-8, 2019.

[41] Eurostat, "Accidents at work statistics," October 2023. [Online]. Available: https://ec.europa.eu/eurostat/statistics-explained/index.php?title=Accidents_at_work_statistics#Number_of_accidents.

[42] R. A. Haslam, S. A. Hide, A. G. Gibb, D. E. Gyi, T. Pavitt, S. Atksinson and A. R. Duff, "Contributing factors in construction accidents," *Applied Ergonomics, Volume 36, Isseu 4,* pp. 401-415, 2005.

[43] M. I. Banton, J. S. Bus, J. J. Collins, E. Delzell, H.-P. Gelbke, J. E. Kester, M. M. Moore, R. Waites and S. S. Sarang, "Evaluation of potential health effects associated with occupational andenvironmental exposure to styrene–an update," *JOURNAL OF TOXICOLOGY AND ENVIRONMENTAL HEALTH, VOL. 22, NOS. ,* pp. 1-130, 2019.

[44] J. Sharman, "12 of the biggest health and safety risks in construction," NBS, 26 March 2018. [Online]. Available: https://www.thenbs.com/knowledge/12-of-the-biggest-health-and-safety-risks-in-construction. [Accessed 15 11 2024].

[45] R. Sarker, S. M. Ali, S. K. Paul and Z. H. Munim, "Measuring sustainability performance using an integrated model," *Measurement,* vol. 184, 2021.

[46] S. Rajabi, S. El-Sayegh and L. Romdhane, "Identification and assessment of sustainability performance indicators for construction projects," *Environmental and sustinability indicators,* vol. 15, 2022.

[47] Online-ISO, "Wat Is Maatschappelijk Verantwoord Ondernemen En Waarom Is Het Belangrijk?," Online-ISO, [Online]. Available: https://www.online-iso.nl/iso-26000/wat-is-maatschappelijk-verantwoord-ondernemen-en-waarom-is-het-belangrijk/.

[48] A. Torti, M. Arena, G. Azzone, P. Secchi and S. Vantini, "Bridge closure in the road network of Lombardy: a spatio-temporal analysis of the socio-economic impacts," *Statistical methods adn applications,* vol. 31, pp. 901-923, 2022.

[49] S. B. Borad, "Life Cycle Cost – Meaning, Importance, Analysis and More," may 2021. [Online]. Available: https://efinancemanagement.com/costing-terms/life-cycle-cost.

[50] D. Macek and V. Snížek, "Innovation in bridge life-cycle cost assesment," ScienceDirect, Elsevier, Primosten, Croatia, 2017.

[51] J. P. Zaniewski, B. C. Butler, G. Cunningham, G. E. Elkins, M. S. Paggi and R. Machemehl, "Vehicle operating costs, fuel consumpion, and pavement type and condition factors," Department of Transporation, Fedeal Highway Administration, Austin, Texas, 1982.

[52] I. Zaabar and K. Chatti, "Estimating Vehicle Operating Costs Caused by Pavement Sufrace conditions," *Sage Jorunal ,* pp. Volume 2455, issue 1, 2014.

[53] Global petrol prices, "Netherlands Gasoline prices," 26 02 2024. [Online]. Available: https://www.globalpetrolprices.com/Netherlands/gasoline_prices/.

[54] G. Erbach, "CO2 emission standards," European Parliamentary Research Service, 2023.

[55] D. Kim, Y. Zhao, M. O. Rodgers and R. Guensler, "Personal Vehicle Ownership and Operating Cost Calculator," National center for sustainable transport, Atlanta, Georgia, 2018.

[56] Composites UK, "Life Cycle Cost of FRP Structures," Composites UK, Berkhamsted, 2016.

[57] A. N. Bleijenberg, "TNO 2021 R10440A Instandhouding infrastructuur Proeve can landelijk prognoserapport vervanging en renovatie," TNO, Delft, 2021.

[58] Rijkswaterstaat, "Bruggen," Rijkswaterstaat, [Online]. Available: https://www.rijkswaterstaat.nl/wegen/wegbeheer/bruggen. [Accessed 04 04 2024].

[59] W. Wu, "Orthotropic Steel Decks," Tu Deflt, [Online]. Available: https://www.tudelft.nl/en/ceg/about-faculty/departments/engineering-structures/sections-labs/steel-and-composite-structures/research/research-lines/orthotropic-steel-decks. [Accessed 7 11 2024].

[60] Rijkswaterstaat , "FACTSHEET DETAILLERING EN ONDERHOUD VAN HOUTEN BRUGGEN," Rijkswaterstaat, Utrecht.

[61] A. v. Eckeveld, "Houten verkeersbruggen," Innovita adives & projectbegeleiding, 2020.

[62] Nationale Millieu Database, "Conservering, onderdeel stalen verkeersportaal, per m2 conservering met een technische levensduur van 20 jaar.," NMD, 13 03 2024. [Online]. Available: https://milieudatabase.nl/nl/viewer/milieuverklaring/nmd_37811/. [Accessed 07 11 2024].

[63] J.-B. Song, L.-S. Wang, H. Dong and J.-T. Yao, "Long lifespan thermal barrier coatings overview: Materials, manufacturing, failure mechanisms, and multiscale structural design," *Ceramics International,* vol. 49, no. 1, pp. 1-23, January 2023.

[64] Nationale Milieu Database, "Thermisch verzinken, toepassing in kustgebied," NMD, 03 06 2022. [Online]. Available: https://milieudatabase.nl/nl/viewer/milieuverklaring/nmd_54881/. [Accessed 07 11 2024].

[65] R. R. Nagavally, "COMPOSITE MATERIALS - HISTORY, TYPES, FABRICATION TECHNIQUES, ADVANTAGES, AND APPLICATIONS," in *29th IRF International Conference*, Bengaluru, India, 2016.

[66] Z. U. Arif, M. Y. Khalid, W. Ahmed, H. Arshad and S. Ullah, "Recycling of the glass/carbon fibre reinforced polymer composites: A step towards the circular economy," *Polymer-Plastics Technology and Materials,* vol. 61, no. 7, pp. 761-788, 2022.

[67] B. Yang, L. Wang, J. Luo, L. Zhaoqing and X. Ding, "Fabrication, Applications, and Prospects of Aramid Nanofiber," *Advanced Funtional materials,* vol. 30, no. 22, 2020.

[68] T. P. Sathiskumar, S. Satheeskumar and J. Naveen, "Glass fiber-reinforced polymer composites – a review," *Journal of Reinforced Plastics and Composites,* vol. 33, no. 13, 2017.

[69] NitPro, "Carbon Fiber Vs. Fiber Glass: What's the Difference," NitPro, [Online]. Available: https://www.nitprocomposites.com/blog/carbon-fiber-vs-fiber-glass#:~:text=Carbon%20fiber%20is%20incredibly%20strong%20and%20lightweight%2C%20making,it%20suitable%20for%20applications%20that%20require%20impact%20resistance.. [Accessed 07 11 2024].

[70] F. Hermansson, S. Heimersson, M. Janssen and M. Svanström, "Can carbon fiber composites have a lower environmental impact than fiberglass?," *Resources, Conservation and Recycling,* vol. 181, p. Volume 181, June 2022.

[71] B. A. Newcomb, "Processing, structure, and properties of carbon fibers," *Composites Part A: Applied Science and Manufacturing,* vol. 91, 2016.

[72] K. Singha, "A Short Review on Basalt Fiber," *International Journal of Textile Science* , vol. 4, pp. 19-28, 2012.

[73] J. Praveenkumara, S. M. Rangappa and S. Siengchin, "Basalt fibers: An environmentally acceptable and sustainable green material for polymer composites," *Construction and Building Materials,* p. Volume 436, 19 July 2024.

[74] A. Pavlovic, T. Donchev, D. Petkova and N. Staletovic, "Sustainability of alternative reinforcement for concrete structures: Life cycle assessment of basalt FRP bars," *Construction and Building Materials,* vol. 334, 2022.

[75] Material-properties, "Kevlar – Material Table – Applications – Price," Material properties, [Online]. Available: https://material-properties.org/kevlar-properties-application-price/?utm_content=cmp-true. [Accessed 19 11 2024].

[76] Teijin, "Teijin Sustainability report," Teijin, 2021.

[77] A. Gholampour and T. Ozbakkaloglu, "A review of natural fiber composites: properties, modification and processing techniques, characterization, applications," *Journal of Materials Science,* vol. 55., pp. 829-892, 2019.

[78] CEN members, "Design of fibre-polymer composite structures," UNI, Brussels, 2022.

[79] W. Wu, "Mechanical Performance/Cost Ratio Analysis of Carbon/Glass Interlayer and Intralayer Hybrid Composites," *Coatings,* p. 810, 28 June 2024.

[80] Ecochain, "Ecochain environmental impact calculator," Mobius, [Online]. Available: https://mobius.ecochain.com/. [Accessed 19 11 2024].

[81] V. Fiore, T. Scalici, G. Di Bella and A. Valenza, "A review on basalt fibre and its composites," *Composites Part B: Engineering,* pp. 74-94, 1 June 2015.

[82] E. Morici and N. T. Dintcheva, "Recycling of Thermoset Materials and Thermoset-Based Composites: Challenge and Opportunity," *Polymers,* vol. 14, no. 19, 2022.

[83] A. v. Schoor, "Polyester Resin vs. Epoxy Resin – Differences Explained," Resin Expert, 1 Februari 2022. [Online]. Available: https://resin-expert.com/en/guide/polyester-resin-vs-epoxy-resin. [Accessed 07 11 2024].

[84] V. Chaudhary and F. Ahmad, "A review on plant fiber reinforced thermoset polymers for structural and frictional composites," *Polymer testing,* vol. 91, 2020.

[85] Polynt Composites, "Compounds Eco-friendly solution," Polynt Reichhold Group, Scanzorosciate, 2021.

[86] ArmaCell, "ArmaPET Struct GR," Armacell, Global, 2021.

[87] A. Rizov, A. Shipsa and D. Zenkert, "Indentation study of foam core sandwich composite panels," *Composite Structures,* vol. 69, no. 1, pp. 95-102, 2005.

[88] J. Galos, R. Das, M. P. Sutcliffe and A. P. Mouritz, "Review of balsa core sandwich composite structures," *Materials & Design,* vol. 221, 2022.

[89] I. Julian, A. Garciá-Jiménez, A. Aguado, C. Arenal, A. Calero, V. Campos, G. Escobar, A. López-Buendía, D. Romero, E. Verdejo and N. García-Polanco, "Advances in the circularity of end-of-life fibre-reinforced polymers by microwave intensification," *Chemical Engineering and Processing - Process Intensification,* p. Volume178, August 2022.

[90] A. Pegoretti, "Towards sustainable structural composites: A review on the recycling," *Advanced Industrial and Engineering Polymer Research,* vol. 4, pp. 105-115, 2021.

[91] F. Meng, E. A. Olivetti, Y. Zhao, J. C. Chang, S. J. Pickering and J. McKechnie, "Comparing Life Cycle Energy and Global Warming Potential of Carbon Fiber Composite Recycling Technologies and Waste Management Options," *ACS Sustainable Chemistry & Engineering,* vol. 6, no. 8, 2018.

[92] L. Giorgini, T. Benelli, G. Brancolini and L. Mazzocchetti, "Recycling of carbon fiber reinforced composite waste to close their life cycle in a cradle-to-cradle approach," *Green and Sustainable Chemistry,* vol. 26, 2020.

[93] F. A. López, O. Rodrígiez, F. J. Alguacil, I. García-Díax, T. A. Centeno, J. L. García-Fierro and C. González, "Recovery of carbon fibres by the thermolysis and gasification of waste prepreg," *Journal of Analytical and Applied Pyrolysis,* vol. 104, pp. 675-863, 2016.

[94] A. E. Krauklis, C. W. Karl, A. I. Gagani and J. K. Jørgensen, "Composite Material Recycling Technology—State-of-the-Art and Sustainable Development for the 2020s," *Journal of Composites Science,* vol. 5, no. 28, 2021.

[95] U. Shubham, V. K. Suriya, M. Neha and R. Adarsh, "Comprehensive study of recycling of thermosetting polymer composites – Driving force, challenges and methods," *Composites Part B,* vol. 207, 2021.

[96] Ministerie van Infrastructuur en Milieu, "Aanpak duurzaam GWW," Ministerie van Infrastructuur en Milieu & Unie can Waterschappen, Den Haag, 2016.

[97] Rijkswaterstaat, "Circulaire ontwerp-principes," Rijkswaterstaat, Utrecht, 2020.

[98] i. E. Fiktorie, "Deelrapport MER Hoogwater-veiligheid," Vlaams-Nederlandse Scheldecomissie, Bergen op Zoom, 2015.

[99] d. F. Vanweert, "Deelrapport MER Verkeer en vervoer," Vlaams-Nederlandse Scheldecommissie, Bergen op Zoom, 2015.

[100] Stichting Koninklijk Nederlands Normalisatie Instituut, "NEN norms," Nen Connect, Delft.

[101] Stichting Koninklijk Nederlands Normalisatie Instituut, "NEN EN 1991-1-1+C1+C11:2019," NEN Connect, Deflt, 2019.

[102] Stichting Koninklijk Nederlands Normalisatie Instituut, "NEN-EN 1991-2+C1:2015," NEN Connect, Delft, 2015.

[103] M. Chairi, J. El Bahaoui, I. Hanafi, F. Favaloro, C. Borsellino, F. Galantini and G. Di Bella, "The effect of span length on the flexural properties of glass and basalt fiber reinforced sandwich structures with balsa wood core for sustainable shipbuilding," *Composite Structures,* vol. 340, pp. 1-18, 2024.

[104] J. Galos, R. Das, M. P. Sutcliffe and A. P. Mouritz, "Review of balsa core sandwich composite structures," *Materials & Design,* vol. 221, no. 111013, 2022.

[105] "Mechanical properties of a balsa wood veneer structural sandwich core material," *Construction and Building Materials,* vol. 265, no. 120193, 2020.

[106] EuRIC, "Metal Recycling Factsheet," EU, Brussels, 2019.

[107] Nationale Milieu Database, "Database viewer," NMD, 24 10 2024. [Online]. Available: https://milieudatabase.nl/nl/viewer/.

[108] Ecoinvent, "Database search," EcoQuery, 24 10 2024. [Online]. Available: https://ecoquery.ecoinvent.org/3.10/cutoff/search.

[109] 3A Composites Core Materials, "BALTEK® SBC & SB (CK LP) balsa wood core material," EPD International AB, 20023.

[110] Polynt, *Polynt Biobased polyester,* Scanzorosciate: Polynt SpA , 2024.

[111] G. S. R. Á. L. A. M. Antón, "Financial risks in construction projects," African Jorunal of Business Management, 2011.

[112] M. S. G. S. S. K. N. P. C. Sukanya Mehra, "Impact of construction material on environment," Ecological and Health Effects of Building Materials, 2021.

[113] S. K. Y. A. Tolga Celik, "Social cost in construction projects," Environmental Impact Assessment Review, 64, 77-86., 2017.

[114] Mar Delos Reyes, "3 Principles of Sustainability: Building a Greener Future," 14 12 2023. [Online]. Available: https://sustainabilityeducationacademy.com/3-principles-of-sustainability-building-a-greener-future/#:~:text=The%203%20principles%20of%20sustainability%20are%20environmental%20sustainability%2C%20social%20sustainability,our%20planet%20and%20its%20inhabita.

[115] J. Elkington, "Cannibals with Forks: The Triple Bottom Line of 21st Century Business," New Society Publishers, Gabriola Island, BC Stony Creek, 1998.

[116] A. Das, "Economic Sustainability Considerations in Asphalt Pavement," in *Sustainability Issues in Civil Engineering*, Singapore, Springer, 2017, pp. 61-72.

[117] K. G. Abraham and J. Mallatt, "Measuring human capital," *Jorunal of economic perspectives,* vol. 36, no. 3, pp. 103-30, 2022.

[118] N. Angrist, S. Djankov, P. Goldberg and H. A. Patrinos, "Measuring Human Capital," SSRN, 2019.

[119] J. D. F. Vidotto, H. A. Ferenhof, P. M. Selig and R. C. Bastos, "A human capital measurement scale," *Jorunal of intellectual capital,* vol. 18, no. 2, pp. 316-329, 2017.

[120] M. Warner, "Social Capital Construction and the Role of the Local State," *Rural Sociology,* vol. 64, no. 3, pp. 373-393, 2009.

[121] F. Baldi and L. Trigeorgis, "Valuing human capital career development: a real options approach," *Jurnal of Intellectual Capital,* vol. 21, no. 5, pp. 781-807, 2020.

[122] C. Bakker and R. Mugge, "Duurzaamheid is een werkwoord," TU Delft, 03 05 2019. [Online]. Available: https://www.tudelft.nl/io/delft-design-stories/duurzaamheid-is-een-werkwoord. [Accessed 01 08 2024].

[123] Nationale milieu database, "Staal constructieprofielen (HEA/HEB/HEM/IPE/UNP)," NMD, 24 11 2023. [Online]. Available: https://milieudatabase.nl/nl/viewer/milieuverklaring/nmd_90901/.

[124] Nationale milieu database, "Conservering, onderdeel stalen verkeersportaal, per m2 conservering met een technische levensduur van 20 jaar.," NMD, 13 03 2024. [Online]. Available: https://milieudatabase.nl/nl/viewer/milieuverklaring/nmd_37811/.

[125] Nationale milieu database, "Kunststof van sluisdeur, type 'rolsluisdeur', herkomst Europa, per kg kunststof, met een technische levensduur van 15 jaar.," NMD, 05 07 2021. [Online]. Available: https://milieudatabase.nl/nl/viewer/milieuverklaring/nmd_36996/.

[126] N. Jungbluth, "glass fibre production," Ecoinvent, 25 02 2011. [Online]. Available: https://ecoquery.ecoinvent.org/3.10/cutoff/dataset/8360/documentation.

[127] J. Fort, J. Koci and R. Cerny, "Environmental Efficiency Aspects of Basalt Fibers Reinforcement in Concrete Mixtures," *Energies,* vol. 14, no. 22, p. 7736, 2021.

Part IV. Appendix

Appendix I, Support position FCP variant 2.

11.1. Introduction

This annex shows the calculations to determine the position of the support for the FCP variant 2. To determine the position of the support, multiple assumptions are made. These assumptions are:

- The current deck profile (position of foot and cycle path) is maintained, this has the consequence of the inability of any load to be placed any closer than 0.7m from the main beam.

- No wheel load can be placed any closer than 0.6m (0.5m + 0.1m) from the edge of the beam

- The concentrated loads are governing for the force distribution in the plates (the distributed loads are analyzed too).

- Although the supports are not continuous, they are assumed as continuous for these calculations (all calculations are done with a schematized 1D beam).

The deck will have the designed like will have a cross section as depicted in Figure 11.1

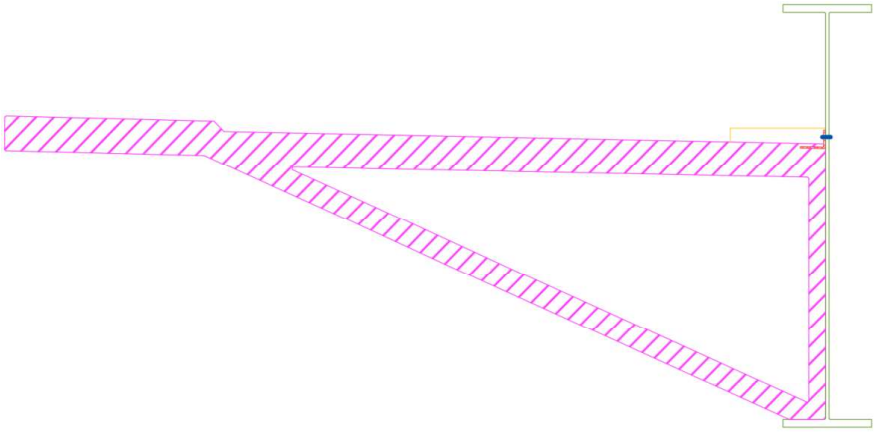

Figure 11.1, Cross section FCP variant 2, FRP deck and support.

And will be schematized as depicted in Figure 11.2

Figure 11.2, Structural scheme for FCP variant 2, FRP deck and support.

11.2. Schemes

To determine the forces in the structure, multiple schemes are implemented. These schemes are depicted in Figure 11.3 and Figure 11.4. The first scheme is used to determine M_B, V_{B-}, R_B and the second scheme is used to determine M_A, M_F, V_{B+}, V_A. The definition of these forces is given in the two figures.

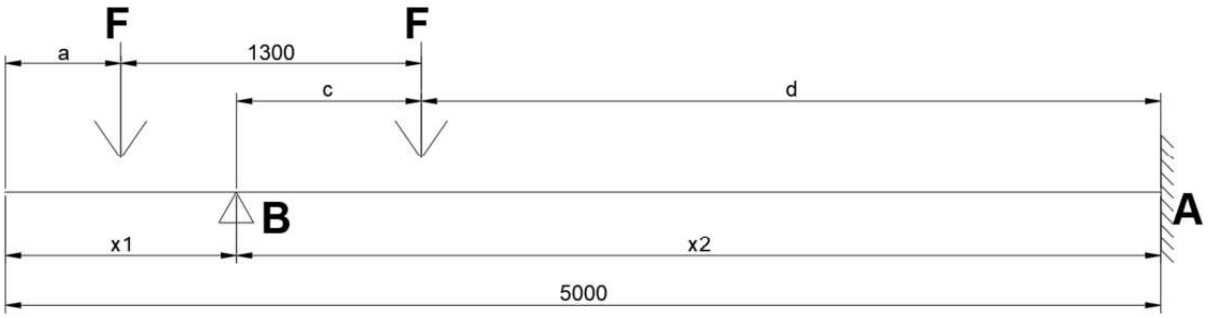

Figure 11.3, FCP variant 2 load scheme 1.

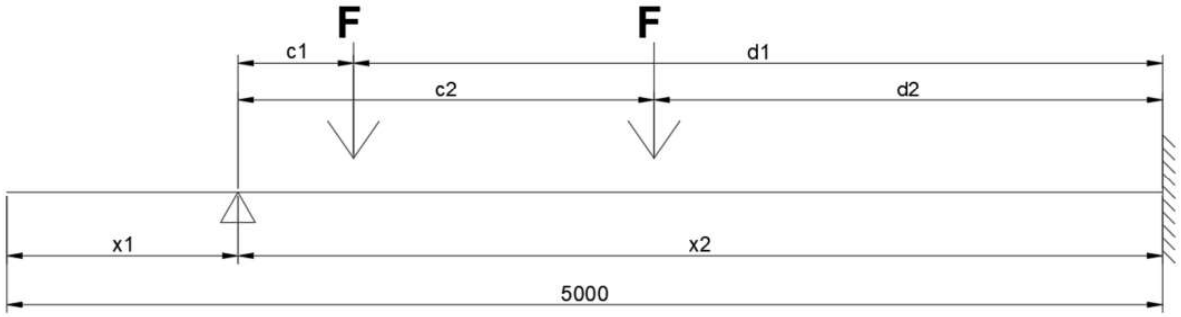

Figure 11.4, FCP variant 2 load scheme 2.

Formula 11.1, Formula 11.2, and Formula 11.3 are used to calculate the shear force left of the support, the bending moments at the support, and the reaction force of the support respectively. These three forces are maximized by load scheme 1.

$$V_{B-} = F$$

(11.1)

$$M_B = F * (x_1 - a)$$

(11.2)

$$R_B = \frac{F * (2 * 5000 - 2 * a - 1300) - M_A}{x_2}; where\ M_A = F * c * d * \frac{x_2 + c}{2 * x_2^2} - \frac{M_B}{2}$$

(11.3)

Formula 11.4, Formula 11.5, Formula 11.6, and Formula 11.7 are used to calculate the shear force right of the support, the shear force at the main beam, the bending moments at the main beam, and the bending moments in the field between the support and the main respectively. These four forces are maximized by load scheme 2.

$$V_{B+} = F * d_1^2 * \frac{c_1 + 2 * x_2}{2 * x_2^3} + F * d_2^2 * \frac{c_2 + 2 * x_2}{2 * x_2^3}$$

(11.4)

$$V_A = 2 * F - V_{B+}$$

(11.5)

$$M_A = F * c_1 * d_1 * \frac{x_2 + c_1}{2 * x_2^2} + F * c_2 * d_2 * \frac{x_2 + c_2}{2 * x_2^2}$$

(11.6)

$$M_F = \max(V_{B+} * c_1, R_{B2} * c_2)\,, where\ R_{B2} = F * d_2^2 * \frac{c_2 + 2 * x_2}{2 * x_2^3}$$

(11.7)

All used formulas are verified with the use of Matrix frame. The definitions of the shear forces and bending moments, from the formulas above. are summarized in Figure 11.5 and Figure 11.6 respectively.

Figure 11.5, Definition of shear and reaction forces.

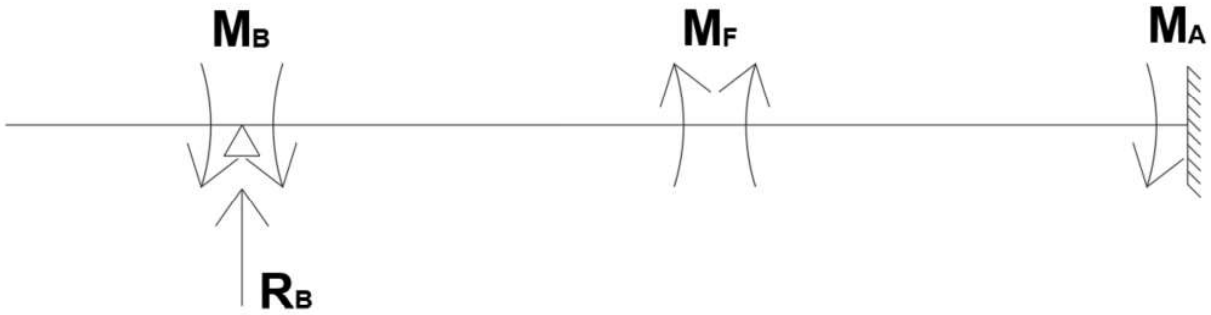

Figure 11.6, Definition of bending moments.

11.3. Results

The following tables contain 2d optimization analysis, where both the position of the forces and the position of the support are moved (this is not the case for forces that are only dependent on 1 or less variables). For the first scheme, the tables containing the bending moments at the support and the reaction force of the support are Table 11.1 and Table 11.2 respectively.

Table 11.1, Bending moments at the support.

$M_B\ (kNm)$												
	x_1	1	1,1	1,2	1,3	1,4	1,5	1,6	1,7	1,8	1,9	2
a												
0,6		16	20	24	28	32	36	40	44	48	-	-
0,7		12	16	20	24	28	32	36	40	44	48	-
0,8		8	12	16	20	24	28	32	36	40	44	48
0,9		4	8	12	16	20	24	28	32	36	40	44
1		-	4	8	12	16	20	24	28	32	36	40
1,1		-	-	4	8	12	16	20	24	28	32	36
1,2		-	-	-	4	8	12	16	20	24	28	32
1,3		-	-	-	-	4	8	12	16	20	24	28
1,4		-	-	-	-	-	4	8	12	16	20	24
1,5		-	-	-	-	-	-	4	8	12	16	20

Table 11.2, Reaction force of the support.

$R_B\ (kN)$												
	x_1	1	1,1	1,2	1,3	1,4	1,5	1,6	1,7	1,8	1,9	2
a												
0,6		72,73	75,56	78,55	81,71	85,05	88,60	92,37	96,37	100,63	-	-
0,7		69,81	72,55	75,45	78,51	81,76	85,20	88,86	92,74	96,88	101,29	-
0,8		66,92	69,57	72,37	75,34	78,48	81,82	85,36	89,13	93,14	97,42	102,00
0,9		64,04	66,60	69,31	72,18	75,22	78,45	81,87	85,52	89,41	93,57	98,01
1		-	63,66	66,27	69,04	71,98	75,10	78,41	81,94	85,70	89,72	94,02
1,1		-	-	63,26	65,93	68,76	71,77	74,97	78,37	82,01	85,89	90,05
1,2		-	-	-	62,84	65,57	68,47	71,55	74,83	78,33	82,08	86,09
1,3		-	-	-	-	62,41	65,19	68,16	71,31	74,69	78,29	82,16
1,4		-	-	-	-	-	61,95	64,79	67,83	71,07	74,54	78,25
1,5		-	-	-	-	-	-	61,47	64,38	67,49	70,81	74,38

For M_B and for R_B the support is optimal to place the support as far as possible. This makes sense as this decreases the overhang on which these forces are greatly dependent.

Table 11.3, Table 11.4, Table 11.5, and Table 11.6 shear force right of the support, shear force at the main beam, bending moments at the main beam and the bending moments in the field between the support and the main beam respectively.

Table 11.3, Shear force right of the support.

V_{B+} (kN)												
	x_1	1	1,1	1,2	1,3	1,4	1,5	1,6	1,7	1,8	1,9	2
c_1												
0,1		58,36	57,85	57,32	56,76	56,18	55,57	54,93	54,25	53,55	52,81	52,03
0,2		55,56	54,99	54,39	53,77	53,12	52,44	51,72	50,97	50,19	49,37	48,51
0,3		52,79	52,16	51,50	50,82	50,10	49,35	48,57	47,75	46,89	45,99	45,05
0,4		50,06	49,37	48,66	47,91	47,13	46,32	45,47	44,59	43,66	42,70	41,69
0,5		47,36	46,62	45,86	45,05	44,22	43,35	42,44	41,50	40,51	39,48	38,41
0,6		44,71	43,92	43,11	42,25	41,37	40,44	39,48	38,48	37,44	36,36	35,24
0,7		42,11	41,27	40,41	39,51	38,58	37,61	36,60	35,55	34,47	33,34	32,18
0,8		39,55	38,68	37,77	36,83	35,86	34,84	33,80	32,71	31,59	30,43	29,24
0,9		37,06	36,14	35,20	34,22	33,21	32,16	31,08	29,97	28,82	27,64	26,43
1		34,61	33,67	32,69	31,69	30,64	29,57	28,46	27,33	26,16	24,97	23,75
1,1		32,24	31,26	30,26	29,23	28,16	27,07	25,95	24,80	23,62	22,43	-
1,2		29,92	28,93	27,90	26,85	25,77	24,67	23,54	22,38	21,22	-	-
1,3		27,68	26,67	25,63	24,56	23,48	22,37	21,24	20,10	-	-	-
1,4		25,51	24,48	23,44	22,37	21,28	20,18	19,06	-	-	-	-
1,5		23,41	22,39	21,34	20,27	19,19	18,10	-	-	-	-	-

Table 11.4, Shear force at the main beam.

V_A (kN)												
	x_1	1	1,1	1,2	1,3	1,4	1,5	1,6	1,7	1,8	1,9	2
c_1												
0,1		21,64	22,15	22,68	23,24	23,82	24,43	25,07	25,75	26,45	27,19	27,97
0,2		24,44	25,01	25,61	26,23	26,88	27,56	28,28	29,03	29,81	30,63	31,49
0,3		27,21	27,84	28,50	29,18	29,90	30,65	31,43	32,25	33,11	34,01	34,95
0,4		29,94	30,63	31,34	32,09	32,87	33,68	34,53	35,41	36,34	37,30	38,31
0,5		32,64	33,38	34,14	34,95	35,78	36,65	37,56	38,50	39,49	40,52	41,59
0,6		35,29	36,08	36,89	37,75	38,63	39,56	40,52	41,52	42,56	43,64	44,76
0,7		37,89	38,73	39,59	40,49	41,42	42,39	43,40	44,45	45,53	46,66	47,82
0,8		40,45	41,32	42,23	43,17	44,14	45,16	46,20	47,29	48,41	49,57	50,76
0,9		42,94	43,86	44,80	45,78	46,79	47,84	48,92	50,03	51,18	52,36	53,57
1		45,39	46,33	47,31	48,31	49,36	50,43	51,54	52,67	53,84	55,03	56,25
1,1		47,76	48,74	49,74	50,77	51,84	52,93	54,05	55,20	56,38	57,57	-
1,2		50,08	51,07	52,10	53,15	54,23	55,33	56,46	57,62	58,78	-	-
1,3		52,32	53,33	54,37	55,44	56,52	57,63	58,76	59,90	-	-	-
1,4		54,49	55,52	56,56	57,63	58,72	59,82	60,94	-	-	-	-
1,5		56,59	57,61	58,66	59,73	60,81	61,90	-	-	-	-	-

Table 11.5, Bending moments at the main beam.

$M_A\ (kNm)$												
	x_1	1	1,1	1,2	1,3	1,4	1,5	1,6	1,7	1,8	1,9	2
c_1												
0,1		26,57	26,39	26,20	25,99	25,76	25,52	25,25	24,96	24,64	24,29	23,90
0,2		29,77	29,55	29,31	29,06	28,78	28,48	28,15	27,79	27,39	26,96	26,48
0,3		32,85	32,58	32,29	31,98	31,64	31,27	30,87	30,43	29,95	29,42	28,84
0,4		35,78	35,46	35,11	34,73	34,32	33,87	33,39	32,86	32,28	31,64	30,94
0,5		38,55	38,17	37,75	37,30	36,81	36,27	35,69	35,06	34,37	33,60	32,76
0,6		41,16	40,70	40,20	39,66	39,08	38,45	37,76	37,01	36,18	35,28	34,28
0,7		43,57	43,03	42,44	41,81	41,13	40,38	39,57	38,68	37,71	36,64	35,46
0,8		45,78	45,15	44,46	43,72	42,92	42,04	41,09	40,05	38,91	37,66	36,28
0,9		47,78	47,04	46,24	45,38	44,44	43,43	42,32	41,11	39,78	38,32	36,72
1		49,54	48,69	47,76	46,76	45,68	44,50	43,22	41,82	40,28	38,60	36,74
1,1		51,06	50,07	49,01	47,86	46,61	45,26	43,78	42,17	40,40	38,46	-
1,2		52,31	51,18	49,97	48,65	47,22	45,67	43,98	42,13	40,11	-	-
1,3		53,28	52,00	50,61	49,11	47,49	45,72	43,79	41,69	-	-	-
1,4		53,97	52,51	50,94	49,24	47,39	45,38	43,20	-	-	-	-
1,5		54,34	52,70	50,92	49,00	46,92	44,65	-	-	-	-	-

Table 11.6, Bending moments in the field between the support and the main beam.

$M_F\ (kNm)$												
	x_1	1	1,1	1,2	1,3	1,4	1,5	1,6	1,7	1,8	1,9	2
c_1												
0,1		27,80	27,14	26,45	25,73	24,98	24,19	23,37	22,50	21,59	20,64	19,65
0,2		27,83	27,09	26,32	25,51	24,67	23,79	22,87	21,91	20,90	19,85	18,75
0,3		27,65	26,82	25,97	25,07	24,14	23,17	22,16	21,10	20,00	18,85	17,65
0,4		27,26	26,35	25,41	24,43	23,41	22,35	21,25	20,10	18,91	17,67	16,67
0,5		26,68	25,69	24,67	23,60	22,50	21,68	21,22	20,75	20,26	19,74	19,21
0,6		26,83	26,35	25,86	25,35	24,82	24,27	23,69	23,09	22,47	21,82	21,14
0,7		29,48	28,89	28,29	27,66	27,00	26,32	25,62	24,89	24,13	23,34	22,53
0,8		31,64	30,94	30,22	29,47	28,68	27,88	27,04	26,17	25,27	24,35	23,39
0,9		33,35	32,53	31,68	30,80	29,89	28,95	27,98	26,97	25,94	24,87	23,78
1		34,61	33,67	32,69	31,69	30,64	29,57	28,46	27,33	26,16	24,97	23,75
1,1		35,46	34,39	33,29	32,15	30,98	29,78	28,54	27,28	25,99	24,68	-
1,2		35,91	34,71	33,48	32,22	30,93	29,60	28,24	26,86	25,46	-	-
1,3		35,98	34,67	33,32	31,93	30,52	29,08	27,61	26,12	-	-	-
1,4		35,71	34,28	32,81	31,32	29,79	28,25	26,68	-	-	-	-
1,5		35,12	33,58	32,00	30,41	28,79	27,15	-	-	-	-	-

For the forces calculated with the second scheme, which focusses on the area between the supports, the conclusions are more nuanced. This is clearly visible in the tables depicted above, where the colors are separated in complicated regions. For V_{B+}, M_A and M_F (generally) the longer the span between the region, the higher the forces. For the shear force in A, V_A, there is a peak visible around 1.5 meters.

11.4. Conclusions

The results clearly depict a complicated situation where the forces need to be balanced. Placing the support inward will decrease the forces from scheme 2 (generally) but increase the forces from scheme 1.

For the shear force a comparison must be made between V_A and V_{B+}, as V_{B-} remains constant and non-governing. An optimum is found between $x_1 = 1.1m$ and $x_1 = 1.2m$. For the bending moments a comparison is made with M_A and M_B, as M_F is non-governing. An optimum is found between $x_1 = 1.6m$ and $x_1 = 1.7m$.

For the reaction force in B, R_B, a small x_1 will result in a smaller R_B.

As mentioned before, distributed loads were also analyzed but were found to be also non-governing. To find a middle ground between the optima, it is determined to design the FCP deck such that $x_1 = 1.5\ m$.

Appendix II, Structural checks steel crossbeam with a wooden deck FCP.

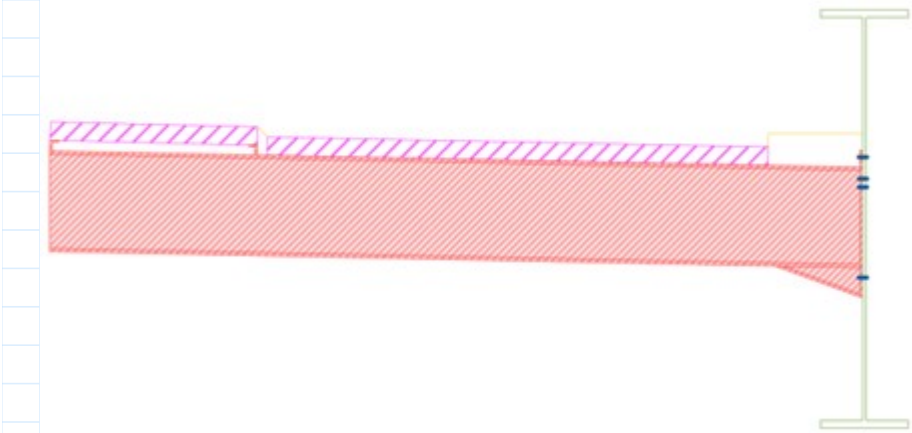

Table of Contents

General

General dimensions

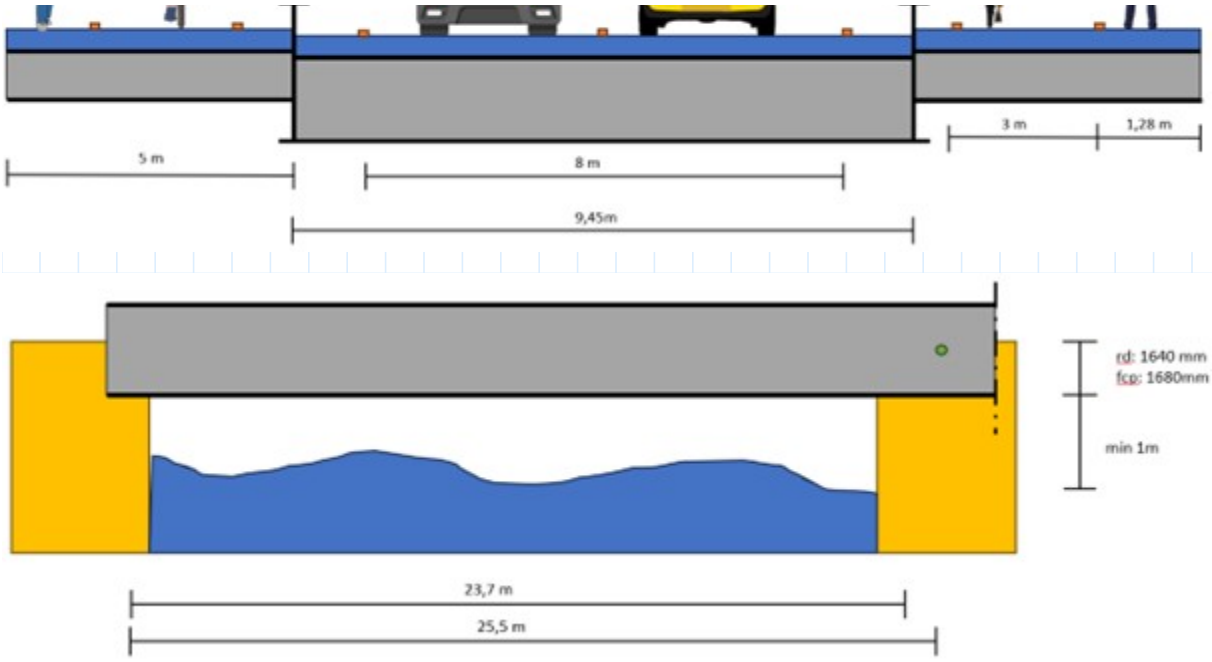

$n_{crossbeam} := 7$ $l := 25250\ mm$

$h.o.h_{crossbeam} := \frac{l}{n_{crossbeam} - 1} = 4.208\ m$

$b_{fcp} := 4.28\ m$ $b_{edge} := 5\ m$ $b_{rd} := 8\ m$ $b_{supp} := 9.45\ m$

$h_{rd} := 5.9\ m$ $h_{fcp} := 6.05\ m$ $h_{water} := 3.3\ m$ $h_{under\_side} := 4.3\ m$

$\theta_{max} := 80\ °$ $h_{top} := \sin(\theta_{max}) \cdot l + h_{rd} = 30.8\ m$ $A_{fcp\_deck} := b_{edge} \cdot l = 126.25\ m^2$

General properties

$T_{s\_sun} := 57\ °C$ $T_{s\_shade} := 31\ °C$

Desing material properties

Properties wood

$\rho_{wood} := 1080\ \frac{kg}{m^3}$ $E_{wood} := 20\ GPa$

Properties steel

$\rho_{steel} := 7800 \frac{kg}{m^3}$ $E_{steel} := 210\ GPa$ $f_{st} := 355\ MPa$

Traffic load calculations

Cross section properties

Load properties

Distirbuted load foot and cycle path

$q_{fcp} := 5 \frac{kN}{m^2}$

Concentrated load service vehicle

$Q_{serv} := 12.5\ kN$

$l_{w\_serv} := 25\ cm$ $w_{w\_serv} := 25\ cm$ $w_{serv} := 1.75\ m$ $h.o.h_{serv} := 3\ m$

Concentrated load accidental vehicle

$Q_{av1} := 40\ kN$ $Q_{av2} := 20\ kN$

$l_{w\_av} := 20\ cm$ $w_{w\_av} := 20\ cm$ $w_{av} := 1.3\ m$ $h.o.h_{av} := 3\ m$

Foot- and cycle path properties

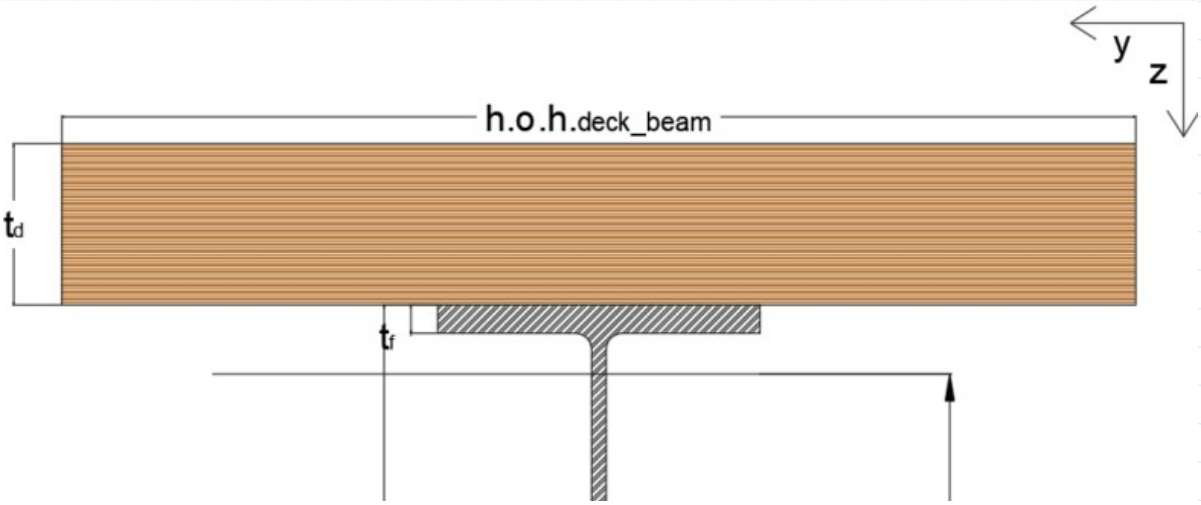

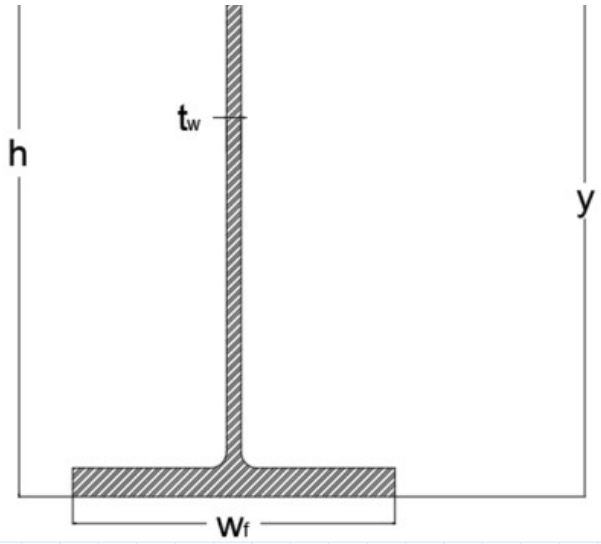

$w_{av\_edge} := 0.5\ m + \frac{w_{w\_av}}{2} = 0.6\ m$ $w_{serv\_edge} := 0.5\ m + \frac{w_{w\_serv}}{2} = 0.625\ m$

$t_{d\_fcp} := 80\ mm$ $A_{deck\_beam} := 2848\ mm^2$ $h_{deck\_beam} := 200\ mm^2$

$n_{deck\_beam} := 6$ $h.o.h_{deck\_beam} := \frac{b_{edge}}{n_{deck\_beam}} = 0.833\ m$ $A_{L\_deck\_beam} := 2848\ mm^2$

$w_{fcp} := w_{w\_av} + t_{d\_fcp} = 280\ mm$

Crossbeam properties

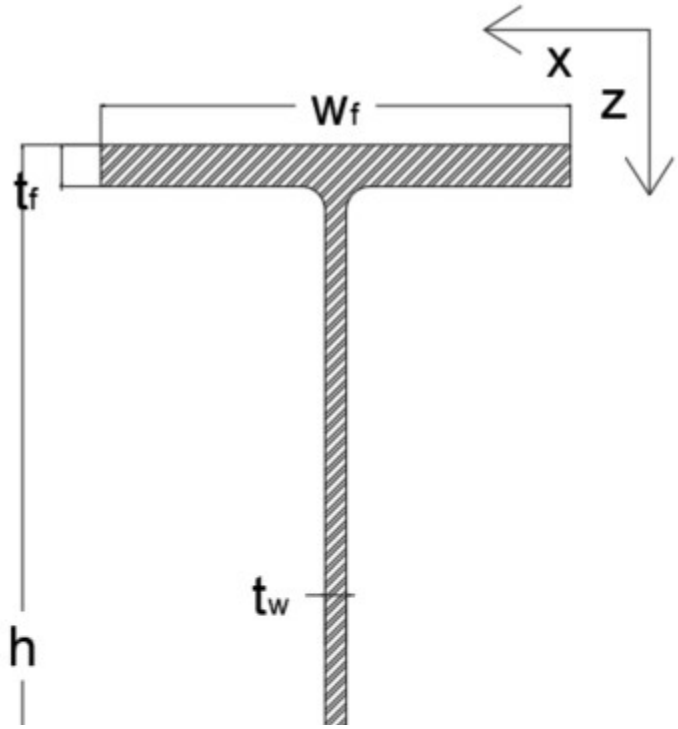

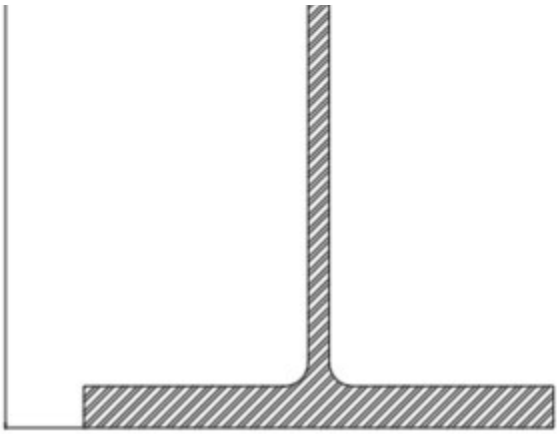

$h_{cb\_side} := 640\ mm$ $t_{cb\_w\_side} := 13.5\ mm$ Edge crossbeam is a HEA650

$t_{cb\_f\_side} := 26.5\ mm$ $w_{cb\_f\_side} := 300\ mm$

$$A_{cb\_side} := 2 \cdot t_{cb\_f\_side} \cdot w_{cb\_f\_side} + t_{cb\_w\_side} \cdot \left(h_{cb\_side} - 2 \cdot t_{cb\_f\_side}\right) = 0.024\ m^2$$

$$A_{cb\_v\_side} := t_{cb\_w\_side} \cdot h_{cb\_side} = 0.009\ m^2$$

$$EI_{cb\_side} := E_{steel} \cdot \left(\begin{array}{l} \frac{1}{12} \cdot t_{cb\_w\_side} \cdot \left(h_{cb\_side} - 2 \cdot t_{cb\_f\_side}\right)^3 \\ + 2 \cdot w_{cb\_f\_side} \cdot t_{cb\_f\_side} \cdot \left(\frac{1}{2} \cdot h_{cb\_side} - \frac{1}{2} \cdot t_{cb\_f\_side}\right)^2 \end{array} \right) = \left(3.62 \cdot 10^5\right)\ kN \cdot m^2$$

$\chi_{LT} := 0.4$

Calculations for deflections

Deflections crossbeam

$$w_{cb\_Q} := \frac{1}{48} \cdot \frac{Q_{serv} \cdot \left(b_{edge} - w_{serv\_edge}\right)^3}{EI_{cb\_side}} + \frac{1}{48} \cdot \frac{Q_{serv} \cdot \left(b_{edge} - w_{serv\_edge} - w_{serv}\right)^3}{EI_{cb\_side}} = 0.1\ mm$$

$$w_{cb\_q} := \frac{5}{384} \cdot \frac{q_{fcp} \cdot h.o.h_{crossbeam} \cdot b_{edge}^{\ 4}}{EI_{cb\_side}} = 0.5\ mm$$

Deflections limit

$w_{limit\_threshold} := 5\ mm$

Unity checks

$$u.c._{deflection\_threshold} := \frac{\max\left(w_{cb\_Q}, w_{cb\_q}\right)}{w_{limit\_threshold}} = 0.09$$

Calculations for crossbeam

Loadcases

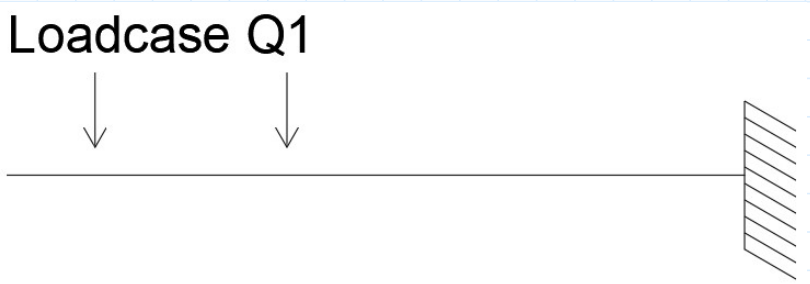

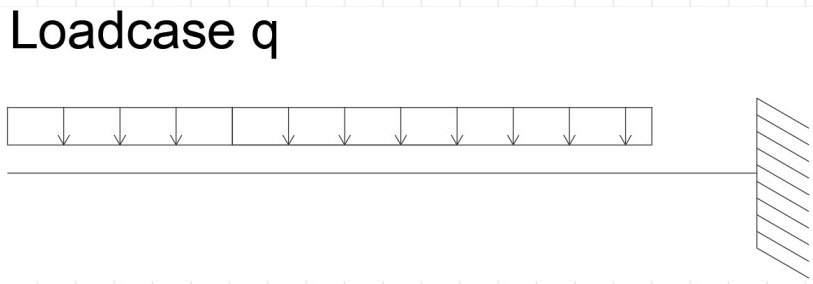

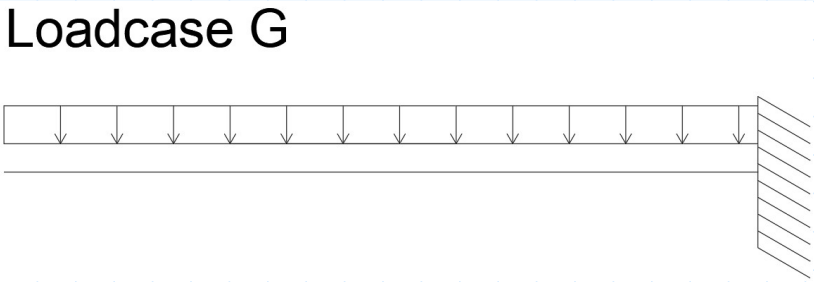

Shearforce

Loadcases q and Q1 were used

$$V_{fcp\_q\_cb} := q_{fcp} \cdot b_{fcp} \cdot h.o.h_{crossbeam} = 90 \ \boldsymbol{kN}$$

$$V_{fcp\_Q\_cb} := 2 \cdot \left(Q_{av1} + Q_{av2}\right) = 120 \ \boldsymbol{kN}$$

Bending moments

Loadcases q and Q1 were used

$$M_{h\_q\_cb} := \frac{1}{2} \cdot q_{fcp} \cdot h.o.h_{crossbeam} \cdot b_{fcp}^{\ 2} + q_{fcp} \cdot h.o.h_{crossbeam} \cdot b_{fcp} \cdot \left(b_{edge} - b_{fcp}\right) = 258 \ \boldsymbol{kN \cdot m}$$

$$M_{h\_Q\_cb} := \left(Q_{av1} + Q_{av2}\right) \cdot \left(2 \cdot b_{edge} - 2 \cdot w_{av\_edge} - w_{av}\right) = 450 \ \boldsymbol{kN \cdot m}$$

Self weight

$$G_{cb\_fcp} := \begin{pmatrix} t_{d\_fcp} \cdot \rho_{wood} \cdot h.o.h_{crossbeam} \\ + \dfrac{n_{deck\_beam} \cdot A_{deck\_beam} \cdot h.o.h_{crossbeam}}{b_{edge}} \cdot \rho_{steel} \\ + A_{cb\_side} \cdot \rho_{steel} \end{pmatrix} \cdot 9.81 \ \frac{\boldsymbol{m}}{\boldsymbol{s}^2} = 6.5 \ \frac{\boldsymbol{kN}}{\boldsymbol{m}}$$

$$G_{cb\_fcp} = 6.5 \ \frac{\boldsymbol{kN}}{\boldsymbol{m}}$$

Resultant forces as a result of self weight

Loadcase G was used

$$V_{G\_cb\_fcp} := G_{cb\_fcp} \cdot b_{edge} = 32.5 \ \boldsymbol{kN}$$

$$M_{G\_cb\_fcp} := \frac{1}{2} \cdot G_{cb\_fcp} \cdot b_{fcp}^{\ 2} + G_{cb\_fcp} \cdot b_{fcp} \cdot \left(b_{edge} - b_{fcp}\right) = 79.4 \ \boldsymbol{kN \cdot m}$$

Combined forces with 6.10 B

$$V_{Ed\_cb\_side} := 1.2 \cdot V_{G\_cb\_fcp} + \max\left(1.5 \cdot V_{fcp\_q\_cb}, V_{fcp\_Q\_cb}\right) = 174.03 \ \boldsymbol{kN}$$

$$M_{Ed\_cb\_side} := 1.2 \cdot M_{G\_cb\_fcp} + \max\left(1.5 \cdot M_{h\_q\_cb}, M_{h\_Q\_cb}\right) = 545.34 \ \boldsymbol{kN \cdot m}$$

Resultant stresses

$$\tau_{Ed\_cb\_side} := \frac{V_{Ed\_cb\_side}}{A_{cb\_v\_side}} = 20.1 \ \boldsymbol{MPa}$$

$$\sigma_{Ed\_cb\_side} := \frac{M_{Ed\_cb\_side}}{EI_{cb\_side}} \cdot E_{steel} \cdot \frac{1}{2} \cdot h_{cb\_side} = 101.2 \ \boldsymbol{MPa}$$

Unity checks

$$u.c._{\tau\_cb} := \frac{\tau_{Ed\_cb\_side}}{f_{st}} = 0.057$$

$$u.c._{\sigma\_cb\_side} := \frac{\sigma_{Ed\_cb\_side}}{\chi_{LT} \cdot f_{st}} = 0.713$$

Auxiliary calculations

Calculations for ship impact forces

$F_{ship} := 1\ MN$ $h_{ship} := 0.25\ m$ $w_{ship} := 3\ m$

$A_{edge} := 15598\ mm^2$ $I_{cr\_edge} := 11271 \cdot 10^4\ mm^4$ Edge crossbeam is an IPE600

$h_{I\_edge} := 600\ mm$ $b_{I\_edge} := 220\ mm$

$t_{w\_I\_edge} := 12\ mm$ $t_{f\_I\_edge} := 19\ mm$ $r_{I\_edge} := 24\ mm$

Beam buckling resistance

$\varepsilon_{I\_edge} := 0.81$ $class_{f\_edge} := 1$ $class_{w\_edge} := 4$ $l_{cr\_edge} := 2 \cdot b_{edge}$

$\lambda_1 := 93.9 \cdot \varepsilon_{I\_edge} = 76$ $\psi_{w\_edge} := 1$ $k_{\sigma\_I\_edge} := 4$

$$\lambda_{p\_w\_edge} := \frac{\frac{h_{I\_edge} - 2 \cdot t_{f\_I\_edge} - 2 \cdot r_{I\_edge}}{t_{w\_I\_edge}}}{28.4 \cdot \varepsilon_{I\_edge} \cdot \sqrt{k_{\sigma\_I\_edge}}} = 0.931$$

$0.5 + \sqrt{0.085 - 0.055 \cdot \psi_{w\_edge}} = 0.673$ $\rho_{I\_edge} := \frac{\lambda_{p\_w\_edge} - 0.055 \cdot (3 + \psi_{w\_edge})}{\lambda_{p\_w\_edge}^2} = 0.82$

$b_{eff\_I\_edge} := \rho_{I\_edge} \cdot (h_{I\_edge} - 2 \cdot (t_{f\_I\_edge} + r_{I\_edge})) = 422\ mm$

$A_{eff\_I\_edge} := (2 \cdot r_{I\_edge} + b_{eff\_I\_edge}) \cdot t_{w\_I\_edge} + \pi \cdot r_{I\_edge}^2 + b_{I\_edge} \cdot t_{f\_I\_edge} = 11625\ mm^2$

$i_{I\_edge} := \sqrt{\frac{I_{cr\_edge}}{A_{eff\_I\_edge}}} = 0.098\ m$ $\lambda_{I\_edge} := \sqrt{\frac{l_{cr\_edge}}{i_{I\_edge} \cdot \lambda_1}} = 1.156$ $\alpha_{I\_edge} := 0.34$

$\phi_{I\_edge} := 0.5 \cdot (1 + \alpha_{I\_edge} \cdot (\lambda_{I\_edge} - 0.2) + \lambda_{I\_edge}^2) = 1.33$

$$\chi_{I\_edge} := \frac{1}{\phi_{I\_edge} + \sqrt{\phi_{I\_edge}^2 + \lambda_{I\_edge}^2}} = 0.323$$

$N_{cr} := \chi_{I\_edge} \cdot A_{eff\_I\_edge} \cdot f_{st} = 1.335\ MN$

Results

Unity checks

Unity checks traffic loads

Deflections

$u.c._{deflection\_threshold} = 0.09$

Crossbeam

$u.c._{\tau\_cb} = 0.06$ $u.c._{\sigma\_cb\_side} = 0.71$

Unity checks ship colision

Reduction of force to main structure due to collision with fcp deck (supp)

$Reduction := 0$

MKI

$€ := 1$ ¤

$Mass_{Steel} := n_{crossbeam} \cdot 2 \cdot A_{edge} \cdot b_{edge} \cdot \rho_{steel} + 2 \cdot n_{deck\_beam} \cdot A_{deck\_beam} \cdot l \cdot \rho_{steel} = 15.247\ tonne$

$A_{Steel} := \left(2 \cdot h_{I\_edge} + 4 \cdot b_{I\_edge} - 2 \cdot t_{w\_I\_edge}\right) \cdot 2 \cdot b_{edge} \cdot n_{crossbeam} + A_{L\_deck\_beam} \cdot n_{deck\_beam} \cdot 2 = 143.954\ m^2$

$A_{Wood} := 2 \cdot l \cdot b_{edge} = 252.5\ m^2$

$Mass_{Wood} := A_{Wood} \cdot t_{d\_fcp} \cdot \rho_{wood} = 21.816\ tonne$ $t_{d\_fcp} \cdot \rho_{wood} = 86.4\ \frac{kg}{m^2}$

$MKI_{Steel} := 0.165\ \frac{€}{kg}$ $MKI_{score\_Steel} := MKI_{Steel} \cdot Mass_{Steel} = 2515.8\ €$

$MKI_{Wood} := 1.26\ \frac{€}{m^2} \cdot \frac{80}{30} = 3.36\ \frac{€}{m^2}$ $MKI_{score\_wood} := MKI_{Wood} \cdot A_{Wood} \cdot 4 = 3393.6\ €$

$MKI_{Steel\_cons} := 0.300 \ \frac{€}{m^2}$ $MKI_{score\_Steel\_cons} := 5 \cdot MKI_{Steel\_cons} \cdot A_{Steel} = 215.9 \ €$

$MKI_{score\_Total} := MKI_{score\_Steel} + MKI_{score\_wood} + MKI_{score\_Steel\_cons} = 6125 \ €$

Mass

$Mass_{total} := Mass_{Steel} + Mass_{Wood} = 37 \ tonne$

Appendix III, Structural checks steel crossbeam with an FRP deck FCP.

Table of Contents

General

General dimensions

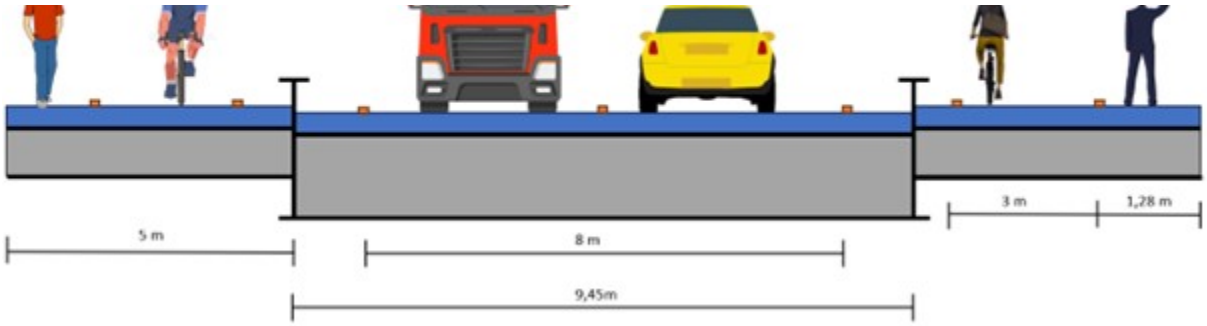

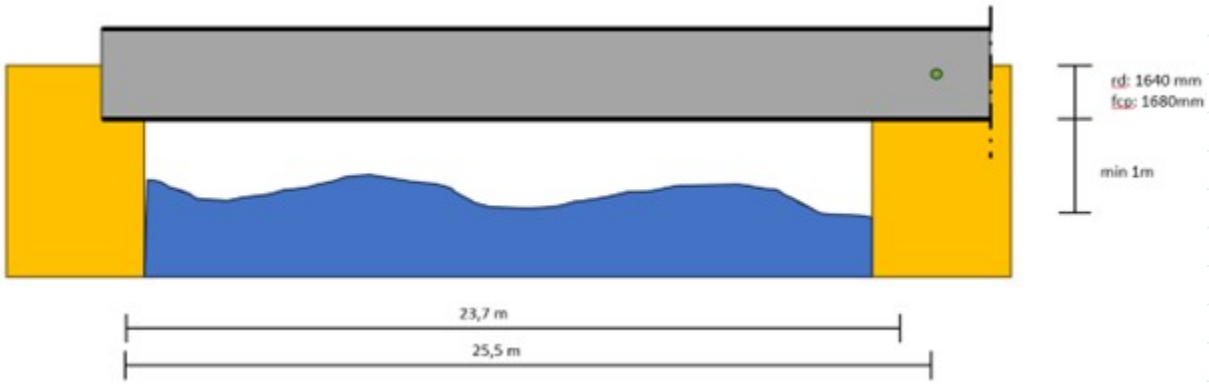

$n_{crossbeam} := 7$ $l := 25250\ mm$

$h.o.h_{crossbeam} := \frac{l}{n_{crossbeam} - 1} = 4.208\ m$

$b_{fcp} := 4.28\ m$ $b_{edge} := 5\ m$ $b_{rd} := 8\ m$ $b_{supp} := 9.45\ m$

$h_{rd} := 5.9\ m$ $h_{fcp} := 6.05\ m$ $h_{water} := 3.3\ m$ $h_{under\_side} := 4.3\ m$

$\theta_{max} := 80\ °$ $h_{top} := \sin(\theta_{max}) \cdot l + h_{rd} = 30.8\ m$ $A_{fcp\_deck} := b_{edge} \cdot l = 126.25\ m^2$

General properties

$T_{s\_sun} := 57\ °C$ $T_{s\_shade} := 31\ °C$

Desing material properties

Properties balsa core

$\rho_{balsa} := 285\ \frac{kg}{m^3}$ $G_{balsa} := 145\ MPa$

$E_{balsa\_\sim} := 720\ MPa$ $E_{balsa\_\sim} := 2642\ MPa$

$f_{c\_xz\_v\_k} := 2.08\ \boldsymbol{MPa}$ $f_{c\_z\_k} := 7.32\ \boldsymbol{MPa}$

$$\eta_{ct\_balsa} := min\left(1 - \left(\frac{0.2\ \frac{\boldsymbol{kg}}{\boldsymbol{m}^3}}{\rho_{balsa}} + 0.004\right) \cdot \left(\frac{T_{s\_sun} - 20\ \boldsymbol{°C}}{1\ \boldsymbol{°C}}\right), 1\right) = 1$$

$\eta_{cm\_balsa} := 1$ $\eta_{c\_balsa} := \eta_{ct\_balsa} \cdot \eta_{cm\_balsa} = 1$

$\gamma_{m\_balsa} := 1.51$ $\gamma_{rd\_balsa} := 1.5$

$$f_{c\_xz\_v\_d} := \frac{\eta_{c\_balsa} \cdot f_{c\_xz\_v\_k}}{\gamma_{m\_balsa} \cdot \gamma_{rd\_balsa}} = 0.92\ \boldsymbol{MPa}$$

$$f_{c\_z\_d} := \frac{\eta_{c\_balsa} \cdot f_{c\_z\_k}}{\gamma_{m\_balsa} \cdot \gamma_{rd\_balsa}} = 3.23\ \boldsymbol{MPa}$$

Properties foot- and cycle path laminate

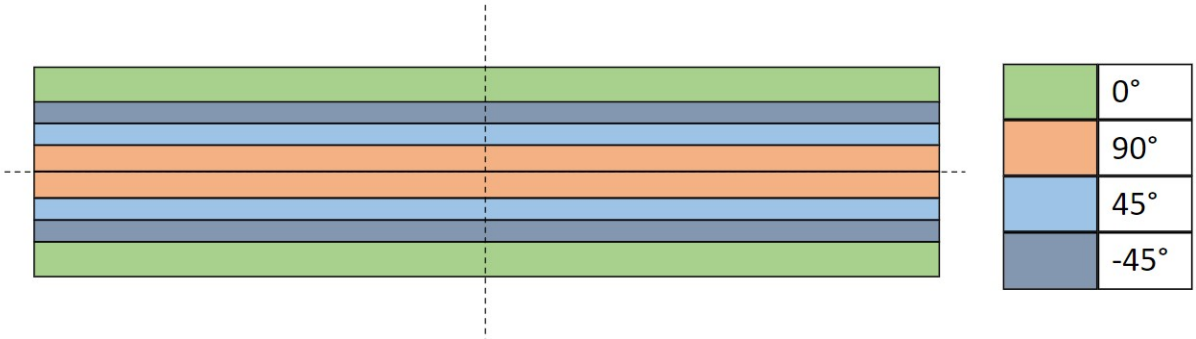

Laminate layup foot- and cycle path

$$\begin{bmatrix} 0 \\ 90 \\ 45 \\ -45 \end{bmatrix} \quad \begin{bmatrix} 50\% \\ 16.67\% \\ 16.67\% \\ 16.67\% \end{bmatrix}$$

$\rho_{l\_fcp} := 1900\ \frac{\boldsymbol{kg}}{\boldsymbol{m}^3}$ $E_{1\_l\_fcp} := 26.2\ \boldsymbol{GPa}$ $E_{2\_l\_fcp} := 17.5\ \boldsymbol{GPa}$

$f_{fcp\_x\_k} := 367\ \boldsymbol{MPa}$ $f_{fcp\_y\_k} := 245\ \boldsymbol{MPa}$ $f_{fcp\_xy\_k} := 150\ \boldsymbol{MPa}$

$T_{s\_fcp} := 90\ \boldsymbol{°C}$

$$\eta_{ct\_f\_fcp} := min\left(1 - 0.25 \cdot \frac{T_{s\_sun} - 20\ °C}{T_{g\_fcp} - 20\ °C}, 1\right) = 0.9$$

$$\eta_{cm\_f\_fcp} := 0.6 \qquad \eta_{c\_f\_fcp} := \eta_{ct\_f\_fcp} \cdot \eta_{cm\_f\_fcp} = 0.521$$

$$\eta_{ct\_m\_fcp} := min\left(1 - 0.80 \cdot \frac{T_{s\_sun} - 20\ °C}{T_{g\_fcp} - 20\ °C}, 1\right) = 0.6$$

$$\eta_{cm\_m\_fcp} := 0.6 \qquad \eta_{c\_m\_fcp} := \eta_{ct\_m\_fcp} \cdot \eta_{cm\_m\_fcp} = 0.346$$

$$\gamma_{m\_fcp} := 1.07 \qquad \gamma_{rd\_fcp} := 1.4$$

$$f_{fcp\_x\_d} := \frac{\eta_{c\_f\_fcp} \cdot f_{fcp\_x\_k}}{\gamma_{rd\_fcp} \cdot \gamma_{m\_fcp}} = 127.6\ MPa$$

$$f_{fcp\_y\_d} := \frac{\eta_{c\_f\_fcp} \cdot f_{fcp\_y\_k}}{\gamma_{rd\_fcp} \cdot \gamma_{m\_fcp}} = 85.2\ MPa$$

$$f_{fcp\_xy\_d} := \frac{\eta_{c\_f\_fcp} \cdot f_{fcp\_xy\_k}}{\gamma_{rd\_fcp} \cdot \gamma_{m\_fcp}} = 52.1\ MPa$$

Properties steel

$$\rho_{steel} := 7800\ \frac{kg}{m^3} \qquad E_{steel} := 210\ GPa \qquad f_{st} := 355\ MPa$$

Traffic load calculations

Cross section properties

Load properties

Distirbuted load foot and cycle path

$$q_{fcp} := 5\ \frac{kN}{m^2}$$

Concentrated load service vehicle

$Q_{serv} := 12.5\ kN$

$l_{w\_serv} := 25\ cm \quad w_{w\_serv} := 25\ cm \quad w_{serv} := 1.75\ m \quad h.o.h_{serv} := 3\ m$

Concentrated load accidental vehicle

$Q_{av1} := 40\ kN \quad Q_{av2} := 20\ kN$

$l_{w\_av} := 20\ cm \quad w_{w\_av} := 20\ cm \quad w_{av} := 1.3\ m \quad h.o.h_{av} := 3\ m$

Foot- and cycle path properties

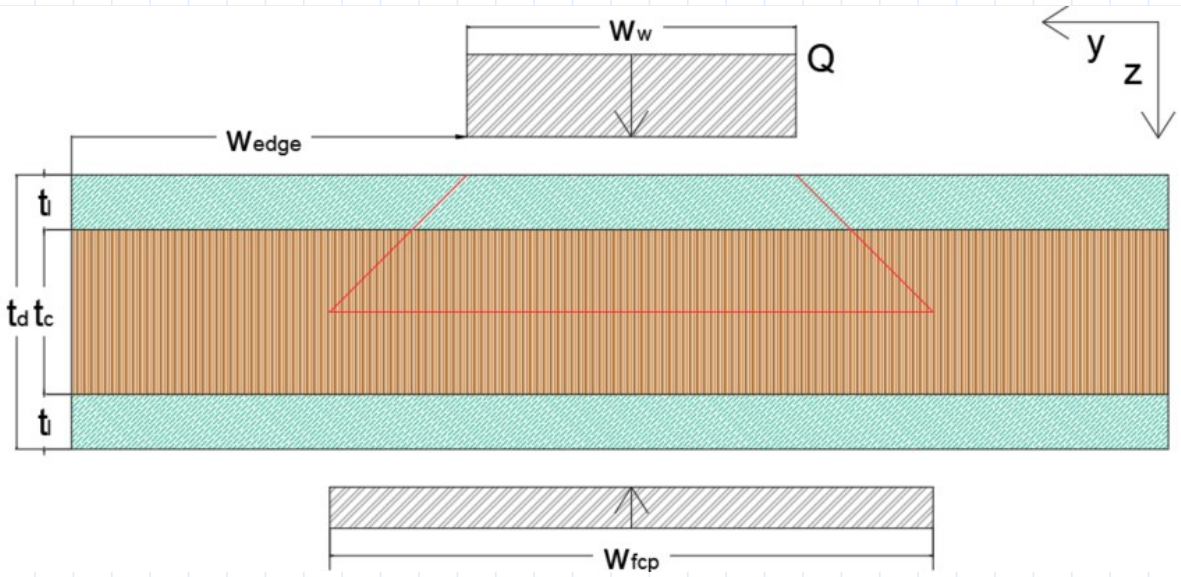

$w_{av\_edge} := 0.5\ m + \frac{w_{w\_av}}{2} = 0.6\ m \quad w_{serv\_edge} := 0.5\ m + \frac{w_{w\_serv}}{2} = 0.625\ m$

$t_{l\_fcp} := 12\ mm \quad t_{c\_fcp} := 200\ mm \quad t_{d\_fcp} := t_{c\_fcp} + 2 \cdot t_{l\_fcp} = 224\ mm$

$w_{fcp} := w_{w\_av} + t_{d\_fcp} = 424\ mm$

$A_{fcp} := w_{fcp} \cdot t_{c\_fcp} = 0.085\ m^2$

$EI_{fcp} := 2 \cdot E_{1\_l\_fcp} \cdot w_{fcp} \cdot t_{l\_fcp} \cdot \left(\frac{t_{c\_fcp} + t_{l\_fcp}}{2} \right)^2 + \frac{1}{12} \cdot E_{balsa\_z} \cdot w_{fcp} \cdot {t_{c\_fcp}}^3 = 3199\ kN \cdot m^2$

Crossbeam properties

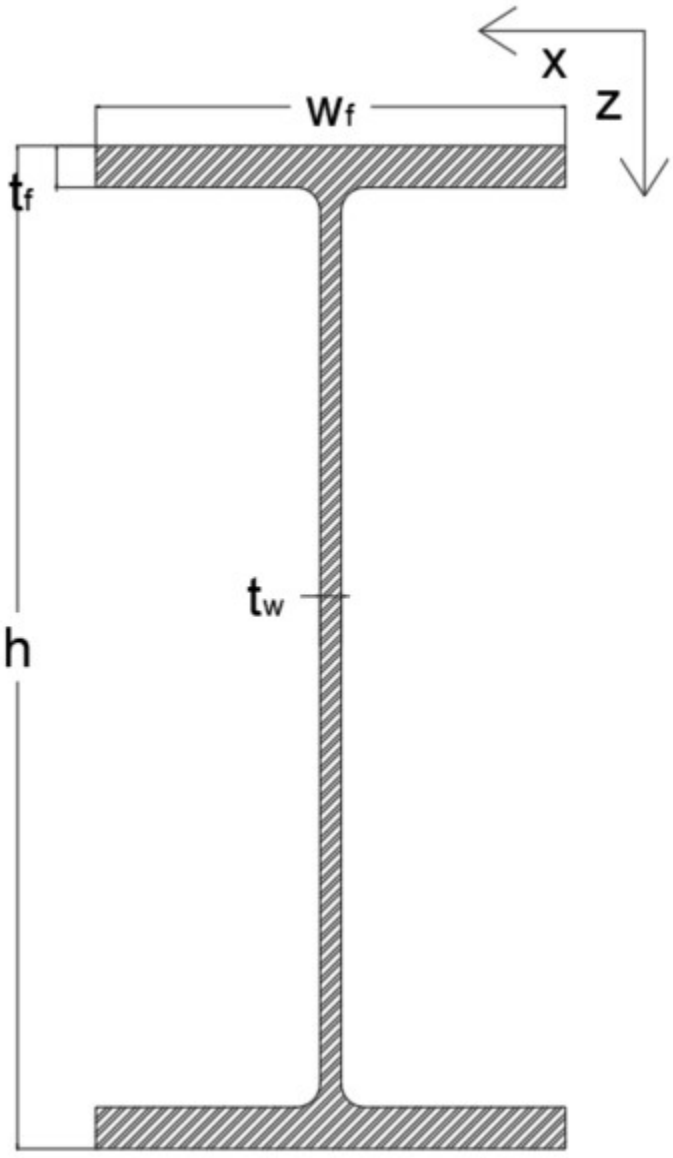

$h_{cb\_side} := 640\ mm \quad t_{cb\_w\_side} := 13.5\ mm$ Edge crossbeam is a HEA650

$t_{cb\_f\_side} := 26.5\ mm \quad w_{cb\_f\_side} := 300\ mm$

$$A_{cb\_side} := 2 \cdot t_{cb\_f\_side} \cdot w_{cb\_f\_side} + t_{cb\_w\_side} \cdot \left(h_{cb\_side} - 2 \cdot t_{cb\_f\_side}\right) = 0.024\ m^2$$

$$A_{cb\_v\_side} := t_{cb\_w\_side} \cdot h_{cb\_side} = 0.009\ m^2$$

$$EI_{cb\_side} := E_{steel} \cdot \left(\begin{array}{l} \frac{1}{12} \cdot t_{cb\_w\_side} \cdot \left(h_{cb\_side} - 2 \cdot t_{cb\_f\_side}\right)^3 \\ + 2 \cdot w_{cb\_f\_side} \cdot t_{cb\_f\_side} \cdot \left(\frac{1}{2} \cdot h_{cb\_side} - \frac{1}{2} \cdot t_{cb\_f\_side}\right)^2 \end{array} \right) = \left(3.62 \cdot 10^5\right)\ kN \cdot m^2$$

$\chi_{LT} := 0.4$

Combined crossbeam + deck properties

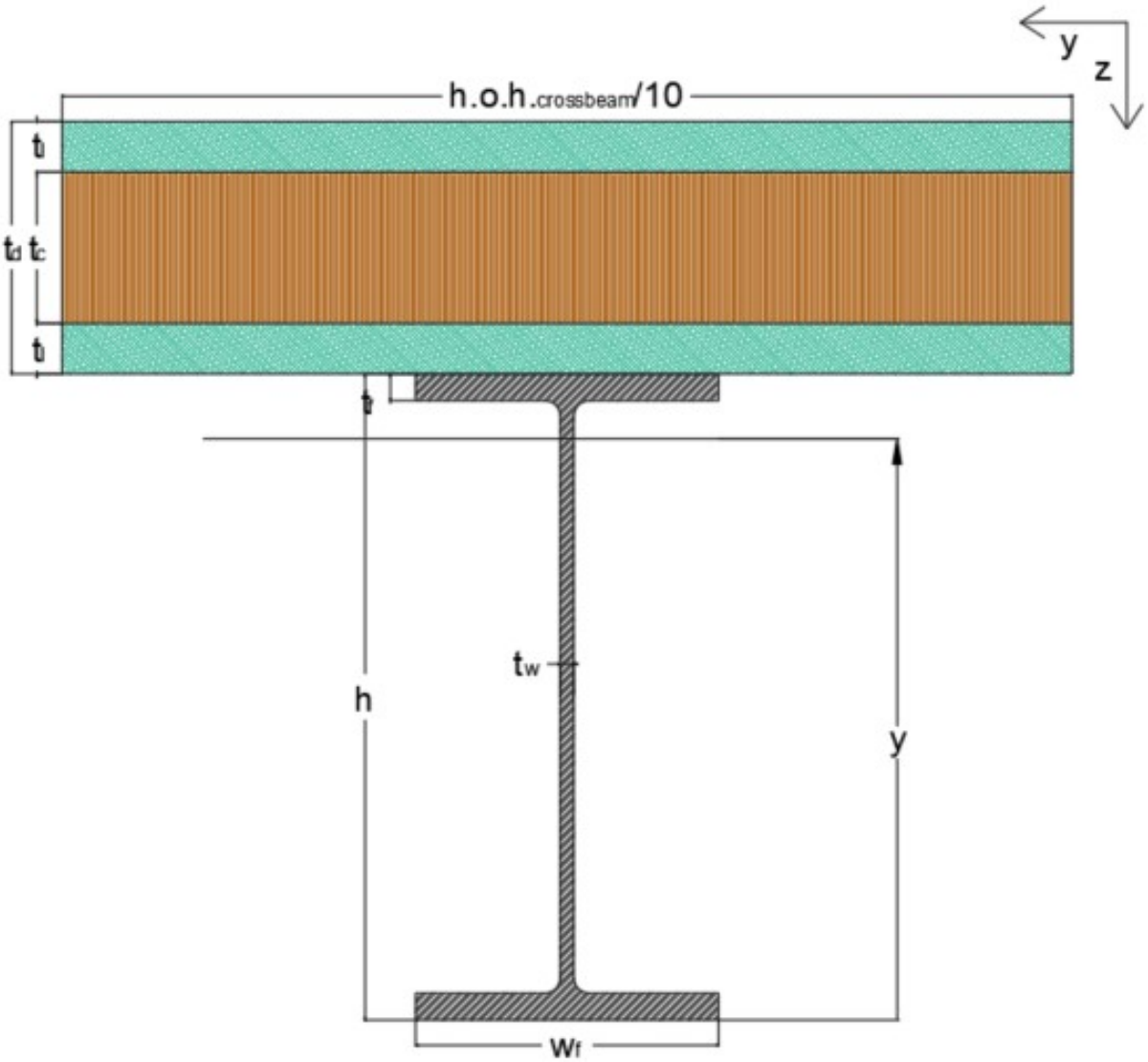

$$y := \frac{\begin{aligned} &A_{cb\_side} \cdot \frac{h_{cb\_side}}{2} \cdot E_{steel} \\ &+ \frac{h.o.h_{crossbeam}}{5} \cdot t_{c\_fcp} \cdot \left(h_{cb\_side} + t_{l\_fcp} + \frac{t_{c\_fcp}}{2} \right) \cdot E_{balsa\_z} \\ &+ \frac{h.o.h_{crossbeam}}{5} \cdot t_{l\_fcp} \cdot \left(2 \cdot h_{cb\_side} + 2 \cdot t_{l\_fcp} + t_{c\_fcp} \right) \cdot E_{2\_l\_fcp} \end{aligned}}{\frac{h.o.h_{crossbeam}}{5} \cdot t_{l\_fcp} \cdot E_{2\_l\_fcp} + A_{cb\_side} \cdot E_{steel} + \frac{h.o.h_{crossbeam}}{5} \cdot t_{c\_fcp} \cdot E_{balsa\_z}} = 0.37\ m$$

$$z_{l\_fcp\_top} := h_{cb\_side} + t_{d\_fcp} - \frac{t_{l\_fcp}}{2} - y = 0.489\ m$$

$$z_{c\_fcp} := h_{cb\_side} + t_{l\_fcp} + \frac{t_{c\_fcp}}{2} - y = 0.383\ m$$

$$z_{l\_fcp\_bot} := h_{cb\_side} + \frac{t_{l\_fcp}}{2} - y = 0.277\ m$$

$$z_{cb} := \frac{h_{cb\_side}}{2} - y = -0.049\ m$$

$$EI_{cb\_comb} := \frac{b_{supp}}{10} \cdot t_{l\_fcp} \cdot \left(z_{l\_fcp\_top}^{\ 2} + z_{l\_fcp\_bot}^{\ 2} \right) \cdot E_{2\_l\_fcp} = \left(4.567 \cdot 10^5 \right)\ kN \cdot m^2$$
$$+ \frac{b_{supp}}{10} \cdot t_{c\_fcp} \cdot z_{c\_fcp}^{\ 2} \cdot E_{balsa\_z}$$
$$+ EI_{cb\_side} + A_{cb\_side} \cdot z_{cb}^{\ 2} \cdot E_{steel}$$

Calculations for deflections

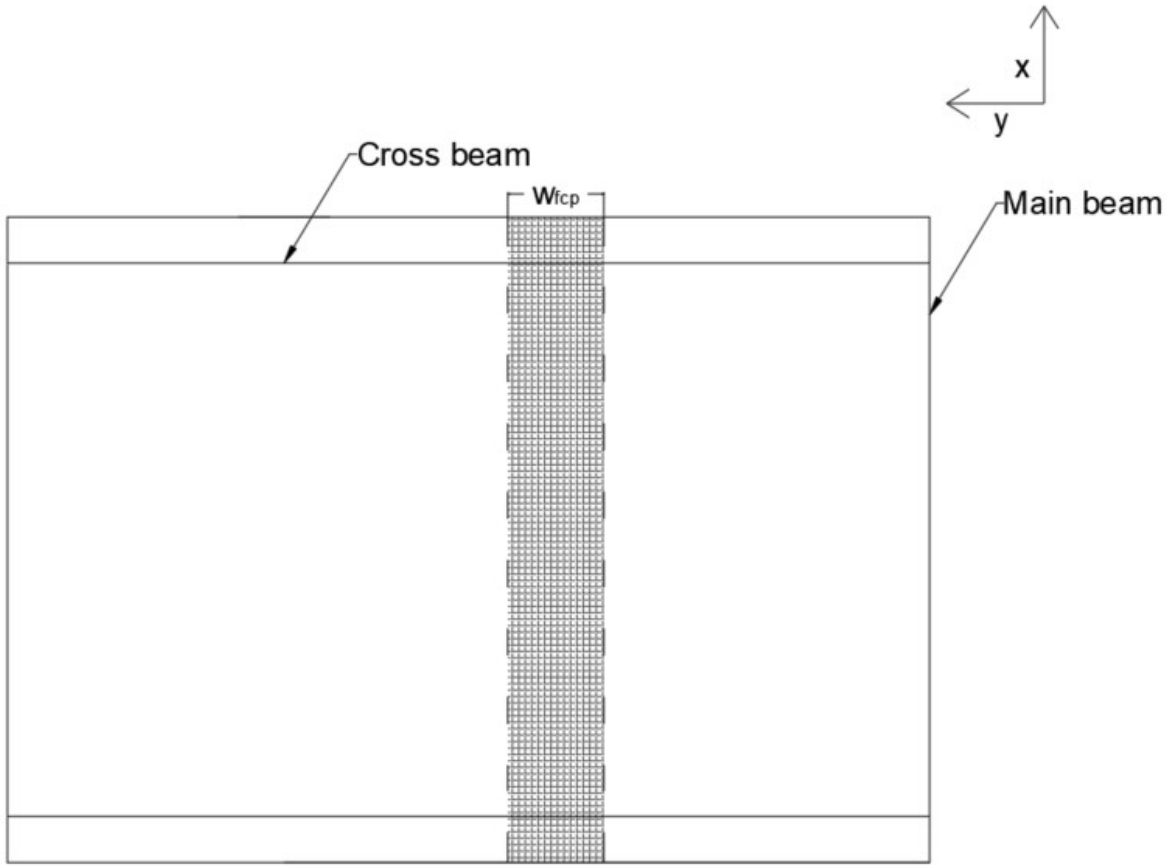

Deflections deck between crossbeams

$$w_{midspan\_q} := \frac{5}{384} \cdot \frac{q_{fcp} \cdot w_{fcp} \cdot h.o.h_{crossbeam}^{4}}{EI_{fcp}} = 2.71 \ mm$$

$$w_{midspan\_Q} := \frac{1}{48} \cdot \frac{Q_{serv} \cdot h.o.h_{crossbeam}^{3}}{EI_{fcp}} = 6.07 \ mm$$

Deflections crossbeam

$$w_{cb\_Q} := \frac{1}{48} \frac{Q_{serv} \cdot \left(b_{edge} - w_{serv\_edge}\right)^{3}}{EI_{cb\_comb}} + \frac{1}{48} \frac{Q_{serv} \cdot \left(b_{edge} - w_{serv\_edge} - w_{serv}\right)^{3}}{EI_{cb\_comb}} = 0.1 \ mm$$

$$w_{cb\_q} := \frac{5}{384} \cdot \frac{q_{fcp} \cdot h.o.h_{crossbeam} \cdot b_{edge}^{4}}{EI_{cb\_comb}} = 0.4 \ mm$$

Deflections limit

$$w_{limit\_midspan} := \frac{h.o.h_{crossbeam}}{250} = 16.83 \ mm \qquad w_{limit\_threshold} := 5 \ mm$$

Unity checks

$$u.c._{deflection\_threshold} := \frac{\max\left(w_{cb\_Q}, w_{cb\_q}\right)}{w_{limit\_threshold}} = 0.07$$

$$u.c._{deflection\_midspan} := \frac{\max\left(w_{midspan\_q} + w_{cb\_q}, w_{midspan\_Q} + w_{cb\_Q}\right)}{w_{limit\_midspan}} = 0.36$$

Calculations for foot- and cycle path deck

Loadcases

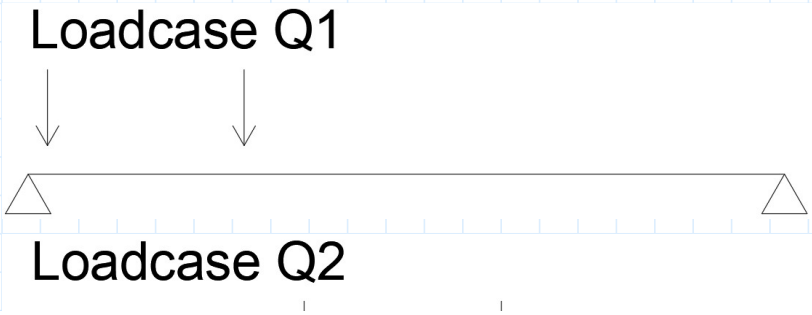

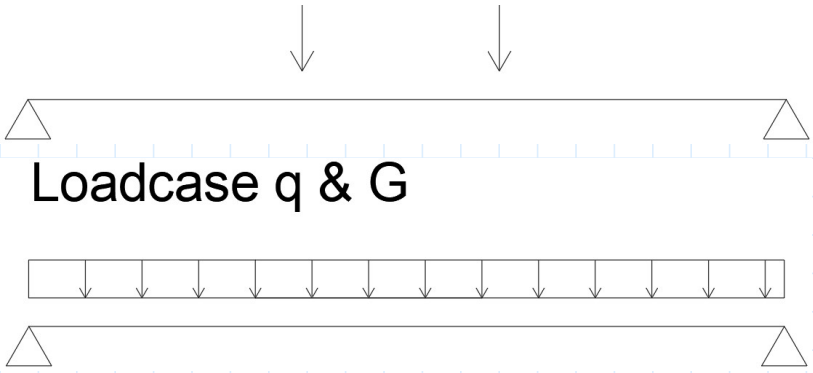

Shearforce

Loadcases q and Q1 were used

$$V_{q\_fcp} := \frac{1}{2} \cdot q_{fcp} \cdot h.o.h_{crossbeam} \cdot w_{fcp} = 4.461 \ \boldsymbol{kN}$$

$$V_{Qav\_fcp} := \frac{h.o.h_{crossbeam} - \frac{l_{w\_av}}{2}}{h.o.h_{crossbeam}} \cdot Q_{av1} + \frac{h.o.h_{crossbeam} - h.o.h_{av} - \frac{l_{w\_av}}{2}}{h.o.h_{crossbeam}} \cdot Q_{av2} = 44.317 \ \boldsymbol{kN}$$

Bending moments

Loadcases q and Q2 were used

$$M_{q\_fcp} := \frac{1}{8} \cdot q_{fcp} \cdot w_{fcp} \cdot h.o.h_{crossbeam}^{\ 2} = 4.693 \ \boldsymbol{kN \cdot m}$$

$$M_{Qav\_fcp} := \frac{1}{4} \cdot Q_{av1} \cdot h.o.h_{crossbeam} - \frac{1}{2} \cdot \frac{Q_{av1}}{l_{w\_av}} \cdot \left(\frac{l_{w\_av}}{2} \right)^2 = 41.083 \ \boldsymbol{kN \cdot m}$$

Self weight

$$G_{fcp} := \left(2 \cdot t_{l\_fcp} \cdot w_{fcp} \cdot \rho_{l\_fcp} + t_{c\_fcp} \cdot w_{fcp} \cdot \rho_{balsa} \right) \cdot 9.81 \ \frac{\boldsymbol{m}}{\boldsymbol{s}^2} = 0.427 \ \frac{\boldsymbol{kN}}{\boldsymbol{m}}$$

Resultant forces as a result of self weight

Loadcase G was used

$$V_{G\_fcp} := \frac{1}{2} \cdot G_{fcp} \cdot h.o.h_{crossbeam} = 0.898 \ \boldsymbol{kN}$$

$$M_{G\_fcp} := \frac{1}{8} \cdot G_{fcp} \cdot h.o.h_{crossbeam}^{\ 2} = 0.945 \ \boldsymbol{kN \cdot m}$$

Combined forces with 6.10 B

$$V_{Ed\_fcp} := 1.2 \cdot V_{G\_fcp} + \max\left(1.5 \cdot V_{q\_fcp}, V_{Qav\_fcp}\right) = 45.394 \ \textbf{kN}$$

$$M_{Ed\_fcp} := 1.2 \cdot M_{G\_fcp} + \max\left(1.5 \ M_{q\_fcp}, M_{Qav\_fcp}\right) = 42.217 \ \textbf{kN} \cdot \textbf{m}$$

$$N_{Ed\_fcp} := 0.6 \cdot 2 \cdot \left(Q_{av1} + Q_{av2}\right) = 72 \ \textbf{kN}$$

Resultant stresses

$$\tau_{c\_fcp} := \frac{V_{Ed\_fcp}}{A_{fcp}} = 0.535 \ \textbf{MPa}$$

$$\sigma_{l\_fcp} := \frac{M_{Ed\_fcp}}{EI_{fcp}} \cdot \frac{t_{d\_fcp}}{2} \cdot E_{1\_l\_fcp} = 39 \ \textbf{MPa}$$

$$\sigma_{n\_fcp} := \frac{N_{Ed\_fcp} \cdot \left(2 \cdot t_{c\_fcp} - t_{l\_fcp}\right)}{2 \cdot t_{l\_fcp} \cdot b_{fcp} \cdot \left(t_{c\_fcp} - t_{l\_fcp}\right)} = 1 \ \textbf{MPa}$$

$$\sigma_{c\_fcp} := \frac{M_{Ed\_fcp}}{EI_{fcp}} \cdot \left(\frac{t_{d\_fcp}}{2} - t_{l\_fcp}\right) \cdot E_{balsa\_z} = 0.95 \ \textbf{MPa}$$

Unity checks

$$u.c._{\tau\_fcp} := \frac{\tau_{c\_fcp}}{f_{c\_xz\_v\_d}} = 0.58$$

$$u.c._{\sigma\_fcp} := \frac{\sigma_{l\_fcp} + \sigma_{n\_fcp}}{f_{fcp\_x\_d}} = 0.31$$

$$u.c._{\sigma\_c\_fcp} := \frac{\sigma_{c\_fcp}}{f_{c\_z\_d}} = 0.29$$

Calculations for crossbeam

Loadcases

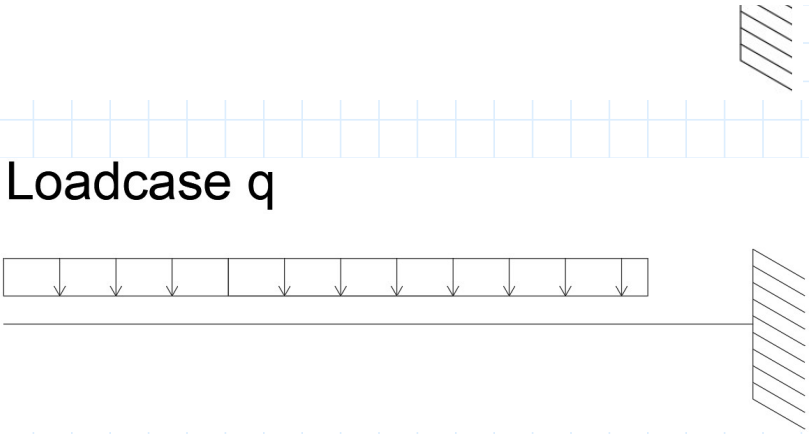

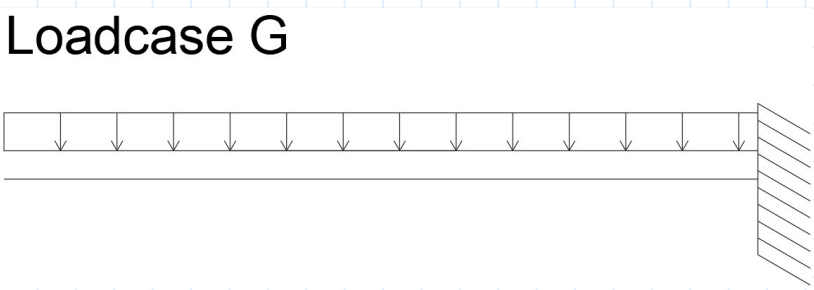

Shearforce

Loadcases q and Q1 were used

$V_{fcp\_q\_cb} := q_{fcp} \cdot b_{fcp} \cdot h.o.h_{crossbeam} = 90\ \boldsymbol{kN}$

$V_{fcp\_Q\_cb} := 2 \cdot \left(Q_{av1} + Q_{av2}\right) = 120\ \boldsymbol{kN}$

Bending moments

Loadcases q and Q1 were used

$M_{h\_q\_cb} := \frac{1}{2} \cdot q_{fcp} \cdot h.o.h_{crossbeam} \cdot b_{fcp}^{\ 2} + q_{fcp} \cdot h.o.h_{crossbeam} \cdot b_{fcp} \cdot \left(b_{edge} - b_{fcp}\right) = 258\ \boldsymbol{kN \cdot m}$

$M_{h\_Q\_cb} := \left(Q_{av1} + Q_{av2}\right) \cdot \left(2 \cdot b_{edge} - 2 \cdot w_{av\_edge} - w_{av}\right) = 450\ \boldsymbol{kN \cdot m}$

Self weight

$$G_{cb\_fcp} := \begin{pmatrix} \left(2 \cdot t_{cb\_f\_side} \cdot w_{cb\_f\_side} + t_{cb\_w\_side} \cdot \left(h_{cb\_side} - 2 \cdot t_{cb\_f\_side}\right)\right) \cdot \rho_{steel} \\ + 2 \cdot t_{l\_fcp} \cdot h.o.h_{crossbeam} \cdot \rho_{l\_fcp} + t_{c\_fcp} \cdot h.o.h_{crossbeam} \cdot \rho_{balsa} \end{pmatrix} \cdot 9.81\ \frac{\boldsymbol{m}}{\boldsymbol{s}^2} = 6.1\ \frac{\boldsymbol{kN}}{\boldsymbol{m}}$$

$G_{cb\_fcp} = 6.1\ \frac{\boldsymbol{kN}}{\boldsymbol{m}}$

Resultant forces as a result of self weight

Loadcase G was used

$V_{G\_cb\_fcp} := G_{cb\_fcp} \cdot b_{edge} = 30.3\ \mathbf{kN}$

$M_{G\_cb\_fcp} := \frac{1}{2} \cdot G_{cb\_fcp} \cdot b_{fcp}{}^2 + G_{cb\_fcp} \cdot b_{fcp} \cdot \left(b_{edge} - b_{fcp}\right) = 74.2\ \mathbf{kN \cdot m}$

Combined forces with 6.10 B

$V_{Ed\_cb\_side} := 1.2 \cdot V_{G\_cb\_fcp} + \max\left(1.5 \cdot V_{fcp\_q\_cb}, V_{fcp\_Q\_cb}\right) = 171.44\ \mathbf{kN}$

$M_{Ed\_cb\_side} := 1.2 \cdot M_{G\_cb\_fcp} + \max\left(1.5 \cdot M_{h\_q\_cb}, M_{h\_Q\_cb}\right) = 539\ \mathbf{kN \cdot m}$

Resultant stresses

$\tau_{Ed\_cb\_side} := \frac{V_{Ed\_cb\_side}}{A_{cb\_v\_side}} = 19.8\ \mathbf{MPa}$

$\sigma_{Ed\_cb\_side} := \frac{M_{Ed\_cb\_side}}{EI_{cb\_side}} \cdot E_{steel} \cdot \frac{1}{2} \cdot h_{cb\_side} = 100.1\ \mathbf{MPa}$

Unity checks

$u.c._{\tau\_cb} := \frac{\tau_{Ed\_cb\_side}}{f_{st}} = 0.056$

$u.c._{\sigma\_cb\_side} := \frac{\sigma_{Ed\_cb\_side}}{\chi_{LT} \cdot f_{st}} = 0.705$

Auxiliary calculations

Calculations for ship impact forces

$F_{ship} := 1\ \mathbf{MN}$ $h_{ship} := 0.25\ \mathbf{m}$ $w_{ship} := 3\ \mathbf{m}$

$A_{edge} := 15598\ \mathbf{mm}^2$ $I_{cr\_edge} := 11271 \cdot 10^4\ \mathbf{mm}^4$ Edge crossbeam is an IPE600

$h_{I\_edge} := 600\ \mathbf{mm}$ $b_{I\_edge} := 220\ \mathbf{mm}$

$t_{w\_I\_edge} := 12\ \mathbf{mm}$ $t_{f\_I\_edge} := 19\ \mathbf{mm}$ $r_{I\_edge} := 24\ \mathbf{mm}$

Beam buckling resistance

$\varepsilon_{I\_edge} := 0.81$ $class_{f\_edge} := 1$ $class_{w\_edge} := 4$ $l_{cr\_edge} := 2 \cdot b_{edge}$

$\lambda_1 := 93.9 \cdot \varepsilon_{I\_edge} = 76$ $\psi_{w\_edge} := 1$ $k_{\sigma\_I\_edge} := 4$

$$\lambda_{p\_w\_edge} := \frac{\frac{h_{I\_edge} - 2 \cdot t_{f\_I\_edge} - 2 \cdot r_{I\_edge}}{t_{w\_I\_edge}}}{28.4 \cdot \varepsilon_{I\_edge} \cdot \sqrt{k_{\sigma\_I\_edge}}} = 0.931$$

$0.5 + \sqrt{0.085 - 0.055 \cdot \psi_{w\_edge}} = 0.673$ $\rho_{I\_edge} := \frac{\lambda_{p\_w\_edge} - 0.055 \cdot (3 + \psi_{w\_edge})}{\lambda_{p\_w\_edge}^{2}} = 0.82$

$b_{eff\_I\_edge} := \rho_{I\_edge} \cdot (h_{I\_edge} - 2 \cdot (t_{f\_I\_edge} + r_{I\_edge})) = 422\ mm$

$A_{eff\_I\_edge} := (2 \cdot r_{I\_edge} + b_{eff\_I\_edge}) \cdot t_{w\_I\_edge} + \pi \cdot r_{I\_edge}^{2} + b_{I\_edge} \cdot t_{f\_I\_edge} = 11625\ mm^2$

$i_{I\_edge} := \sqrt{\frac{I_{cr\_edge}}{A_{eff\_I\_edge}}} = 0.098\ m$ $\lambda_{I\_edge} := \sqrt{\frac{l_{cr\_edge}}{i_{I\_edge} \cdot \lambda_1}} = 1.156$ $\alpha_{I\_edge} := 0.34$

$\phi_{I\_edge} := 0.5 \cdot (1 + \alpha_{I\_edge} \cdot (\lambda_{I\_edge} - 0.2) + \lambda_{I\_edge}^{2}) = 1.33$

$$\chi_{I\_edge} := \frac{1}{\phi_{I\_edge} + \sqrt{\phi_{I\_edge}^{2} + \lambda_{I\_edge}^{2}}} = 0.323$$

$N_{cr} := \chi_{I\_edge} \cdot A_{eff\_I\_edge} \cdot f_{st} = 1.335\ MN$

Results

Unity checks

Unity checks traffic loads

Deflections

$u.c._{deflection\_threshold} = 0.07$ $u.c._{deflection\_midspan} = 0.36$

Foot and cycle paths

$u.c._{\tau\_fcp} = 0.58$ $u.c._{\sigma\_fcp} = 0.31$ $u.c._{\sigma\_c\_fcp} = 0.29$

Crossbeam

$u.c._{\tau\_cb} = 0.06$ $u.c._{\sigma\_cb\_side} = 0.7$

Unity checks ship colision

Reduction of force to main structure due to collision with fcp deck (supp)

$Reduction := 0$

MKI

$€ := 1$ ¤

$Mass_{E\_glass} := 4 \cdot t_{l\_fcp} \cdot b_{edge} \cdot l \cdot \rho_{l\_fcp} = 11.5$ *tonne*

$Mass_{Balsa} := 2 \cdot t_{c\_fcp} \cdot b_{edge} \cdot l \cdot \rho_{balsa} = 14.393$ *tonne*

$Mass_{Steel} := n_{crossbeam} \cdot 2 \cdot A_{edge} \cdot b_{edge} \cdot \rho_{steel} = 8.517$ *tonne*

$A_{E\_glass} := 4 \cdot \left(b_{edge} + t_{d\_fcp}\right) \cdot l = 527.624$ m^2

$A_{Steel} := \left(2 \cdot h_{I\_edge} + 4 \cdot b_{I\_edge} - 2 \cdot t_{w\_I\_edge}\right) \cdot 2 \cdot b_{edge} \cdot n_{crossbeam} = 143.92$ m^2

$MKI_{Steel} := 0.165 \ \frac{€}{kg}$ $\quad MKI_{score\_Steel} := MKI_{Steel} \cdot Mass_{Steel} = 1405.2$ €

$MKI_{E\_glass} := 0.265 \ \frac{€}{kg}$ $\quad MKI_{score\_E\_glass} := MKI_{E\_glass} \cdot Mass_{E\_glass} = 3051.2$ €

$MKI_{Balsa} := -0.15 \ \frac{€}{kg}$ $\quad MKI_{score\_Balsa} := MKI_{Balsa} \cdot Mass_{Balsa} = -2158.9$ €

$MKI_{Steel\_cons} := 0.300 \ \frac{€}{m^2}$ $\quad MKI_{score\_Steel\_cons} := 5 \cdot MKI_{Steel\_cons} \cdot A_{Steel} = 215.9$ €

$MKI_{E\_glass\_cons} := 1.173 \ \frac{€}{m^2}$ $\quad MKI_{score\_E\_glass\_cons} := MKI_{E\_glass\_cons} \cdot A_{E\_glass} = 618.9$ €

$MKI_{score\_Total} := MKI_{score\_Steel} + MKI_{score\_E\_glass} + MKI_{score\_Balsa} + MKI_{score\_Steel\_cons} + MKI_{score\_E\_glass\_cons} = 3132$ €

Mass

$Mass_{total} := Mass_{Steel} + Mass_{E\_glass} + Mass_{Balsa} = 34$ *tonne*

Appendix IV, Structural checks full FRP FCP.

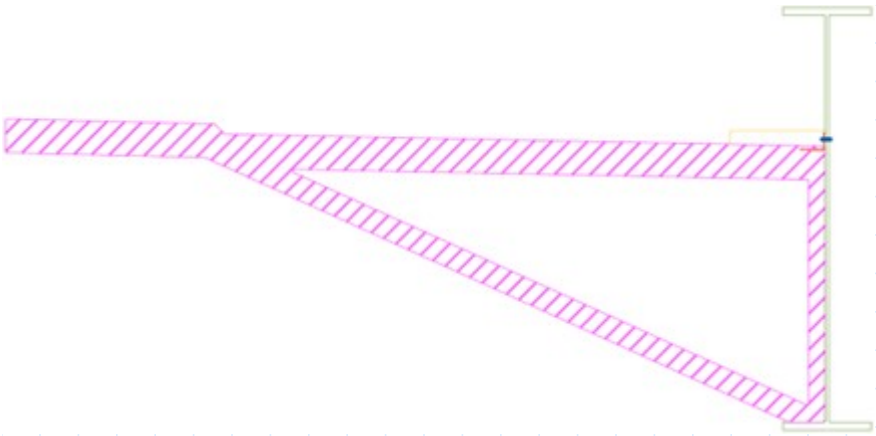

Table of Contents

General

General dimensions

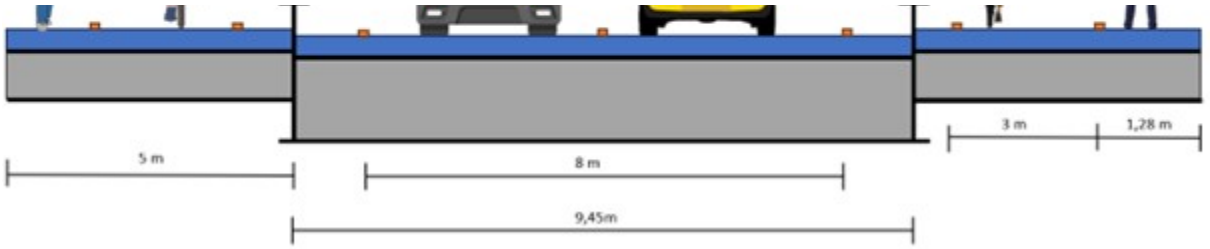

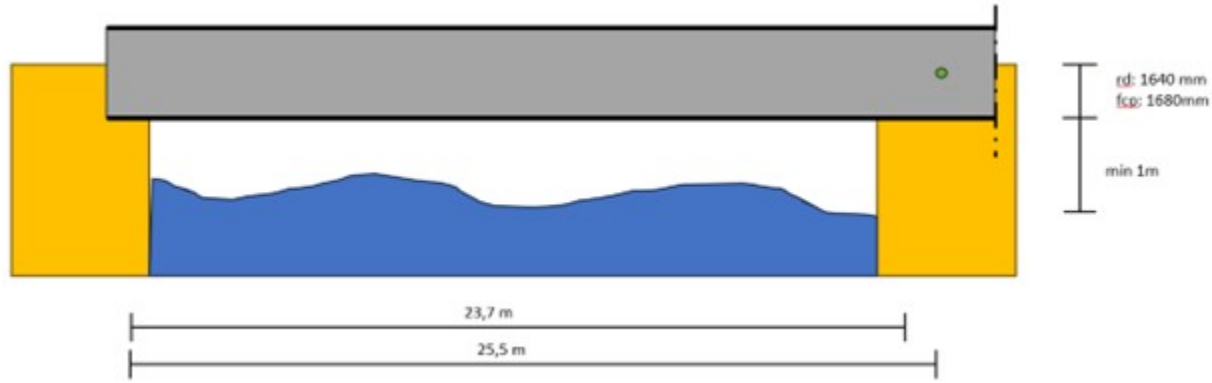

$l := 25250\ mm$

$b_{fcp} := 4.28\ m$ $b_{edge} := 5\ m$ $b_{rd} := 8\ m$ $b_{supp} := 9.45\ m$

$n_{fcp\_supp} := 17$ $h.o.h_{fcp\_supp} := \frac{l}{n_{fcp\_supp} - 1} = 1.58\ m$

$h_{rd} := 5.9\ m$ $h_{fcp} := 6.05\ m$ $h_{water} := 3.3\ m$ $h_{under\_side} := 4.3\ m$

$\theta_{max} := 80\ °$ $h_{top} := \sin\left(\theta_{max}\right) \cdot l + h_{rd} = 30.8\ m$

General properties

$T_{s\_sun} := 57\ °C$ $T_{s\_shade} := 31\ °C$

Partial Safety Factors

Partial factors balsa

$\rho_{balsa} := 285\ \frac{kg}{m^3}$ $G_{balsa} := 145\ MPa$

$E_{balsa\_z} := 720\ MPa$ $E_{balsa\_x} := 2642\ MPa$

$f_{c\_zz\_k} := 2.08\ MPa$ $f_{c\_xx\_k} := 7.32\ MPa$

$$\eta_{ct\_balsa} := min\left(1 - \left(\frac{0.2\ \frac{kg}{m^3}}{\rho_{balsa}} + 0.004\right) \cdot \left(\frac{T_{s\_sun} - 20\ °C}{1\ °C}\right), 1\right) = 1$$

$\eta_{cm\_balsa} := 1$ $\eta_{c\_balsa} := \eta_{ct\_balsa} \cdot \eta_{cm\_balsa} = 1$

$\gamma_{m\_balsa} := 1.51$ $\gamma_{rd\_balsa} := 1.5$

$$f_{c\_xz\_v\_d} := \frac{\eta_{c\_balsa} \cdot f_{c\_xz\_v\_k}}{\gamma_{m\_balsa} \cdot \gamma_{rd\_balsa}} = 0.92\ MPa$$

$$f_{c\_z\_d} := \frac{\eta_{c\_balsa} \cdot f_{c\_z\_k}}{\gamma_{m\_balsa} \cdot \gamma_{rd\_balsa}} = 3.23\ MPa$$

Partial factors frp foot- and cycle path

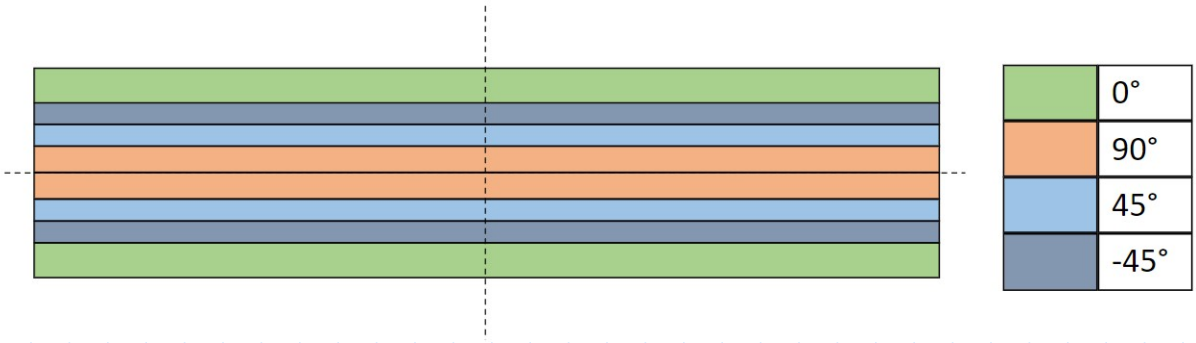

Laminate layup foot- and cycle path

$$\begin{bmatrix} 0 \\ 90 \\ 45 \\ -45 \end{bmatrix} \quad \begin{bmatrix} 50\% \\ 16.67\% \\ 16.67\% \\ 16.67\% \end{bmatrix}$$

$\rho_{l\_fcp} := 1900\ \frac{kg}{m^3}$ $E_{1\_l\_fcp} := 26.2\ GPa$ $E_{2\_l\_fcp} := 17.5\ GPa$

$f_{fcp\_x\_k} := 367\ MPa$ $f_{fcp\_y\_k} := 245\ MPa$ $f_{fcp\_xy\_k} := 150\ MPa$

$T_{g\_fcp} := 90\ °C$

$$\eta_{ct\_f\_fcp} := min\left(1 - 0.25 \cdot \frac{T_{s\_sun} - 20\ °C}{T_{g\_fcp} - 20\ °C}, 1\right) = 0.9$$

$$\eta_{cm\_f\_fcp} := 0.6 \qquad \eta_{c\_f\_fcp} := \eta_{ct\_f\_fcp} \cdot \eta_{cm\_f\_fcp} = 0.521$$

$$\eta_{ct\_m\_fcp} := min\left(1 - 0.80 \cdot \frac{T_{s\_sun} - 20\ °C}{T_{g\_fcp} - 20\ °C}, 1\right) = 0.6$$

$$\eta_{cm\_m\_fcp} := 0.6 \qquad \eta_{c\_m\_fcp} := \eta_{ct\_m\_fcp} \cdot \eta_{cm\_m\_fcp} = 0.346$$

$$\gamma_{m\_fcp} := 1.07 \qquad \gamma_{rd\_fcp} := 1.4$$

$$f_{fcp\_x\_d} := \frac{\eta_{c\_f\_fcp} \cdot f_{fcp\_x\_k}}{\gamma_{rd\_fcp} \cdot \gamma_{m\_fcp}} = 127.6\ \textbf{\textit{MPa}}$$

$$f_{fcp\_y\_d} := \frac{\eta_{c\_f\_fcp} \cdot f_{fcp\_y\_k}}{\gamma_{rd\_fcp} \cdot \gamma_{m\_fcp}} = 85.2\ \textbf{\textit{MPa}}$$

$$f_{fcp\_xy\_d} := \frac{\eta_{c\_f\_fcp} \cdot f_{fcp\_xy\_k}}{\gamma_{rd\_fcp} \cdot \gamma_{m\_fcp}} = 52.1\ \textbf{\textit{MPa}}$$

Partial factors frp foot- and cycle path support

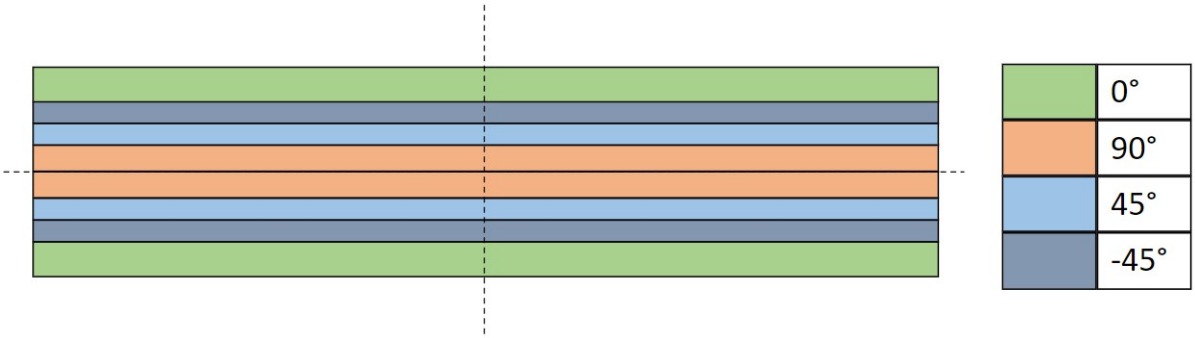

Laminate layup support

$$\begin{bmatrix} 0 \\ 90 \\ 45 \\ -45 \end{bmatrix} \quad \begin{bmatrix} 62.5\% \\ 12.5\% \\ 12.5\% \\ 12.5\% \end{bmatrix}$$

$\rho_{l\_fcp\_supp} := 1900\ \frac{kg}{m^3}$ $E_{l\_fcp\_supp} := 27.5\ GPa$

$f_{fcp\_supp\_x\_k} := 385\ MPa$ $f_{fcp\_supp\_y\_k} := 262\ MPa$ $f_{fcp\_supp\_xy\_k} := 132\ MPa$

$\eta_{ct\_f\_fcp\_supp} := min\left(1 - 0.25 \cdot \frac{T_{s\_shade} - 20\ °C}{T_{g\_fcp} - 20\ °C}, 1\right) = 1$

$\eta_{cm\_f\_fcp\_supp} := 0.6$ $\eta_{c\_f\_fcp\_supp} := \eta_{ct\_f\_fcp\_supp} \cdot \eta_{cm\_f\_fcp\_supp} = 0.576$

$\eta_{ct\_m\_fcp\_supp} := min\left(1 - 0.80 \cdot \frac{T_{s\_shade} - 20\ °C}{T_{g\_fcp} - 20\ °C}, 1\right) = 0.9$

$\eta_{cm\_m\_fcp\_supp} := 0.6$ $\eta_{c\_m\_fcp\_supp} := \eta_{ct\_m\_fcp\_supp} \cdot \eta_{cm\_m\_fcp\_supp} = 0.525$

$f_{fcp\_supp\_x\_d} := \frac{\eta_{c\_f\_fcp\_supp} \cdot f_{fcp\_supp\_x\_k}}{\gamma_{rd\_fcp} \cdot \gamma_{m\_fcp}} = 148.1\ MPa$

$f_{fcp\_supp\_y\_d} := \frac{\eta_{c\_f\_fcp\_supp} \cdot f_{fcp\_supp\_y\_k}}{\gamma_{rd\_fcp} \cdot \gamma_{m\_fcp}} = 100.8\ MPa$

$f_{fcp\_supp\_xy\_d} := \frac{\eta_{c\_f\_fcp\_supp} \cdot f_{fcp\_supp\_xy\_k}}{\gamma_{rd\_fcp} \cdot \gamma_{m\_fcp}} = 50.8\ MPa$

Traffic load calculations

Cross section properties

Load properties

Distirbuted load foot and cycle path

$q_{fcp} := 5\ \frac{kN}{m^2}$

Concentrated load service vehicle

$Q_{serv} := 12.5\ kN$

$l_{w\_serv} := 25\ cm$ $w_{w\_serv} := 25\ cm$ $w_{serv} := 1.75\ m$ $h.o.h_{serv} := 3\ m$

Concentrated load accidental vehicle

$Q_{av1} := 40\ kN \quad Q_{av2} := 20\ kN$

$l_{w\_av} := 20\ cm \quad w_{w\_av} := 20\ cm \quad w_{av} := 1.3\ m \quad h.o.h_{av} := 3\ m$

Foot- and cycle path properties

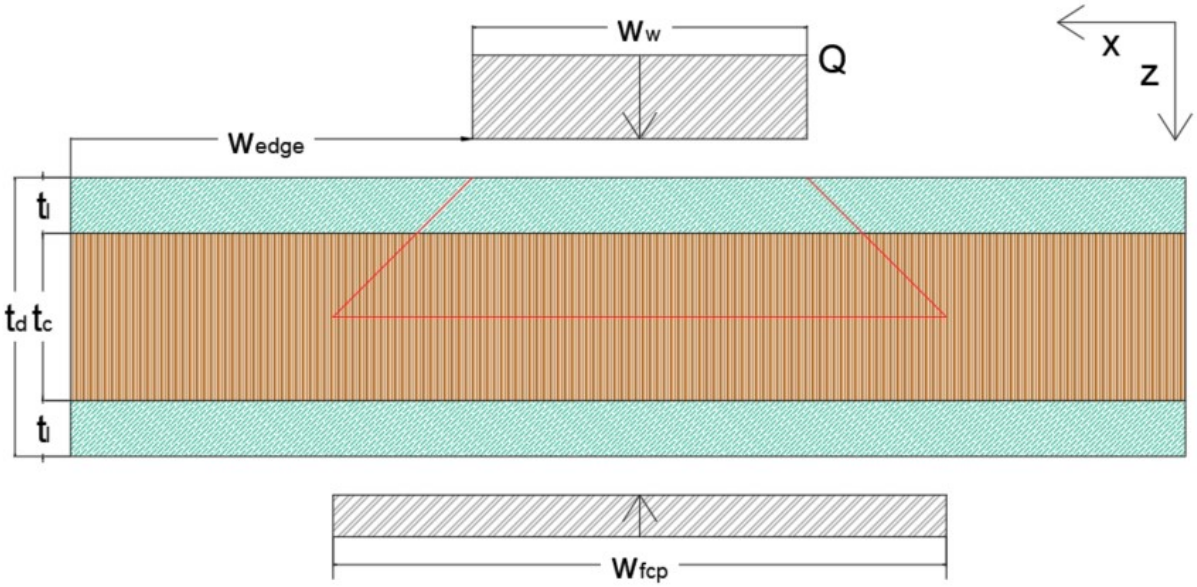

$t_{l\_fcp} := 12\ mm \quad t_{c\_fcp} := 250\ mm \quad t_{d\_fcp} := t_{c\_fcp} + 2 \cdot t_{l\_fcp} = 274\ mm$

$x_{1\_fcp} := 1.5\ m \quad x_{2\_fcp} := b_{edge} - x_{1\_fcp} = 3.5\ m$

$w_{av\_edge} := 0.5\ m + \frac{w_{w\_av}}{2} = 0.6\ m \quad w_{fcp} := l_{w\_av} + t_{d\_fcp} = 474\ mm$

$A_{fcp} := w_{fcp} \cdot t_{c\_fcp} = 0.119\ m^2$

$EI_{fcp\_yz} := 2 \cdot E_{1\_l\_fcp} \cdot w_{fcp} \cdot t_{l\_fcp} \cdot \left(\frac{t_{c\_fcp} + t_{l\_fcp}}{2} \right)^2 = 5559\ kN \cdot m^2$

$+ \frac{1}{12} \cdot E_{balsa\_z} \cdot w_{fcp} \cdot t_{c\_fcp}^{\ 3}$

$EI_{fcp\_xz} := 2 \cdot E_{2\_l\_fcp} \cdot w_{fcp} \cdot t_{l\_fcp} \cdot \left(\frac{t_{c\_fcp} + t_{l\_fcp}}{2} \right)^2 = 3861\ kN \cdot m^2$

$+ \frac{1}{12} \cdot E_{\ldots} \cdot w_{\ldots} \cdot t_{\ldots}^{\ 3}$

$$\frac{1}{12} \cdot E_{balsa\_z} \cdot w_{fcp} \cdot t_{c\_fcp}$$

Support properties

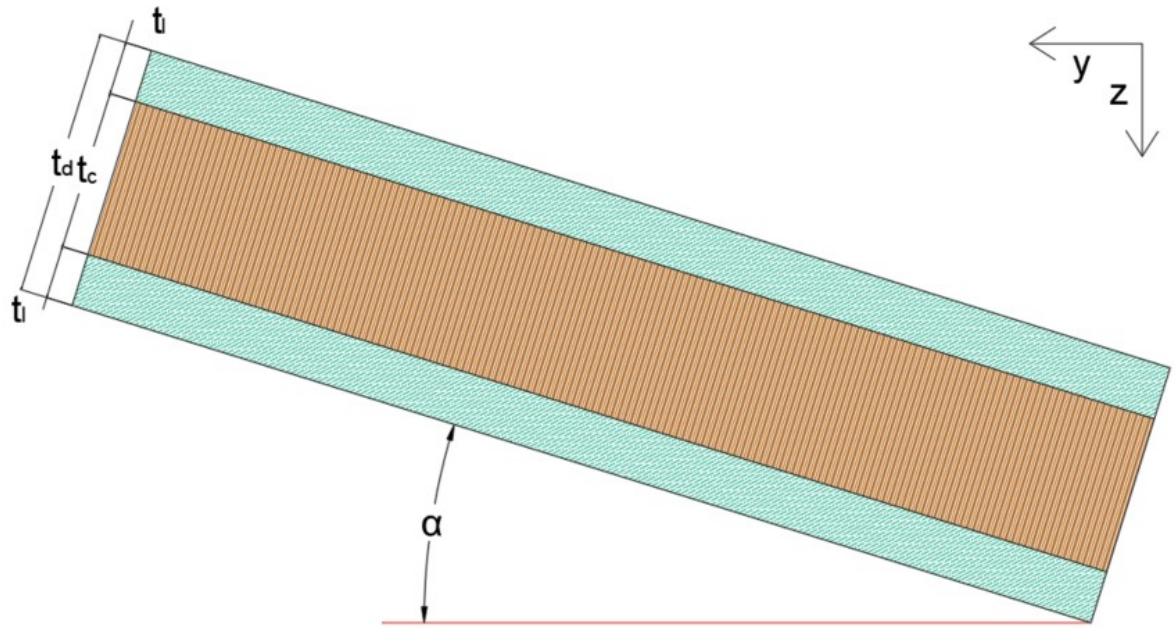

$w_{fcp\_supp} := 0.5\ m$ $t_{l\_fcp\_supp} := 18\ mm$ $t_{c\_fcp\_supp} := 160\ mm$

$t_{d\_fcp\_supp} := 2 \cdot t_{l\_fcp\_supp} + t_{c\_fcp\_supp} = 196\ mm$

$l_{fcp\_supp} := \sqrt{\left(h_{fcp} - t_{d\_fcp} - h_{under\_side}\right)^2 + \left(b_{edge} - x_{1\_fcp}\right)^2} = 3.798\ m$

$\alpha := \operatorname{atan}\left(\frac{h_{fcp} - t_{d\_fcp} - h_{under\_side}}{x_{2\_fcp}}\right) = 22.866\ °$

$A_{V\_fcp\_supp} := t_{c\_fcp\_supp} \cdot w_{fcp\_supp} = 0.08\ m^2$

$EI_{fcp\_supp} := 2 \cdot E_{l\_fcp\_supp} \cdot w_{fcp\_supp} \cdot t_{l\_fcp\_supp} \cdot \left(\frac{t_{c\_fcp\_supp} + t_{l\_fcp\_supp}}{2}\right)^2 = 4044\ kN \cdot m^2$

$+ \frac{1}{12} \cdot E_{balsa\_z} \cdot w_{fcp\_supp} \cdot t_{c\_fcp\_supp}^3$

Calculations for deflections

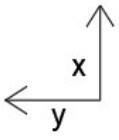

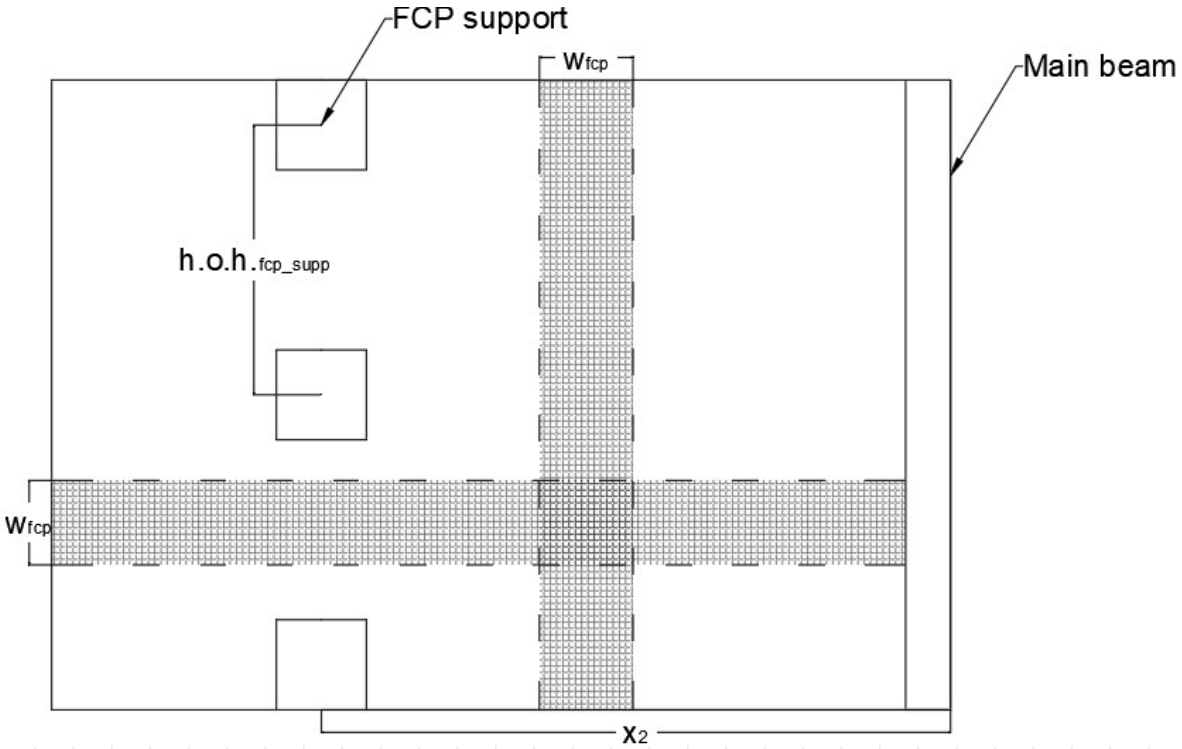

Deflections deck between supports

$$w_{midspan\_q\_yz} := \frac{5}{384} \cdot \frac{q_{fcp} \cdot w_{fcp} \cdot x_{2\_fcp}^{4}}{EI_{fcp\_yz}} = 0.83\ mm$$

$$w_{midspan\_q\_xz} := \frac{5}{384} \cdot \frac{q_{fcp} \cdot w_{fcp} \cdot h.o.h_{fcp\_supp}^{4}}{EI_{fcp\_xz}} = 0.05\ mm$$

$$w_{midspan\_q} := w_{midspan\_q\_yz} + w_{midspan\_q\_xz} = 0.883\ mm$$

$$w_{midspan\_Q\_yz} := \frac{1}{48} \cdot \frac{Q_{serv} \cdot x_{2\_fcp}^{3}}{EI_{fcp\_yz}} = 2.01\ mm$$

$$w_{midspan\_Q\_xz} := \frac{1}{48} \cdot \frac{Q_{serv} \cdot h.o.h_{fcp\_supp}^{3}}{EI_{fcp\_xz}} = 0.265\ mm$$

$$w_{midspan\_Q} := w_{midspan\_Q\_yz} + w_{midspan\_Q\_xz} = 2.274\ mm$$

Deflections limit

$$w_{limit\_midspan} := \frac{h.o.h_{fcp\_supp}}{250} = 6.31\ mm \qquad w_{limit\_threshold} := 5\ mm$$

Unity checks

$$u.c._{deflection\_threshold} := \frac{\max\left(w_{midspan\_q\_yz}, w_{midspan\_Q\_yz}\right)}{w_{limit\_threshold}} = 0.4$$

$$u.c._{deflection\_midspan} := \frac{\max\left(w_{midspan\_q}, w_{midspan\_Q}\right)}{w_{limit\_midspan}} = 0.36$$

Calculations for foot- and cycle path deck

Loadcases forces in x-y plane

Loadcase q1

Loadcase q2

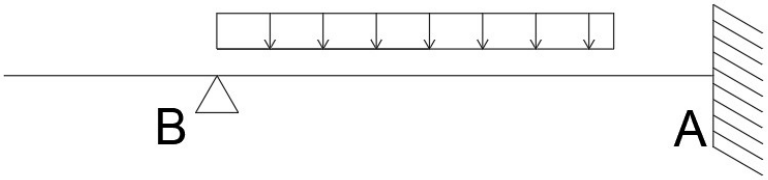

Loadcase q3

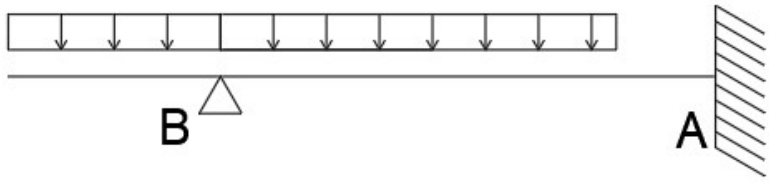

Loadcase Q1

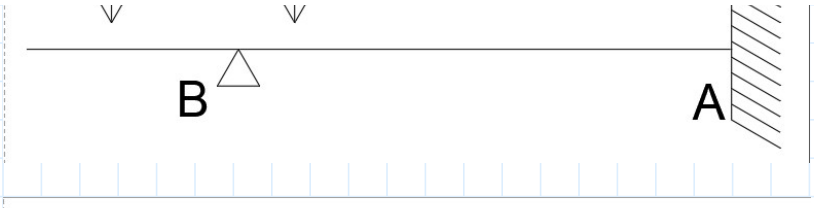

Loadcase Q2

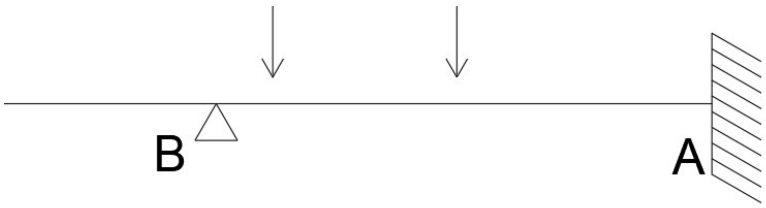

Loadcase G

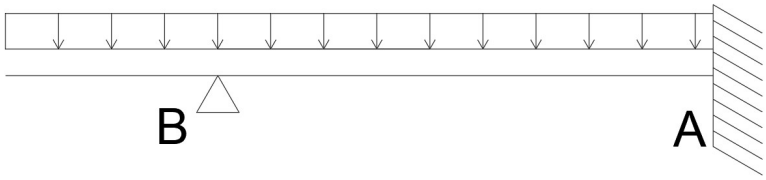

Shearforce at B-

Loadcases q1 and Q1 were used

$V_{q\_fcp\_B\_left} := q_{fcp} \cdot x_{1\_fcp} \cdot w_{fcp} = 3.555\ kN$

$V_{Qav\_fcp\_B\_left} := Q_{av1} = 40\ kN$

Shearforce at B+

Loadcases q2 and Q2 were used

$V_{q\_fcp\_B\_right} := 3.79\ kN$ Calculated with Matrixframe

$V_{Qav\_fcp\_B\_right} := 55.57\ kN$ Calculated with Matrixframe

Shearforce at A

Loadcases q2 and Q2 were used

$V_{q\_fcp\_A} := 3.14\ kN$ Calculated with Matrixframe

$V_{Qav\_fcp\_A} := 61.49\ kN$ Calculated with Matrixframe

$Q_{av\_fcp\_A}$

Moment at B

Loadcases q1 and Q1 were used

$M_{q\_fcp\_B} := \frac{1}{2} \cdot q_{fcp} \cdot w_{fcp} \cdot x_{1\_fcp}^{2} = 2.67\ \boldsymbol{kN \cdot m}$

$M_{Qav\_fcp\_B} := Q_{av1} \cdot \left(x_{1\_fcp} - w_{av\_edge}\right) = 36\ \boldsymbol{kN \cdot m}$

Moment at A

Loadcases q2 and Q2 were used

$M_{q\_fcp\_A} := 2.8\ \boldsymbol{kN \cdot m}$ Calculated with Matrixframe

$M_{Qav\_fcp\_A} := 45.72\ \boldsymbol{kN \cdot m}$ Calculated with Matrixframe

Moment in field AB

Loadcases q2 and Q2 were used

$M_{q\_fcp\_F} := 1.78\ \boldsymbol{kN \cdot m}$ Calculated with Matrixframe

$M_{Qav\_fcp\_F} := 29.78\ \boldsymbol{kN \cdot m}$ Calculated with Matrixframe

Reactionforce at B

Loadcases q3 and Q1 were used

$R_{q\_fcp\_B} := 22.12\ \boldsymbol{kN}$ Calculated with Matrixframe

$R_{Qav\_fcp\_B} := 88.6\ \boldsymbol{kN}$ Calculated with Matrixframe

Self weight of wheel width and component width respectivly

$G_{fcp\_w} := \left(2 \cdot t_{l\_fcp} \cdot w_{fcp} \cdot \rho_{l\_fcp} + t_{c\_fcp} \cdot w_{fcp} \cdot \rho_{balsa}\right) \cdot 9.81\ \frac{\boldsymbol{m}}{\boldsymbol{s}^{2}} = 0.543\ \frac{\boldsymbol{kN}}{\boldsymbol{m}}$

$G_{fcp\_hoh\_fcp\_supp} := \begin{pmatrix} 2 \cdot t_{l\_fcp} \cdot h.o.h_{fcp\_supp} \cdot \rho_{l\_fcp} \\ + t_{c\_fcp} \cdot h.o.h_{fcp\_supp} \cdot \rho_{balsa} \end{pmatrix} \cdot 9.81\ \frac{\boldsymbol{m}}{\boldsymbol{s}^{2}} = 1.809\ \frac{\boldsymbol{kN}}{\boldsymbol{m}}$

Forces as a result of self weight

Loadcase G was used

$V_{G\_fcp\_B\_left} := G_{fcp\_w} \cdot x_{1\_fcp} = 0.82\ kN$

$V_{G\_fcp\_B\_right} := 0.93\ kN$ Calculated with Matrixframe

$V_{G\_fcp\_A} := 0.88\ kN$ Calculated with Matrixframe

$M_{G\_fcp\_B} := \frac{1}{2} \cdot G_{fcp\_w} \cdot x_{1\_fcp}^{\ 2} = 0.61\ kN \cdot m$

$M_{G\_fcp\_A} := 1.53\ m^2 \cdot G_{fcp\_w} = 0.83\ kN \cdot m$ Calculated with Matrixframe

$M_{G\_fcp\_F} := 3.05 \cdot m^2 \cdot G_{fcp\_w} = 1.657\ kN \cdot m$ Calculated with Matrixframe

$R_{G\_fcp\_B} := 5.40\ kN$ Calculated with Matrixframe

Combined forces with 6.10 B

$V_{fcp\_B\_left} := \max\left(1.5 \cdot V_{q\_fcp\_B\_left}, V_{Qav\_fcp\_B\_left}\right) + 1.2 \cdot V_{G\_fcp\_B\_left} = 40.98\ kN$

$V_{fcp\_B\_right} := \max\left(1.5 \cdot V_{q\_fcp\_B\_right}, V_{Qav\_fcp\_B\_right}\right) + 1.2 \cdot V_{G\_fcp\_B\_right} = 56.69\ kN$

$V_{fcp\_A} := \max\left(1.5 \cdot V_{q\_fcp\_A}, V_{Qav\_fcp\_A}\right) + 1.2 \cdot V_{G\_fcp\_A} = 62.55\ kN$

$M_{fcp\_B} := \max\left(1.5 \cdot M_{q\_fcp\_B}, M_{Qav\_fcp\_B}\right) + 1.2 \cdot M_{G\_fcp\_B} = 36.73\ kN \cdot m$

$M_{fcp\_A} := \max\left(1.5 \cdot M_{q\_fcp\_A}, M_{Qav\_fcp\_A}\right) + 1.2 \cdot M_{G\_fcp\_A} = 46.72\ kN \cdot m$

$M_{fcp\_F} := \max\left(1.5 \cdot M_{q\_fcp\_F}, M_{Qav\_fcp\_F}\right) + 1.2 \cdot M_{G\_fcp\_F} = 31.77\ kN \cdot m$

$V_{Ed\_fcp\_yz} := \max\left(V_{fcp\_B\_left}, V_{fcp\_B\_right}, V_{fcp\_A}\right) = 62.546\ kN$

$M_{Ed\_fcp\_yz} := \max\left(M_{fcp\_B}, M_{fcp\_A}, M_{fcp\_F}\right) = 46.718\ kN \cdot m$

$V_{Ed\_fcp\_s\_yz} := 0.6 \cdot 2\ Q_{av1} = 48\ kN$

$R_{Ed\_fcp\_B} := R_{Qav\_fcp\_B} + 1.2 \cdot R_{G\_fcp\_B} = 95.1\ kN$

Forces in x-z plane

Shearforce

Loadcases q and Q1 were used

$$V_{q\_fcp} := \frac{1}{2} \cdot q_{fcp} \cdot h.o.h_{fcp\_supp} \cdot w_{fcp} = 1.87 \ \mathbf{kN}$$

$$V_{Qav\_fcp} := \frac{h.o.h_{fcp\_supp} - \frac{l_{w\_av}}{2}}{h.o.h_{fcp\_supp}} \cdot Q_{av1} = 37.465 \ \mathbf{kN}$$

Bending moments

Loadcases q and Q2 were used

$$M_{q\_fcp} := \frac{1}{8} \cdot q_{fcp} \cdot w_{fcp} \cdot h.o.h_{fcp\_supp}^{\ 2} = 0.738 \ \mathbf{kN \cdot m}$$

$$M_{Qav\_fcp} := \frac{1}{4} \cdot Q_{av1} \cdot h.o.h_{fcp\_supp} = 15.781 \ \mathbf{kN \cdot m}$$

Maximal resultant forces

$$V_{fcp} := \max\left(V_{q\_fcp}, V_{Qav\_fcp}\right) = 37.465 \ \mathbf{kN}$$

$$M_{fcp} := \max\left(M_{q\_fcp}, M_{Qav\_fcp}\right) = 15.781 \ \mathbf{kN \cdot m}$$

Forces as a result of self weight

Loadcase G was used

$$V_{G\_fcp} := \frac{1}{2} \cdot G_{fcp\_w} \cdot h.o.h_{fcp\_supp} = 0.429 \ \mathbf{kN}$$

$$M_{G\_fcp} := \frac{1}{8} \cdot G_{fcp\_w} \cdot h.o.h_{fcp\_supp}^{\ 2} = 0.169 \ \mathbf{kN \cdot m}$$

Combined forces with 6.10 B

$$V_{Ed\_fcp\_xz} := \max\left(1.5 \cdot V_{q\_fcp}, V_{Qav\_fcp}\right) + 1.2 \cdot V_{G\_fcp} = 37.98 \ \mathbf{kN}$$

$$M_{Ed\_fcp\_xz} := \max\left(1.5 \cdot M_{q\_fcp}, M_{Qav\_fcp}\right) + 1.2 \cdot M_{G\_fcp} = 15.984 \ \mathbf{kN \cdot m}$$

Resultant stresses

$$\tau_{\_fcp\_xz} := \frac{V_{Ed\_fcp\_yz}}{\_} = 0.528 \ \mathbf{MPa}$$

$$\sigma_{c\_fcp\_yz} := \frac{V_{Ed\_fcp\_yz}}{A_{fcp}}$$

$$\tau_{c\_fcp\_xz} := \frac{V_{Ed\_fcp\_xz}}{A_{fcp}} = 0.321\ \textbf{MPa}$$

$$\sigma_{c\_fcp\_xz} := \frac{M_{Ed\_fcp\_xz}}{EI_{fcp\_xz}} \cdot \left(\frac{t_{d\_fcp}}{2} - t_{l\_fcp} \right) \cdot E_{balsa\_z} = 0.373\ \textbf{MPa}$$

$$\sigma_{c\_fcp\_yz} := \frac{M_{Ed\_fcp\_yz}}{EI_{fcp\_yz}} \cdot \left(\frac{t_{d\_fcp}}{2} - t_{l\_fcp} \right) \cdot E_{balsa\_z} = 0.756\ \textbf{MPa}$$

$$\sigma_{l\_fcp\_yz} := \frac{M_{Ed\_fcp\_yz}}{EI_{fcp\_yz}} \cdot \frac{t_{d\_fcp}}{2} \cdot E_{1\_l\_fcp} = 30\ \textbf{MPa}$$

$$\sigma_{l\_fcp\_xz} := \frac{M_{Ed\_fcp\_xz}}{EI_{fcp\_yz}} \cdot \frac{t_{d\_fcp}}{2} \cdot E_{2\_l\_fcp} = 7\ \textbf{MPa}$$

$$\tau_{l\_fcp} := \frac{V_{Ed\_fcp\_s\_yz}}{2 \cdot t_{l\_fcp} \cdot l_{w\_av}} = 10\ \textbf{MPa}$$

Unity checks

$$u.c._{\tau\_c\_fcp} := \max\left(\frac{\tau_{c\_fcp\_yz}}{f_{c\_z\_d}}, \frac{\tau_{c\_fcp\_xz}}{f_{c\_xz\_v\_d}} \right) = 0.349$$

$$u.c._{\sigma\_fcp\_yz} := \frac{\sigma_{l\_fcp\_yz}}{f_{fcp\_x\_d}} = 0.236 \qquad u.c._{\sigma\_fcp\_xz} := \frac{\sigma_{l\_fcp\_xz}}{f_{fcp\_y\_d}} = 0.081$$

$$u.c._{\sigma\_c\_fcp} := \frac{\sigma_{c\_fcp\_xz} + \sigma_{c\_fcp\_yz}}{f_{c\_z\_d}} = 0.35$$

$$u.c._{\tau\_l\_fcp} := \frac{\tau_{l\_fcp}}{f_{fcp\_xy\_d}} = 0.192$$

$$u.c._{comb\_fcp} := u.c._{\sigma\_fcp\_yz} + u.c._{\sigma\_fcp\_xz} + u.c._{\tau\_l\_fcp} = 0.51$$

Calculations for foot- and cycle path support

Loadcase

Loadcase Support

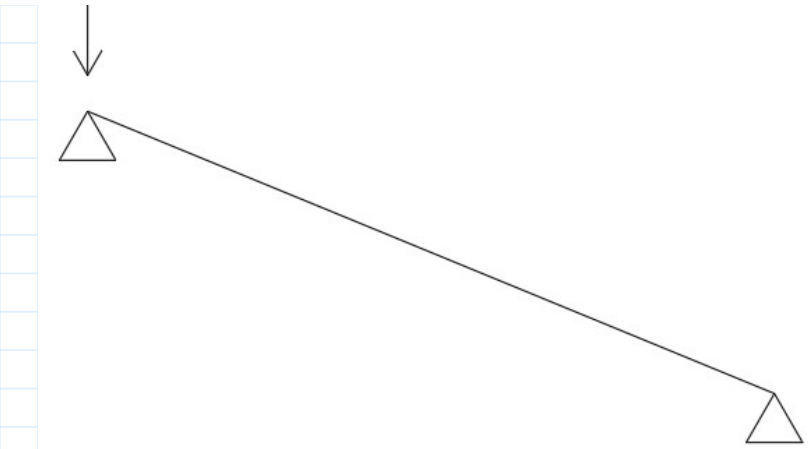

Forces recieved from deck

$F_{applied} := R_{Ed\_fcp\_B} = 95.1\ \boldsymbol{kN}$

Normal force in support

$N_{Ed\_fcp\_supp} := \frac{1}{\sin(\alpha)} \cdot F_{applied} = 244.7\ \boldsymbol{kN}$

Additional tension in deck

$N_{Ed\_fcp} := \frac{1}{\tan(\alpha)} \cdot F_{applied} = 225.461\ \boldsymbol{kN}$

Bow imperfections equivalent force

$e_{0\_d} := 1\%$

$q_{fcp\_supp\_imp} := \frac{8 \cdot N_{Ed\_fcp\_supp} \cdot e_{0\_d} \cdot l_{fcp\_supp}}{l_{fcp\_supp}^{\ 2}} = 5.153\ \frac{\boldsymbol{kN}}{\boldsymbol{m}}$

$V_{fcp\_supp\_imp} := \frac{1}{2} \cdot q_{fcp\_supp\_imp} \cdot l_{fcp\_supp} = 9.788\ \boldsymbol{kN}$

$M_{fcp\_supp\_imp} := \frac{1}{8} \cdot q_{fcp\_supp\_imp} \cdot l_{fcp\_supp}^{\ 2} = 9.295\ \boldsymbol{kN \cdot m}$

FRP sandwich buckling resistance

$\gamma_{rd\_gb} := 1.4 \qquad l_{cr} := l_{fcp\_supp} = 3.8\ \boldsymbol{m}$

$$D_f := \frac{\eta_{c\_m\_fcp} \cdot E_{l\_fcp\_supp} \cdot t_{l\_fcp\_supp}}{12} = 4.628 \ \boldsymbol{kN \cdot m}$$

$$D_0 := \frac{\eta_{c\_m\_fcp} \cdot E_{l\_fcp\_supp} \cdot t_{l\_fcp\_supp} \cdot \left(t_{c\_fcp\_supp} + t_{l\_fcp\_supp}\right)^2}{2} = \left(2.715 \cdot 10^3\right) \ \boldsymbol{kN \cdot m}$$

$$D_c := \frac{\eta_{c\_balsa} \cdot E_{balsa\_x} \cdot t_{c\_fcp\_supp}^{\ 3}}{12} = 901.23 \ \boldsymbol{kN \cdot m}$$

$$D_k := 2 \cdot D_f + D_0 + D_c = \left(3.626 \cdot 10^3\right) \ \boldsymbol{kN \cdot m}$$

$$P_{cb\_d} := \frac{1}{\gamma_{m\_fcp} \cdot \gamma_{rd\_gb}} \cdot \frac{\pi^2 \cdot D_k}{l_{cr}^{\ 2}} = 1656 \ \frac{\boldsymbol{kN}}{\boldsymbol{m}}$$

$$P_{cs\_d} := \frac{\eta_{c\_balsa}}{\gamma_{m\_balsa} \cdot \gamma_{rd\_gb}} \cdot \frac{G_{balsa} \cdot \left(t_{c\_fcp\_supp} + t_{l\_fcp\_supp}\right)^2}{t_{c\_fcp\_supp}} = 13574 \ \frac{\boldsymbol{kN}}{\boldsymbol{m}}$$

$$P_{c\_d} := \frac{P_{cb\_d} \cdot P_{cs\_d}}{P_{cb\_d} + P_{cs\_d}} = \left(1.476 \cdot 10^3\right) \ \frac{\boldsymbol{kN}}{\boldsymbol{m}}$$

Resultant stresses

$$\tau_{fcp\_supp\_imp} := \frac{V_{fcp\_supp\_imp}}{A_{V\_fcp\_supp}} = 0.122 \ \boldsymbol{MPa}$$

$$\sigma_{fcp\_supp\_imp} := \frac{M_{fcp\_supp\_imp}}{EI_{fcp\_supp}} \cdot \frac{t_{d\_fcp\_supp}}{2} \cdot E_{l\_fcp\_supp} = 6.194 \ \boldsymbol{MPa}$$

$$\sigma_{fcp\_deck\_tension} := \frac{N_{Ed\_fcp}}{2 \cdot t_{l\_fcp} \cdot \frac{h.o.h_{fcp\_supp}}{5}} = 29.764 \ \boldsymbol{MPa}$$

Unity checks

$$u.c._{buck\_fcp\_supp} := \frac{N_{Ed\_fcp\_supp}}{P_{c\_d} \cdot w_{fcp\_supp}} = 0.33$$

$$u.c._{\tau\_imp\_fcp\_supp} := \frac{\tau_{fcp\_supp\_imp}}{f_{c\_xz\_v\_d}} = 0.13$$

$$u.c._{\sigma\_imp\_fcp\_supp} := \frac{\sigma_{fcp\_supp\_imp}}{f_{fcp\_supp\_x\_d}} = 0.042$$

$$u.c._{fcp\_supp\_comb} := u.c._{buck\_fcp\_supp} + u.c._{\sigma\_imp\_fcp\_supp} = 0.37$$

$$u.c._{comb\_fcp\_add\_tension} := u.c._{comb\_fcp} + \frac{\sigma_{fcp\_deck\_tension}}{f_{fcp\_x\_d}} = 0.74$$

Auxiliary calculations

Calculations for ship impact forces

$F_{ship} := 1\ \boldsymbol{MN}$ $h_{ship} := 0.25\ \boldsymbol{m}$ $w_{ship} := 3\ \boldsymbol{m}$

Loadcase

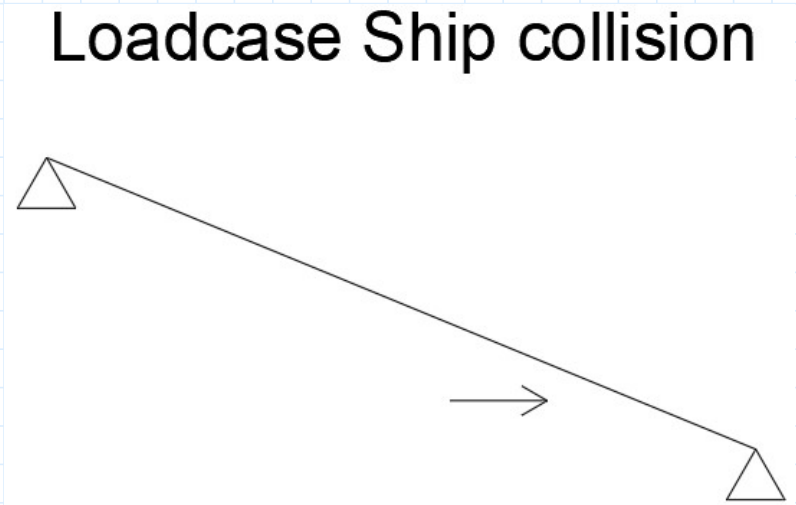

Number of supports activated by ship colision

$$n_{fcp\_supp\_coll} := \mathrm{Floor}\left(\frac{w_{ship}}{h.o.h_{fcp\_supp}}, 1\right) = 1$$

Forces in principle direction

$N_{Ed\_sh} := F_{ship} \cdot \cos(\alpha) = 921\ \boldsymbol{kN}$

$V_{Ed\_sh} := F_{ship} \cdot \sin(\alpha) = 389\ \boldsymbol{kN}$

$M_{Ed\_sh} := \frac{1}{4} \cdot F_{ship} \cdot \sin(\alpha) \cdot l_{fcp\_supp} = 369\ \boldsymbol{kN \cdot m}$

Resitance to shear force

$$V_{Rd\_sh} := f_{c\_xz\_v\_d} \cdot A_{V\_fcp\_supp} \cdot n_{fcp\_supp\_coll} = 73.4\ \mathbf{kN}$$

$$M_{Rd\_sh} := \frac{f_{fcp\_supp\_x\_d} \cdot 2 \cdot EI_{fcp\_supp}}{t_{d\_fcp\_supp} \cdot E_{l\_fcp\_supp}} = 222.3\ \mathbf{kN \cdot m}$$

Buckling resistance

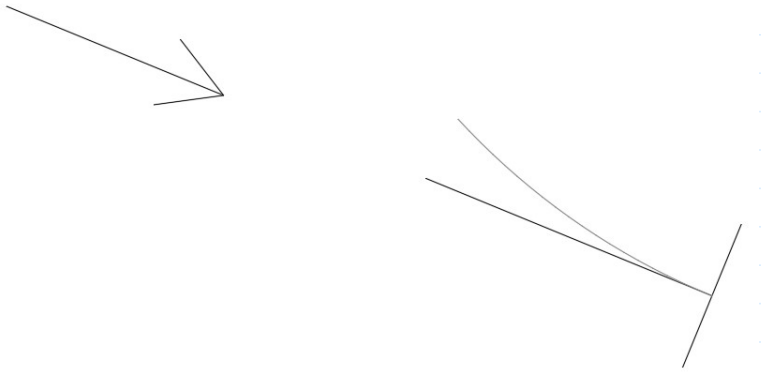

$$\gamma_{rd\_sh} := 1.4 \qquad D_{k\_sh} := \frac{\eta_{c\_balsa} \cdot E_{balsa\_x} \cdot t_{c\_fcp\_supp}^{\ 3}}{12} \qquad l_{cr\_sh} := 2 \cdot \frac{h_{ship}}{\sin(\alpha)} = 1.287\ \mathbf{m}$$

$$P_{cb\_d\_sh} := \frac{1}{\gamma_{m\_fcp} \cdot \gamma_{rd\_fcp}} \cdot \frac{\pi^2 \cdot D_k}{l_{cr\_sh}^{\ 2}} = 14\ \frac{\mathbf{MN}}{\mathbf{m}}$$

$$P_{cs\_d\_sh} := \frac{\eta_{c\_f\_fcp}}{\gamma_{m\_fcp} \cdot \gamma_{rd\_fcp}} \cdot \frac{G_{balsa} \cdot \left(t_{c\_fcp\_supp} + t_{l\_fcp\_supp}\right)^2}{t_{c\_fcp\_supp}} = 9981.038\ \frac{\mathbf{kN}}{\mathbf{m}}$$

$$P_{c\_d\_sh} := n_{fcp\_supp\_coll} \cdot \frac{P_{cb\_d\_sh} \cdot P_{cs\_d\_sh}}{P_{cb\_d\_sh} + P_{cs\_d\_sh}} = 5.9\ \frac{\mathbf{MN}}{\mathbf{m}}$$

Reduction of forces due to absorbtion of energy by supports

$$N_{res} := \max\left(0, N_{Ed\_sh} - P_{c\_d\_sh} \cdot w_{ship}\right) = 0\ \mathbf{MN}$$

$$V_{res} := \max\left(0, V_{Ed\_sh} - V_{Rd\_sh}\right) = 0.315\ \mathbf{MN}$$

$$M_{res} := \max\left(0, M_{Ed\_sh} - M_{Rd\_sh}\right) = 146.709\ \mathbf{kN \cdot m}$$

$$F_{ship\_res} := \max\left(\frac{N_{res}}{\cos(\alpha)}, \frac{V_{res}}{\sin(\alpha)}, \frac{4 \cdot M_{res}}{\sin(\alpha) \cdot l_{fcp\_supp}}\right) = 0.811\ \mathbf{MN}$$

Results

Unity checks

Unity checks traffic loads

Foot and cycle paths

$u.c._{\tau\_c\_fcp} = 0.35$ $u.c._{comb\_fcp\_add\_tension} = 0.74$

fcp supports

$u.c._{fcp\_supp\_comb} = 0.37$

Unity checks ship colision

Reduction of force to main structure due to collision with fcp deck (supp)

$$Reduction := \frac{F_{ship\_res} - F_{ship}}{F_{ship}} = -18.9\%$$

MKI

€ := 1 ¤

$$Mass_{E\_glass} := 2 \cdot t_{l\_fcp} \cdot b_{edge} \cdot l \cdot \rho_{l\_fcp} + 2 \cdot n_{fcp\_supp} \cdot t_{l\_fcp\_supp} \cdot w_{fcp\_supp} \cdot \rho_{l\_fcp\_supp} \cdot l_{fcp\_supp} = 8\ tonne$$

$$Mass_{Balsa} := t_{c\_fcp} \cdot b_{edge} \cdot l \cdot \rho_{balsa} + n_{fcp\_supp} \cdot t_{c\_fcp\_supp} \cdot w_{fcp\_supp} \cdot l_{fcp\_supp} \cdot \rho_{balsa} = 10.468\ tonne$$

$$A_{E\_glass} := \left(2 \cdot b_{edge} + 2 \cdot l_{fcp\_supp}\right) \cdot l = 444.324\ m^2$$

$$MKI_{E\_glass} := 0.265\ \frac{€}{kg} \qquad MKI_{score\_E\_glass} := MKI_{E\_glass} \cdot Mass_{E\_glass} = 2110.8\ €$$

$$MKI_{Balsa} := -0.129\ \frac{€}{kg} \qquad MKI_{score\_Balsa} := MKI_{Balsa} \cdot Mass_{Balsa} = -1350.3\ €$$

$$MKI_{E\_glass\_cons} := 1.173\ \frac{€}{m^2} \qquad MKI_{score\_E\_glass\_cons} := MKI_{E\_glass\_cons} \cdot A_{E\_glass} = 521.2\ €$$

$$MKI_{score\_Total} := MKI_{score\_E\_glass} + MKI_{score\_Balsa} + MKI_{score\_E\_glass\_cons} = 1282\ €$$

Mass

$$Mass_{total} := Mass_{E\_glass} + Mass_{Balsa} = 18.43\ tonne$$

Appendix V, Structural checks steel crossbeam, main beam, and orthotropic deck main structure.

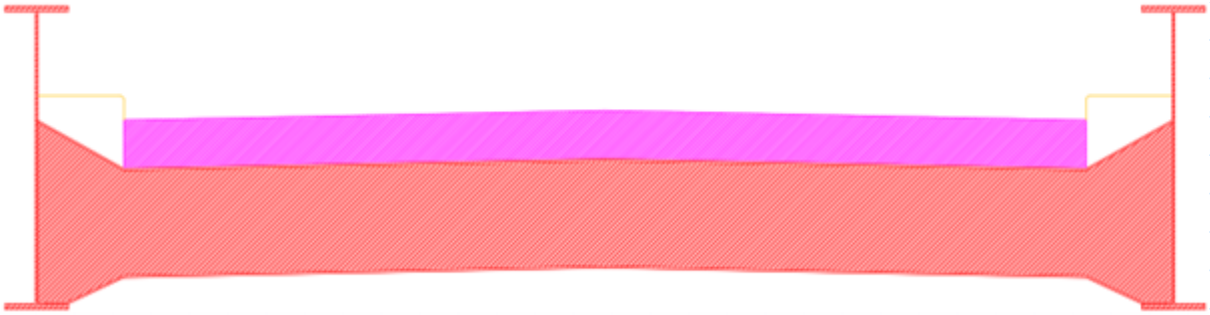

Table of Contents

General

General dimensions

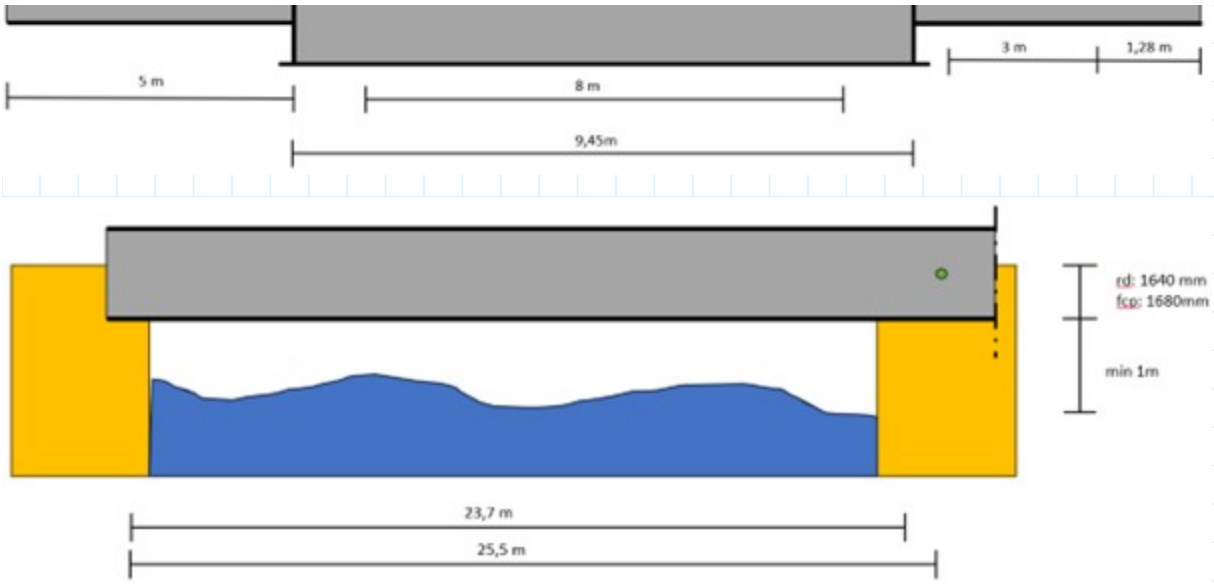

$n_{crossbeam} := 7$ $l := 25250\ mm$

$h.o.h_{crossbeam} := \frac{l}{n_{crossbeam} - 1} = 4.208\ m$

$b_{fcp} := 4.28\ m$ $b_{edge} := 5\ m$ $b_{rd} := 8\ m$ $b_{supp} := 9.45\ m$

$h_{rd} := 5.9\ m$ $h_{fcp} := 6.05\ m$ $h_{water} := 3.3\ m$ $h_{under\_side} := 4.3\ m$

$\theta_{max} := 80\ °$ $h_{top} := \sin(\theta_{max}) \cdot l + h_{rd} = 30.8\ m$

Design material properties

Properties steel

$\rho_{steel} := 7800\ \frac{kg}{m^3}$ $E_{steel} := 210\ GPa$ $f_{st} := 355\ MPa$

Traffic load calculations

Cross section properties

load properties

Distributed load BM1

$q_{bm1} := 9\ \frac{kN}{m^2}$

Concentrated load BM1

$Q_{bm1} := 300\ kN$ $l_{w\_bm1} := 40\ cm$ $w_{w\_bm1} := 40\ cm$ $w_{bm1} := 2\ m$ $h.o.h_{bm1} := 1.2\ m$

$w_{bm1\_mid} := 0.5\ m$

Distirbuted load foot and cycle path

$q_{fcp} := 5\ \frac{kN}{m^2}$

Concentrated load accidental vehicle

$Q_{av1} := 80\ kN$ $Q_{av2} := 40\ kN$

Ship collision force

$F_{ship} := 0.811\ MN$ $h_{ship} := 0.25\ m$ $w_{ship} := 3\ m$

Cross beam properties

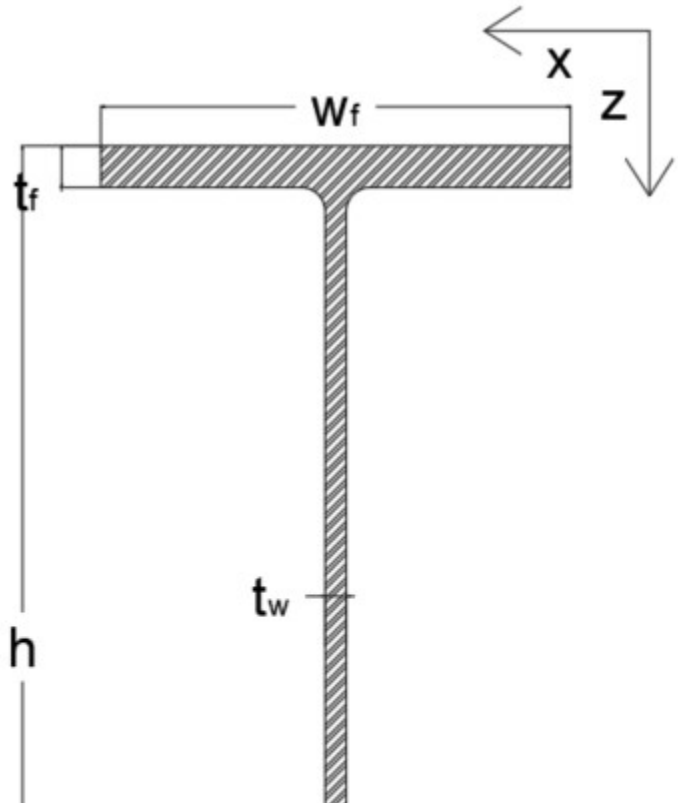

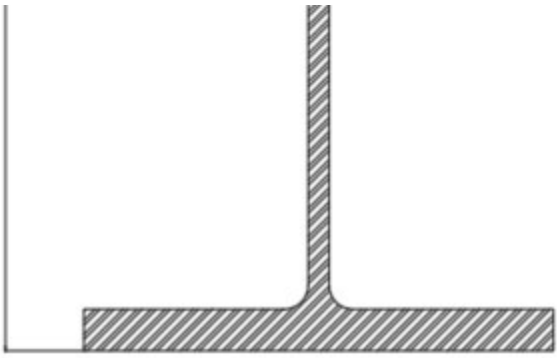

$h_{cb\_main} := 1000\ mm \qquad w_{cb\_f} := 300\ mm \qquad t_{cb\_f} := 16\ mm \qquad t_{cb\_w} := 12\ mm$

$A_{cb\_v} := h_{cb\_main} \cdot t_{cb\_w} = 0.012\ m^2$

$A_{cb} := 2 \cdot t_{cb\_f} \cdot w_{cb\_f} + t_{cb\_w} \cdot \left(h_{cb\_main} - 2 \cdot t_{cb\_f}\right) = 0.021\ m^2$

$$EI_{cb} := E_{steel} \cdot \left(\frac{1}{12} \cdot t_{cb\_w} \cdot \left(h_{cb\_main} - 2 \cdot t_{cb\_f}\right)^3 \hookleftarrow + 2 \cdot w_{cb\_f} \cdot t_{cb\_f} \cdot \left(\frac{1}{2} \cdot h_{cb\_main} - \frac{1}{2} \cdot t_{cb\_f} \right)^2 \right) = \left(678.5 \cdot 10^3\right)\ kN \cdot m^2$$

Main beam properties

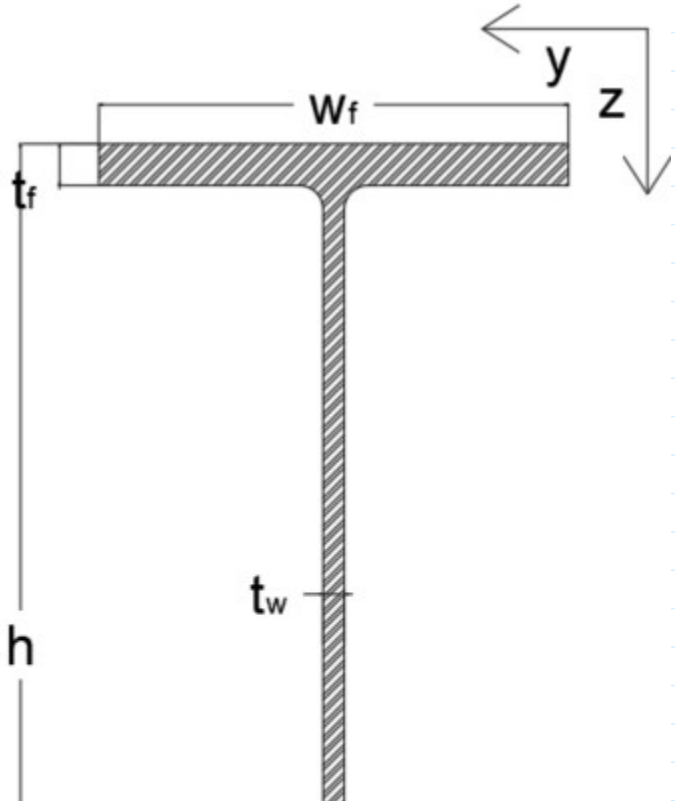

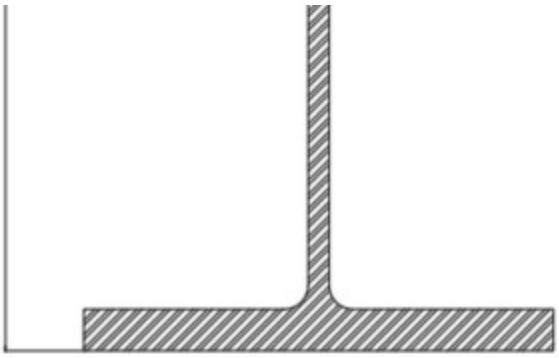

$h_{mb} := 2500\ mm$ $w_{mb\_f} := 525\ mm$ $t_{mb\_f} := 45\ mm$ $t_{mb\_w} := 20\ mm$

$A_{mb\_v} := h_{mb} \cdot t_{mb\_w} = 0.05\ m^2$

$A_{mb} := 2 \cdot t_{mb\_f} \cdot w_{mb\_f} + t_{mb\_w} \cdot \left(h_{mb} - 2 \cdot t_{mb\_f}\right) = 0.095\ m^2$

$$EI_{mb} := E_{steel} \cdot \left(\frac{1}{12} \cdot t_{mb\_w} \cdot \left(h_{mb} - 2 \cdot t_{mb\_f}\right)^3 \hookleftarrow + 2 \cdot w_{mb\_f} \cdot t_{mb\_f} \cdot \left(\frac{1}{2} \cdot h_{mb} - \frac{1}{2} \cdot t_{mb\_f} \right)^2 \right) = \left(19.8 \cdot 10^6\right)\ kN \cdot m^2$$

Road deck

$t_{rd} := 20\ mm$ $n_{trough} := 16$ $h.o.h_{trough} := \frac{b_{supp}}{n_{trough}} = 0.591\ m$

$h_{trough} := 350\ mm$ $b_{trough\_top} := 285\ mm$ $b_{trough\_bot} := 150\ mm$ $t_{trough} := 6\ mm$

$$A_{trough} := \left(2 \cdot \sqrt[2]{h_{trough}^{\ 2} + \left(b_{trough\_top} - b_{trough\_bot}\right)^2} + b_{trough\_bot}\right) \cdot t_{trough} = 0.005\ m^2$$

Calculations for crossbeam

Load cases

Loadcase BM1 1

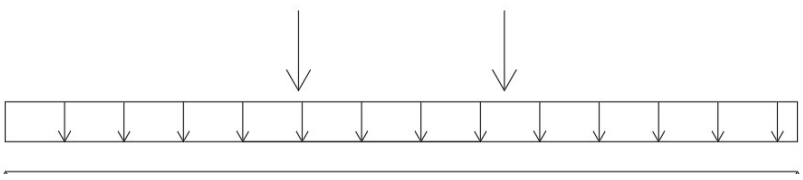

Loadcase BM1 2

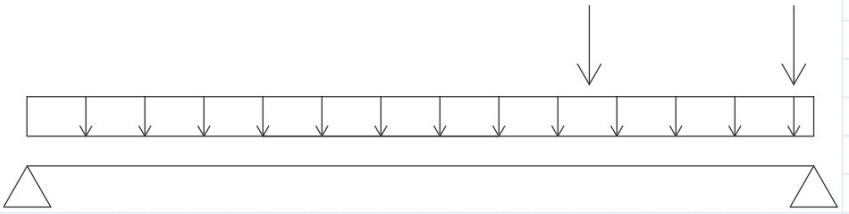

Loadcase G

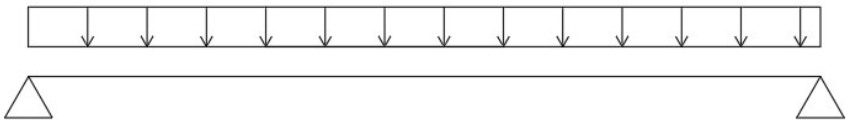

Shear force

Loadcases BM1 2 was used

$$V_{cb} := \frac{1}{2} \cdot q_{bm1} \cdot h.o.h_{crossbeam} \cdot b_{rd} + \frac{Q_{bm1}}{2} \cdot \frac{2 \cdot b_{supp} - 2 \cdot \frac{b_{supp} - b_{rd}}{2} - w_{bm1} + 2 \cdot \frac{b_{supp}}{2} - 2 \cdot \left(w_{bm1\_mid} - w_{bm1}\right)}{b_{supp}} = 594 \ kN$$

Bending moments

Loadcases BM1 1 was used

$$M_{cb} := \frac{1}{2} \cdot q_{bm1} \cdot h.o.h_{crossbeam} \cdot b_{rd} \cdot \left(\frac{1}{2} \cdot b_{supp} - \frac{1}{4} \cdot b_{rd}\right) + \frac{Q_{bm1}}{2} \cdot \left(b_{supp} - 2 \cdot w_{bm1\_mid} - w_{bm1}\right) = 1380 \ kN \cdot m$$

Self weight

$$G_{cb} := \left(\begin{array}{l} \left(2 \cdot t_{cb\_f} \cdot w_{cb\_f} + t_{cb\_w} \cdot \left(h_{cb\_main} - 2 \cdot t_{cb\_f}\right)\right) \cdot \rho_{steel} \\ + t_{rd} \cdot h.o.h_{crossbeam} \cdot \rho_{steel} + \frac{h.o.h_{crossbeam} \cdot A_{trough}}{h.o.h_{trough}} \cdot \rho_{steel} \end{array} \right) \cdot 9.81 \ \frac{m}{s^2} = 11.009 \ \frac{kN}{m}$$

Forces as a result of self weight

Loadcase G was used

$$V_{G\_cb} := \frac{1}{2} \cdot G_{cb} \cdot b_{supp} = 52 \ \textbf{kN}$$

$$M_{G\_cb} := \frac{1}{2} \cdot G_{cb} \cdot b_{rd} \cdot \left(\frac{1}{2} \cdot b_{supp} - \frac{1}{4} \cdot b_{rd} \right) = 120 \ \textbf{kN} \cdot \textbf{m}$$

Combined forces with 6.10 B

$$V_{Ed\_cb} := 1.2 \cdot V_{G\_cb} + 1.5 \ V_{cb} = 953.955 \ \textbf{kN}$$

$$M_{Ed\_cb} := 1.2 \cdot M_{G\_cb} + 1.5 \ M_{cb} = \left(2.214 \cdot 10^3 \right) \ \textbf{kN} \cdot \textbf{m}$$

Resultant stresses

$$\tau_{Ed\_cb} := \frac{V_{Ed\_cb}}{A_{cb\_v}} = 79.496 \ \textbf{MPa}$$

$$\sigma_{Ed\_cb} := \frac{M_{Ed\_cb}}{EI_{cb}} \cdot E_{steel} \cdot \frac{1}{2} \cdot h_{cb\_main} = 342.711 \ \textbf{MPa}$$

Unity checks

$$u.c._{\tau\_cb} := \frac{\tau_{Ed\_cb}}{f_{st}} = 0.224$$

$$u.c._{\sigma\_cb} := \frac{\sigma_{Ed\_cb}}{f_{st}} = 0.965$$

Calculations for mainbeam

Loads

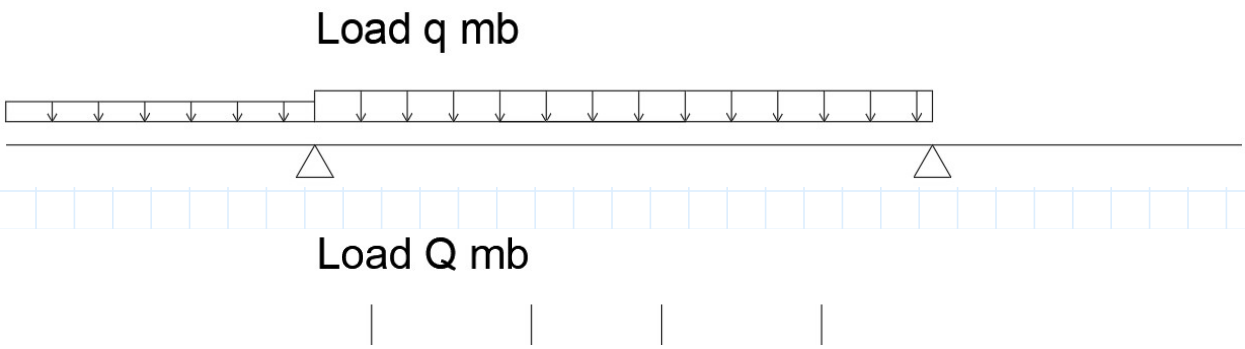

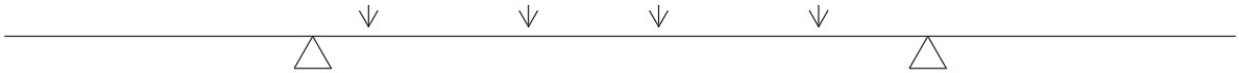

$$q_{mb} := \frac{b_{fcp} \cdot q_{fcp} \cdot \left(\frac{b_{fcp}}{2} + \left(b_{edge} - b_{fcp} \right) + b_{supp} \right) + b_{rd} \cdot q_{bm1} \cdot b_{supp}}{b_{supp}} = 99.877 \ \frac{kN}{m}$$

$$Q_{mb} := \frac{Q_{bm1} \cdot \left(\begin{array}{l} 2 \cdot b_{supp} - 2 \cdot \frac{\left(b_{supp} - b_{rd} \right)}{2} - 2 \cdot w_{bm1\_mid} \\ -w_{bm1} + 2 \cdot \frac{b_{supp}}{2} - 2 \cdot w_{bm1\_mid} - w_{bm1} \end{array} \right)}{b_{supp}} = 663.5 \ kN$$

Load cases

Loadcase M MB

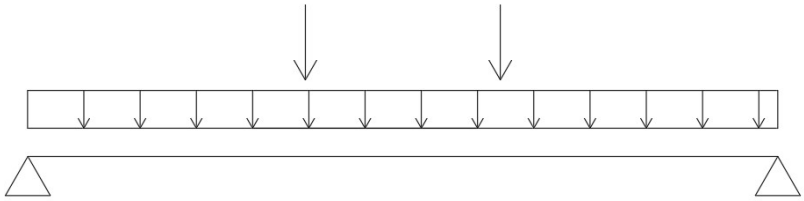

Loadcase V MB

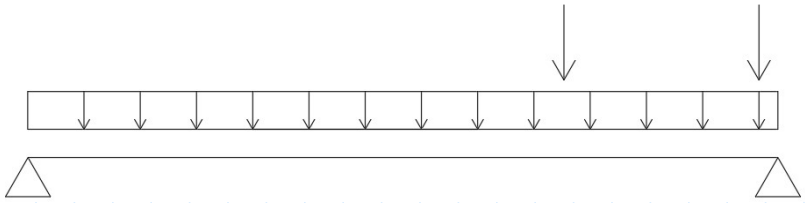

Loadcase G

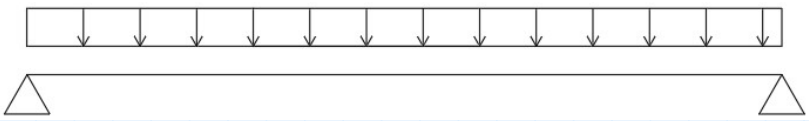

Shear force

Loadcases V MB was used

$$V_{bm1\_mb} := \frac{1}{2} \cdot q_{mb} \cdot l + 2 \cdot Q_{mb} = \left(2.6 \cdot 10^{3} \right) \ kN$$

Bending moment

Loadcases M MB was used

$$M_{bm1\_mb} := \frac{1}{8} \cdot q_{mb} \cdot l^2 + \frac{1}{4} \cdot Q_{mb} \cdot l = \left(1.215 \cdot 10^4\right)\ \mathbf{kN \cdot m}$$

Self weight

$$Mass_{dist} := \left(\begin{array}{l} \left(2 \cdot \left(2 \cdot w_{mb\_f} \cdot t_{mb\_f} + \left(h_{mb} - 2 \cdot t_{mb\_f}\right) \cdot t_{mb\_w}\right)\right) \\ + \dfrac{n_{crossbeam} \cdot \left(b_{supp} + 2 \cdot b_{edge}\right) \cdot \left(\begin{array}{r} 2 \cdot w_{cb\_f} \cdot t_{cb\_f} \\ + \left(h_{cb\_main} - 2 \cdot t_{cb\_f}\right) \cdot t_{cb\_w} \end{array}\right)}{l} \\ + t_{rd} \cdot b_{supp} + n_{trough} \cdot A_{trough} \end{array} \right) \cdot \rho_{steel} = 4530\ \frac{\mathbf{kg}}{\mathbf{m}}$$

$$G_{mb} := Mass_{dist} \cdot 9.81\ \frac{\mathbf{m}}{\mathbf{s}^2} = 44.436\ \frac{\mathbf{kN}}{\mathbf{m}}$$

Forces as a result of self weight

Loadcase G was used

$$V_{G\_mb} := \frac{1}{2} \cdot G_{mb} \cdot l = 561\ \mathbf{kN}$$

$$M_{G\_mb} := \frac{1}{8} \cdot G_{mb} \cdot l^2 = 3541\ \mathbf{kN \cdot m}$$

Combined forces with 6.10 B

$$V_{Ed\_mb} := 1.2 \cdot V_{G\_mb} + 1.5 \cdot V_{bm1\_mb} = \left(4.555 \cdot 10^3\right)\ \mathbf{kN}$$

$$M_{Ed\_mb} := 1.2 \cdot M_{G\_mb} + 1.5 \cdot M_{bm1\_mb} = \left(2.247 \cdot 10^4\right)\ \mathbf{kN \cdot m}$$

Resultant stresses

$$\tau_{Ed\_mb} := \frac{V_{Ed\_mb}}{A_{mb\_v}} = 91.1\ \mathbf{MPa}$$

$$\sigma_{Ed\_mb} := \frac{M_{Ed\_mb}}{EI_{mb}} \cdot E_{steel} \cdot \frac{1}{2} \cdot h_{mb} = 297.2\ \mathbf{MPa}$$

Unity checks

$$u.c._{mb} := \frac{\tau_{Ed\_mb}}{} = 0.257$$

$$f_{st}$$

$$u.c._{\sigma\_mb} := \frac{\sigma_{Ed\_mb}}{f_{st}} = 0.837$$

Auxiliary calculations

Calculations for ship impact forces

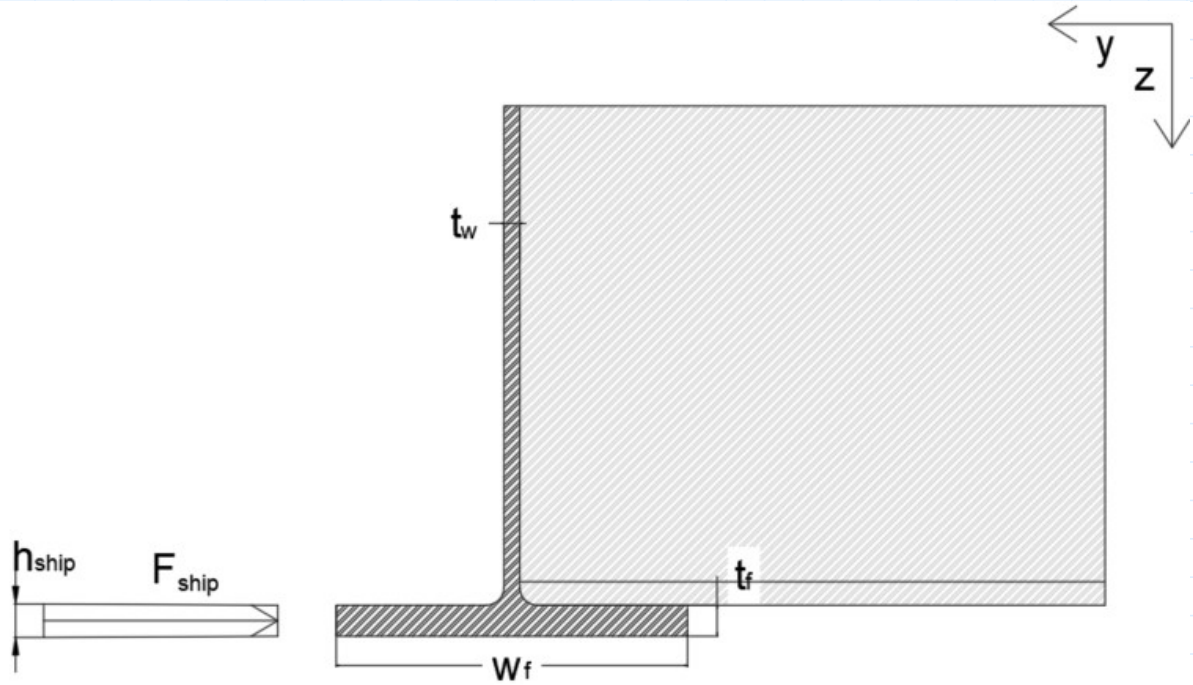

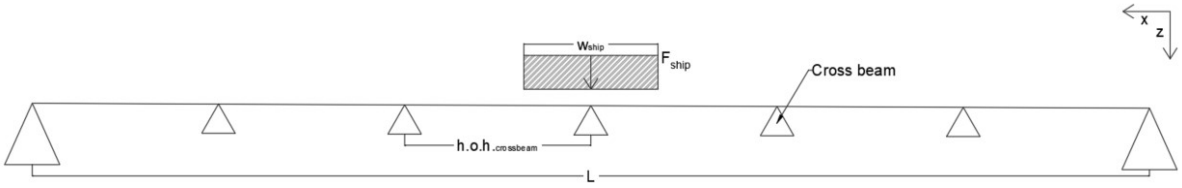

Global bending moment

$$M_{ship\_glob} := \frac{1}{2} \cdot F_{ship} \cdot \left(\frac{1}{2} \cdot l - \frac{1}{4} \cdot w_{ship} \right) = 4.8 \ \boldsymbol{MN \cdot m}$$

Local bending moment

$$M_{ship\_loc} := \frac{1}{2} \cdot F_{ship} \cdot \left(\frac{1}{2} \cdot h.o.h_{crossbeam} - \frac{1}{4} \cdot w_{ship} \right) = 549.115 \ \boldsymbol{kN \cdot m}$$

Shear forve

$$V_{ship} := F_{ship} = 811\ \boldsymbol{kN}$$

Section properties

$$A_{V\_mb\_f} := t_{mb\_f} \cdot w_{mb\_f} = 0.024\ \boldsymbol{m^2} \qquad W_{loc\_mb\_f} := \frac{1}{6} \cdot t_{mb\_f} \cdot w_{mb\_f}^{\ 2}$$

$$I_{sc} := 2 \cdot \frac{1}{12} \cdot t_{mb\_f} \cdot w_{mb\_f}^{\ 3} + 2 \cdot t_{mb\_f} \cdot w_{mb\_f} \cdot \left(\frac{b_{supp}}{2} \right)^2 = 1.056\ \boldsymbol{m^4}$$

Resultant stresses

$$\tau_{sc} := \frac{V_{ship}}{A_{V\_mb\_f}} = 34.3\ \boldsymbol{MPa}$$

$$\sigma_{sc\_glob} := \frac{M_{ship\_glob}}{I_{sc}} \cdot \frac{b_{supp} + w_{mb\_f}}{2} = 22.7\ \boldsymbol{MPa}$$

$$\sigma_{sc\_loc} := \frac{M_{ship\_loc}}{W_{loc\_mb\_f}} = 265.6\ \boldsymbol{MPa}$$

Unity checks

$$u.c._{\tau\_sc} := \frac{\tau_{sc}}{f_{st}} = 0.097$$

$$u.c._{\sigma\_sc\_loc} := \frac{\sigma_{sc\_loc}}{f_{st}} = 0.748$$

$$u.c._{\sigma\_sc\_glob} := \frac{\sigma_{sc\_glob}}{f_{st}} = 0.064$$

Calculations for opened structure

Wind loads

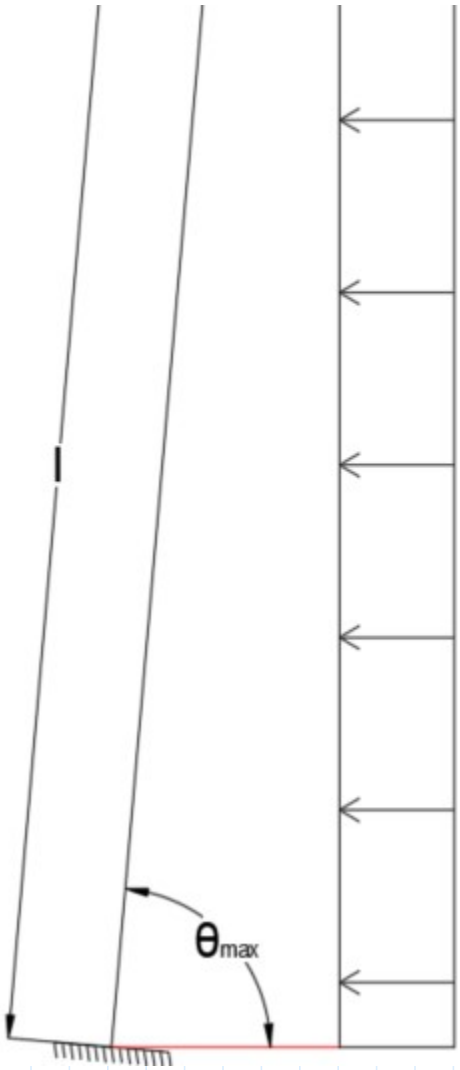

$z_e := h_{under\_side} + \sin(\theta_{max}) \cdot l = 29.2\ m$ $q_{p\_0} := 1.94\ \frac{kN}{m^2}$ $slenderness := \frac{b_{supp} + 2 \cdot b_{edge}}{h_{mb}} = 8$

$\rho := 1.25\ \frac{kg}{m^3}$ $v_b := 29.5\ \frac{m}{s}$

$c_{fx\_0} := \begin{cases} \text{if } slenderness \le 4 \\ \quad 2.4 - 0.275 \cdot slenderness \\ \text{else} \\ \quad 1.3 \end{cases} = 1.3$ $c_e := \frac{q_{p\_0}}{\frac{1}{2} \cdot \rho \cdot v_b^{\,2}} = 3.6$ $C_t := c_{fx\_0} \cdot c_e = 4.6$

$q_p := \frac{1}{2} \cdot \rho \cdot v_b^{\,2} \cdot C_t = 2.5\ \frac{kN}{m^2}$

$\ln\left(\frac{t_{open}}{}\right)$

$t_{open} := 15 \quad \psi_t := 1 + \frac{\left(50 \right)}{9} = 0.9$

Principle resultant forces

$N_{mb\_G\_open} := \frac{G_{mb} \cdot l}{2 \cdot \sin\left(\theta_{max}\right)} = 569.7 \ \boldsymbol{kN}$

$M_{mb\_G\_open} := \frac{1}{2} \cdot G_{mb} \cdot \cos\left(\theta_{max}\right) \cdot l^2 = \left(2.46 \cdot 10^3\right) \ \boldsymbol{kN \cdot m}$

$N_{mb\_wind} := \frac{\frac{1}{2} \cdot q_p \cdot h_{mb} \cdot \left(\sin\left(\theta_{max}\right) \cdot l\right)^2}{b_{supp}} = 206.276 \ \boldsymbol{kN}$

$M_{mb\_wind\_y} := \frac{1}{2} \cdot \frac{1}{2} \cdot q_p \cdot \left(2 \cdot b_{edge} + b_{supp}\right) \cdot \left(\sin\left(\theta_{max}\right) \cdot l\right)^2 = \left(7.583 \cdot 10^3\right) \ \boldsymbol{kN \cdot m}$

Resultant stresses

$\sigma_{mb\_G\_open} := \frac{M_{mb\_G\_open}}{EI_{mb}} \cdot E_{steel} \cdot \frac{1}{2} \cdot h_{mb} + \frac{N_{mb\_G\_open}}{A_{mb}} = 38.5 \ \boldsymbol{MPa}$

$\sigma_{mb\_wind\_1} := \frac{M_{mb\_wind\_y}}{EI_{mb}} \cdot E_{steel} \cdot \frac{1}{2} \cdot h_{mb} + 0.4 \cdot \frac{N_{mb\_wind}}{A_{mb}} = 101.1 \ \boldsymbol{MPa}$

$\sigma_{mb\_wind\_2} := 0.4 \cdot \frac{M_{mb\_wind\_y}}{EI_{mb}} \cdot E_{steel} \cdot \frac{1}{2} \cdot h_{mb} + \frac{N_{mb\_wind}}{A_{mb}} = 42.3 \ \boldsymbol{MPa}$

$\sigma_{mb\_wind} := \max\left(\sigma_{mb\_wind\_1}, \sigma_{mb\_wind\_2}\right) = 101.1 \ \boldsymbol{MPa}$

Unity checks

$u.c._{\sigma\_open} := \frac{1.2 \cdot \sigma_{mb\_G\_open} + 1.8 \cdot \psi_t \cdot \sigma_{mb\_wind}}{f_{st}} = 0.57$

Results

Unity Checks

Unity checks traffic loads

Cross beam

$u.c._{\tau\_cb} = 0.22 \qquad u.c._{\sigma\_cb} = 0.97$

Main beam

$u.c._{\tau\_mb} = 0.26$ $u.c._{\sigma\_mb} = 0.84$

Unity checks ship colision

Main Beam

$u.c._{\tau\_sc} = 0.097$ $u.c._{\sigma\_sc\_loc} = 0.748$ $u.c._{\sigma\_sc\_glob} = 0.064$

Unity checks opened position

$u.c._{\sigma\_open} = 0.57$

MKI

$€ := 1$ ¤

$$Mass_{Steel} := \begin{pmatrix} n_{crossbeam} \cdot \left(2 \cdot w_{cb\_f} \cdot t_{cb\_f} + t_{cb\_w} \cdot \left(h_{cb\_main} - 2 \cdot t_{cb\_f}\right)\right) \cdot b_{supp} \\ + 2 \cdot \left(2 \cdot w_{mb\_f} \cdot t_{mb\_f} + t_{mb\_w} \cdot \left(h_{mb} - 2 \cdot t_{mb\_f}\right)\right) \cdot l \\ + \left(t_{rd} \cdot b_{supp} + n_{trough} \cdot A_{trough}\right) \cdot l \end{pmatrix} \cdot \rho_{steel} = 102.8 \ tonne$$

$$A_{Steel} := n_{crossbeam} \cdot \left(4 \cdot t_{cb\_f} + 4 \cdot w_{cb\_f} + 2 \cdot h_{cb\_main} - 2 \cdot t_{cb\_w}\right) \cdot b_{supp} = 1101.4 \ m^2$$
$$+ 2 \cdot \left(4 \cdot t_{mb\_f} + 4 \cdot w_{mb\_f} + 2 \cdot h_{mb} - 2 \cdot t_{mb\_w}\right) \cdot l$$
$$+ \left(h.o.h_{trough} + 2 \cdot h_{trough}\right) \ n_{trough} \cdot l$$

$MKI_{Steel} := 0.165 \ \frac{€}{kg}$ $MKI_{score\_Steel} := MKI_{Steel} \cdot Mass_{Steel} = 16960.3 \ €$

$MKI_{Steel\_cons} := 0.300 \ \frac{€}{m^2}$ $MKI_{score\_Steel\_cons} := 5 \cdot MKI_{Steel\_cons} \cdot A_{Steel} = 1652 \ €$

$MKI_{score\_Total} := MKI_{score\_Steel} + MKI_{score\_Steel\_cons} = 18612 \ €$

Mass

$Mass_{total} := Mass_{Steel} = 103 \ tonne$

Appendix VI, Structural checks steel crossbeam and main beam with an FRP deck main structure.

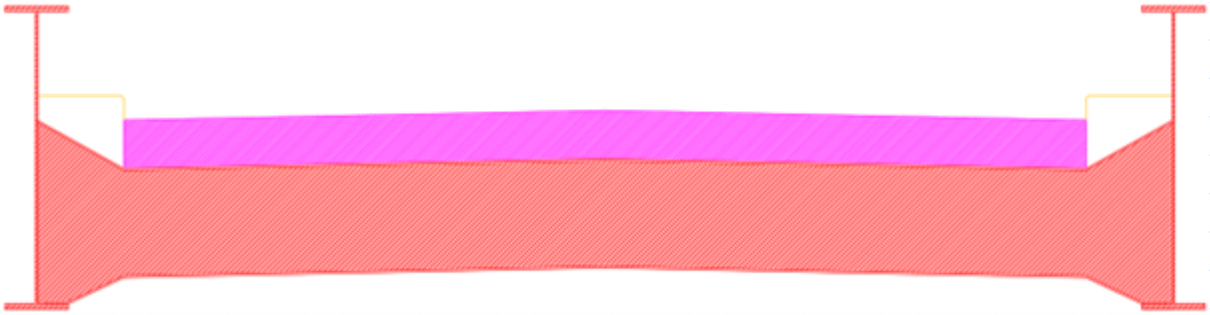

Table of Contents

General

General dimensions

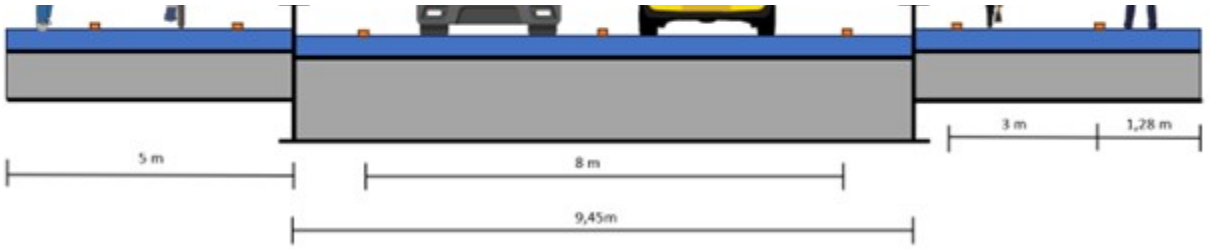

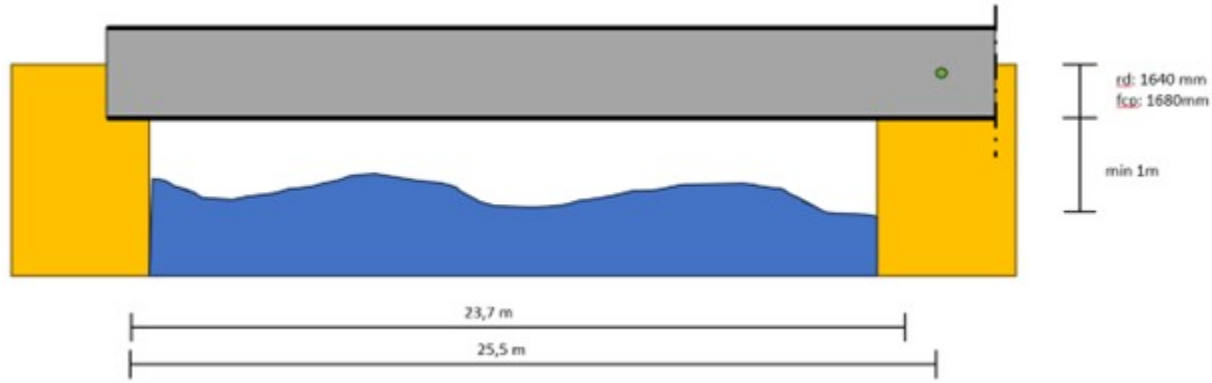

$n_{crossbeam} := 7$ $l := 25250\ mm$

$h.o.h_{crossbeam} := \frac{l}{n_{crossbeam} - 1} = 4.208\ m$

$b_{fcp} := 4.28\ m$ $b_{edge} := 5\ m$ $b_{rd} := 8\ m$ $b_{supp} := 9.45\ m$

$h_{rd} := 5.9\ m$ $h_{fcp} := 6.05\ m$ $h_{water} := 3.3\ m$ $h_{under\_side} := 4.3\ m$

$\theta_{max} := 80\ °$ $h_{top} := \sin(\theta_{max}) \cdot l + h_{rd} = 30.8\ m$

$Mass_{fcp} := 15.45\ tonne$

General properties

$T_{s\_sun} := 57\ °C$ $T_{s\_shade} := 31\ °C$

Design material properties

Properties balsa core

$\rho_{balsa} := 285\ \frac{kg}{m^3}$ $G_{balsa} := 145\ MPa$

$E_{balsa\_z} := 720\ MPa$ $E_{balsa\_x} := 2642\ MPa$

$f_{c\_xz\_v\_k} := 2.08\ \mathit{MPa}$ $f_{c\_z\_k} := 7.32\ \mathit{MPa}$

$$\eta_{ct\_balsa} := min\left(1 - \left(\frac{0.2\ \frac{kg}{m^3}}{\rho_{balsa}} + 0.004\right) \cdot \left(\frac{T_{s\_sun} - 20\ °C}{1\ °C}\right), 1\right) = 1$$

$\eta_{cm\_balsa} := 1$ $\eta_{c\_balsa} := \eta_{ct\_balsa} \cdot \eta_{cm\_balsa} = 1$

$\gamma_{m\_balsa} := 1.51$ $\gamma_{rd\_balsa} := 1.5$

$$f_{c\_xz\_v\_d} := \frac{\eta_{c\_balsa} \cdot f_{c\_xz\_v\_k}}{\gamma_{m\_balsa} \cdot \gamma_{rd\_balsa}} = 0.92\ \mathit{MPa}$$

$$f_{c\_z\_d} := \frac{\eta_{c\_balsa} \cdot f_{c\_z\_k}}{\gamma_{m\_balsa} \cdot \gamma_{rd\_balsa}} = 3.23\ \mathit{MPa}$$

Properties road deck laminate

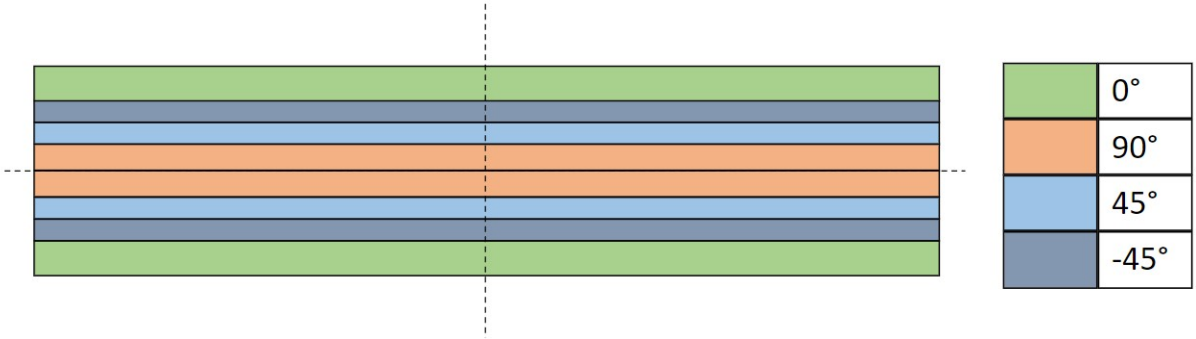

Laminate layup road deck

$$\begin{bmatrix} 0 \\ 90 \\ 45 \\ -45 \end{bmatrix} \quad \begin{bmatrix} 50\% \\ 16.67\% \\ 16.67\% \\ 16.67\% \end{bmatrix}$$

$$\rho_{l\_rd} := 1900\ \frac{kg}{m^3}$$

$E_{1\_l\_rd} := 26.2\ \mathit{GPa}$ $E_{2\_l\_rd} := 17.5\ \mathit{GPa}$

$f_{rd\_x\_k} := 367\ \mathit{MPa}$ $f_{rd\_y\_k} := 245\ \mathit{MPa}$ $f_{rd\_xy\_k} := 150\ \mathit{MPa}$

$T_{g\_rd} := 90\ °C$

$$\eta_{ct\_f\_rd} := min\left(1 - 0.25 \cdot \frac{T_{s\_sun} - 20\ °C}{T_{g\_rd} - 20\ °C}, 1\right) = 0.9$$

$$\eta_{cm\_f\_rd} := 0.6 \qquad \eta_{c\_f\_rd} := \eta_{ct\_f\_rd} \cdot \eta_{cm\_f\_rd} = 0.521$$

$$\eta_{ct\_m\_rd} := min\left(1 - 0.80 \cdot \frac{T_{s\_sun} - 20\ °C}{T_{g\_rd} - 20\ °C}, 1\right) = 0.6$$

$$\eta_{cm\_m\_rd} := 0.6 \qquad \eta_{c\_m\_rd} := \eta_{ct\_m\_rd} \cdot \eta_{cm\_m\_rd} = 0.346$$

$$\gamma_{m\_rd} := 1.07 \qquad \gamma_{rd\_rd} := 1.4$$

$$f_{rd\_x\_50} := \frac{\eta_{c\_f\_rd} \cdot f_{rd\_x\_k}}{\gamma_{rd\_rd} \cdot \gamma_{m\_rd}} = 127.6\ MPa$$

$$f_{rd\_y\_50} := \frac{\eta_{c\_f\_rd} \cdot f_{rd\_y\_k}}{\gamma_{rd\_rd} \cdot \gamma_{m\_rd}} = 85.2\ MPa$$

$$f_{rd\_xy\_d} := \frac{\eta_{ct\_f\_rd} \cdot f_{rd\_xy\_k}}{\gamma_{rd\_rd} \cdot \gamma_{m\_rd}} = 86.9\ MPa$$

Properties steel

$$\rho_{steel} := 7800\ \frac{kg}{m^3} \qquad E_{steel} := 210\ GPa \qquad f_{st} := 355\ MPa$$

Traffic load calculations

Cross section properties

load properties

Distributed load BM1

$$q_{bm1} := 9\ \frac{kN}{m^2}$$

Concentrated load BM1

$Q_{bm1} := 300\ kN$ $l_{w\_bm1} := 40\ cm$ $w_{w\_bm1} := 40\ cm$ $w_{bm1} := 2\ m$ $h.o.h_{bm1} := 1.2\ m$

Distirbuted load foot and cycle path

$q_{fcp} := 5\ \frac{kN}{m^2}$

Concentrated load accidental vehicle

$Q_{av1} := 80\ kN$ $Q_{av2} := 40\ kN$

Ship collision force

$F_{ship} := 0.811\ MN$ $h_{ship} := 0.25\ m$ $w_{ship} := 3\ m$

Road deck properties

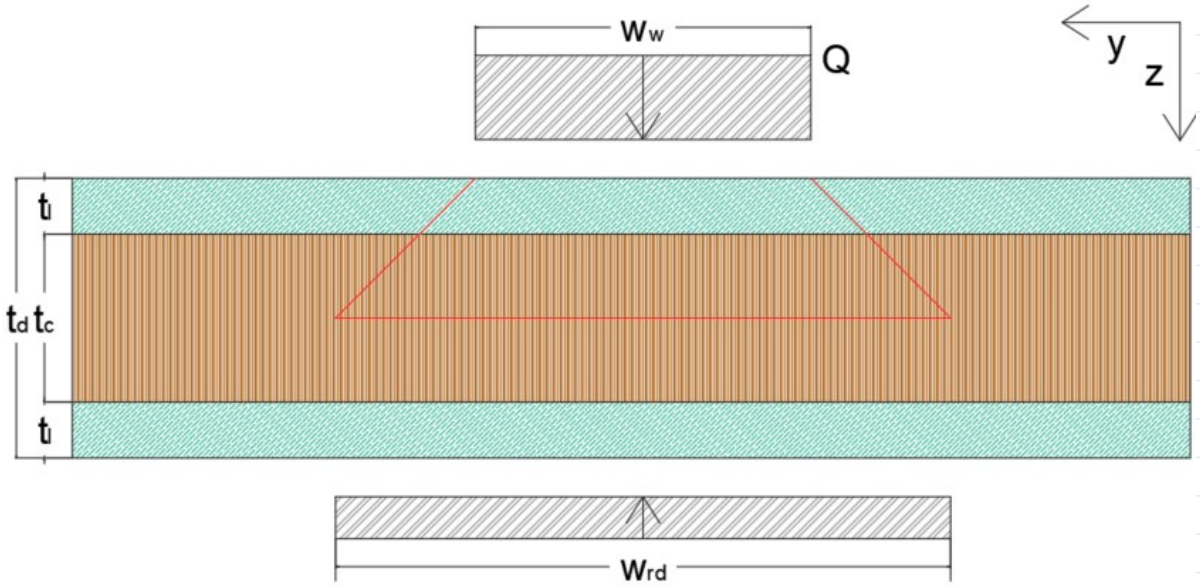

$w_{bm1\_mid} := 0.5\ m$

$t_{l\_rd} := 12\ mm$ $t_{c\_rd} := 500\ mm$ $t_{d\_rd} := t_{c\_rd} + 2 \cdot t_{l\_rd} = 524\ mm$

$w_{rd} := w_{w\_bm1} + t_{d\_rd} = 924\ mm$

$A_{rd} := w_{rd} \cdot t_{c\_rd} = 0.462\ m^2$

$$EI_{rd} := 2 \cdot E_{1\_l\_rd} \cdot w_{rd} \cdot t_{l\_rd} \cdot \left(\frac{t_{c\_rd} + t_{l\_rd}}{2} \right)^2 + \frac{1}{12} \cdot E_{balsa\_z} \cdot w_{rd} \cdot {t_{c\_rd}}^3 = 45007 \ kN \cdot m^2$$

Cross beam properties

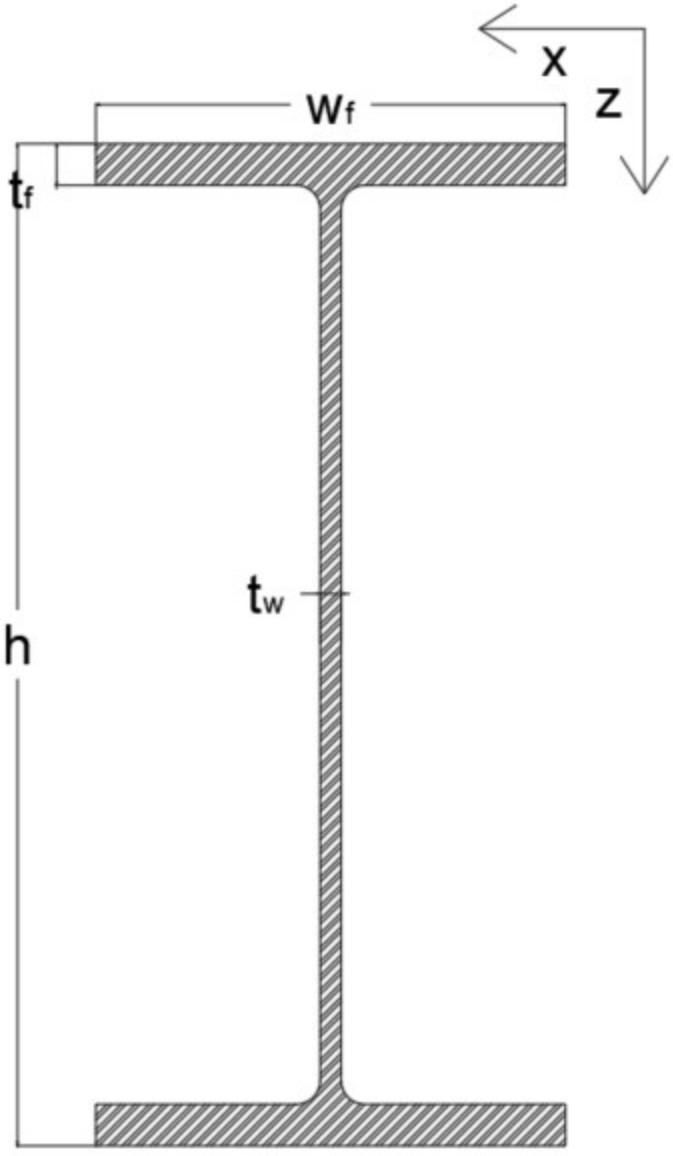

$h_{cb\_main} := 1000 \ mm$ $w_{cb\_f} := 300 \ mm$ $t_{cb\_f} := 16 \ mm$ $t_{cb\_w} := 12 \ mm$

$$A_{cb\_v} := h_{cb\_main} \cdot t_{cb\_w} = 0.012 \ m^2$$

$$A_{cb} := 2 \cdot t_{cb\_f} \cdot w_{cb\_f} + t_{cb\_w} \cdot \left(h_{cb\_main} - 2 \cdot t_{cb\_f} \right) = 0.021 \ m^2$$

$$EI_{cb} := E_{steel} \cdot \left(\frac{1}{12} \cdot t_{cb\_w} \cdot \left(h_{cb\_main} - 2 \cdot t_{cb\_f} \right)^3 \right) = \left(678.5 \cdot 10^3 \right) \ kN \cdot m^2$$

$$\left(+2\cdot w_{cb\_f}\cdot t_{cb\_f}\cdot\left(\frac{1}{2}\cdot h_{cb\_main}-\frac{1}{2}\cdot t_{cb\_f}\right)^2\right)$$

Main beam properties

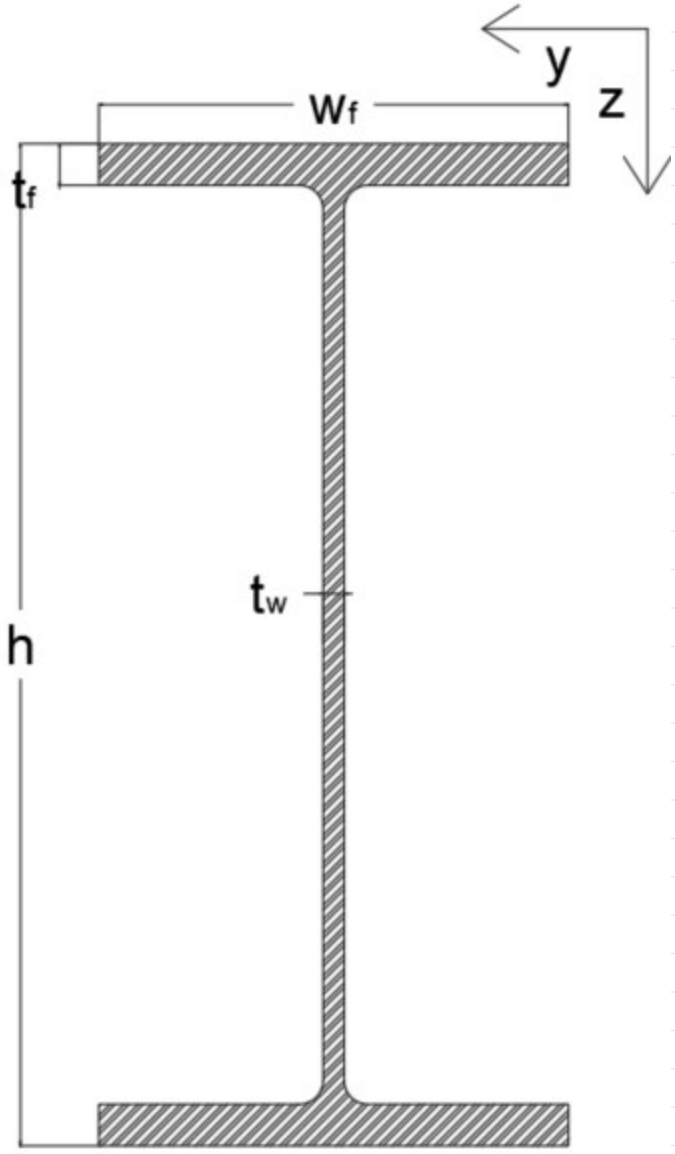

$h_{mb} := 2500\ mm$ $w_{mb\_f} := 525\ mm$ $t_{mb\_f} := 45\ mm$ $t_{mb\_w} := 20\ mm$

$A_{mb\_v} := h_{mb}\cdot t_{mb\_w} = 0.05\ m^2$

$A_{mb} := 2\cdot t_{mb\_f}\cdot w_{mb\_f} + t_{mb\_w}\cdot\left(h_{mb} - 2\cdot t_{mb\_f}\right) = 0.095\ m^2$

$EI_{mb} := E_{steel}\cdot\left(\frac{1}{12}\cdot t_{mb\_w}\cdot\left(h_{mb} - 2\cdot t_{mb\_f}\right)^3 \right.$ $\left.\right) = (19.8\cdot 10^6)\ kN\cdot m^2$

$$\left| \frac{1}{12} \cdot w_{mb\_f} \cdot t_{mb\_f}^3 + 2 \cdot w_{mb\_f} \cdot t_{mb\_f} \cdot \left(\frac{1}{2} \cdot h_{mb} - \frac{1}{2} \cdot t_{mb\_f} \right)^2 \right|$$

Stiffness properties head board

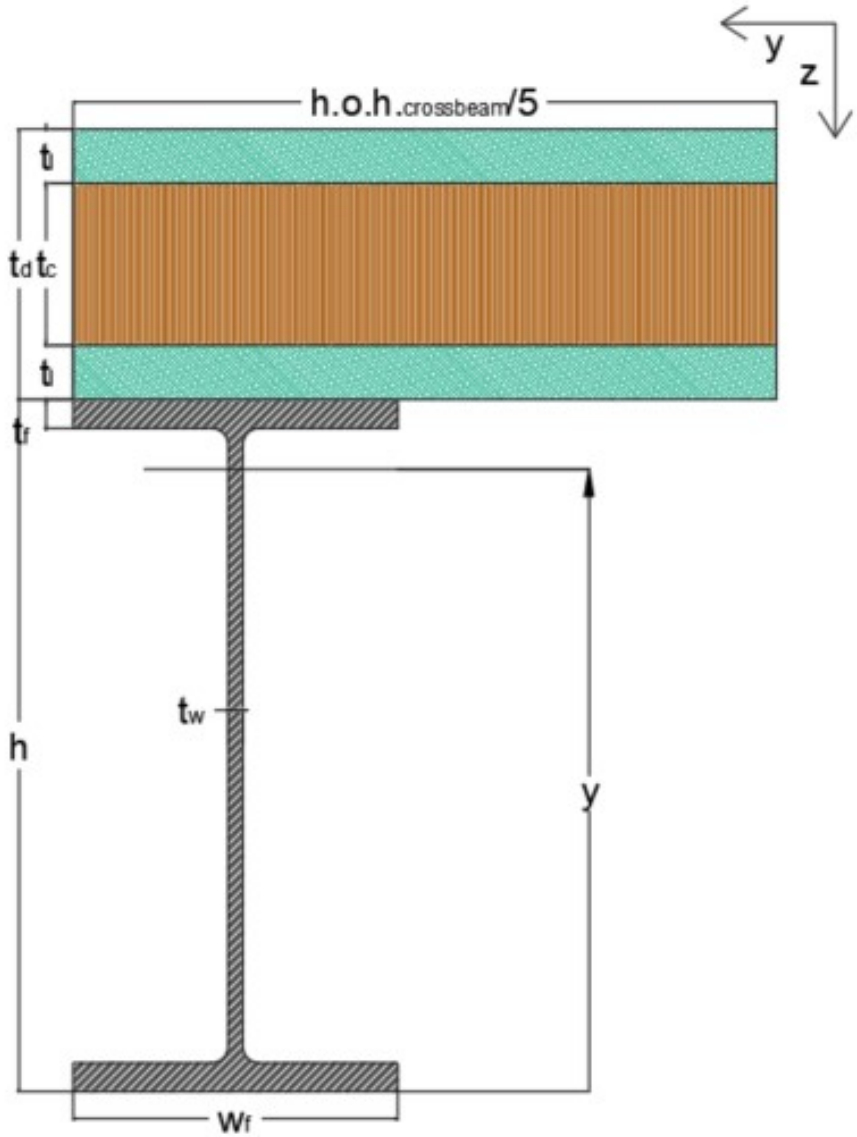

$$A_{cb} \cdot \frac{h_{cb\_main}}{2} \cdot E_{steel} \hookleft$$

$$+ \frac{b_{supp}}{10} \cdot t_{c\_rd} \cdot \left(h_{rd} - h_{under\_side} - t_{l\_rd} - \frac{t_{c\_rd}}{2} \right) \cdot E_{balsa\_z} \hookleft$$

$$+ \frac{b_{supp}}{10} \cdot t_{l\_rd} \cdot \left(h_{rd} - h_{under\_side} - \frac{t_{l\_rd}}{2} \right) \cdot E_{2\_l\_rd} \hookleft$$

$$y := \frac{\left(\frac{b_{supp}}{10} \cdot t_{l\_rd} \cdot \left(h_{rd} - h_{under\_side} - t_{c\_rd} - \frac{3 \cdot t_{l\_rd}}{2}\right) \cdot E_{2\_l\_rd}\right)}{2 \cdot \frac{b_{supp}}{10} \cdot t_{l\_rd} \cdot E_{1\_l\_rd} + \frac{b_{supp}}{10} \cdot t_{c\_rd} \cdot E_{balsa\_z} + A_{cb} \cdot E_{steel}} = 0.6\ m$$

$$z_{l\_rd\_top} := h_{rd} - h_{under\_side} - \frac{t_{l\_rd}}{2} - y = 0.998\ m$$

$$z_{c\_rd} := h_{rd} - h_{under\_side} - t_{l\_rd} - \frac{t_{c\_rd}}{2} - y = 0.742\ m$$

$$z_{l\_rd\_bot} := h_{rd} - h_{under\_side} - t_{c\_rd} - \frac{3\ t_{l\_rd}}{2} - y = 0.486\ m$$

$$z_{cb} := \frac{h_{cb\_main}}{2} - y = -0.096\ m$$

$$EI_{hb} := \frac{b_{supp}}{10} \cdot t_{l\_rd} \cdot \left(z_{l\_rd\_top}^{\ 2} + z_{l\_rd\_bot}^{\ 2}\right) \cdot E_{1\_l\_rd} \hookleftarrow = \left(1.273 \cdot 10^{6}\right)\ kN \cdot m^2$$
$$+ \frac{b_{supp}}{10} \cdot t_{c\_rd} \cdot z_{c\_rd}^{\ 2} \cdot E_{balsa\_z} \hookleftarrow$$
$$+ EI_{cb} + A_{cb} \cdot z_{cb}^{\ 2} \cdot E_{steel}$$

Calculations for deflections

Deflections at the supports in the middle of the deck

$$w_{middle\_at\_supports} := \frac{1}{48} \cdot \frac{Q_{bm1} \cdot b_{supp}^{\ 3}}{EI_{hb}} + \frac{5}{384} \cdot \frac{q_{bm1} \cdot \frac{b_{supp}}{10} \cdot b_{supp}^{\ 4}}{EI_{hb}} = 4.84\ mm$$

Deflections at midspan in the middle of the deck

$$w_{middle\_midspan} := \frac{1}{48} \frac{4 \cdot Q_{bm1} \cdot l^3}{2 \cdot EI_{mb}} + \frac{5}{384} \cdot \frac{q_{bm1} \cdot b_{supp} \cdot l^4}{2 \cdot EI_{mb}} = 21.5\ mm$$

Deflections limit

$$w_{limit\_midspan} := \frac{l}{250} = 101\ mm \qquad w_{limit\_threshold} := 5\ mm$$

Unity checks

$$u.c._{deflection\_threshold} := \frac{w_{middle\_at\_supports}}{w_{limit\_threshold}} = 0.97$$

$$u.c._{deflection\_midspan} := \frac{w_{middle\_midspan}}{w_{limit\_midspan}} = 0.21$$

Calculations for road deck

Load cases

Loadcase BM1 1

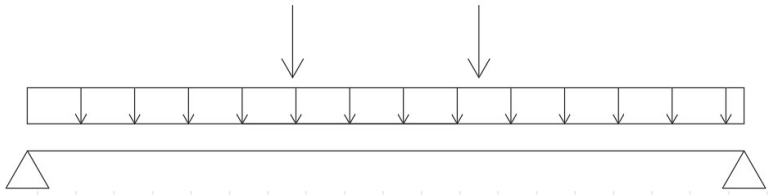

Loadcase BM1 2

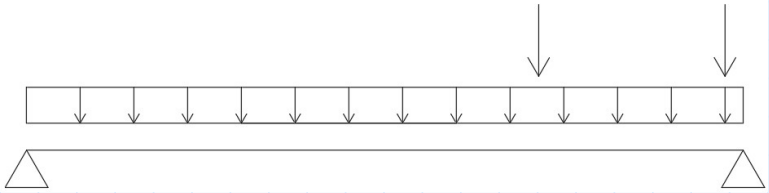

Loadcase G

Shear force

Loadcases BM1 2 was used

$$V_{bm1} := \frac{1}{2} \cdot q_{bm1} \cdot h.o.h_{crossbeam} \cdot w_{rd} \; = 260.469 \; kN$$

$$+ \frac{h.o.h_{crossbeam} - \frac{l_{w\_bm1}}{2}}{h.o.h_{crossbeam}} \cdot \frac{Q_{bm1}}{2}$$

$$+ \frac{h.o.h_{crossbeam} - h.o.h_{bm1} - \frac{l_{w\_bm1}}{2}}{} \cdot \frac{Q_{bm1}}{}$$

$h.o.h_{crossbeam}$ 2

Bending moments

Loadcases BM1 1 was used

$$M_{bm1} := \frac{1}{8} \cdot q_{bm1} \cdot w_{rd} \cdot h.o.h_{crossbeam}^{2} = 244\ \mathbf{kN \cdot m}$$
$$+ 2 \cdot \left(\left(\frac{h.o.h_{crossbeam} + h.o.h_{bm1}}{2 \cdot h.o.h_{crossbeam}} \right) \cdot \frac{Q_{bm1}}{2} \cdot \left(\frac{h.o.h_{crossbeam}}{2} - \frac{h.o.h_{bm1}}{2} \right) \right.$$
$$\left. - \left(\frac{h.o.h_{crossbeam} - h.o.h_{bm1}}{2 \cdot h.o.h_{crossbeam}} \right) \cdot \frac{Q_{bm1}}{2} \cdot \frac{h.o.h_{bm1}}{2} \right)$$

Self weight

$$G_{rd} := \left(2 \cdot t_{l\_rd} \cdot w_{rd} \cdot \rho_{l\_rd} + t_{c\_rd} \cdot w_{rd} \cdot \rho_{balsa}\right) \cdot 9.81\ \frac{\mathbf{m}}{\mathbf{s}^2} = 1.705\ \frac{\mathbf{kN}}{\mathbf{m}}$$

Forces as a result of self weight

Loadcase G was used

$$V_{G\_rd} := \frac{1}{2} \cdot G_{rd} \cdot h.o.h_{crossbeam} = 3.588\ \mathbf{kN}$$

$$M_{G\_rd} := \frac{1}{8} \cdot G_{rd} \cdot h.o.h_{crossbeam}^{2} = 3.775\ \mathbf{kN \cdot m}$$

Combined forces with 6.10 B

$$V_{Ed\_rd} := 1.2 \cdot V_{G\_rd} + 1.5 \cdot V_{bm1} = 395\ \mathbf{kN}$$

$$M_{Ed\_rd} := 1.2 \cdot M_{G\_rd} + 1.5 \cdot M_{bm1} = 371\ \mathbf{kN \cdot m}$$

$$N_{Ed\_rd} := 1.5 \cdot \left(0.6 \cdot Q_{bm1} + 0.1 \cdot q_{bm1} \cdot w_{w\_bm1} \cdot \frac{h.o.h_{crossbeam}}{2}\right) = 271\ \mathbf{kN}$$

Resultant stresses

$$\tau_{c\_rd} := \frac{V_{Ed\_rd}}{A_{rd}} = 0.9\ \mathbf{MPa}$$

$$\sigma_{l\_rd} := \frac{M_{Ed\_rd}}{EI_{rd}} \cdot \frac{t_{d\_rd}}{2} \cdot E_{1\_l\_rd} = 57\ \mathbf{MPa}$$

$$\sigma_{\_rd} := \frac{N_{Ed\_rd} \cdot \left(2 \cdot t_{c\_rd} - t_{l\_rd}\right)}{} = 57\ \mathbf{MPa}$$

$$2 \cdot t_{l\_rd} \cdot w_{w\_bm1} \cdot \left(t_{c\_rd} - t_{l\_rd}\right)$$

$$\sigma_{c\_rd} := \frac{M_{Ed\_rd}}{EI_{rd}} \cdot \left(\frac{t_{d\_rd}}{2} - t_{l\_rd}\right) \cdot E_{balsa\_z} = 1.482\ \textit{MPa}$$

Unity checks

$$u.c._{\tau\_rd} := \frac{\tau_{c\_rd}}{f_{c\_xz\_v\_d}} = 0.932$$

$$u.c._{\sigma\_rd} := \frac{\sigma_{l\_rd} + \sigma_{n\_rd}}{f_{rd\_x\_50}} = 0.891$$

$$u.c._{\sigma\_c\_rd} := \frac{\sigma_{c\_rd}}{f_{c\_z\_d}} = 0.459$$

Calculations for crossbeam

Load cases

Loadcase BM1 1

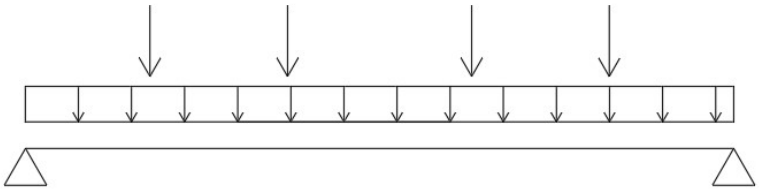

Loadcase BM1 2

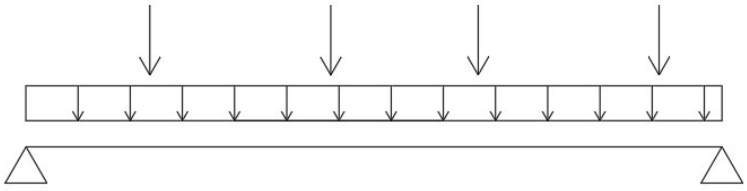

Loadcase G

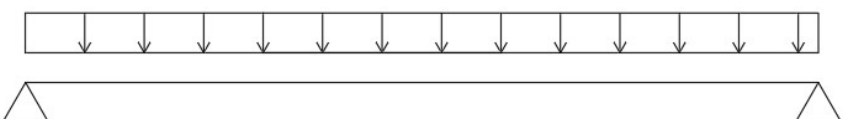

Shear force

Loadcases BM1 2 was used

$$V_{cb} := \frac{1}{2} \cdot q_{bm1} \cdot h.o.h_{crossbeam} \cdot b_{rd} + \frac{Q_{bm1}}{2} \cdot \frac{2 \cdot b_{supp} - 2 \cdot \frac{b_{supp} - b_{rd}}{2} - w_{bm1} + 2 \cdot \frac{b_{supp}}{2} - 2 \cdot w_{bm1\_mid} - w_{bm1}}{b_{supp}} = 499 \ \mathbf{kN}$$

Bending moments

Loadcases BM1 1 was used

$$M_{cb} := \frac{1}{2} \cdot q_{bm1} \cdot h.o.h_{crossbeam} \cdot b_{rd} \cdot \left(\frac{1}{2} \cdot b_{supp} - \frac{1}{4} \cdot b_{rd} \right) + \frac{Q_{bm1}}{2} \cdot \left(b_{supp} - 2 \cdot w_{bm1\_mid} - w_{bm1} \right) = 1380 \ \mathbf{kN \cdot m}$$

Self weight

$$G_{cb} := \begin{pmatrix} \left(2 \cdot t_{cb\_f} \cdot w_{cb\_f} + t_{cb\_w} \cdot \left(h_{cb\_main} - 2 \cdot t_{cb\_f} \right) \right) \cdot \rho_{steel} \\ + 2 \cdot t_{l\_rd} \cdot h.o.h_{crossbeam} \cdot \rho_{l\_rd} + t_{c\_rd} \cdot h.o.h_{crossbeam} \cdot \rho_{balsa} \end{pmatrix} \cdot 9.81 \ \frac{\mathbf{m}}{\mathbf{s}^2} = 9.389 \ \frac{\mathbf{kN}}{\mathbf{m}}$$

Forces as a result of self weight

Loadcase G was used

$$V_{G\_cb} := \frac{1}{2} \cdot G_{cb} \cdot b_{supp} = 44.4 \ \mathbf{kN}$$

$$M_{G\_cb} := \frac{1}{2} \cdot G_{cb} \cdot b_{rd} \cdot \left(\frac{1}{2} \cdot b_{supp} - \frac{1}{4} \cdot b_{rd} \right) = 102.3 \ \mathbf{kN \cdot m}$$

Combined forces with 6.10 B

$$V_{Ed\_cb} := 1.2 \cdot V_{G\_cb} + 1.5 \ V_{cb} = 801.914 \ \mathbf{kN}$$

$$M_{Ed\_cb} := 1.2 \cdot M_{G\_cb} + 1.5 \ M_{cb} = \left(2.193 \cdot 10^3 \right) \ \mathbf{kN \cdot m}$$

Resultant stresses

$$\tau_{Ed\_cb} := \frac{V_{Ed\_cb}}{} = 66.826 \ \mathbf{MPa}$$

$$\tau_{Ed\_cb} := \frac{V_{Ed\_cb}}{A_{cb\_v}}$$

$$\sigma_{Ed\_cb} := \frac{M_{Ed\_cb}}{EI_{cb}} \cdot E_{steel} \cdot \frac{1}{2} \cdot h_{cb\_main} = 339.432\ \textit{MPa}$$

Unity checks

$$u.c._{\tau\_cb} := \frac{\tau_{Ed\_cb}}{f_{st}} = 0.188$$

$$u.c._{\sigma\_cb} := \frac{\sigma_{Ed\_cb}}{f_{st}} = 0.956$$

Calculations for mainbeam

Loads

Load q mb

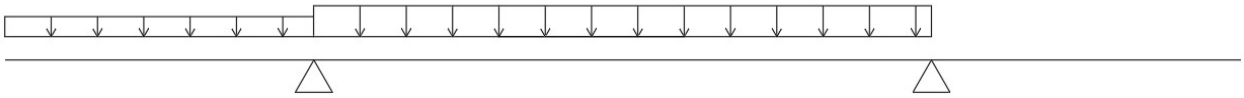

Load Q mb

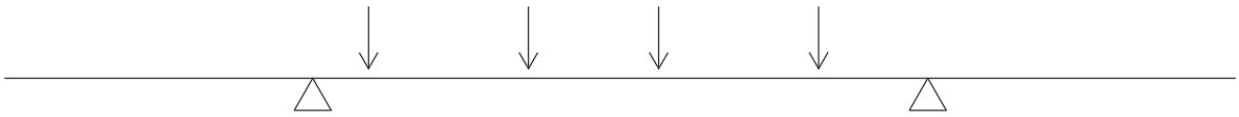

$$q_{mb} := \frac{b_{fcp} \cdot q_{fcp} \cdot \left(\frac{b_{fcp}}{2} + \left(b_{edge} - b_{fcp} \right) + b_{supp} \right) + b_{rd} \cdot q_{bm1} \cdot b_{supp}}{b_{supp}} = 99.877\ \frac{\textit{kN}}{\textit{m}}$$

$$Q_{mb} := \frac{Q_{bm1} \cdot \begin{pmatrix} 2 \cdot b_{supp} - 2 \cdot \frac{\left(b_{supp} - b_{rd} \right)}{2} - 2 \cdot w_{bm1\_mid} \\ -w_{bm1} + 2 \cdot \frac{b_{supp}}{2} - 2 \cdot w_{bm1\_mid} - w_{bm1} \end{pmatrix}}{b_{supp}} = 663.5\ \textit{kN}$$

Load cases

Loadcase V MB

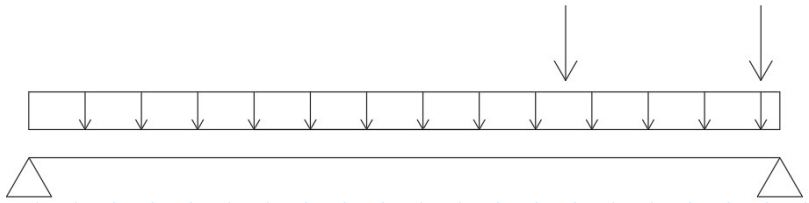

Loadcase M MB

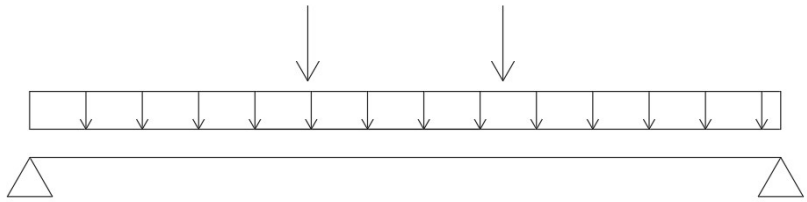

Loadcase G

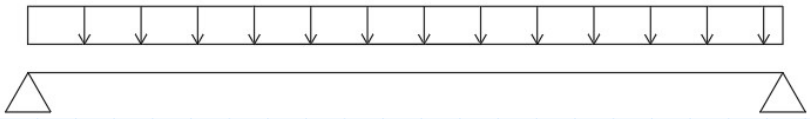

Shear force

Loadcases V MB was used

$$V_{bm1\_mb} := \frac{1}{2} \cdot q_{mb} \cdot l + 2 \cdot Q_{mb} = \left(2.6 \cdot 10^3\right)\ \mathbf{kN}$$

Bending moment

Loadcases M MB was used

$$M_{bm1\_mb} := \frac{1}{8} \cdot q_{mb} \cdot l^2 + \frac{1}{4} \cdot Q_{mb} \cdot l = \left(1.215 \cdot 10^4\right)\ \mathbf{kN \cdot m}$$

Self weight

$$Mass_{dist} := \left(\begin{array}{l} \left(2 \cdot \left(2 \cdot w_{mb\_f} \cdot t_{mb\_f} + \left(h_{mb} - 2 \cdot t_{mb\_f}\right) \cdot t_{mb\_w}\right)\right) \\ \quad + n_{crossbeam} \cdot \left(b_{supp} + 2 \cdot b_{edge}\right) \cdot \left(2 \cdot w_{cb\_f} \cdot t_{cb\_f} + \left(h_{cb\_main} - 2 \cdot t_{cb\_f}\right) \cdot t_{cb\_w}\right) \\ \quad + \dfrac{}{l} \end{array} \right) \cdot \rho_{steel} = 5383\ \frac{\mathbf{kg}}{\mathbf{m}}$$

$$+ t_{c\_rd} \cdot b_{supp} \cdot \rho_{balsa} + 2 \cdot t_{l\_rd} \cdot b_{supp} \cdot \rho_{l\_rd} + 2 \cdot \frac{Mass_{fcp}}{l}$$

$$G_{mb} := Mass_{dist} \cdot 9.81\ \frac{\mathbf{m}}{\mathbf{s}^2} = 52.804\ \frac{\mathbf{kN}}{\mathbf{m}}$$

Forces as a result of self weight

Loadcase G was used

$$V_{G\_mb} := \frac{1}{2} \cdot G_{mb} \cdot l = 667 \ \textbf{kN}$$

$$M_{G\_mb} := \frac{1}{8} \cdot G_{mb} \cdot l^2 = 4208 \ \textbf{kN} \cdot \textbf{m}$$

Combined forces with 6.10 B

$$V_{Ed\_mb} := 1.2 \cdot V_{G\_mb} + 1.5 \cdot V_{bm1\_mb} = \left(4.682 \cdot 10^3\right) \ \textbf{kN}$$

$$M_{Ed\_mb} := 1.2 \cdot M_{G\_mb} + 1.5 \cdot M_{bm1\_mb} = \left(2.327 \cdot 10^4\right) \ \textbf{kN} \cdot \textbf{m}$$

Resultant stresses

$$\tau_{Ed\_mb} := \frac{V_{Ed\_mb}}{A_{mb\_v}} = 93.6 \ \textbf{MPa}$$

$$\sigma_{Ed\_mb} := \frac{M_{Ed\_mb}}{EI_{mb}} \cdot E_{steel} \cdot \frac{1}{2} \cdot h_{mb} = 307.8 \ \textbf{MPa}$$

Unity checks

$$u.c._{\tau\_mb} := \frac{\tau_{Ed\_mb}}{f_{st}} = 0.264$$

$$u.c._{\sigma\_mb} := \frac{\sigma_{Ed\_mb}}{f_{st}} = 0.867$$

Auxiliary calculations

Calculations for ship impact forces

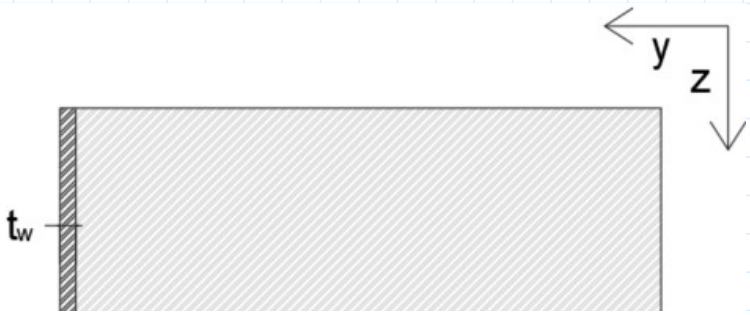

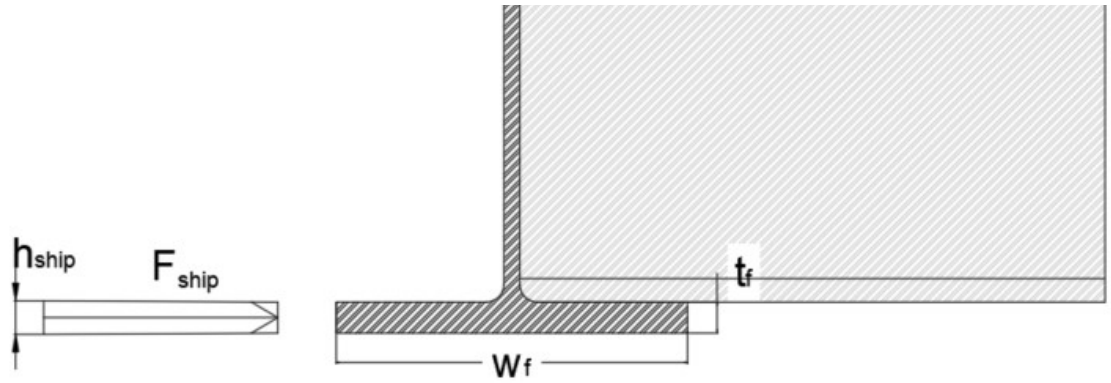

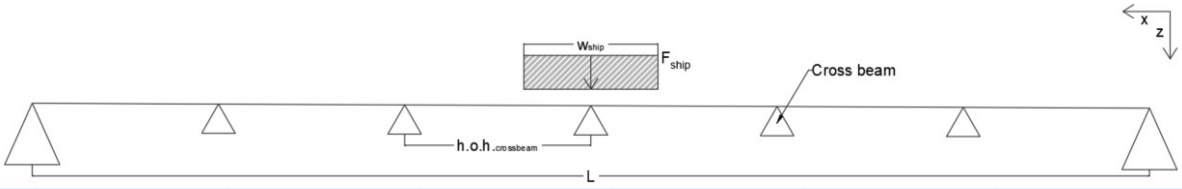

Global bending moment

$$M_{ship\_glob} := \frac{1}{2} \cdot F_{ship} \cdot \left(\frac{1}{2} \cdot l - \frac{1}{4} \cdot w_{ship} \right) = 4.8 \ \boldsymbol{MN \cdot m}$$

Local bending moment

$$M_{ship\_loc} := \frac{1}{2} \cdot F_{ship} \cdot \left(\frac{1}{2} \cdot h.o.h_{crossbeam} - \frac{1}{4} \cdot w_{ship} \right) = 549.115 \ \boldsymbol{kN \cdot m}$$

Shear forve

$$V_{ship} := F_{ship} = 811 \ \boldsymbol{kN}$$

Section properties

$$A_{V\_mb\_f} := t_{mb\_f} \cdot w_{mb\_f} = 0.024 \ \boldsymbol{m^2} \qquad W_{loc\_mb\_f} := \frac{1}{6} \cdot t_{mb\_f} \cdot w_{mb\_f}^{\ 2}$$

$$I_{sc} := 2 \cdot \frac{1}{12} \cdot t_{mb\_f} \cdot w_{mb\_f}^{\ 3} + 2 \cdot t_{mb\_f} \cdot w_{mb\_f} \cdot \left(\frac{b_{supp}}{2} \right)^2 = 1.056 \ \boldsymbol{m^4}$$

Resultant stresses

$$\tau_{sc} := \frac{V_{ship}}{A_{V\_mb\_f}} = 34.3 \ \boldsymbol{MPa}$$

$$\sigma_{sc\_glob} := \frac{M_{ship\_glob}}{I_{sc}} \cdot \frac{b_{supp} + w_{mb\_f}}{2} = 22.7\ \textit{MPa}$$

$$\sigma_{sc\_loc} := \frac{M_{ship\_loc}}{W_{loc\_mb\_f}} = 265.6\ \textit{MPa}$$

Unity checks

$$u.c._{\tau\_sc} := \frac{\tau_{sc}}{f_{st}} = 0.097$$

$$u.c._{\sigma\_sc\_loc} := \frac{\sigma_{sc\_loc}}{f_{st}} = 0.748$$

$$u.c._{\sigma\_sc\_glob} := \frac{\sigma_{sc\_glob}}{f_{st}} = 0.064$$

Calculations for opened structure

Wind loads

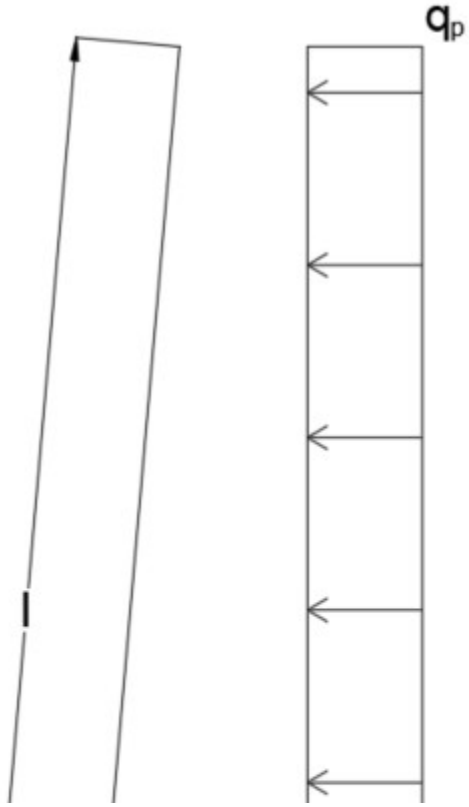

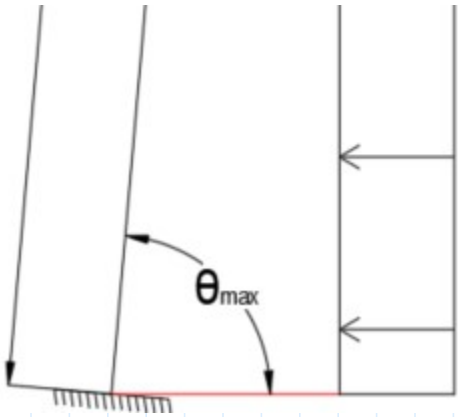

$z_e := h_{under\_side} + \sin(\theta_{max}) \cdot l = 29.2\ m$ $q_{p\_0} := 1.94\ \frac{kN}{m^2}$ $slenderness := \frac{b_{supp} + 2 \cdot b_{edge}}{h_{mb}} = 8$

$\rho := 1.25\ \frac{kg}{m^3}$ $v_b := 29.5\ \frac{m}{s}$

$c_{fx\_0} := \begin{cases} \text{if } slenderness \le 4 \\ \quad 2.4 - 0.275 \cdot slenderness \\ \text{else} \\ \quad 1.3 \end{cases} = 1.3$ $c_e := \frac{q_{p\_0}}{\frac{1}{2} \cdot \rho \cdot v_b^{\,2}} = 3.6$ $C_t := c_{fx\_0} \cdot c_e = 4.6$

$q_p := \frac{1}{2} \cdot \rho \cdot v_b^{\,2} \cdot C_t = 2.5\ \frac{kN}{m^2}$

$t_{open} := 15$ $\psi_t := 1 + \frac{\ln\left(\frac{t_{open}}{50}\right)}{9} = 0.9$

Principle resultant forces

$N_{mb\_G\_open} := \frac{G_{mb} \cdot l}{2 \cdot \sin(\theta_{max})} = 676.9\ kN$

$M_{mb\_G\_open} := \frac{1}{2} \cdot G_{mb} \cdot \cos(\theta_{max}) \cdot l^2 = (2.923 \cdot 10^3)\ kN \cdot m$

$N_{mb\_wind} := \frac{\frac{1}{2} \cdot q_p \cdot h_{mb} \cdot (\sin(\theta_{max}) \cdot l)^2}{b_{supp}} = 206.276\ kN$

$M_{mb\_wind\_y} := \frac{1}{2} \cdot \frac{1}{2} \cdot q_p \cdot (2 \cdot b_{edge} + b_{supp}) \cdot (\sin(\theta_{max}) \cdot l)^2 = (7.583 \cdot 10^3)\ kN \cdot m$

Resultant stresses

$$\sigma_{mb\_G\_open} := \frac{M_{mb\_G\_open}}{EI_{mb}} \cdot E_{steel} \cdot \frac{1}{2} \cdot h_{mb} + \frac{N_{mb\_G\_open}}{A_{mb}} = 45.7\ \textbf{MPa}$$

$$\sigma_{mb\_wind\_1} := \frac{M_{mb\_wind\_y}}{EI_{mb}} \cdot E_{steel} \cdot \frac{1}{2} \cdot h_{mb} + 0.4 \cdot \frac{N_{mb\_wind}}{A_{mb}} = 101.1\ \textbf{MPa}$$

$$\sigma_{mb\_wind\_2} := 0.4 \cdot \frac{M_{mb\_wind\_y}}{EI_{mb}} \cdot E_{steel} \cdot \frac{1}{2} \cdot h_{mb} + \frac{N_{mb\_wind}}{A_{mb}} = 42.3\ \textbf{MPa}$$

$$\sigma_{mb\_wind} := \max\left(\sigma_{mb\_wind\_1}, \sigma_{mb\_wind\_2}\right) = 101.1\ \textbf{MPa}$$

Unity checks

$$u.c._{\sigma\_open} := \frac{1.2 \cdot \sigma_{mb\_G\_open} + 1.8 \cdot \psi_t \cdot \sigma_{mb\_wind}}{f_{st}} = 0.6$$

Results

Unity Checks

Unity checks traffic loads

deflection

$u.c._{deflection\_midspan} = 0.21$ $u.c._{deflection\_threshold} = 0.97$

Road deck

$u.c._{\tau\_rd} = 0.93$ $u.c._{\sigma\_rd} = 0.89$ $u.c._{\sigma\_c\_rd} = 0.46$

Cross beam

$u.c._{\tau\_cb} = 0.19$ $u.c._{\sigma\_cb} = 0.96$

Main beam

$u.c._{\tau\_mb} = 0.26$ $u.c._{\sigma\_mb} = 0.87$

Unity checks ship colision

Main Beam

$u.c._{\tau\_sc} = 0.097$ $u.c._{\sigma\_sc\_loc} = 0.748$ $u.c._{\sigma\_sc\_glob} = 0.064$

Unity checks opened position

$u.c._{\sigma\_open} = 0.6$

MKI

$€ := 1$ ¤

$Mass_{E\_glass} := 2 \cdot t_{l\_rd} \cdot b_{supp} \cdot l \cdot \rho_{l\_rd} = 10.9$ *tonne*

$Mass_{Balsa} := t_{c\_rd} \cdot b_{supp} \cdot l \cdot \rho_{balsa} = 34.002$ *tonne*

$$Mass_{Steel} := \begin{pmatrix} n_{crossbeam} \cdot \left(2 \cdot w_{cb\_f} \cdot t_{cb\_f} + t_{cb\_w} \cdot \left(h_{cb\_main} - 2 \cdot t_{cb\_f}\right)\right) \cdot b_{supp} \\ +2 \cdot \left(2 \cdot w_{mb\_f} \cdot t_{mb\_f} + t_{mb\_w} \cdot \left(h_{mb} - 2 \cdot t_{mb\_f}\right)\right) \cdot l \end{pmatrix} \cdot \rho_{steel} = 48.5 \text{ tonne}$$

$A_{E\_glass} := 2 \cdot \left(b_{supp} + t_{d\_rd}\right) \cdot l = 503.687$ m^2

$$A_{Steel} := n_{crossbeam} \cdot \left(4 \cdot t_{cb\_f} + 4 \cdot w_{cb\_f} + 2 \cdot h_{cb\_main} - 2 \cdot t_{cb\_w}\right) \cdot b_{supp} = 579.9 \text{ m}^2$$
$$+ 2 \cdot \left(4 \cdot t_{mb\_f} + 4 \cdot w_{mb\_f} + 2 \cdot h_{mb} - 2 \cdot t_{mb\_w}\right) \cdot l$$

$MKI_{Steel} := 0.165 \frac{€}{kg}$ $\quad MKI_{score\_Steel} := MKI_{Steel} \cdot Mass_{Steel} = 8009.9$ €

$MKI_{E\_glass} := 0.265 \frac{€}{kg}$ $\quad MKI_{score\_E\_glass} := MKI_{E\_glass} \cdot Mass_{E\_glass} = 2883.4$ €

$MKI_{Balsa} := -0.129 \frac{€}{kg}$ $\quad MKI_{score\_Balsa} := MKI_{Balsa} \cdot Mass_{Balsa} = -4386.3$ €

$MKI_{Steel\_cons} := 0.300 \frac{€}{m^2}$ $\quad MKI_{score\_Steel\_cons} := 5 \cdot MKI_{Steel\_cons} \cdot A_{Steel} = 869.9$ €

$MKI_{E\_glass\_cons} := 1.173 \frac{€}{m^2}$ $\quad MKI_{score\_E\_glass\_cons} := MKI_{E\_glass\_cons} \cdot A_{E\_glass} = 590.8$ €

$$MKI_{score\_Total} := MKI_{score\_Steel} + MKI_{score\_E\_glass} + MKI_{score\_Balsa} = 7968 \text{ €}$$
$$+ MKI_{score\_Steel\_cons} + MKI_{score\_E\_glass\_cons}$$

Mass

$Mass_{total} := Mass_{Steel} + Mass_{E\_glass} + Mass_{Balsa} = 93$ *tonne*

Appendix VII Structural checks steel main beam with an FRP deck main structure.

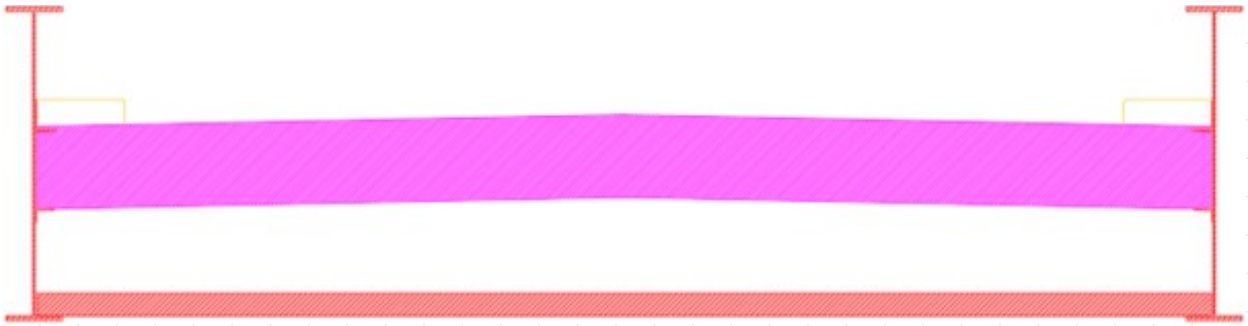

Table of Contents

General

General dimensions

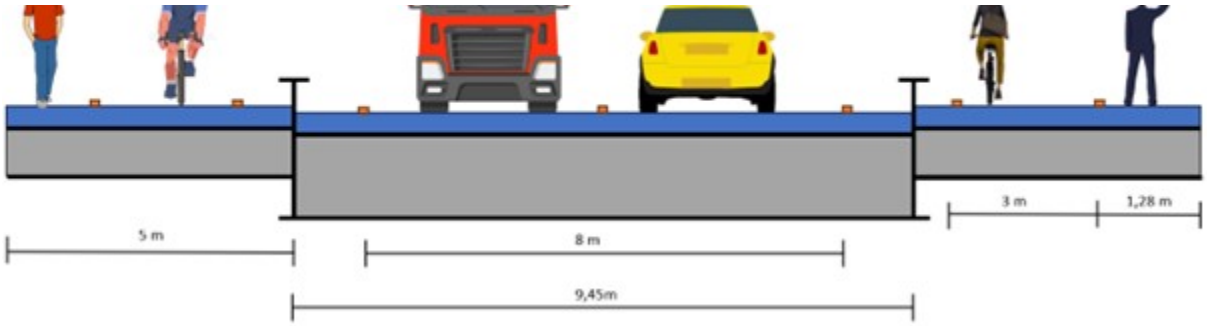

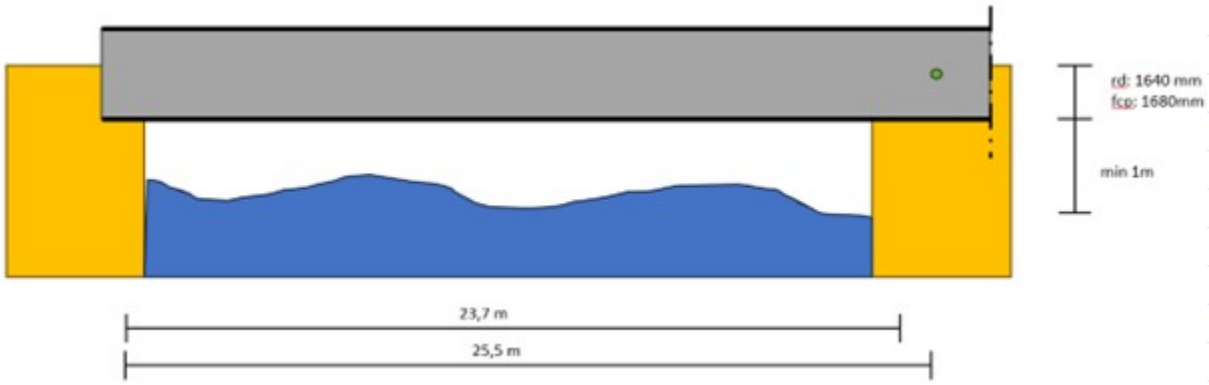

$l := 25250\ mm$

$b_{fcp} := 4.28\ m$ $b_{edge} := 5\ m$ $b_{rd} := 8\ m$ $b_{supp} := 9.45\ m$

$h_{rd} := 5.9\ m$ $h_{fcp} := 6.05\ m$ $h_{water} := 3.3\ m$ $h_{under\_side} := 4.3\ m$

$\theta_{max} := 80\ °$ $h_{top} := \sin\left(\theta_{max}\right) \cdot l + h_{rd} = 30.8\ m$

$Mass_{fcp} := 15.45\ tonne$

General properties

$T_{s\_sun} := 57\ °C$ $T_{s\_shade} := 31\ °C$

Design material properties

Properties balsa core

$\rho_{balsa} := 285\ \frac{kg}{m^3}$ $G_{balsa} := 145\ MPa$

$E_{balsa\_z} := 720\ MPa$ $E_{balsa\_x} := 2642\ MPa$

$f_{c\_zz\_k} := 2.08\ MPa$ $f_{c\_xx\_k} := 7.32\ MPa$

$$\eta_{ct\_balsa} := min\left(1 - \left(\frac{0.2\ \frac{kg}{m^3}}{\rho_{balsa}} + 0.004\right) \cdot \left(\frac{T_{s\_sun} - 20\ °C}{1\ °C}\right), 1\right) = 1$$

$$\eta_{cm\_balsa} := 1 \qquad \eta_{c\_balsa} := \eta_{ct\_balsa} \cdot \eta_{cm\_balsa} = 1$$

$$\gamma_{m\_balsa} := 1.51 \qquad \gamma_{rd\_balsa} := 1.5$$

$$f_{c\_xz\_d} := \frac{\eta_{c\_balsa} \cdot f_{c\_xz\_v\_k}}{\gamma_{m\_balsa} \cdot \gamma_{rd\_balsa}} = 0.92\ MPa$$

$$f_{c\_z\_d} := \frac{\eta_{c\_balsa} \cdot f_{c\_z\_k}}{\gamma_{m\_balsa} \cdot \gamma_{rd\_balsa}} = 3.23\ MPa$$

Properties road deck laminate

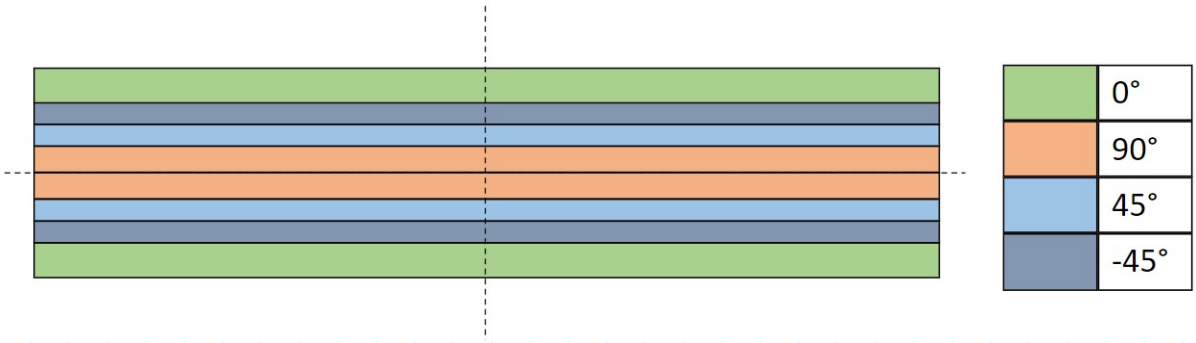

Laminate layup road deck

$$\begin{bmatrix} 0 \\ 90 \\ 45 \\ -45 \end{bmatrix} \quad \begin{bmatrix} 50\% \\ 16.67\% \\ 16.67\% \\ 16.67\% \end{bmatrix}$$

$$\rho_{l\_rd} := 1900\ \frac{kg}{m^3} \qquad E_{1\_l\_rd} := 26.2\ GPa \qquad E_{2\_l\_rd} := 17.4\ GPa$$

$$f_{rd\_x\_k} := 366\ MPa \qquad f_{rd\_y\_k} := 244\ MPa \qquad f_{rd\_xy\_k} := 153\ MPa$$

$$T_{g\_rd} := 90\ °C$$

$$\eta_{ct\_f\_rd} := min\left(1 - 0.25 \cdot \frac{T_{s\_sun} - 20\ °C}{T_{g\_rd} - 20\ °C}, 1\right) = 0.9$$

$$\eta_{cm\_f\_rd} := 0.6 \qquad \eta_{c\_f\_rd} := \eta_{ct\_f\_rd} \cdot \eta_{cm\_f\_rd} = 0.521$$

$$\eta_{ct\_m\_rd} := min\left(1 - 0.80 \cdot \frac{T_{s\_sun} - 20\ °C}{T_{g\_rd} - 20\ °C}, 1\right) = 0.6$$

$$\eta_{cm\_m\_rd} := 0.6 \qquad \eta_{c\_m\_rd} := \eta_{ct\_m\_rd} \cdot \eta_{cm\_m\_rd} = 0.346$$

$$\gamma_{m\_rd} := 1.07 \qquad \gamma_{rd\_rd} := 1.4$$

$$f_{rd\_x\_d} := \frac{\eta_{ct\_f\_rd} \cdot f_{rd\_x\_k}}{\gamma_{rd\_rd} \cdot \gamma_{m\_rd}} = 212\ MPa$$

$$f_{rd\_y\_d} := \frac{\eta_{ct\_f\_rd} \cdot f_{rd\_y\_k}}{\gamma_{rd\_rd} \cdot \gamma_{m\_rd}} = 141.4\ MPa$$

$$f_{rd\_xy\_d} := \frac{\eta_{ct\_f\_rd} \cdot f_{rd\_xy\_k}}{\gamma_{rd\_rd} \cdot \gamma_{m\_rd}} = 88.6\ MPa$$

Properties head board web

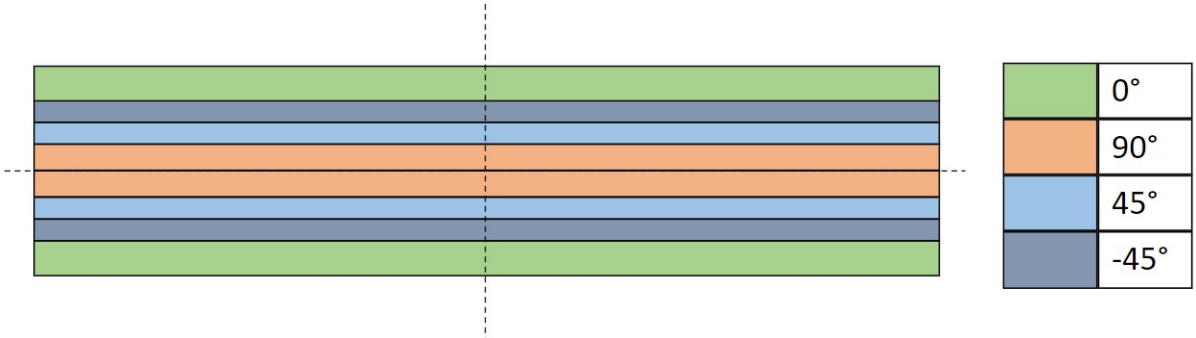

Laminate layup web

$$\begin{bmatrix} 0 \\ 90 \\ 45 \\ -45 \end{bmatrix} \quad \begin{bmatrix} 25\% \\ 25\% \\ 25\% \\ 25\% \end{bmatrix}$$

$$E_{w\_mb} := 19.9\ GPa$$

Properties steel

$\rho_{steel} := 7800 \ \frac{kg}{m^3}$ $E_{steel} := 210 \ GPa$ $f_{st} := 355 \ MPa$

Traffic load calculations

Cross section properties

load properties

Distributed load BM1

$q_{bm1} := 9 \ \frac{kN}{m^2}$

Concentrated load BM1

$Q_{bm1} := 300 \ kN$ $l_{w\_bm1} := 40 \ cm$ $w_{w\_bm1} := 40 \ cm$ $w_{bm1} := 2 \ m$ $h.o.h_{bm1} := 1.2 \ m$

Distirbuted load foot and cycle path

$q_{fcp} := 5 \ \frac{kN}{m^2}$

Concentrated load accidental vehicle

$Q_{av1} := 80 \ kN$ $Q_{av2} := 40 \ kN$

Ship collision force

$F_{ship} := 0.811 \ MN$ $h_{ship} := 0.25 \ m$ $w_{ship} := 3 \ m$

Road deck properties

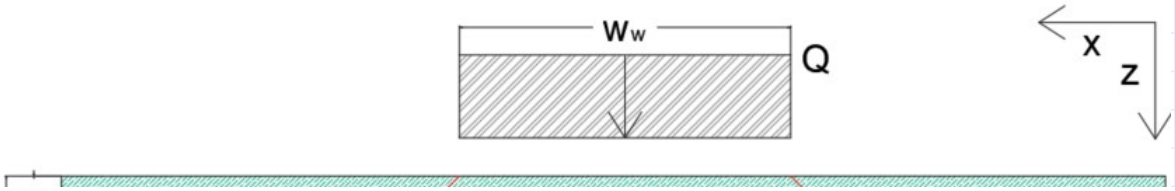

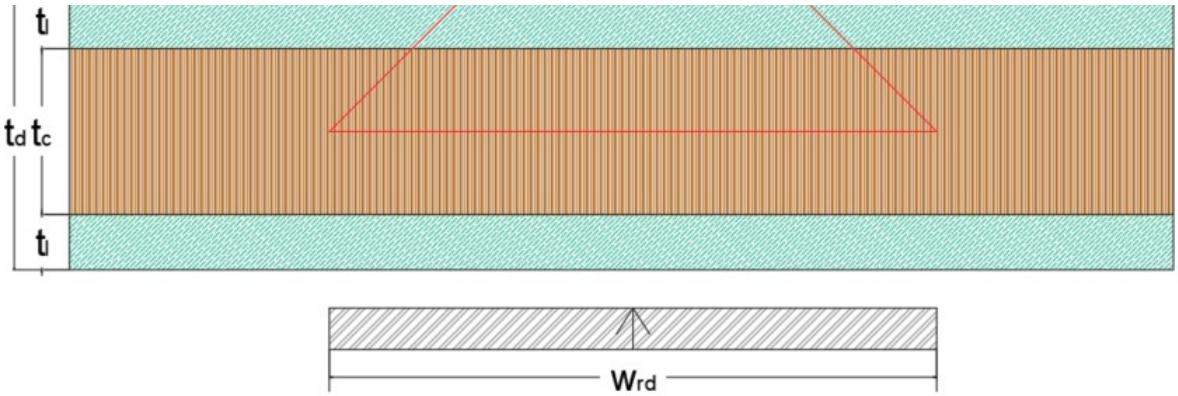

$w_{bm1\_mid} := 0.5\ m$

$t_{l\_rd} := 30\ mm \qquad t_{c\_rd} := 700\ mm \qquad t_{d\_rd} := t_{c\_rd} + 2 \cdot t_{l\_rd} = 760\ mm$

$w_{rd} := l_{w\_bm1} + t_{d\_rd} = (1.16 \cdot 10^3)\ mm$

$A_{rd} := w_{rd} \cdot t_{c\_rd} = 0.812\ m^2$

$EI_{rd} := 2 \cdot E_{1\_l\_rd} \cdot w_{rd} \cdot t_{l\_rd} \cdot \left(\frac{t_{c\_rd} + t_{l\_rd}}{2} \right)^2 = 266811\ kN \cdot m^2$

$+ \frac{1}{12} \cdot E_{balsa\_z} \cdot w_{rd} \cdot t_{c\_rd}^{\ 3}$

Main beam properties

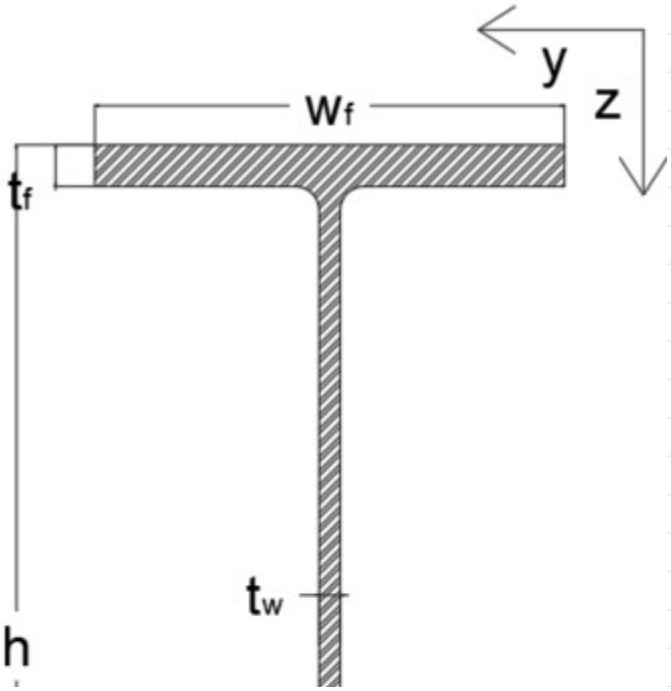

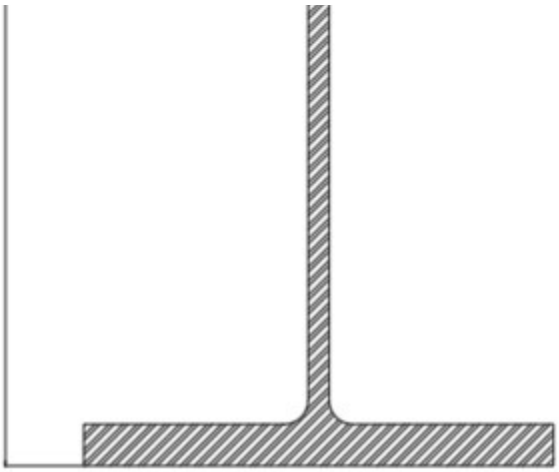

$h_{mb} := 2500\ mm$ $w_{mb\_f} := 525\ mm$ $t_{mb\_f} := 45\ mm$ $t_{mb\_w} := 20\ mm$

$A_{mb\_v} := t_{mb\_w} \cdot h_{mb} = 0.05\ m^2$

$A_{mb} := 2 \cdot t_{mb\_f} \cdot w_{mb\_f} + t_{mb\_w} \cdot \left(h_{mb} - 2 \cdot t_{mb\_f}\right) = 0.095\ m^2$

$$EI_{mb} := E_{steel} \cdot \left(\frac{1}{12} \cdot t_{mb\_w} \cdot \left(h_{mb} - 2 \cdot t_{mb\_f}\right)^3 + 2 \cdot w_{mb\_f} \cdot t_{mb\_f} \cdot \left(\frac{1}{2} \cdot h_{mb} - \frac{1}{2} \cdot t_{mb\_f} \right)^2 \right) = \left(19.8 \cdot 10^6\right)\ kN \cdot m^2$$

Stiffness properties head board

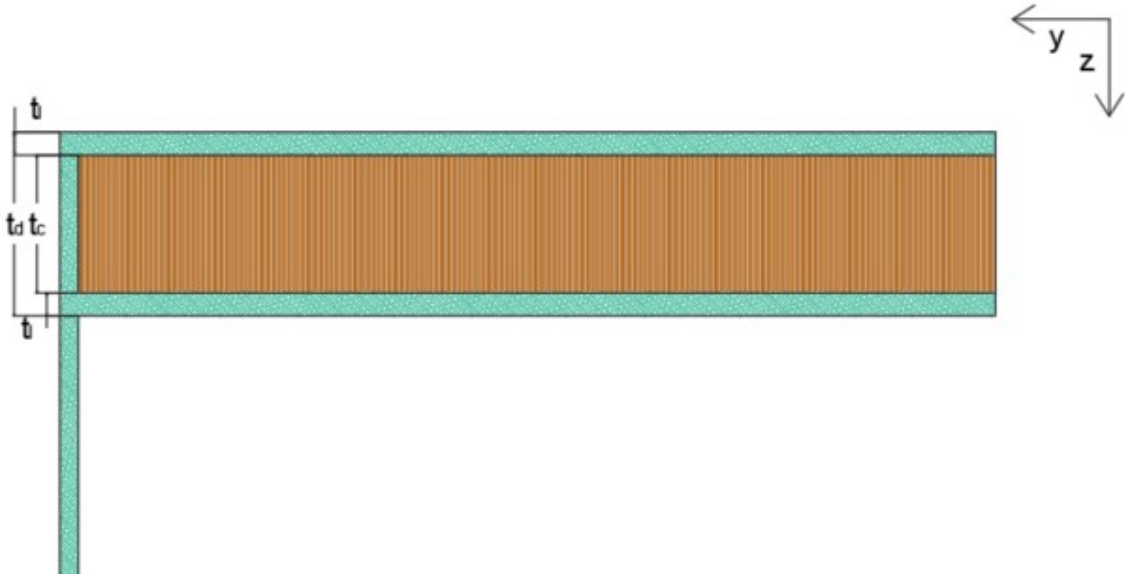

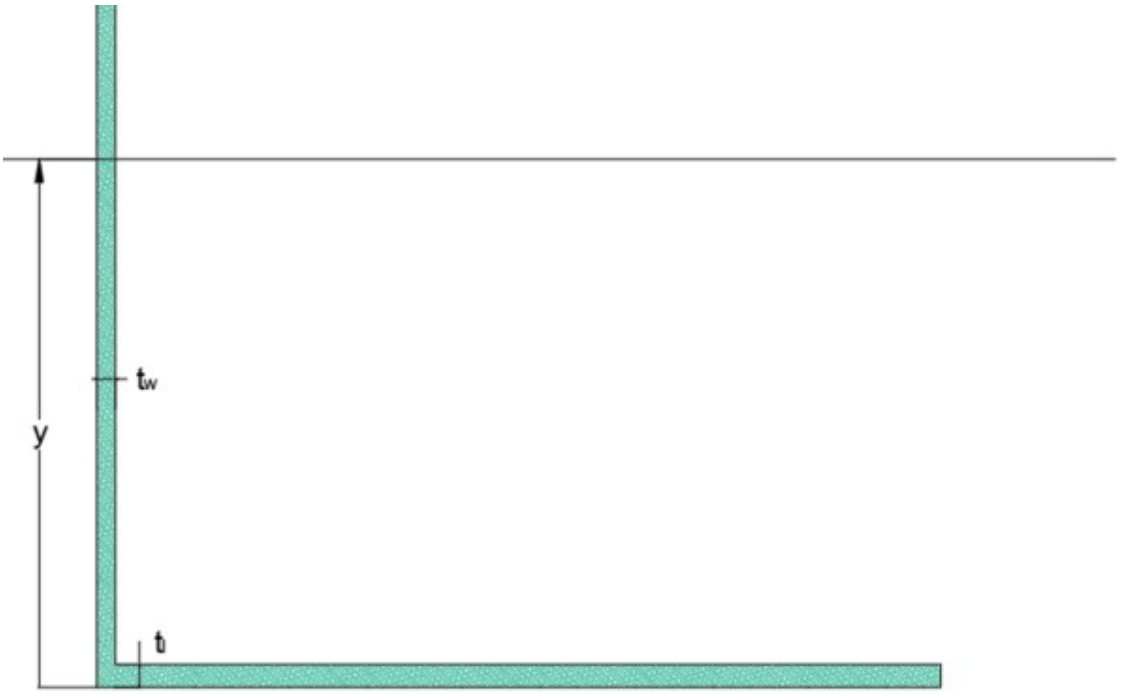

$t_{l\_hb} := 34\ mm \qquad t_{l\_hb\_w} := 28\ mm$

$$y := \frac{\begin{aligned}&\frac{1}{2}\cdot\frac{b_{supp}}{10}\cdot t_{l\_hb}^{\ 2}\cdot E_{1\_l\_rd} + \frac{b_{supp}}{10}\cdot t_{c\_rd}\cdot\left(h_{rd} - h_{under\_side} - t_{l\_rd} - \frac{t_{c\_rd}}{2}\right)\cdot E_{balsa\_z} \\ &+ \frac{b_{supp}}{10}\cdot t_{l\_rd}\cdot\left(h_{rd} - h_{under\_side} - \frac{t_{l\_rd}}{2}\right)\cdot E_{1\_l\_rd} \\ &+ \frac{b_{supp}}{10}\cdot t_{l\_rd}\cdot\left(h_{rd} - h_{under\_side} - t_{c\_rd} - \frac{3\cdot t_{l\_rd}}{2}\right)\cdot E_{1\_l\_rd} \\ &+ \frac{1}{12}\cdot t_{l\_hb\_w}\cdot\left(h_{rd} - h_{under\_side}\right)\cdot E_{w\_mb}\cdot\frac{1}{2}\cdot\left(h_{rd} - h_{under\_side}\right)\end{aligned}}{3\cdot\frac{b_{supp}}{10}\cdot t_{l\_rd}\cdot E_{1\_l\_rd} + \frac{b_{supp}}{10}\cdot t_{c\_rd}\cdot E_{balsa\_z} + \left(h_{rd} - h_{under\_side}\right)\cdot t_{mb\_w}\cdot E_{w\_mb}} = 0.74\ m$$

$$z_{l\_rd\_top} := h_{rd} - h_{under\_side} - \frac{t_{l\_rd}}{2} - y = 0.847\ m$$

$$z_{c\_rd} := h_{rd} - h_{under\_side} - t_{l\_rd} - \frac{t_{c\_rd}}{2} - y = 0.482\ m$$

$$z_{l\_rd\_bot} := h_{rd} - h_{under\_side} - t_{c\_rd} - \frac{3\ t_{l\_rd}}{2} - y = 0.117\ m$$

$$z_{l\_beam\_bot} := -y + \frac{t_{l\_rd}}{2} = -0.723\ m$$

$$EI_{hb} := \frac{b_{supp}}{10}\cdot t_{l\_rd}\cdot z_{l\_rd\_bot}^{\ 2}\cdot E_{1\_l\_rd} = \left(1.284\cdot 10^{6}\right)\ kN\cdot m^{2}$$

$$\frac{b_{supp}}{\ }\cdot t\ \cdot\ z\ ^{2}\cdot E$$

$$+\frac{b_{supp}}{10}\cdot t_{l\_rd}\cdot z_{l\_rd\_top}{}^{2}\cdot E_{1\_l\_rd}$$

$$+\frac{b_{supp}}{10}\cdot t_{l\_hb}\cdot z_{l\_beam\_bot}{}^{2}\cdot E_{1\_l\_rd}$$

$$+\frac{b_{supp}}{10}\cdot t_{c\_rd}\cdot z_{c\_rd}{}^{2}\cdot E_{balsa\_z}$$

$$+\frac{1}{12}\cdot t_{l\_hb\_w}\cdot\left(h_{rd}-h_{under\_side}\right)^{3}\cdot E_{w\_mb}$$

Calculations for deflections

Deflections at the supports in the middle of the deck

$$w_{middle\_at\_supports}:=\frac{1}{48}\cdot\frac{Q_{bm1}\cdot b_{supp}{}^{3}}{EI_{hb}}+\frac{5}{384}\cdot\frac{q_{bm1}\cdot\frac{b_{supp}}{10}\cdot b_{supp}{}^{4}}{EI_{hb}}=4.8\ mm$$

Deflections at midspan in the middle of the deck

$$w_{middle\_midspan}:=\frac{1}{48}\ \frac{4\cdot Q_{bm1}\cdot l^{3}}{2\cdot EI_{mb}}+\frac{5}{384}\cdot\frac{q_{bm1}\cdot b_{supp}\cdot l^{4}}{2\cdot EI_{mb}}=21.5\ mm$$

Deflections limit

$$w_{limit\_midspan}:=\frac{l}{250}=101\ mm \qquad w_{limit\_threshold}:=5\ mm$$

Unity checks

$$u.c._{deflection\_threshold}:=\frac{w_{middle\_at\_supports}}{w_{limit\_threshold}}=0.96$$

$$u.c._{deflection\_midspan}:=\frac{w_{middle\_midspan}}{w_{limit\_midspan}}=0.21$$

Calculations for road deck

Load cases

Loadcase BM1.1

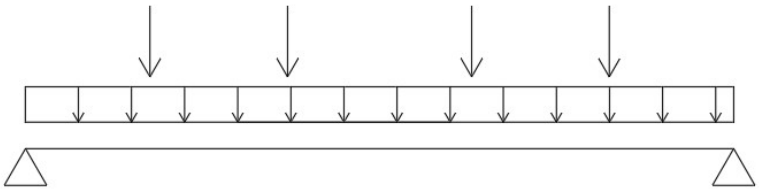

Loadcase BM1 2

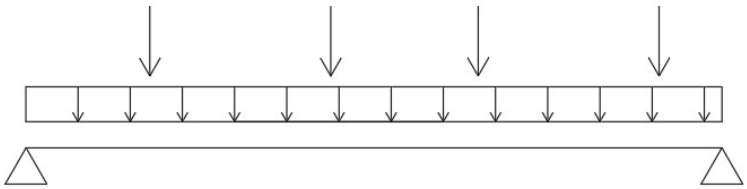

Loadcase G

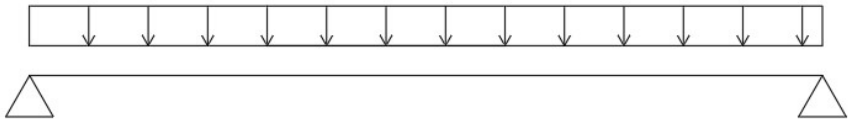

Shear force

Load case BM1 2 was used

$$V_{bm1} := \frac{1}{2} \cdot q_{bm1} \cdot b_{rd} \cdot w_{rd} + 1.105 \cdot Q_{bm1} = 373.26 \ \boldsymbol{kN}$$

Bending moments

Load case BM1 1 was used

$$M_{bm1} := \frac{1}{2} \cdot q_{bm1} \cdot w_{rd} \cdot b_{rd} \cdot \left(\frac{1}{2} \cdot b_{supp} - \frac{1}{4} \cdot b_{rd} \right) + \frac{Q_{bm1}}{2} \cdot \left(b_{supp} - 2 \cdot w_{bm1\_mid} - w_{bm1} \right) = 1081 \ \boldsymbol{kN \cdot m}$$

Self weight

$$G_{rd} := \left(2 \cdot t_{l\_rd} \cdot w_{rd} \cdot \rho_{l\_rd} + t_{c\_rd} \cdot w_{rd} \cdot \rho_{balsa} \right) \cdot 9.81 \ \frac{\boldsymbol{m}}{\boldsymbol{s}^2} = 3.568 \ \frac{\boldsymbol{kN}}{\boldsymbol{m}}$$

Forces as a result of self weight

Loadcase G was used

$$V_{G\_rd} := \frac{1}{2} \cdot G_{rd} \cdot b_{supp} = 16.9 \ \boldsymbol{kN}$$

$$M_{G\_rd} := \frac{1}{8} \cdot G_{rd} \cdot b_{supp}{}^{2} = 39.8 \ \boldsymbol{kN \cdot m}$$

Combined forces with 6.10 B

$$V_{Ed\_rd} := 1.2 \cdot V_{G\_rd} + 1.5 \cdot V_{bm1} = 580 \ \boldsymbol{kN}$$

$$M_{Ed\_rd} := 1.2 \cdot M_{G\_rd} + 1.5 \cdot M_{bm1} = 1670 \ \boldsymbol{kN \cdot m}$$

$$V_{Ed\_rd\_s} := 1.5 \cdot \left(2 \cdot 0.6 \cdot Q_{bm1} + 0.1 \cdot q_{bm1} \cdot w_{w\_bm1} \cdot b_{rd}\right) = 544 \ \boldsymbol{kN}$$

Resultant stresses

$$\tau_{c\_rd} := \frac{V_{Ed\_rd}}{A_{rd}} = 0.7 \ \boldsymbol{MPa}$$

$$\sigma_{l\_rd} := \frac{M_{Ed\_rd}}{EI_{rd}} \cdot \frac{t_{d\_rd}}{2} \cdot E_{1\_l\_rd} = 62 \ \boldsymbol{MPa}$$

$$\tau_{l\_rd} := \frac{V_{Ed\_rd\_s}}{t_{l\_rd} \cdot w_{w\_bm1}} = 45 \ \boldsymbol{MPa}$$

$$\sigma_{c\_fcp} := \frac{M_{Ed\_rd}}{EI_{rd}} \cdot \left(\frac{t_{d\_rd}}{2} - t_{l\_rd}\right) \cdot E_{balsa\_z} = 1.577 \ \boldsymbol{MPa}$$

Unity checks

$$u.c._{\tau\_c\_rd} := \frac{\tau_{c\_rd}}{f_{c\_xz\_d}} = 0.78$$

$$u.c._{\sigma\_rd} := \frac{\sigma_{l\_rd}}{f_{rd\_x\_d}} = 0.29$$

$$u.c._{\tau\_l\_rd} := \frac{\tau_{l\_rd}}{f_{rd\_xy\_d}} = 0.51$$

$$u.c._{comb\_rd} := u.c._{\sigma\_rd} + u.c._{\tau\_l\_rd} = 0.81$$

$$u.c._{\sigma\_c\_rd} := \frac{\sigma_{c\_fcp}}{f_{c\_z\_d}} = 0.49$$

Calculations for mainbeam

Loads

Load q mb

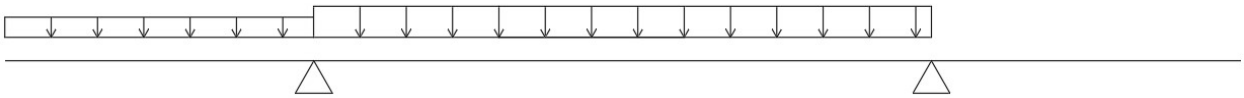

Load Q mb

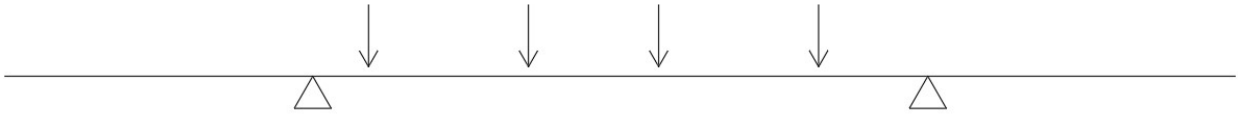

$$q_{mb} := \frac{b_{fcp} \cdot q_{fcp} \cdot \left(\frac{b_{fcp}}{2} + \left(b_{edge} - b_{fcp} \right) + b_{supp} \right) + b_{rd} \cdot q_{bm1} \cdot b_{supp}}{b_{supp}} = 99.877 \ \frac{kN}{m}$$

$$Q_{mb} := \frac{\left(\begin{array}{l} Q_{bm1} \cdot \left(2 \cdot b_{supp} - 2 \cdot \frac{\left(b_{supp} - b_{rd} \right)}{2} - 2 \cdot w_{bm1\_mid} - w_{bm1} \right) \\ + 2 \cdot \frac{b_{supp}}{2} - 2 \cdot w_{bm1\_mid} - w_{bm1} \end{array} \right)}{b_{supp}} = 663.5 \ kN$$

Load cases

Loadcase V MB

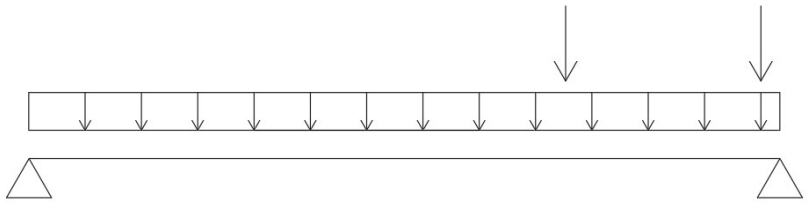

Loadcase M MB

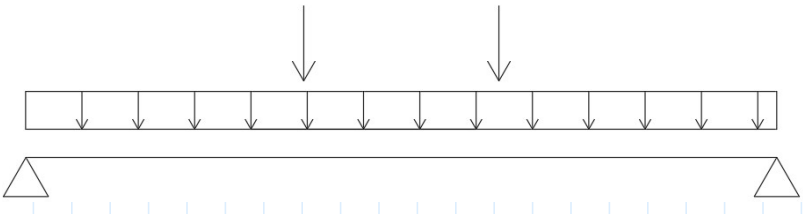

Loadcase G

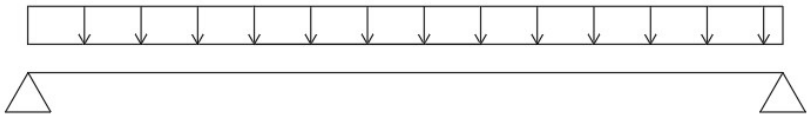

Shear force

Loadcases V MB was used

$$V_{bm1\_mb} := \frac{1}{2} \cdot q_{mb} \cdot l + Q_{mb} = \left(1.9 \cdot 10^3\right)\ \mathbf{kN}$$

Bending moment

Loadcases M MB was used

$$M_{bm1\_mb} := \frac{1}{8} \cdot q_{mb} \cdot l^2 + \frac{1}{4} \cdot Q_{mb} \cdot l = \left(1.215 \cdot 10^4\right)\ \mathbf{kN \cdot m}$$

Self weight

$$Mass_{dist} := 2 \cdot \left(2 \cdot w_{mb\_f} \cdot t_{mb\_f} + \left(h_{mb} - 2 \cdot t_{mb\_f}\right) \cdot t_{mb\_w}\right) \cdot \rho_{steel} + t_{c\_rd} \cdot b_{supp} \cdot \rho_{balsa} + 2 \cdot t_{l\_rd} \cdot b_{supp} \cdot \rho_{l\_rd} + 2 \cdot \frac{Mass_{fcp}}{l} = 5675\ \frac{\mathbf{kg}}{\mathbf{m}}$$

$$G_{mb} := Mass_{dist} \cdot 9.81\ \frac{\mathbf{m}}{\mathbf{s}^2} = 55.675\ \frac{\mathbf{kN}}{\mathbf{m}}$$

Forces as a result of self weight

Loadcase G was used

$$V_{G\_mb} := \frac{1}{2} \cdot G_{mb} \cdot l = 703\ \mathbf{kN}$$

$$M_{G\_mb} := \frac{1}{8} \cdot G_{mb} \cdot l^2 = 4437\ \mathbf{kN \cdot m}$$

Combined forces with 6.10 B

$$V_{Ed\_mb} := 1.2 \cdot V_{G\_mb} + 1.5 \cdot V_{bm1\_mb} = \left(3.73 \cdot 10^3\right)\ \mathbf{kN}$$

$$M_{Ed\_mb} := 1.2 \cdot M_{G\_mb} + 1.5 \cdot M_{bm1\_mb} = \left(2.355 \cdot 10^4\right)\ \mathbf{kN \cdot m}$$

Resultant stresses

$$\tau_{Ed\_mb} := \frac{V_{Ed\_mb}}{A_{mb\_v}} = 74.6 \ \textbf{\textit{MPa}}$$

$$\sigma_{Ed\_mb} := \frac{M_{Ed\_mb}}{EI_{mb}} \cdot E_{steel} \cdot \frac{1}{2} \cdot h_{mb} = 311.4 \ \textbf{\textit{MPa}}$$

Unity checks

$$u.c._{\tau\_mb} := \frac{\tau_{Ed\_mb}}{f_{st}} = 0.21$$

$$u.c._{\sigma\_mb} := \frac{\sigma_{Ed\_mb}}{f_{st}} = 0.877$$

Auxiliary calculations

Calculations for ship impact forces

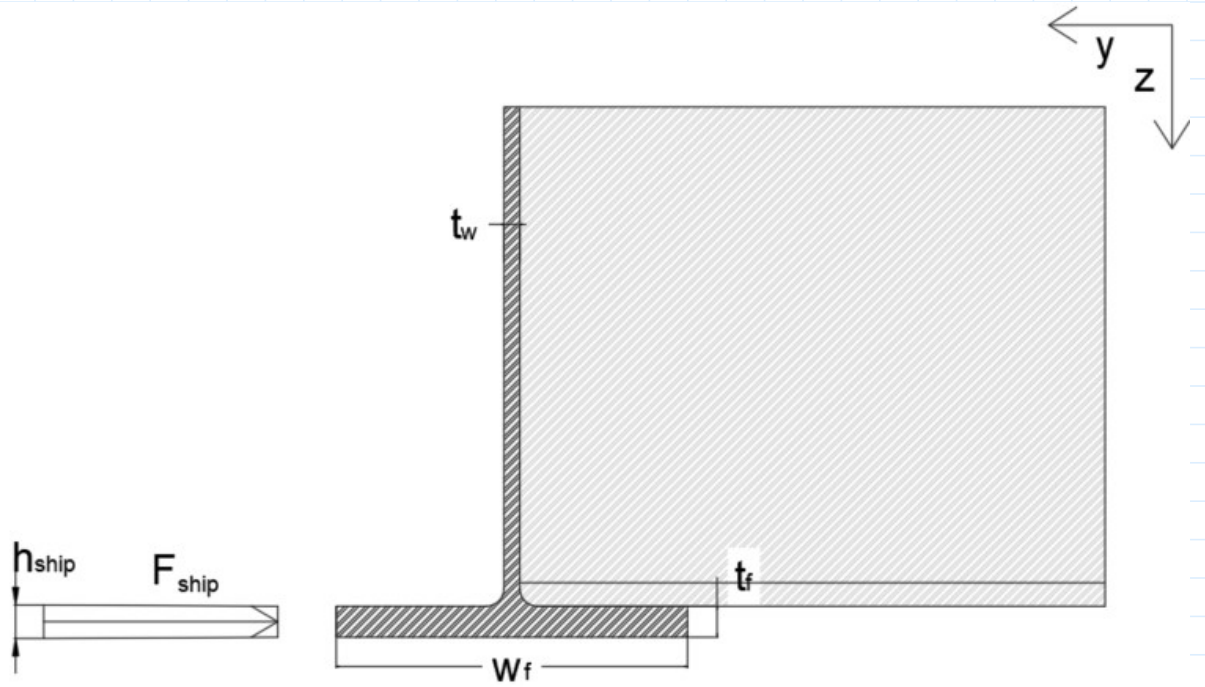

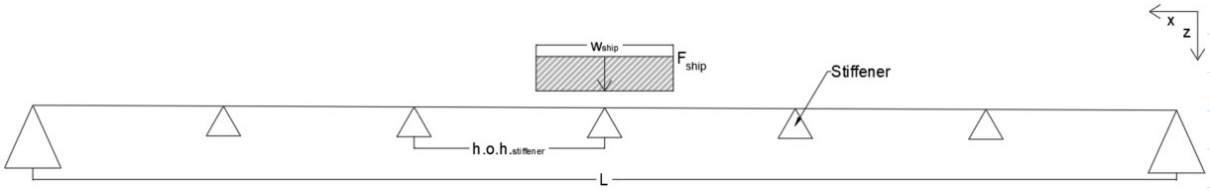

$n_{stiffeners} := 18$ $h.o.h._{stiffener} := \frac{l}{n_{stiffeners} - 1} = 1.485\ m$

$A_{stiff} := 6457\ mm^2$ $I_{cr\_stiff} := 3017 \cdot 10^4\ mm^4$

Stiffeners are square tubes, 180 x 180 x10

Activated stiffeners

$$n_{stiff\_active} := \text{floor}\left(\frac{w_{ship}}{h.o.h._{stiffener}}\right) = 2$$

Normal force

$N_{ship} := F_{ship} = 0.811\ MN$

Shear force

$$V_{ship} := \frac{1}{2} \cdot \frac{F_{ship}}{w_{ship}} \cdot h.o.h._{stiffener} = 0.201\ MN$$

Global bending moment

$$M_{ship\_glob} := \frac{1}{2} \cdot F_{ship} \cdot \left(\frac{1}{2} \cdot l - \frac{1}{4} \cdot w_{ship}\right) = 4.8\ MN \cdot m$$

Local bending moment

$$M_{ship\_loc} := \frac{1}{8} \cdot \frac{F_{ship}}{w_{ship}} \cdot h.o.h._{stiffener}^2 = 74.548\ kN \cdot m$$

Section properties

$$A_{V\_mb\_f} := t_{mb\_f} \cdot w_{mb\_f} = 0.024\ m^2$$

$$W_{loc\_mb\_f} := \frac{1}{6} \cdot t_{mb\_f} \cdot w_{mb\_f}^2$$

$$I_{sc} := 2 \cdot \frac{1}{12} \cdot t_{mb\_f} \cdot w_{mb\_f}^3 + 2 \cdot t_{mb\_f} \cdot w_{mb\_f} \cdot \left(\frac{b_{supp}}{2}\right)^2 = 1.056\ m^4$$

Critical buckling force

$\varepsilon := 0.81$ $class_{f\_stiff} := 1$ $class_{w\_stiff} := 2$ $l_{m\_stiff} := b_{supp}$ $\lambda_1 := 93.9 \cdot \varepsilon = 76$

$$i := \sqrt{\frac{I_{cr\_stiff}}{A_{stiff}}} = 0.068\ m \qquad \lambda := \frac{l_{cr\_stiff}}{i \cdot \lambda_1} = 1.818 \qquad \alpha_{stiff} := 0.49$$

$$\phi := 0.5 \cdot \left(1 + \alpha_{stiff} \cdot (\lambda - 0.2) + \lambda^2\right) = 2.548 \qquad \chi := \frac{1}{\phi + \sqrt{\phi^2 + \lambda^2}} = 0.176$$

$$N_{cr} := \chi \cdot A_{stiff} \cdot f_{st} = 0.404\ MN$$

Resultant stresses

$$\tau_{sc} := \frac{V_{ship}}{A_{V\_mb\_f}} = 8.5\ MPa$$

$$\sigma_{sc\_glob} := \frac{M_{ship\_glob}}{I_{sc}} \cdot \frac{b_{supp} + w_{mb\_f}}{2} = 22.7\ MPa$$

$$\sigma_{sc\_loc} := \frac{M_{ship\_loc}}{W_{loc\_mb\_f}} = 36.1\ MPa$$

Unity checks

$$u.c._{\tau\_sc} := \frac{\tau_{sc}}{f_{st}} = 0.02$$

$$u.c._{\sigma\_sc\_loc} := \frac{\sigma_{sc\_loc}}{f_{st}} = 0.1$$

$$u.c._{s\_sc\_glob} := \frac{\sigma_{sc\_glob}}{f_{st}} = 0.06$$

$$u.c._{\sigma\_sc\_s\_stiff} := \frac{N_{ship}}{n_{stiff\_active} \cdot N_{cr}} = 1$$

Calculations for opened structure

Wind loads

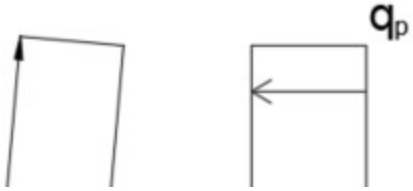

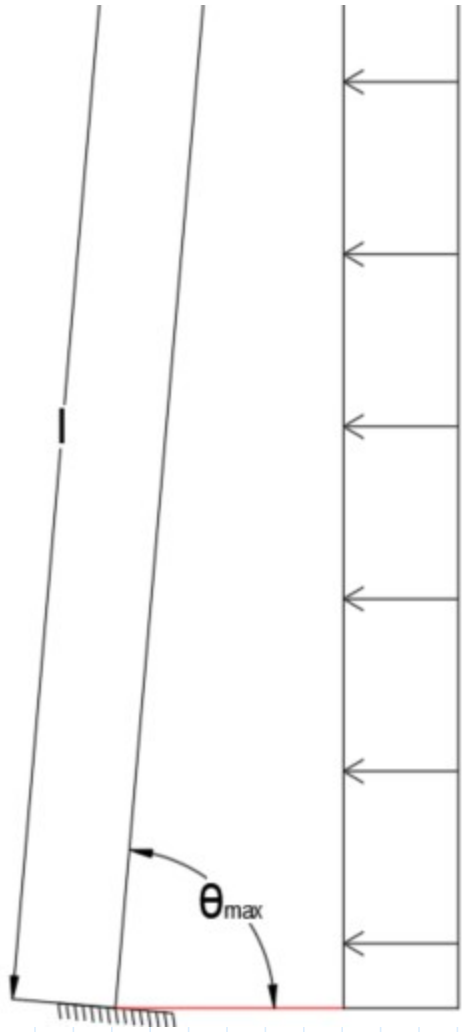

$z_e := h_{under\_side} + \sin(\theta_{max}) \cdot l = 29.2\ m$ $q_{p\_0} := 1.94\ \frac{kN}{m^2}$ $slenderness := \frac{b_{supp} + 2 \cdot b_{edge}}{h_{mb}} = 8$

$\rho := 1.25\ \frac{kg}{m^3}$ $v_b := 29.5\ \frac{m}{s}$

$c_{fx\_0} := \begin{cases} \text{if } slenderness \le 4 \\ \quad 2.4 - 0.275 \cdot slenderness \\ \text{else} \\ \quad 1.3 \end{cases} = 1.3$ $c_e := \frac{q_{p\_0}}{\frac{1}{2} \cdot \rho \cdot v_b^{\,2}} = 3.6$ $C_t := c_{fx\_0} \cdot c_e = 4.6$

$q_p := \frac{1}{2} \cdot \rho \cdot v_b^{\,2} \cdot C_t = 2.5\ \frac{kN}{m^2}$

$t_{open} := 15$ $\psi_t := 1 + \frac{\ln\left(\frac{t_{open}}{50}\right)}{} = 0.9$

Principle resultant forces

$$N_{mb\_G\_open} := \frac{G_{mb} \cdot l}{2 \cdot \sin\left(\theta_{max}\right)} = 713.7\ \textbf{kN}$$

$$M_{mb\_G\_open} := \frac{1}{2} \cdot G_{mb} \cdot \cos\left(\theta_{max}\right) \cdot l^2 = \left(3.082 \cdot 10^3\right)\ \textbf{kN} \cdot \textbf{m}$$

$$N_{mb\_wind} := \frac{\frac{1}{2} \cdot q_p \cdot h_{mb} \cdot \left(\sin\left(\theta_{max}\right) \cdot l\right)^2}{b_{supp}} = 206.276\ \textbf{kN}$$

$$M_{mb\_wind\_y} := \frac{1}{2} \cdot \frac{1}{2} \cdot q_p \cdot \left(2 \cdot b_{edge} + b_{supp}\right) \cdot \left(\sin\left(\theta_{max}\right) \cdot l\right)^2 = \left(7.583 \cdot 10^3\right)\ \textbf{kN} \cdot \textbf{m}$$

Resultant stresses

$$\sigma_{mb\_G\_open} := \frac{M_{mb\_G\_open}}{EI_{mb}} \cdot E_{steel} \cdot \frac{1}{2} \cdot h_{mb} + \frac{N_{mb\_G\_open}}{A_{mb}} = 48.2\ \textbf{MPa}$$

$$\sigma_{mb\_wind\_1} := \frac{M_{mb\_wind\_y}}{EI_{mb}} \cdot E_{steel} \cdot \frac{1}{2} \cdot h_{mb} + 0.4 \cdot \frac{N_{mb\_wind}}{A_{mb}} = 101.1\ \textbf{MPa}$$

$$\sigma_{mb\_wind\_2} := 0.4 \cdot \frac{M_{mb\_wind\_y}}{EI_{mb}} \cdot E_{steel} \cdot \frac{1}{2} \cdot h_{mb} + \frac{N_{mb\_wind}}{A_{mb}} = 42.3\ \textbf{MPa}$$

$$\sigma_{mb\_wind} := \max\left(\sigma_{mb\_wind\_1}, \sigma_{mb\_wind\_2}\right) = 101.1\ \textbf{MPa}$$

Unity checks

$$u.c._{\sigma\_open} := \frac{1.2 \cdot \sigma_{mb\_G\_open} + 1.8 \cdot \psi_t \cdot \sigma_{mb\_wind}}{f_{st}} = 0.61$$

Results

Unity checks

Unity checks traffic loads

deflection

$u.c._{deflection\_midspan} = 0.21$ $u.c._{deflection\_threshold} = 0.96$

Road deck

$u.c._{\sigma\_rd} = 0.78$ $u.c._{\sigma\_rd} = 0.49$ $u.c._{comb\_rd} = 0.81$

Main beam

$u.c._{\tau\_mb} = 0.21$ $u.c._{\sigma\_mb} = 0.88$

Unity checks ship colision

Main beam

$u.c._{\tau\_sc} = 0.024$ $u.c._{\sigma\_sc\_loc} = 0.102$ $u.c._{s\_sc\_glob} = 0.064$

Stiffener

$u.c._{\sigma\_sc\_s\_stiff} = 1$

Unity checks opened position

$u.c._{\sigma\_open} = 0.61$

MKI

$€ := 1$ ¤

$Mass_{E\_glass} := 2 \cdot t_{l\_rd} \cdot b_{supp} \cdot l \cdot \rho_{l\_rd} = 27.2$ *tonne*

$Mass_{Balsa} := \left(t_{c\_rd} \cdot b_{supp}\right) \cdot l \cdot \rho_{balsa} = 47.6$ *tonne*

$Mass_{Steel} := \begin{pmatrix} 2 \cdot \left(2 \cdot w_{mb\_f} \cdot t_{mb\_f} + t_{mb\_w} \cdot \left(h_{mb} - 2 \cdot t_{mb\_f}\right)\right) \cdot l \\ + A_{stiff} \cdot n_{stiffeners} \cdot b_{supp} \end{pmatrix} \cdot \rho_{steel} = 46.2$ *tonne*

$A_{E\_glass} := 2 \cdot \left(b_{supp} + t_{d\_rd}\right) \cdot l = 515.605\ m^2$

$A_{Steel} := 2 \cdot \left(4 \cdot t_{mb\_f} + 4 \cdot w_{mb\_f} + 2 \cdot h_{mb} - 2 \cdot t_{mb\_w}\right) \cdot l = 365.6\ m^2$

$MKI_{Steel} := 0.165\ \frac{€}{kg}$ $MKI_{score\_Steel} := MKI_{Steel} \cdot Mass_{Steel} = 7617.2$ €

$MKI_{E\_glass} := 0.265\ \frac{€}{kg}$ $MKI_{score\_E\_glass} := MKI_{E\_glass} \cdot Mass_{E\_glass} = 7208.5$ €

$MKI_{Balsa} := -0.129\ \frac{€}{kg}$ $MKI_{score\_Balsa} := MKI_{Balsa} \cdot Mass_{Balsa} = -6140.8$ €

$MKI_{Steel\_cons} := 0.300\ \frac{€}{m^2}$ $MKI_{score\_Steel\_cons} := 5 \cdot MKI_{Steel\_cons} \cdot A_{Steel} = 548.4$ €

$MKI_{E\_glass\_cons} := 1.173\ \frac{€}{m^2}$ $MKI_{score\_E\_glass\_cons} := MKI_{E\_glass\_cons} \cdot A_{E\_glass} = 604.8$ €

$MKI_{score\_Total} := MKI_{score\_Steel} + MKI_{score\_E\_glass} = 9838$ €

$$score_{Total} \quad score_{Steel} \quad score_{E\_glass}$$
$$+MKI_{score\_Balsa}+MKI_{score\_Steel\_cons}+MKI_{score\_E\_glass\_cons}$$

Mass

$$Mass_{total}:=Mass_{E\_glass}+Mass_{Balsa}+Mass_{Steel}=121\ tonne$$

Appendix VIII Structural checks FRP main beam and deck main structure.

Table of Contents

General

General dimensions

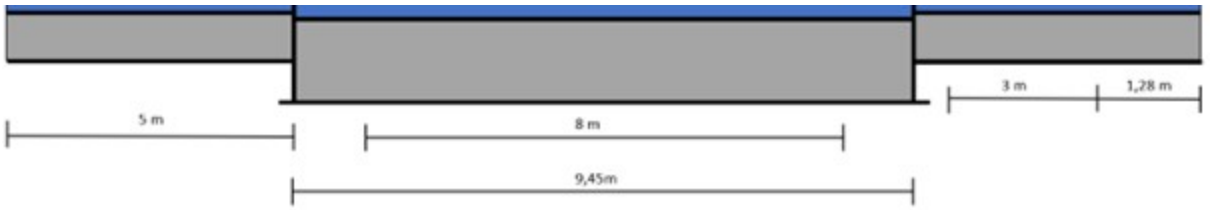

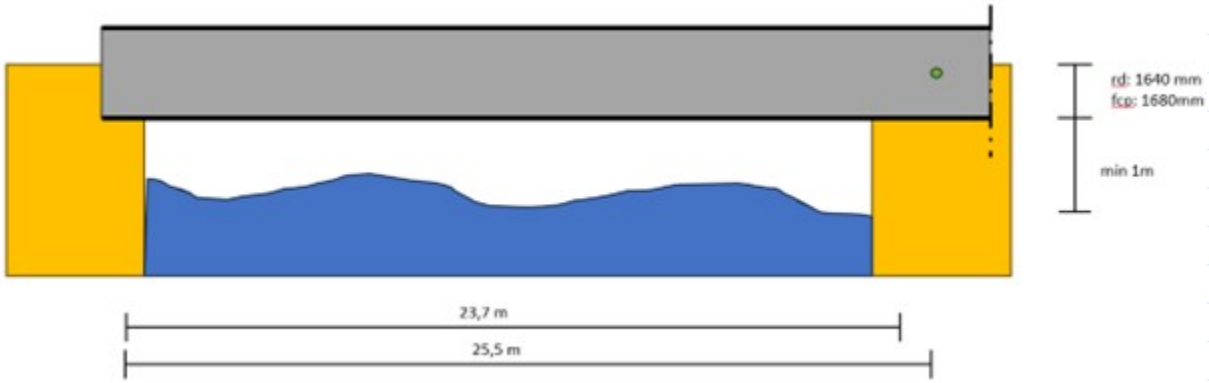

$l := 25250\ mm$

$b_{fcp} := 4.28\ m$ $b_{edge} := 5\ m$ $b_{rd} := 8\ m$ $b_{supp} := 9.45\ m$

$h_{rd} := 5.9\ m$ $h_{fcp} := 6.05\ m$ $h_{water} := 3.3\ m$ $h_{under\_side} := 4.3\ m$

$\theta_{max} := 80\ °$ $h_{top} := \sin\left(\theta_{max}\right) \cdot l + h_{rd} = 30.8\ m$

$Mass_{fcp} := 15.45\ tonne$

General properties

$T_{s\_sun} := 57\ °C$ $T_{s\_shade} := 31\ °C$

Partial safety factors

Properties balsa core

$\rho_{balsa} := 285\ \frac{kg}{m^3}$ $G_{balsa} := 145\ MPa$

$E_{balsa\_z} := 720\ MPa$ $E_{balsa\_x} := 2642\ MPa$

$f_{c\_xz\_v\_k} := 2.08\ MPa$ $f_{c\_z\_k} := 7.32\ MPa$

$$\eta_{rt\_balsa} := min\left(1 - \left(\frac{0.2\ \frac{kg}{m^3}}{\rho_{balsa}} + 0.004\right) \cdot \left(\frac{T_{s\_sun} - 20\ °C}{1\ °C}\right), 1\right) = 1$$

$\eta_{ct\_balsa} := \left(\left(\rho_{balsa}\right)\left(1\ °C\right)\right)$

$\eta_{cm\_balsa} := 1$ $\eta_{c\_balsa} := \eta_{ct\_balsa} \cdot \eta_{cm\_balsa} = 1$

$\gamma_{m\_balsa} := 1.51$ $\gamma_{rd\_balsa} := 1.5$

$f_{c\_xz\_d} := \frac{\eta_{c\_balsa} \cdot f_{c\_xz\_v\_k}}{\gamma_{m\_balsa} \cdot \gamma_{rd\_balsa}} = 0.92\ MPa$

$f_{c\_z\_d} := \frac{\eta_{c\_balsa} \cdot f_{c\_z\_k}}{\gamma_{m\_balsa} \cdot \gamma_{rd\_balsa}} = 3.23\ MPa$

Properties road deck laminate

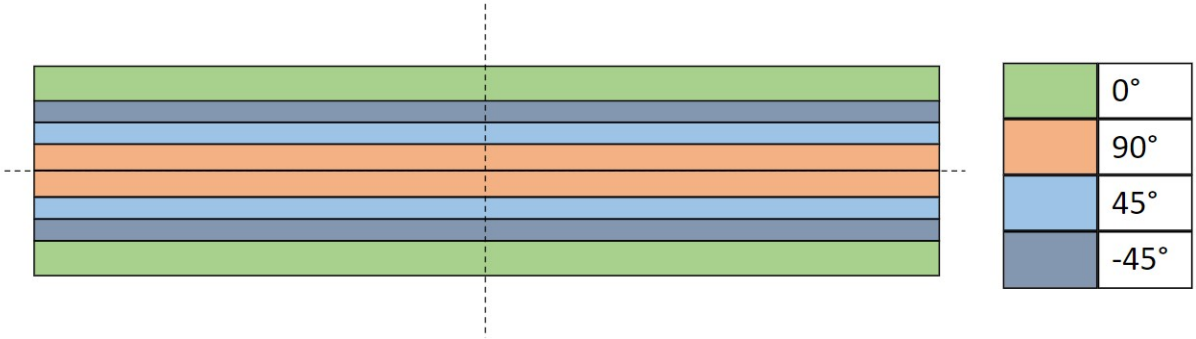

Laminate layup road deck

$\begin{bmatrix} 0 \\ 90 \\ 45 \\ -45 \end{bmatrix}$ $\begin{bmatrix} 50\% \\ 16.67\% \\ 16.67\% \\ 16.67\% \end{bmatrix}$

$\rho_{l\_rd} := 1900\ \frac{kg}{m^3}$ $E_{1\_l\_rd} := 26.2\ GPa$ $E_{2\_l\_rd} := 17.4\ GPa$

$f_{rd\_x\_k} := 366\ MPa$ $f_{rd\_y\_k} := 244\ MPa$ $f_{rd\_xy\_k} := 153\ MPa$

$T_{g\_rd} := 90\ °C$

$\eta_{ct\_f\_rd} := min\left(1 - 0.25 \cdot \frac{T_{s\_sun} - 20\ °C}{T_{g\_rd} - 20\ °C}, 1\right) = 0.9$

$\eta_{cm\_f\_rd} := 0.6$ $\eta_{c\_f\_rd} := \eta_{ct\_f\_rd} \cdot \eta_{cm\_f\_rd} = 0.521$

$$\eta_{ct\_m\_rd} := min\left(1 - 0.80 \cdot \frac{T_{s\_sun} - 20\ °C}{T_{g\_rd} - 20\ °C}, 1\right) = 0.6$$

$$\eta_{cm\_m\_rd} := 0.6 \qquad \eta_{c\_m\_rd} := \eta_{ct\_m\_rd} \cdot \eta_{cm\_m\_rd} = 0.346$$

$$\gamma_{m\_rd} := 1.07 \qquad \gamma_{rd\_rd} := 1.4$$

$$f_{rd\_x\_d} := \frac{\eta_{ct\_f\_rd} \cdot f_{rd\_x\_k}}{\gamma_{rd\_rd} \cdot \gamma_{m\_rd}} = 212\ \textbf{MPa}$$

$$f_{rd\_y\_d} := \frac{\eta_{ct\_f\_rd} \cdot f_{rd\_y\_k}}{\gamma_{rd\_rd} \cdot \gamma_{m\_rd}} = 141.4\ \textbf{MPa}$$

$$f_{rd\_xy\_d} := \frac{\eta_{ct\_f\_rd} \cdot f_{rd\_xy\_k}}{\gamma_{rd\_rd} \cdot \gamma_{m\_rd}} = 88.6\ \textbf{MPa}$$

Partial factors frp main beam

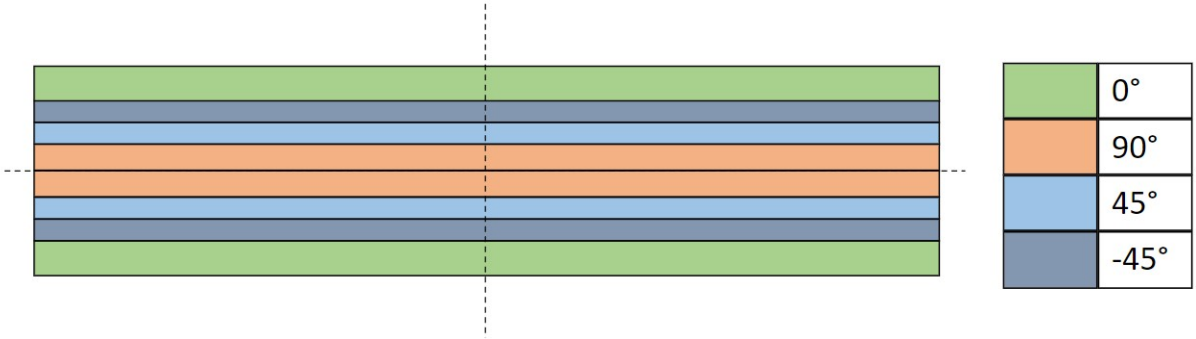

Laminate layup flange

$$\begin{bmatrix} 0 \\ 90 \\ 45 \\ -45 \end{bmatrix} \quad \begin{bmatrix} 62.5\% \\ 12.5\% \\ 12.5\% \\ 12.5\% \end{bmatrix}$$

Laminate layup web

$$\begin{bmatrix} 0 \\ 90 \\ 45 \end{bmatrix} \quad \begin{bmatrix} 25\% \\ 25\% \\ 25\% \end{bmatrix}$$

$\lfloor -45 \rfloor \quad \lfloor 25\% \rfloor$

$\rho_{l\_mb} := 1900 \ \frac{kg}{m^3} \qquad E_{f\_mb} := 29.4 \ GPa \qquad E_{w\_mb} := 19.9 \ GPa$

$f_{mb\_x\_k} := 412 \ MPa \qquad f_{mb\_xz\_k} := 180 \ MPa$

$T_{g\_mb} := 90 \ °C \qquad \phi_{50\_mb\_x\_t} := 0.14 \qquad \phi_{50\_mb\_x\_c} := 0.41$

$\eta_{ct\_f\_mb} := min\left(1 - 0.25 \cdot \frac{T_{s\_sun} - 20 \ °C}{T_{g\_mb} - 20 \ °C}, 1\right) = 0.9$

$\eta_{cm\_f\_mb} := 0.6 \qquad \eta_{c\_f\_mb} := \eta_{ct\_f\_mb} \cdot \eta_{cm\_f\_mb} = 0.521$

$\eta_{ct\_f\_stiff} := min\left(1 - 0.25 \cdot \frac{T_{s\_shade} - 20 \ °C}{T_{g\_mb} - 20 \ °C}, 1\right) = 0.961$

$\eta_{cm\_f\_stiff} := 0.6 \qquad \eta_{c\_f\_stiff} := \eta_{ct\_f\_stiff} \cdot \eta_{cm\_f\_stiff} = 0.576$

$\eta_{ct\_m\_mb} := min\left(1 - 0.80 \cdot \frac{T_{s\_sun} - 20 \ °C}{T_{g\_mb} - 20 \ °C}, 1\right) = 0.6$

$\eta_{cm\_m\_mb} := 0.6 \qquad \eta_{c\_m\_mb} := \eta_{ct\_m\_mb} \cdot \eta_{cm\_m\_mb} = 0.346$

$\gamma_{m\_mb} := 1.07 \qquad \gamma_{rd\_mb} := 1.5$

$f_{mb\_x\_50} := \frac{\eta_{c\_f\_mb} \cdot f_{mb\_x\_k}}{\gamma_{rd\_mb} \cdot \gamma_{m\_mb}} = 133.7 \ MPa$

$f_{mb\_xz\_50} := \frac{\eta_{c\_f\_mb} \cdot f_{mb\_xz\_k}}{\gamma_{rd\_mb} \cdot \gamma_{m\_mb}} = 58.4 \ MPa$

Traffic load calculations

Cross section properties

load properties

Distributed load BM1

$q_{bm1} := 9 \ \frac{kN}{m^2}$

Concentrated load BM1

$Q_{bm1} := 300 \ kN \quad l_{w\_bm1} := 40 \ cm \quad w_{w\_bm1} := 40 \ cm \quad w_{bm1} := 2 \ m \quad h.o.h_{bm1} := 1.2 \ m$

Distirbuted load foot and cycle path

$q_{fcp} := 5 \ \frac{kN}{m^2}$

Concentrated load accidental vehicle

$Q_{av1} := 80 \ kN \quad Q_{av2} := 40 \ kN$

Ship collision force

$F_{ship} := 0.811 \ MN \quad h_{ship} := 0.25 \ m \quad w_{ship} := 3 \ m$

Road deck properties

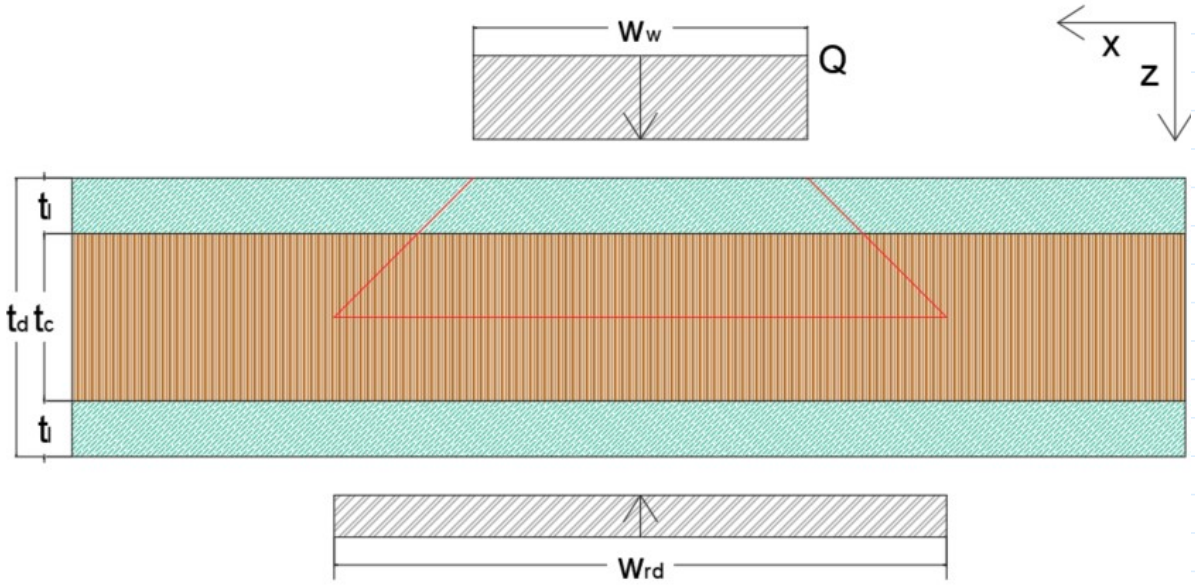

$w_{bm1\_mid} := 0.5 \ m$

$t_{l\_rd} := 30\ mm \qquad t_{c\_rd} := 700\ mm \qquad t_{d\_rd} := t_{c\_rd} + 2 \cdot t_{l\_rd} = 760\ mm$

$w_{rd} := l_{w\_bm1} + t_{d\_rd} = (1.16 \cdot 10^3)\ mm$

$A_{rd} := w_{rd} \cdot t_{c\_rd} = 0.812\ m^2$

$EI_{rd} := 2 \cdot E_{1\_l\_rd} \cdot w_{rd} \cdot t_{l\_rd} \cdot \left(\frac{t_{c\_rd} + t_{l\_rd}}{2} \right)^2 = 266811\ kN \cdot m^2$

$+ \frac{1}{12} \cdot E_{balsa\_z} \cdot w_{rd} \cdot t_{c\_rd}^{\ 3}$

Main beam properties

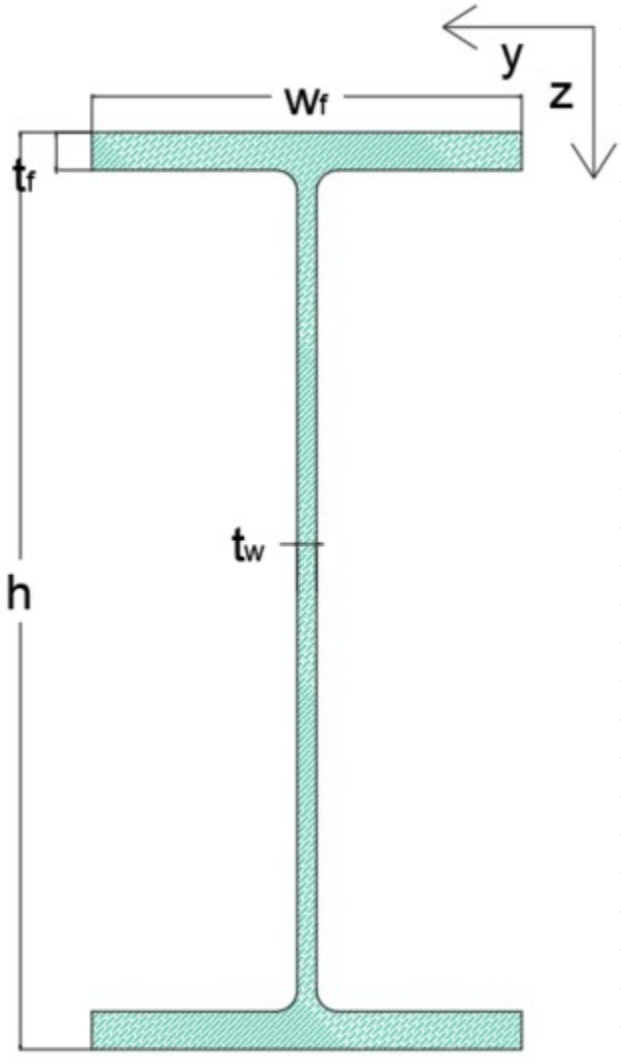

$h_{mb} := 3200\ mm \qquad w_{mb\_f} := 600\ mm \qquad t_{mb\_f} := 80\ mm \qquad t_{mb\_w} := 28\ mm$

$$A_{mb\_v} := t_{mb\_w} \cdot h_{mb} = 0.09\ m^2$$

$$A_{mb} := 2 \cdot t_{mb\_f} \cdot w_{mb\_f} + t_{mb\_w} \cdot \left(h_{mb} - 2 \cdot t_{mb\_f}\right) = 0.181\ m^2$$

$$EI_{mb} := E_{w\_mb} \cdot \frac{1}{12} \cdot t_{mb\_w} \cdot \left(h_{mb} - 2 \cdot t_{mb\_f}\right)^3 + 2 \cdot E_{f\_mb} \cdot w_{mb\_f} \cdot t_{mb\_f} \cdot \left(\frac{1}{2} \cdot h_{mb} - \frac{1}{2} \cdot t_{mb\_f}\right)^2 = \left(8.2 \cdot 10^6\right)\ kN \cdot m^2$$

Stiffness properties head board

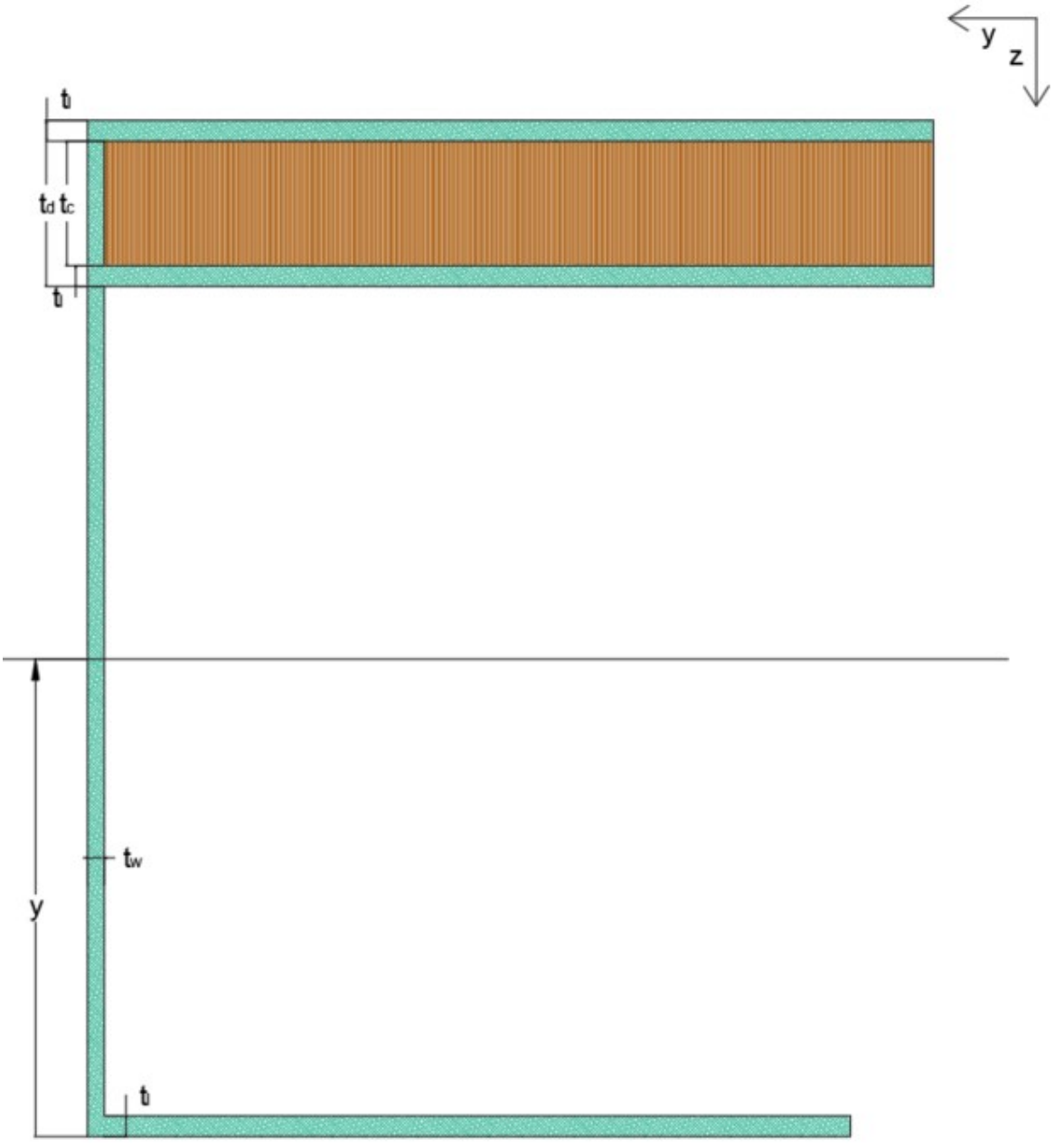

$$t_{l\_hb} := 34\ mm$$

$$y := \frac{\begin{aligned}&\frac{1}{2}\cdot\frac{b_{supp}}{10}\cdot t_{l\_hb}^{\ 2}\cdot E_{1\_l\_rd} + \frac{b_{supp}}{10}\cdot t_{c\_rd}\cdot\left(h_{rd} - h_{under\_side} - t_{l\_rd} - \frac{t_{c\_rd}}{2}\right)\cdot E_{balsa\_z} \\ &+\frac{b_{supp}}{10}\cdot t_{l\_rd}\cdot\left(h_{rd} - h_{under\_side} - \frac{t_{l\_rd}}{2}\right)\cdot E_{1\_l\_rd} \\ &+\frac{b_{supp}}{10}\cdot t_{l\_rd}\cdot\left(h_{rd} - h_{under\_side} - t_{c\_rd} - \frac{3\cdot t_{l\_rd}}{2}\right)\cdot E_{1\_l\_rd} \\ &+\frac{1}{12}\cdot t_{mb\_w}\cdot\left(h_{rd} - h_{under\_side}\right)\cdot E_{w\_mb}\cdot\frac{1}{2}\cdot\left(h_{rd} - h_{under\_side}\right)\end{aligned}}{3\cdot\frac{b_{supp}}{10}\cdot t_{l\_rd}\cdot E_{1\_l\_rd} + \frac{b_{supp}}{10}\cdot t_{c\_rd}\cdot E_{balsa\_z} + \left(h_{rd} - h_{under\_side}\right)\cdot t_{mb\_w}\cdot E_{w\_mb}} = 0.69\ m$$

$$z_{l\_rd\_top} := h_{rd} - h_{under\_side} - \frac{t_{l\_rd}}{2} - y = 0.899\ m$$

$$z_{c\_rd} := h_{rd} - h_{under\_side} - t_{l\_rd} - \frac{t_{c\_rd}}{2} - y = 0.534\ m$$

$$z_{l\_rd\_bot} := h_{rd} - h_{under\_side} - t_{c\_rd} - \frac{3\ t_{l\_rd}}{2} - y = 0.169\ m$$

$$z_{l\_beam\_bot} := -y + \frac{t_{l\_rd}}{2} = -0.671\ m$$

$$\begin{aligned}EI_{hb} := &\frac{b_{supp}}{10}\cdot t_{l\_rd}\cdot z_{l\_rd\_bot}^{\ 2}\cdot E_{1\_l\_rd} \\ &+\frac{b_{supp}}{10}\cdot t_{l\_rd}\cdot z_{l\_rd\_top}^{\ 2}\cdot E_{1\_l\_rd} \\ &+\frac{b_{supp}}{10}\cdot t_{l\_hb}\cdot z_{l\_beam\_bot}^{\ 2}\cdot E_{1\_l\_rd} \\ &+\frac{b_{supp}}{10}\cdot t_{c\_rd}\cdot z_{c\_rd}^{\ 2}\cdot E_{balsa\_z} \\ &+\frac{1}{12}\cdot t_{mb\_w}\cdot\left(h_{rd} - h_{under\_side}\right)^3\cdot E_{w\_mb}\end{aligned} = \left(1.326\cdot 10^6\right)\ kN\cdot m^2$$

Calculations for deflections

Deflections at the supports in the middle of the deck

$$w_{middle\_at\_supports} := \frac{1}{48}\cdot\frac{Q_{bm1}\cdot b_{supp}^{\ 3}}{EI_{hb}} + \frac{5}{384}\cdot\frac{q_{bm1}\cdot\frac{b_{supp}}{10}\cdot b_{supp}^{\ 4}}{EI_{hb}} = 4.64\ mm$$

Deflections at midspan in the middle of the deck

$$w_{middle\_midspan} := \frac{1}{48}\cdot\frac{4\cdot Q_{bm1}\cdot l^3}{2\cdot EI_{mb}} + \frac{5}{384}\cdot\frac{q_{bm1}\cdot b_{supp}\cdot l^4}{2\cdot EI_{mb}} = 52.2\ mm$$

Deflections limit

$$w_{limit\_midspan} := \frac{l}{250} = 101\ mm \qquad w_{limit\_threshold} := 5\ mm$$

Unity checks

$$u.c._{deflection\_threshold} := \frac{w_{middle\_at\_supports}}{w_{limit\_threshold}} = 0.93$$

$$u.c._{deflection\_midspan} := \frac{w_{middle\_midspan}}{w_{limit\_midspan}} = 0.52$$

Calculations for road deck

Load cases

Loadcase BM1 1

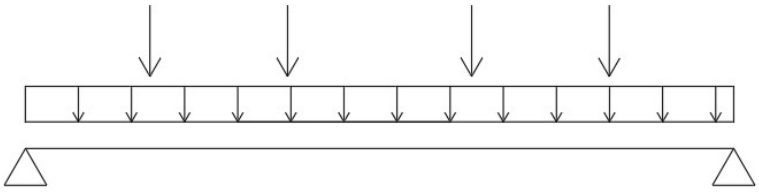

Loadcase BM1 2

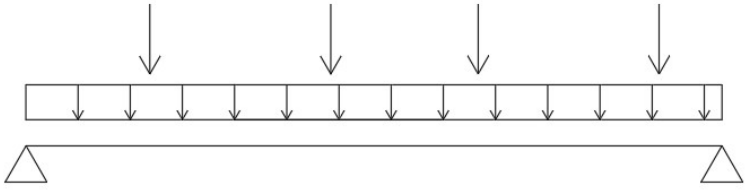

Loadcase G

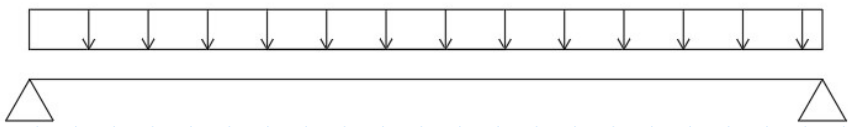

Shear force

Load case BM1 2 was used

$$V_{bm1} := \frac{1}{2} \cdot q_{bm1} \cdot b_{rd} \cdot w_{rd} + 1.2 \cdot Q_{bm1} = 401.76 \ \boldsymbol{kN}$$

Bending moments

Load case BM1 1 was used

$$M_{bm1} := \frac{1}{2} \cdot q_{bm1} \cdot w_{rd} \cdot b_{rd} \cdot \left(\frac{1}{2} \cdot b_{supp} - \frac{1}{4} \cdot b_{rd} \right) = 1081 \ \boldsymbol{kN \cdot m}$$
$$+ \frac{Q_{bm1}}{2} \cdot \left(b_{supp} - 2 \cdot w_{bm1\_mid} - w_{bm1} \right)$$

Self weight

$$G_{rd} := \left(2 \cdot t_{l\_rd} \cdot w_{rd} \cdot \rho_{l\_rd} + t_{c\_rd} \cdot w_{rd} \cdot \rho_{balsa} \right) \cdot 9.81 \ \frac{\boldsymbol{m}}{\boldsymbol{s}^2} = 3.568 \ \frac{\boldsymbol{kN}}{\boldsymbol{m}}$$

Forces as a result of self weight

Loadcase G was used

$$V_{G\_rd} := \frac{1}{2} \cdot G_{rd} \cdot b_{supp} = 16.9 \ \boldsymbol{kN}$$

$$M_{G\_rd} := \frac{1}{8} \cdot G_{rd} \cdot b_{supp}{}^2 = 39.8 \ \boldsymbol{kN \cdot m}$$

Combined forces with 6.10 B

$$V_{Ed\_rd} := 1.2 \cdot V_{G\_rd} + 1.5 \cdot V_{bm1} = 623 \ \boldsymbol{kN}$$

$$M_{Ed\_rd} := 1.2 \cdot M_{G\_rd} + 1.5 \cdot M_{bm1} = 1670 \ \boldsymbol{kN \cdot m}$$

$$V_{Ed\_rd\_s} := 1.5 \cdot \left(2 \cdot 0.6 \cdot Q_{bm1} + 0.1 \cdot q_{bm1} \cdot w_{w\_bm1} \cdot \frac{b_{rd}}{2} \right) = 542 \ \boldsymbol{kN}$$

Resultant stresses

$$\tau_{c\_rd} := \frac{V_{Ed\_rd}}{A_{rd}} = 0.8\ \textit{MPa}$$

$$\sigma_{l\_rd} := \frac{M_{Ed\_rd}}{EI_{rd}} \cdot \frac{t_{d\_rd}}{2} \cdot E_{1\_l\_rd} = 62\ \textit{MPa}$$

$$\tau_{l\_rd} := \frac{V_{Ed\_rd\_s}}{2 \cdot t_{l\_rd} \cdot w_{w\_bm1}} = 23\ \textit{MPa}$$

$$\sigma_{c\_fcp} := \frac{M_{Ed\_rd}}{EI_{rd}} \cdot \left(\frac{t_{d\_rd}}{2} - t_{l\_rd} \right) \cdot E_{balsa\_z} = 1.577\ \textit{MPa}$$

Unity checks

$$u.c._{\tau\_c\_rd} := \frac{\tau_{c\_rd}}{f_{c\_xz\_d}} = 0.836$$

$$u.c._{\sigma\_rd} := \frac{\sigma_{l\_rd}}{f_{rd\_x\_d}} = 0.294$$

$$u.c._{\tau\_l\_rd} := \frac{\tau_{l\_rd}}{f_{rd\_xy\_d}} = 0.255$$

$$u.c._{comb\_rd} := u.c._{\sigma\_rd} + u.c._{\tau\_l\_rd} = 0.5$$

$$u.c._{\sigma\_c\_rd} := \frac{\sigma_{c\_fcp}}{f_{c\_z\_d}} = 0.49$$

Calculations for mainbeam

Loads

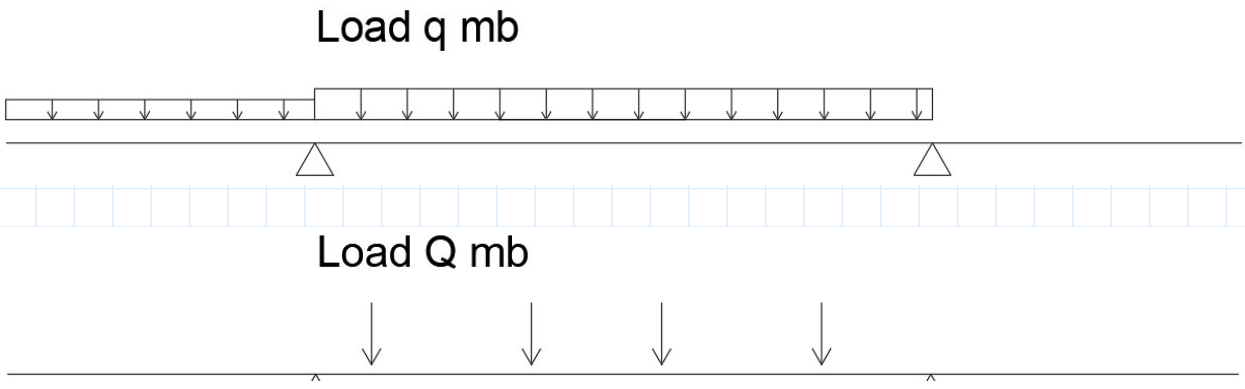

$$q_{mb} := \frac{b_{fcp} \cdot q_{fcp} \cdot \left(\frac{b_{fcp}}{2} + \left(b_{edge} - b_{fcp} \right) + b_{supp} \right) + b_{rd} \cdot q_{bm1} \cdot b_{supp}}{b_{supp}} = 99.877 \ \frac{kN}{m}$$

$$Q_{mb} := \frac{Q_{bm1} \cdot \left(\begin{array}{l} 2 \cdot b_{supp} - 2 \cdot \frac{\left(b_{supp} - b_{rd} \right)}{2} - 2 \cdot w_{bm1\_mid} - w_{bm1} \\ + 2 \cdot \frac{b_{supp}}{2} - 2 \cdot w_{bm1\_mid} - w_{bm1} \end{array} \right)}{b_{supp}} = 663.5 \ kN$$

Load cases

Loadcase V MB

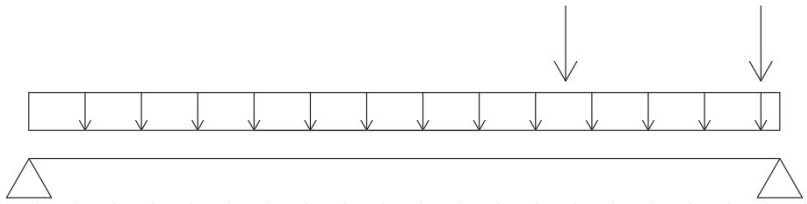

Loadcase M MB

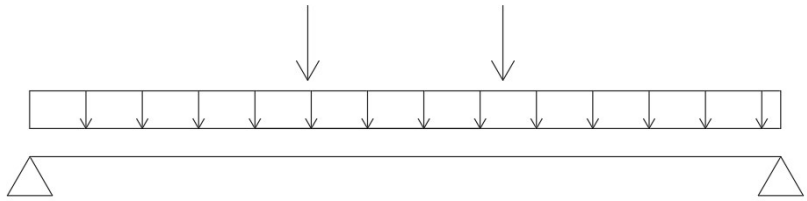

Loadcase G

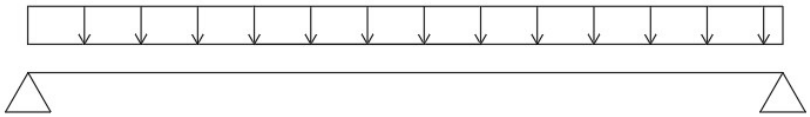

Shear force

Loadcases V MB was used

$$V_{bm1\_mb} := \frac{1}{2} \cdot q_{mb} \cdot l + Q_{mb} = \left(1.9 \cdot 10^{3} \right) \ kN$$

Bending moment

Loadcases M MB was used

$$M_{bm1\_mb} := \frac{1}{8} \cdot q_{mb} \cdot l^2 + \frac{1}{4} \cdot Q_{mb} \cdot l = \left(1.215 \cdot 10^4\right)\ \mathbf{kN \cdot m}$$

Self weight

$$Mass_{dist} := 2 \cdot \left(2 \cdot w_{mb\_f} \cdot t_{mb\_f} + \left(h_{mb} - 2 \cdot t_{mb\_f}\right) \cdot t_{mb\_w}\right) \cdot \rho_{l\_mb} \dots = 4875\ \frac{\mathbf{kg}}{\mathbf{m}}$$

$$\dots + t_{c\_rd} \cdot b_{supp} \cdot \rho_{balsa} + 2 \cdot t_{l\_rd} \cdot b_{supp} \cdot \rho_{l\_rd} + 2 \cdot \frac{Mass_{fcp}}{l}$$

$$G_{mb} := Mass_{dist} \cdot 9.81\ \frac{\mathbf{m}}{\mathbf{s}^2} = 47.82\ \frac{\mathbf{kN}}{\mathbf{m}}$$

Forces as a result of self weight

Loadcase G was used

$$V_{G\_mb} := \frac{1}{2} \cdot G_{mb} \cdot l = 604\ \mathbf{kN}$$

$$M_{G\_mb} := \frac{1}{8} \cdot G_{mb} \cdot l^2 = 3811\ \mathbf{kN \cdot m}$$

Combined forces with 6.10 B

$$V_{Ed\_mb} := 1.2 \cdot V_{G\_mb} + 1.5 \cdot V_{bm1\_mb} = \left(3.611 \cdot 10^3\right)\ \mathbf{kN}$$

$$M_{Ed\_mb} := 1.2 \cdot M_{G\_mb} + 1.5 \cdot M_{bm1\_mb} = \left(2.28 \cdot 10^4\right)\ \mathbf{kN \cdot m}$$

Resultant stresses

$$\tau_{Ed\_mb} := \frac{V_{Ed\_mb}}{A_{mb\_v}} = 40.3\ \mathbf{MPa}$$

$$\sigma_{Ed\_mb} := \frac{M_{Ed\_mb}}{EI_{mb}} \cdot E_{f\_mb} \cdot \frac{1}{2} \cdot h_{mb} = 131.2\ \mathbf{MPa}$$

Unity checks

$$u.c._{\tau\_mb} := \frac{\tau_{Ed\_mb}}{f_{mb\_xz\_50}} = 0.69$$

$$u.c._{\sigma\_mb} := \frac{\sigma_{Ed\_mb}}{\dots} = 0.982$$

$f_{mb\_x\_50}$

Auxiliary calculations

Calculations for ship impact forces

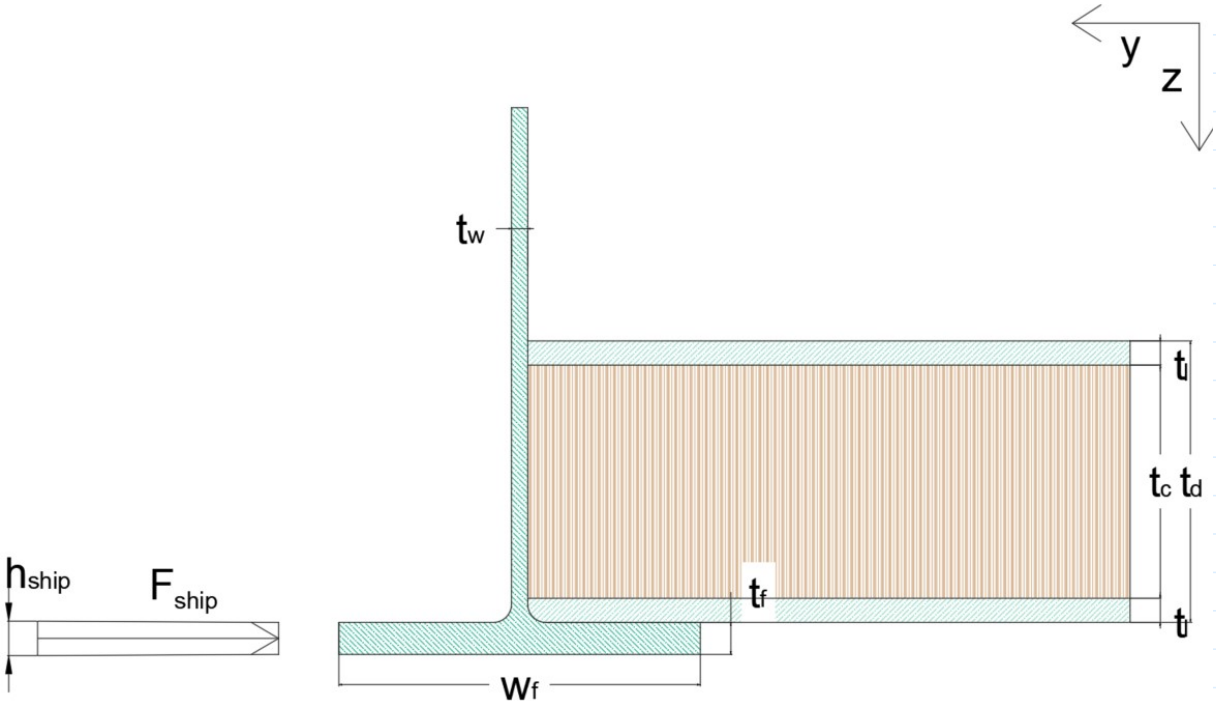

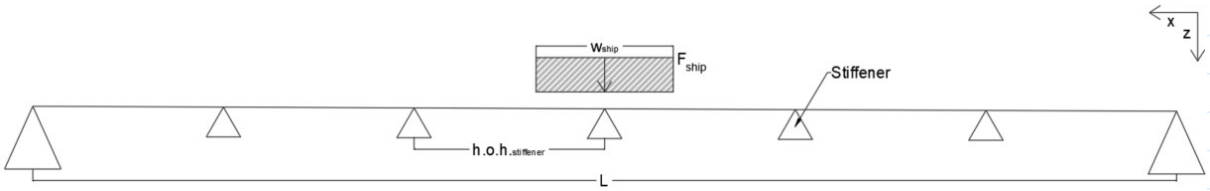

$t_{l\_stiff} := 16\ mm$ $t_{c\_stiff} := 250\ mm$ $l_{cr\_stiff} := b_{supp}$

$w_{stiff} := 0.625\ m$ $n_{stiff} := 18$ $h.o.h_{stiff} := \frac{l}{n_{stiff} - 1} = 1.485\ m$

$t_{d\_stiff} := t_{c\_stiff} + 2 \cdot t_{l\_stiff} = 282\ mm$

Activated stiffeners

$n_{stiff\_active} := \text{floor}\left(\frac{w_{ship}}{h.o.h_{stiff}}\right) = 2$

Normal force

$$N_{ship} := F_{ship}$$

Global bending moment

$$M_{ship\_glob} := \frac{1}{2} \cdot F_{ship} \cdot \left(\frac{1}{2} \cdot l - \frac{1}{4} \cdot w_{ship} \right) = 4.8 \ \boldsymbol{MN \cdot m}$$

Section properties

$$I_{sc} := 2 \cdot \frac{1}{12} \cdot t_{mb\_f} \cdot {w_{mb\_f}}^3 + 2 \cdot t_{mb\_f} \cdot w_{mb\_f} \cdot \left(\frac{b_{supp}}{2} \right)^2 = 2.146 \ \boldsymbol{m^4}$$

Critical buckling force

$$\gamma_{rd\_gb\_stiff} := 1.4$$

$$D_f := \frac{\eta_{c\_m\_mb} \cdot E_{f\_mb} \cdot {t_{l\_stiff}}^3}{12} = 3.475 \ \boldsymbol{kN \cdot m}$$

$$D_0 := \frac{\eta_{c\_m\_mb} \cdot E_{f\_mb} \cdot t_{l\_stiff} \cdot \left(t_{c\_stiff} + t_{l\_stiff} \right)^2}{2} = \left(5.763 \cdot 10^3 \right) \ \boldsymbol{kN \cdot m}$$

$$D_c := \frac{\eta_{c\_balsa} \cdot E_{balsa\_x} \cdot {t_{c\_stiff}}^3}{12} = \left(3.438 \cdot 10^3 \right) \ \boldsymbol{kN \cdot m}$$

$$D_{k\_stiff} := 2 \cdot D_f + D_0 + D_c = \left(9.208 \cdot 10^3 \right) \ \boldsymbol{kN \cdot m}$$

$$P_{cb\_d\_stiff} := \frac{1}{\gamma_{m\_rd} \cdot \gamma_{rd\_gb\_stiff}} \cdot \frac{\pi^2 \cdot D_{k\_stiff}}{{l_{cr\_stiff}}^2} = 679 \ \frac{\boldsymbol{kN}}{\boldsymbol{m}}$$

$$P_{cs\_d\_stiff} := \frac{\eta_{c\_f\_stiff}}{\gamma_{m\_mb} \cdot \gamma_{rd\_mb}} \cdot \frac{G_{balsa} \cdot \left(t_{c\_stiff} + t_{l\_stiff} \right)^2}{t_{c\_stiff}} = 14739 \ \frac{\boldsymbol{kN}}{\boldsymbol{m}}$$

$$P_{c\_d\_stiff} := \frac{P_{cb\_d\_stiff} \cdot P_{cs\_d\_stiff}}{P_{cb\_d\_stiff} + P_{cs\_d\_stiff}} = 0.649 \ \frac{\boldsymbol{MN}}{\boldsymbol{m}}$$

Resultant stresses

$$\sigma_{sc\_glob} := \frac{M_{ship\_glob}}{I_{sc}} \cdot \frac{b_{supp} + w_{mb\_f}}{2} = 11.3 \ \boldsymbol{MPa}$$

Unity checks

$$u.c._{s\_sc\_stiff} := \frac{N_{ship}}{n_{stiff\_active} \cdot w_{stiff} \cdot P_{c\_d\_stiff}} = 1$$

$$u.c._{s\_sc\_glob} := \frac{\sigma_{sc\_glob}}{f_{mb\_x\_50}} = 0.084$$

Calculations for opened structure

Wind loads

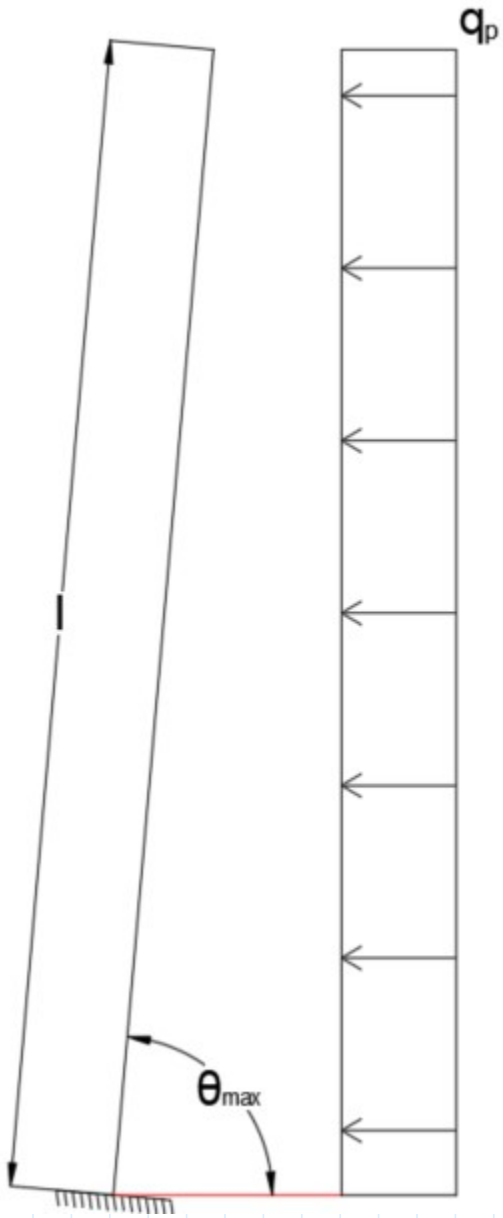

$z_e := h_{under\_side} + \sin(\theta_{max}) \cdot l = 29.2\ m$ $q_{p\_0} := 1.94\ \frac{kN}{m^2}$ $slenderness := \frac{b_{supp} + 2 \cdot b_{edge}}{h_{mb}} = 6$

$\rho := 1.25\ \frac{kg}{m^3}$ $v_b := 29.5\ \frac{m}{s}$

$c_{fx\_0} := \begin{cases} \text{if } slenderness \le 4 \\ \quad 2.4 - 0.275 \cdot slenderness \\ \text{else} \\ \quad 1.3 \end{cases} = 1.3$ $c_e := \frac{q_{p\_0}}{\frac{1}{2} \cdot \rho \cdot v_b^2} = 3.6$ $C_t := c_{fx\_0} \cdot c_e = 4.6$

$q_p := \frac{1}{2} \cdot \rho \cdot v_b^2 \cdot C_t = 2.5\ \frac{kN}{m^2}$

$t_{open} := 15$ $\psi_t := 1 + \frac{\ln\left(\frac{t_{open}}{50}\right)}{9} = 0.9$

Principle resultant forces

$N_{mb\_G\_open} := \frac{G_{mb} \cdot l}{2 \cdot \sin(\theta_{max})} = 613\ kN$

$M_{mb\_G\_open} := \frac{1}{2} \cdot G_{mb} \cdot \cos(\theta_{max}) \cdot l^2 = (2.647 \cdot 10^3)\ kN \cdot m$

$N_{mb\_wind} := \frac{\frac{1}{2} \cdot q_p \cdot h_{mb} \cdot (\sin(\theta_{max}) \cdot l)^2}{b_{supp}} = 264.033\ kN$

$M_{mb\_wind\_y} := \frac{1}{2} \cdot \frac{1}{2} \cdot q_p \cdot (2 \cdot b_{edge} + b_{supp}) \cdot (\sin(\theta_{max}) \cdot l)^2 = (7.583 \cdot 10^3)\ kN \cdot m$

Resultant stresses

$\sigma_{mb\_G\_open} := \frac{M_{mb\_G\_open}}{EI_{mb}} \cdot E_{f\_mb} \cdot \frac{1}{2} \cdot h_{mb} + \frac{N_{mb\_G\_open}}{A_{mb}} = 18.6\ MPa$

$\sigma_{mb\_wind\_1} := \frac{M_{mb\_wind\_y}}{EI_{mb}} \cdot E_{f\_mb} \cdot \frac{1}{2} \cdot h_{mb} + 0.4 \cdot \frac{N_{mb\_wind}}{A_{mb}} = 44.2\ MPa$

$\sigma_{mb\_wind\_2} := 0.4 \cdot \frac{M_{mb\_wind\_y}}{EI_{mb}} \cdot E_{f\_mb} \cdot \frac{1}{2} \cdot h_{mb} + \frac{N_{mb\_wind}}{A_{mb}} = 18.9\ MPa$

$\sigma_{mb\_wind} := \max(\sigma_{mb\_wind\_1}, \sigma_{mb\_wind\_2}) = 44.2\ MPa$

σ_{mb_wind} $\left(\sigma_{mb\_wind\_1}\ \sigma_{mb\_wind\_2}\right)$

Unity checks

$$u.c._{\sigma\_open} := \frac{1.2 \cdot \sigma_{mb\_G\_open} + 1.8 \cdot \psi_t \cdot \sigma_{mb\_wind}}{f_{mb\_x\_50}} = 0.68$$

Results

Unity checks

Unity checks traffic loads

deflection

$u.c._{deflection\_midspan} = 0.52$ $u.c._{deflection\_threshold} = 0.93$

Road deck

$u.c._{\tau\_c\_rd} = 0.84$ $u.c._{\sigma\_c\_rd} = 0.49$ $u.c._{comb\_rd} = 0.55$

Main beam

$u.c._{\tau\_mb} = 0.69$ $u.c._{\sigma\_mb} = 0.98$

Unity checks ship colision

Main beam

$u.c._{s\_sc\_glob} = 0.084$

Stiffener

$u.c._{s\_sc\_stiff} = 0.999$

Unity checks opened position

$u.c._{\sigma\_open} = 0.68$

MKI

€ := 1 ¤

$$Mass_{E\_glass} := 2 \cdot t_{l\_rd} \cdot b_{supp} \cdot l \cdot \rho_{l\_rd} + 2 \cdot \left(2 \cdot w_{mb\_f} \cdot t_{mb\_f} + t_{mb\_w} \cdot \left(h_{mb} - 2 \cdot t_{mb\_f}\right)\right) \cdot l \cdot \rho_{l\_mb} = 44.6\ tonne$$

$$Mass_{Balsa} := \left(t_{c\_rd} \cdot b_{supp}\right) \cdot l \cdot \rho_{balsa} = 47.6\ tonne$$

$$A_{E\_glass} := 2 \cdot \left(b_{supp} + t_{d\_rd}\right) \cdot l + 2 \cdot \left(2 \cdot h_{mb} + 2 \cdot w_{mb\_f} + 2\ \left(w_{mb\_f} - t_{mb\_w}\right)\right) \cdot l = 957.177\ m^2$$

$MKI_{E\_glass} := 0.265 \ \frac{€}{kg}$ $MKI_{score\_E\_glass} := MKI_{E\_glass} \cdot Mass_{E\_glass} = 11813.8 \ €$

$MKI_{Balsa} := -0.129 \ \frac{€}{kg}$ $MKI_{score\_Balsa} := MKI_{Balsa} \cdot Mass_{Balsa} = -6140.8 \ €$

$MKI_{E\_glass\_cons} := 1.173 \ \frac{€}{m^2}$ $MKI_{score\_E\_glass\_cons} := MKI_{E\_glass\_cons} \cdot A_{E\_glass} = 1122.8 \ €$

$MKI_{score\_Total} := MKI_{score\_E\_glass} + MKI_{score\_Balsa} + MKI_{score\_E\_glass\_cons} = 6796 \ €$

Mass

$Mass_{total} := Mass_{E\_glass} + Mass_{Balsa} = 92 \ tonne$

Appendix IX Structural checks full FRP main structure.

Table of Contents

General

General dimensions

Bac

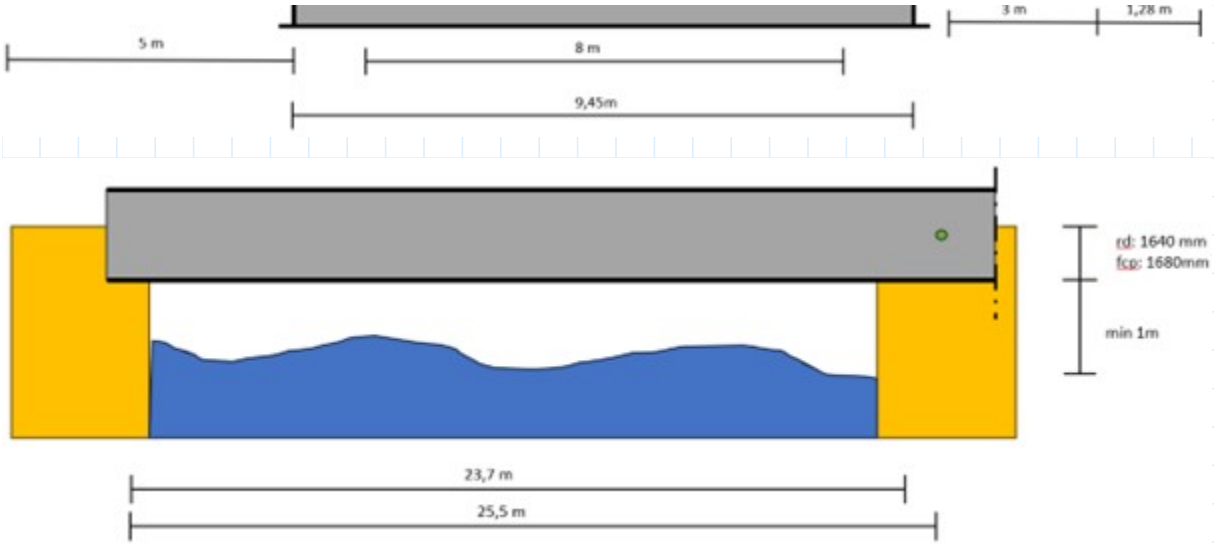

$l := 25250\ mm$

$b_{fcp} := 4.28\ m$ $b_{edge} := 5\ m$ $b_{rd} := 8\ m$ $b_{supp} := 9.45\ m$

$h_{rd} := 5.9\ m$ $h_{fcp} := 6.05\ m$ $h_{water} := 3.3\ m$ $h_{under\_side} := 4.3\ m$

$\theta_{max} := 80\ °$ $h_{top} := \sin\left(\theta_{max}\right) \cdot l + h_{rd} = 30.8\ m$

$n_{main\_webs} := 6$ $h.o.h._{main\_webs} := \frac{b_{supp}}{n_{main\_webs} - 1} = 1.89\ m$

$mass_{fcp} := 15.45\ tonne$

General properties

Bac

$T_{s\_sun} := 57\ °C$ $T_{s\_shade} := 31\ °C$

Desing material properties

Properties balsa core

Bac

$\rho_{balsa} := 285\ \frac{kg}{m^3}$ $G_{balsa} := 145\ MPa$

$E_{balsa\_z} := 720\ MPa$ $E_{balsa\_x} := 2642\ MPa$

$f_{c\_xz\_v\_k} := 2.08\ MPa$ $f_{c\_z\_k} := 7.32\ MPa$

$\left(\left(0.2\ \frac{kg}{} \right) \right.$ $\left. \right)$

$$\eta_{ct\_balsa} := min\left(1 - \left(\frac{m^3}{\rho_{balsa}} + 0.004\right) \cdot \left(\frac{T_{s\_sun} - 20\ °C}{1\ °C}\right), 1\right) = 1$$

$\eta_{cm\_balsa} := 1$ $\eta_{c\_balsa} := \eta_{ct\_balsa} \cdot \eta_{cm\_balsa} = 1$

$\gamma_{m\_balsa} := 1.51$ $\gamma_{rd\_balsa} := 1.5$

$$f_{c\_xz\_d} := \frac{\eta_{c\_balsa} \cdot f_{c\_xz\_v\_k}}{\gamma_{m\_balsa} \cdot \gamma_{rd\_balsa}} = 0.92\ MPa$$

$$f_{c\_z\_d} := \frac{\eta_{c\_balsa} \cdot f_{c\_z\_k}}{\gamma_{m\_balsa} \cdot \gamma_{rd\_balsa}} = 3.23\ MPa$$

Properties road deck laminate

Bac

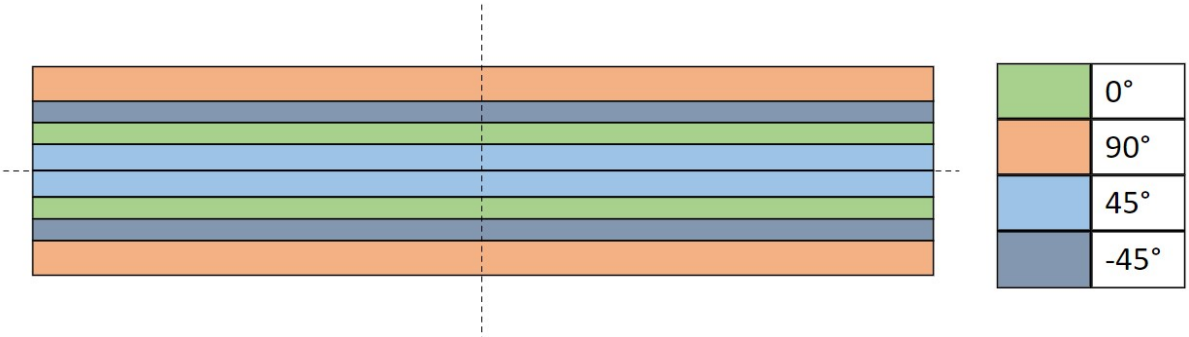

Laminate layup road deck

$$\begin{bmatrix} 90 \\ 0 \\ 45 \\ -45 \end{bmatrix} \quad \begin{bmatrix} 16.67\% \\ 50\% \\ 16.67\% \\ 16.67\% \end{bmatrix}$$

$\rho_{l\_rd} := 1900\ \frac{kg}{m^3}$ $E_{1\_l\_rd} := 17.5\ GPa$ $E_{2\_l\_rd} := 26.2\ GPa$

$f_{rd\_x\_k} := 245\ MPa$ $f_{rd\_y\_k} := 367\ MPa$ $f_{rd\_xy\_k} := 150\ MPa$

$T_{g\_rd} := 90\ °C$

$$\eta_{ct\_f\_rd} := min\left(1 - 0.25 \cdot \frac{T_{s\_sun} - 20\ °C}{T_{g\_rd} - 20\ °C}, 1\right) = 0.9$$

$\eta_{cm\_f\_rd} := 0.8$ $\eta_{c\_f\_rd} := \eta_{ct\_f\_rd} \cdot \eta_{cm\_f\_rd} = 0.694$

$$\eta_{ct\_m\_rd} := min\left(1 - 0.80 \cdot \frac{T_{s\_sun} - 20\ °C}{T_{g\_rd} - 20\ °C}, 1\right) = 0.6$$

$$\eta_{cm\_m\_rd} := 0.8 \qquad \eta_{c\_m\_rd} := \eta_{ct\_m\_rd} \cdot \eta_{cm\_m\_rd} = 0.462$$

$$\gamma_{m\_rd} := 1.07 \qquad \gamma_{rd\_rd} := 1.4$$

$$f_{rd\_x\_d} := \frac{\eta_{c\_f\_rd} \cdot f_{rd\_x\_k}}{\gamma_{rd\_rd} \cdot \gamma_{m\_rd}} = 113.6\ MPa$$

$$f_{rd\_y\_d} := \frac{\eta_{c\_f\_rd} \cdot f_{rd\_y\_k}}{\gamma_{rd\_rd} \cdot \gamma_{m\_rd}} = 170.1\ MPa$$

$$f_{rd\_xy\_d} := \frac{\eta_{c\_f\_rd} \cdot f_{rd\_xy\_k}}{\gamma_{rd\_rd} \cdot \gamma_{m\_rd}} = 69.5\ MPa$$

Properties frp main beam laminate

Bac

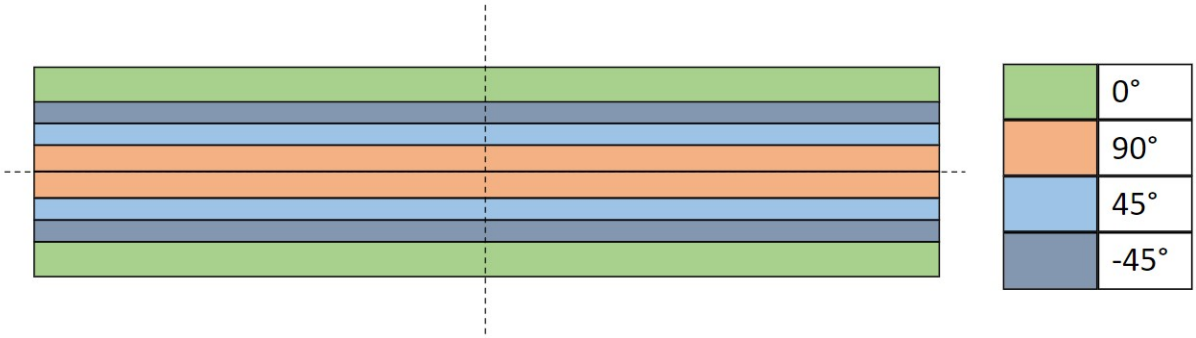

Laminate layup flange

$$\begin{bmatrix} 0 \\ 90 \\ 45 \\ -45 \end{bmatrix} \quad \begin{bmatrix} 50\% \\ 16.67\% \\ 16.67\% \\ 16.67\% \end{bmatrix}$$

Laminate layup web

$$\begin{bmatrix} 0 \\ 90 \\ 45 \\ -45 \end{bmatrix} \quad \begin{bmatrix} 25\% \\ 25\% \\ 25\% \\ 25\% \end{bmatrix}$$

$\rho_{l\_mb} := 1900 \ \frac{kg}{m^3}$ $E_{f\_mb} := 26.2 \ GPa$ $E_{w\_mb} := 19.9 \ GPa$

$f_{mb\_x\_k} := 367 \ MPa$ $f_{mb\_y\_k} := 246 \ MPa$ $f_{mb\_xz\_k} := 180 \ MPa$

$f_{w\_y\_k} := 278 \ MPa$

$T_{g\_mb} := 90 \ °C$

$\eta_{ct\_f\_mb} := min\left(1 - 0.25 \cdot \frac{T_{s\_shade} - 20 \ °C}{T_{g\_mb} - 20 \ °C}, 1\right) = 1$

$\eta_{cm\_f\_mb} := 0.8$ $\eta_{c\_f\_mb} := \eta_{ct\_f\_mb} \cdot \eta_{cm\_f\_mb} = 0.769$

$\eta_{ct\_m\_mb} := min\left(1 - 0.80 \cdot \frac{T_{s\_shade} - 20 \ °C}{T_{g\_mb} - 20 \ °C}, 1\right) = 0.9$

$\eta_{cm\_m\_mb} := 0.8$ $\eta_{c\_m\_mb} := \eta_{ct\_m\_mb} \cdot \eta_{cm\_m\_mb} = 0.699$

$\gamma_{m\_mb} := 1.07$ $\gamma_{rd\_mb} := 1.5$

$f_{mb\_x\_d} := \frac{\eta_{c\_f\_mb} \cdot f_{mb\_x\_k}}{\gamma_{rd\_mb} \cdot \gamma_{m\_mb}} = 175.7 \ MPa$

$f_{mb\_y\_d} := \frac{\eta_{c\_f\_mb} \cdot f_{mb\_y\_k}}{\gamma_{rd\_mb} \cdot \gamma_{m\_mb}} = 117.8 \ MPa$

$f_{mb\_xz\_d} := \frac{\eta_{c\_f\_mb} \cdot f_{mb\_xz\_k}}{\gamma_{rd\_mb} \cdot \gamma_{m\_mb}} = 86.2 \ MPa$

$f_{mb\_w\_y\_d} := \frac{\eta_{c\_f\_mb} \cdot f_{w\_y\_k}}{\gamma_{rd\_mb} \cdot \gamma_{m\_mb}} = 133.1 \ MPa$

Properties frp connection arm laminate

$\rho_{l\_ca} := 1900 \ \frac{kg}{m^3}$ $E_{f\_ca} := 28.0 \ GPa$ $E_{w\_ca} := 19.9 \ GPa$

$f_{ca\_x\_k} := 392 \ MPa$ $f_{c\_xz\_k} := 180 \ MPa$

$T_{g\_ca} := 90 \ °C$

$$\eta_{ct\_f\_ca} := min\left(1 - 0.25 \cdot \frac{T_{s\_shade} - 20\ °C}{T_{g\_ca} - 20\ °C}, 1\right) = 1$$

$\eta_{cm\_f\_ca} := 0.8$ $\eta_{c\_f\_ca} := \eta_{ct\_f\_ca} \cdot \eta_{cm\_f\_ca} = 0.769$

$$\eta_{ct\_m\_ca} := min\left(1 - 0.80 \cdot \frac{T_{s\_shade} - 20\ °C}{T_{g\_ca} - 20\ °C}, 1\right) = 0.9$$

$\eta_{cm\_m\_ca} := 0.8$ $\eta_{c\_m\_ca} := \eta_{ct\_m\_ca} \cdot \eta_{cm\_m\_ca} = 0.699$

$\gamma_{m\_ca} := 1.07$ $\gamma_{rd\_ca} := 1.5$

$$f_{ca\_x\_d} := \frac{\eta_{c\_f\_ca} \cdot f_{ca\_x\_k}}{\gamma_{rd\_ca} \cdot \gamma_{m\_ca}} = 187.7\ MPa$$

$$f_{ca\_w\_y\_d} := \frac{\eta_{c\_f\_ca} \cdot f_{w\_y\_k}}{\gamma_{rd\_ca} \cdot \gamma_{m\_ca}} = 133.1\ MPa$$

Traffic load calculations

Cross section properties

load properties

Distributed load BM1

$$q_{bm1} := 9\ \frac{kN}{m^2}$$

Concentrated load BM1

$Q_{bm1} := 300\ kN$ $l_{w\_bm1} := 40\ cm$ $w_{w\_bm1} := 40\ cm$ $w_{bm1} := 2\ m$ $h.o.h_{bm1} := 1.2\ m$

Distirbuted load foot and cycle path

$$q_{fcp} := 5\ \frac{kN}{m^2}$$

Concentrated load accidental vehicle

$Q_{av1} := 80\ kN$ $Q_{av2} := 40\ kN$

Ship collision force

$F_{ship} := 0.811\ MN$ $h_{ship} := 0.25\ m$ $w_{ship} := 3\ m$

Road deck properties

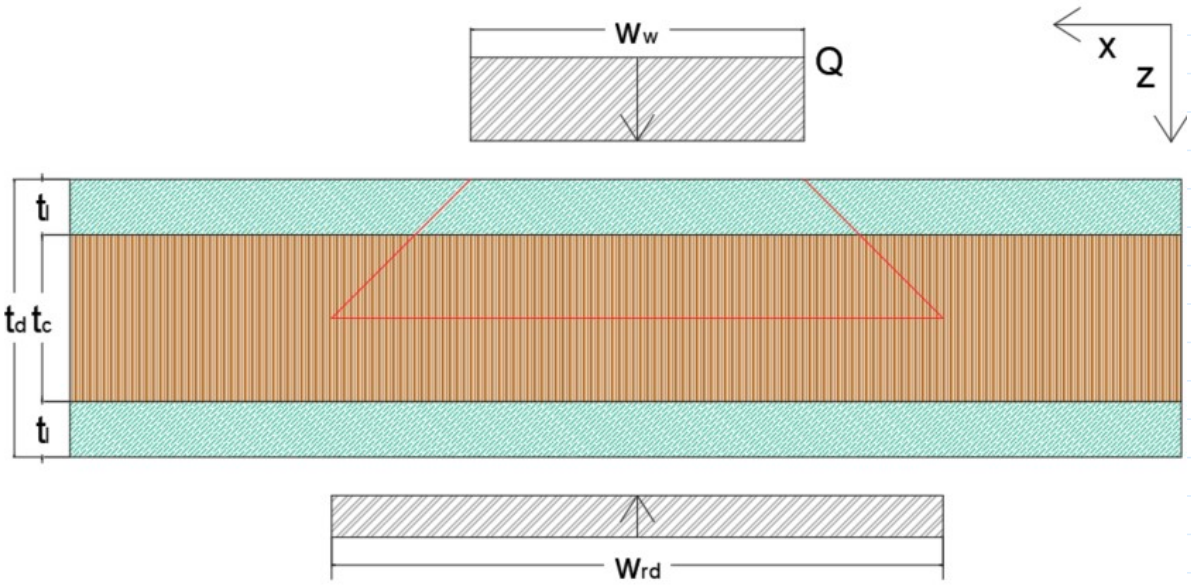

$w_{bm1\_mid} := 0.5\ m$

$t_{l\_rd} := 16\ mm$ $t_{c\_rd} := 500\ mm$ $t_{d\_rd} := t_{c\_rd} + 2 \cdot t_{l\_rd} = 532\ mm$

$w_{rd} := l_{w\_bm1} + t_{d\_rd} = 932\ mm$

$A_{rd} := w_{rd} \cdot t_{c\_rd} = 0.466\ m^2$

$$EI_{rd} := 2 \cdot E_{1\_l\_rd} \cdot w_{rd} \cdot t_{l\_rd} \cdot \left(\frac{t_{c\_rd} + t_{l\_rd}}{2} \right)^2 = 60390\ kN \cdot m^2$$
$$+ \frac{1}{12} \cdot E_{balsa\_x} \cdot w_{rd} \cdot t_{c\_rd}^{\ 3}$$

Main beam properties

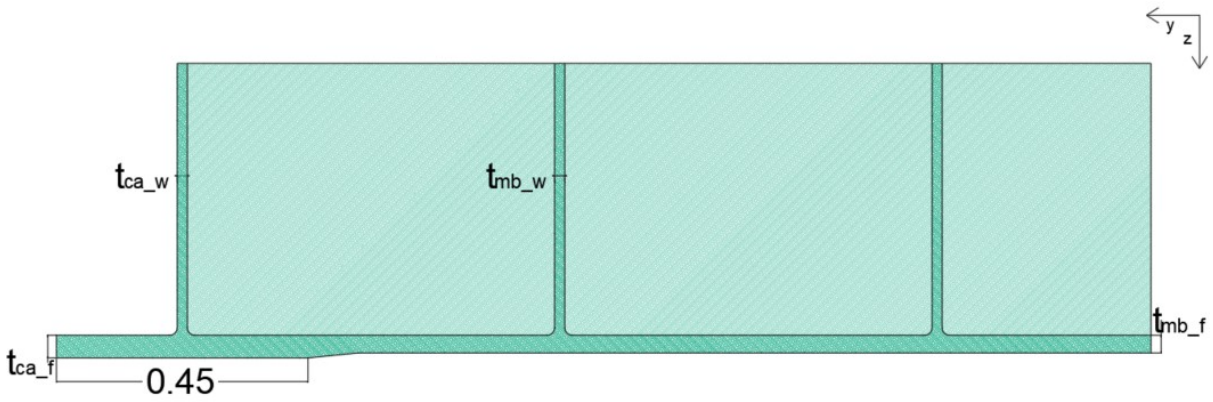

$t_{mb\_f} := 24\ mm$ $t_{mb\_w} := 16\ mm$

$t_{ca\_f} := 48\ mm$ $t_{ca\_w} := 16\ mm$

$h_{mb} := h_{rd} - h_{under\_side} - t_{d\_rd} = 1.068\ m$

$h_{ca} := h_{rd} - h_{under\_side} = 1.6\ m$

Main beam fictional beams properties

Stiffness properties head board

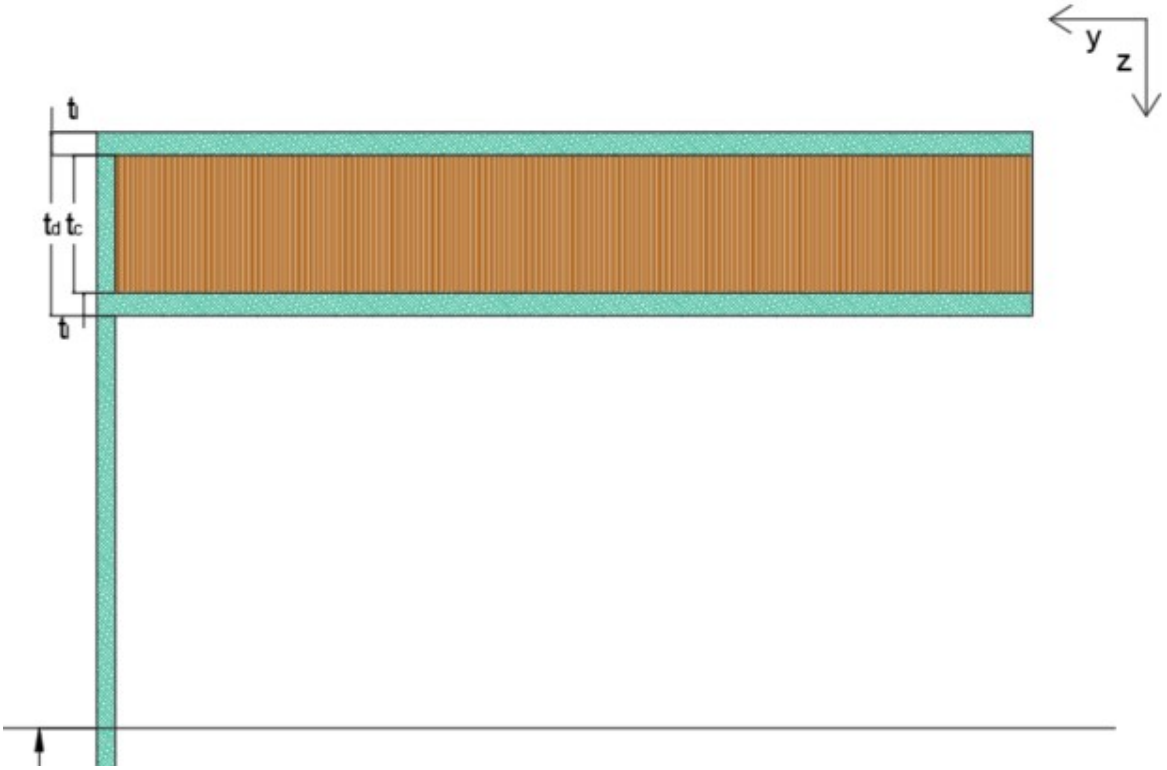

$$t_{l\_hb} := t_{mb\_w} = 16\ mm$$

$$y_{hb} := \frac{\begin{aligned}&\frac{1}{2}\cdot\frac{b_{supp}}{10}\cdot {t_{l\_hb}}^2\cdot E_{f\_mb} \\ &+\frac{b_{supp}}{10}\cdot\frac{1}{2}\cdot {t_{mb\_f}}^2\cdot E_{w\_mb} \\ &+\frac{b_{supp}}{10}\cdot t_{c\_rd}\cdot\left(h_{mb}+t_{l\_rd}+\frac{1}{2}\cdot t_{c\_rd}\right)\cdot E_{balsa\_z} \\ &+\frac{b_{supp}}{10}\cdot t_{l\_rd}\cdot\left(2\cdot h_{mb}+2\cdot t_{l\_rd}+t_{c\_rd}\right)\cdot E_{2\_l\_rd}\end{aligned}}{\begin{aligned}&\frac{b_{supp}}{10}\cdot t_{mb\_f}\cdot E_{f\_mb}+t_{mb\_w}\cdot\left(h_{mb}-t_{mb\_f}\right)\cdot E_{w\_mb} \\ &+\frac{b_{supp}}{10}\cdot t_{c\_rd}\cdot E_{balsa\_z}+\frac{b_{supp}}{10}\cdot 2\cdot t_{l\_rd}\cdot E_{2\_l\_rd}\end{aligned}} = 0.738\ m$$

$$z_{hb\_mb\_f} := \left(y_{hb}-\frac{1}{2}\cdot t_{mb\_f}\right) = 0.726\ m$$

$$z_{hb\_c\_rd} := h_{mb}-y_{hb}+t_{l\_rd}+\frac{1}{2}\cdot t_{c\_rd} = 0.596\ m$$

$$z_{hb\_l\_rd\_bot} := h_{mb}-y_{hb}+\frac{1}{2}\cdot t_{l\_rd} = 0.338\ m$$

$$z_{hb\_l\_rd\_top} := h_{mb}-y_{hb}+\frac{3}{2}\cdot t_{l\_rd}+t_{c\_rd} = 0.854\ m$$

$$EI_{hb} := \begin{aligned}&E_{w\_mb}\cdot\frac{1}{12}\cdot t_{mb\_w}\cdot\left(h_{mb}-2\cdot t_{mb\_f}\right)^3 \\ &+E_{f\_mb}\cdot\frac{b_{supp}}{10}\cdot 2\cdot t_{mb\_f}\cdot {z_{hb\_mb\_f}}^2 \\ &+E_{balsa\_z}\cdot t_{c\_rd}\cdot\frac{b_{supp}}{10}\cdot {z_{hb\_c\_rd}}^2\end{aligned} = \left(1.444\cdot 10^6\right)\ kN\cdot m^2$$

$$+E_{2\_l\_rd}\cdot\frac{b_{supp}}{10}\cdot 2\cdot t_{l\_rd}\cdot\left(z_{hb\_l\_rd\_bot}{}^{2}+z_{hb\_l\_rd\_top}{}^{2}\right)$$

$$k_{hb}:=\frac{48\cdot EI_{hb}}{l^{3}}=4305\ \frac{kN}{m}$$

Stiffness properties inside fictional beam

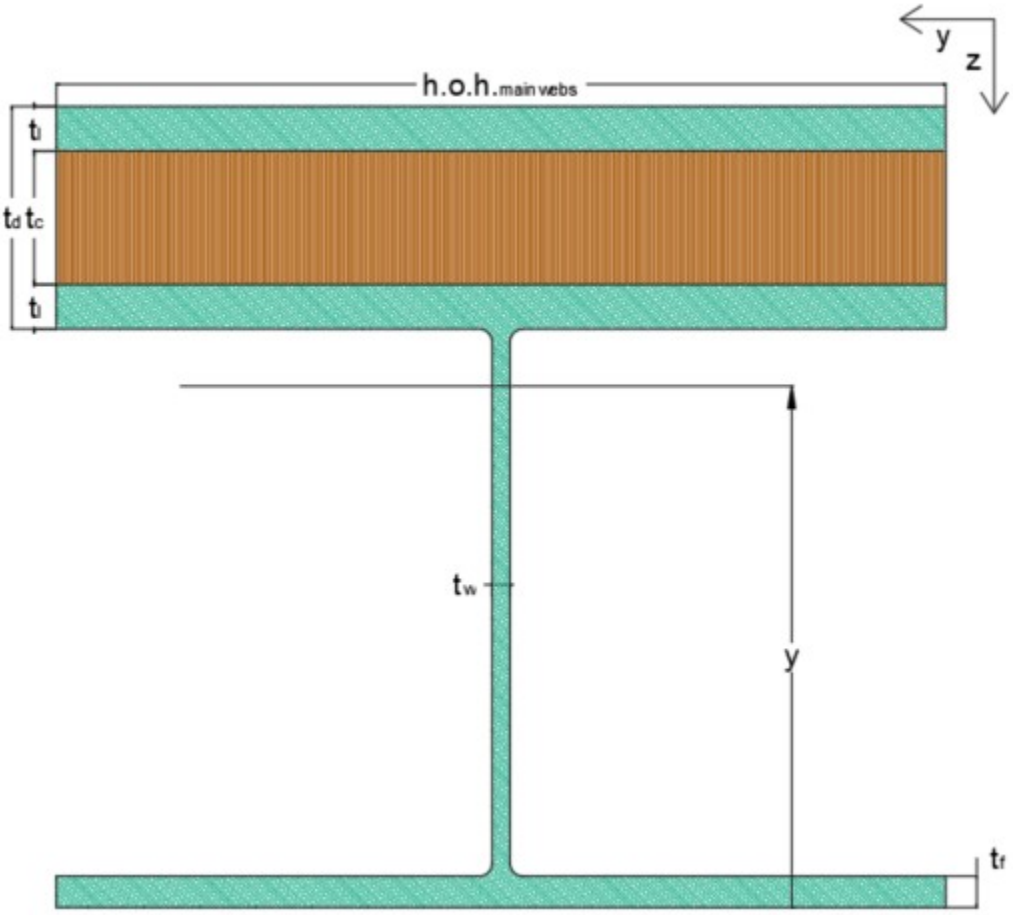

$$y_2:=\frac{\begin{array}{l}\frac{1}{2}\cdot h.o.h._{main\_webs}\cdot t_{mb\_f}{}^{2}\cdot E_{f\_mb}\\ +t_{mb\_w}\cdot\left(h_{mb}-t_{mb\_f}\right)\cdot\frac{1}{2}\cdot\left(h_{mb}+t_{mb\_f}\right)\cdot E_{w\_mb}\\ +h.o.h._{main\_webs}\cdot t_{c\_rd}\cdot\left(h_{mb}+t_{l\_rd}+\frac{1}{2}\cdot t_{c\_rd}\right)\cdot E_{balsa\_z}\\ +h.o.h._{main\_webs}\cdot t_{l\_rd}\cdot\left(2\cdot h_{mb}+2\cdot t_{l\_rd}+t_{c\_rd}\right)\cdot E_{2\_l\_rd}\end{array}}{\begin{array}{l}h.o.h._{main\_webs}\cdot t_{mb\_f}\cdot E_{f\_mb}+t_{mb\_w}\cdot\left(h_{mb}-t_{mb\_f}\right)\cdot E_{w\_mb}\\ +h.o.h._{main\_webs}\cdot t_{c\_rd}\cdot E_{balsa\_z}+h.o.h._{main\_webs}\cdot 2\cdot t_{l\_rd}\cdot E_{2\_l\_rd}\end{array}}=0.85\ m$$

$$z_{2mb\_f} := \left(y_2 - \frac{1}{2} \cdot t_{mb\_f}\right) = 0.838\ m$$

$$z_{2c\_rd} := h_{mb} - y_2 + t_{l\_rd} + \frac{1}{2} \cdot t_{c\_rd} = 0.484\ m$$

$$z_{2l\_rd\_bot} := h_{mb} - y_2 + \frac{1}{2} \cdot t_{l\_rd} = 0.226\ m$$

$$z_{2l\_rd\_top} := h_{mb} - y_2 + \frac{3}{2} \cdot t_{l\_rd} + t_{c\_rd} = 0.742\ m$$

$$EI_{fb\_mid} := E_{w\_mb} \cdot \frac{1}{12} \cdot t_{mb\_w} \cdot \left(h_{mb} - 2 \cdot t_{mb\_f}\right)^3 + E_{f\_mb} \cdot h.o.h._{main\_webs} \cdot t_{mb\_f} \cdot z_{2mb\_f}^{\ 2} + E_{balsa\_z} \cdot t_{c\_rd} \cdot h.o.h._{main\_webs} \cdot z_{2c\_rd}^{\ 2} + E_{2\_l\_rd} \cdot h.o.h._{main\_webs} \cdot t_{l\_rd} \cdot \left(z_{2l\_rd\_bot}^{\ 2} + z_{2l\_rd\_top}^{\ 2}\right) = \left(1.499 \cdot 10^6\right)\ kN \cdot m^2$$

$$k_{mid} := \frac{48 \cdot EI_{fb\_mid}}{l^3} = 4469\ \frac{kN}{m}$$

Stiffness properties outside fictional beam

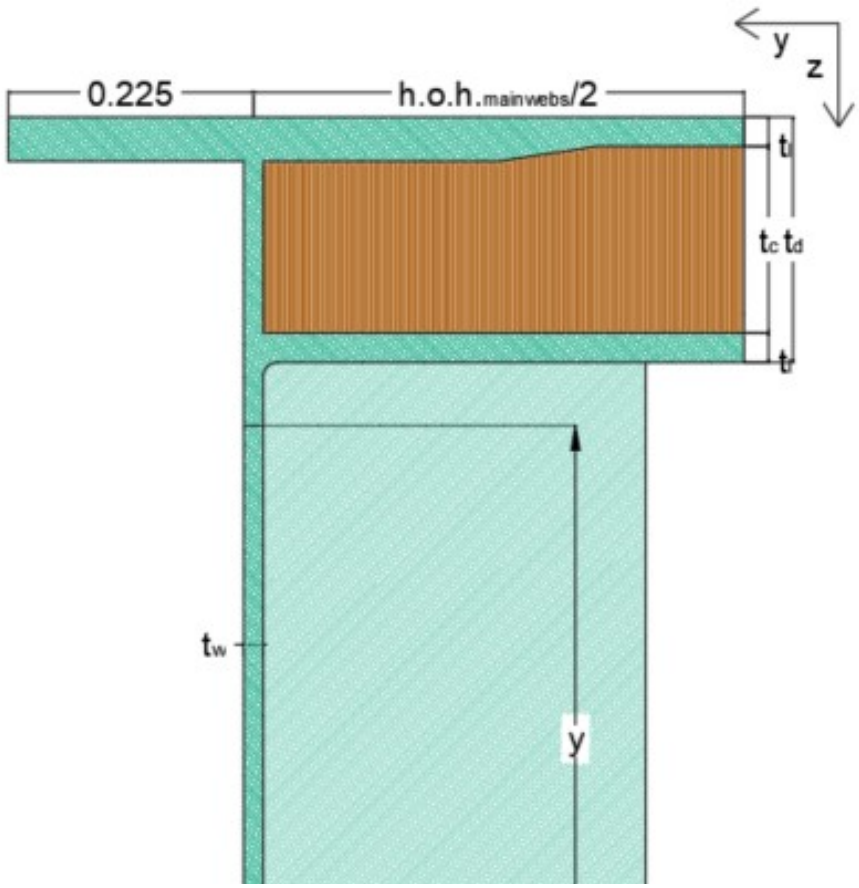

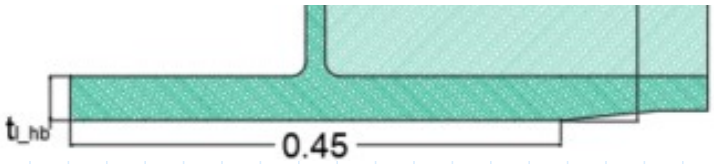

$$y_3 := \frac{\begin{aligned} &0.45\ m \cdot t_{ca\_f} \cdot h_{mb} \cdot E_{f\_ca} \\ &+ t_{ca\_w} \cdot \left(h_{mb} - t_{mb\_f}\right) \cdot \frac{1}{2} \cdot \left(h_{mb} + t_{mb\_f}\right) \cdot E_{w\_ca} \\ &+ \left(\frac{h.o.h._{main\_webs}}{2} + 0.225\ m\right) \cdot t_{c\_rd} \cdot \left(h_{mb} + t_{l\_rd} + \frac{1}{2} \cdot t_{c\_rd}\right) \cdot E_{balsa\_z} \\ &+ \left(\frac{h.o.h._{main\_webs}}{2} + 0.225\ m\right) \cdot t_{l\_rd} \cdot \left(2 \cdot h_{mb} + 2 \cdot t_{l\_rd} + t_{c\_rd}\right) \cdot E_{2\_l\_rd} \end{aligned}}{\begin{aligned} &2 \cdot 0.45\ m \cdot t_{ca\_f} \cdot E_{f\_ca} + t_{ca\_w} \cdot \left(h_{mb} - t_{mb\_f}\right) \cdot E_{w\_ca} \\ &+ \left(\frac{h.o.h._{main\_webs}}{2} - 0.25\ m\right) \cdot t_{c\_rd} \cdot E_{balsa\_z} \\ &+ \left(\frac{h.o.h._{main\_webs}}{2} - 0.25\ m\right) \cdot 2 \cdot t_{l\_rd} \cdot E_{2\_l\_rd} \end{aligned}} = 1.136\ m$$

$$z_{3ca\_f\_bot} := y_3 - \frac{1}{2} \cdot 2 \cdot t_{ca\_f} = 1.088\ m$$

$$z_{3ca\_f\_top} := h_{ca} - y_3 - \frac{1}{2} \cdot t_{ca\_f} = 0.44\ m$$

$$z_{3c\_rd} := h_{mb} - y_3 + t_{l\_rd} + \frac{1}{2} \cdot t_{c\_rd} = 0.198\ m$$

$$z_{3l\_rd\_bot} := h_{mb} - y_3 + \frac{1}{2} \cdot t_{l\_rd} = -0.06\ m$$

$$z_{3l\_rd\_top} := h_{mb} - y_3 + \frac{3}{2} \cdot t_{l\_rd} + t_{c\_rd} = 0.456\ m$$

$$EI_{fb\_edge} := \begin{aligned} &E_{w\_ca} \cdot \frac{1}{12} \cdot t_{ca\_w} \cdot \left(h_{mb} - 2 \cdot t_{ca\_f}\right)^3 \\ &+ E_{f\_ca} \cdot 0.45\ m \cdot t_{ca\_f} \cdot \left(z_{3ca\_f\_bot}{}^2 + z_{3ca\_f\_top}{}^2\right) \\ &+ E_{balsa\_z} \cdot t_{c\_rd} \cdot \frac{h.o.h._{main\_webs}}{2} \cdot z_{3c\_rd}{}^2 \\ &+ E_{2\_l\_rd} \cdot \left(\frac{h.o.h._{main\_webs}}{2} + 0.225\ m\right) \cdot 2 \cdot t_{l\_rd} \cdot z_{3l\_rd\_bot}{}^2 \\ &+ E_{2\_l\_rd} \cdot \left(\frac{h.o.h._{main\_webs}}{2} + 0.225\ m\right) \cdot 2\ t_{l\_rd} \cdot z_{3l\_rd\_top}{}^2 \end{aligned} = \left(1.078 \cdot 10^6\right)\ kN \cdot m^2$$

$$k_{edge} := \frac{48 \cdot EI_{fb\_edge}}{l^3} = 3215\ \frac{kN}{m}$$

Combined stiffness properties inside fictional beams

$$k_{comb} := \frac{1}{\frac{1}{k_{mid}} + \frac{1}{k_{hb}}} = 2193 \ \frac{kN}{m}$$

$$k_{inbetween} := \frac{k_{edge} + k_{comb}}{2} = 2704 \ \frac{kN}{m}$$

Properties entire crossection

$$A_{mb\_v} := \frac{\left(2 + \frac{k_{comb}}{k_{edge}} \cdot 4\right) \cdot t_{mb\_w} \cdot h_{mb}}{2} = 0.04 \ m^2$$

$$EI_{mb} := 2 \cdot EI_{fb\_edge} + 4 \cdot \frac{k_{comb}}{k_{edge}} \cdot EI_{fb\_mid} = \left(6.246 \cdot 10^6\right) \ kN \cdot m^2$$

Stiffness properties beam continuing from deck to rotation axis

$$EI_{ca} := \frac{1}{12} \cdot t_{ca\_w} \cdot {h_{ca}}^3 \cdot E_{w\_ca} \hookleftarrow \quad = \left(8.828 \cdot 10^5\right) \ kN \cdot m^2$$
$$+ 2 \cdot t_{ca\_f} \cdot (0.45 \ m) \cdot \left(\frac{h_{ca}}{2}\right)^2 \cdot E_{f\_ca}$$

$$A_{V\_main\_beam} := t_{ca\_w} \cdot h_{ca} = 0.026 \ m^2$$

$$A_{N\_main\_beam} := t_{ca\_w} \cdot h_{ca} + 2 \cdot t_{ca\_f} \cdot 0.45 \ m = 0.069 \ m^2$$

Calculations for deflections

Deflections at the supports in the middle of the deck

$$w_{middle\_at\_supports} := \frac{1}{48} \cdot \frac{Q_{bm1} \cdot {b_{supp}}^3}{EI_{hb}} + \frac{5}{384} \cdot \frac{q_{bm1} \cdot w_{rd} \cdot {b_{supp}}^4}{EI_{hb}} = 4.26 \ mm$$

Deflections at midspan in the middle of the deck

$$w_{middle\_midspan} := \frac{1}{48} \cdot \frac{4 \cdot Q_{bm1} \cdot l^3}{EI_{mb}} + \frac{5}{384} \cdot \frac{q_{bm1} \cdot h.o.h._{main\_webs} \cdot l^4}{EI_{mb}} = 78.855 \ mm$$

Deflections limit

$$w_{limit} := \frac{l}{250} = 101\ mm$$

Unity checks

$$u.c._{deflection\_threshold} := \frac{w_{middle\_at\_supports}}{5\ mm} = 0.851$$

$$u.c._{deflection\_midspan} := \frac{w_{middle\_midspan}}{w_{limit}} = 0.781$$

Calculations for road deck strength

Self weight

$$G_{rd} := \left(2 \cdot t_{l\_rd} \cdot w_{rd} \cdot \rho_{l\_rd} + t_{c\_rd} \cdot w_{rd} \cdot \rho_{balsa}\right) \cdot 9.81\ \frac{m}{s^2} = 1.859\ \frac{kN}{m}$$

Important dimensions

$$x_1 := \frac{b_{supp}}{2} - w_{bm1\_mid} - w_{bm1} = 2.225\ m \qquad x_2 := w_{bm1} = 2\ m \qquad x_3 := w_{bm1\_mid} = 0.5\ m$$

Load cases

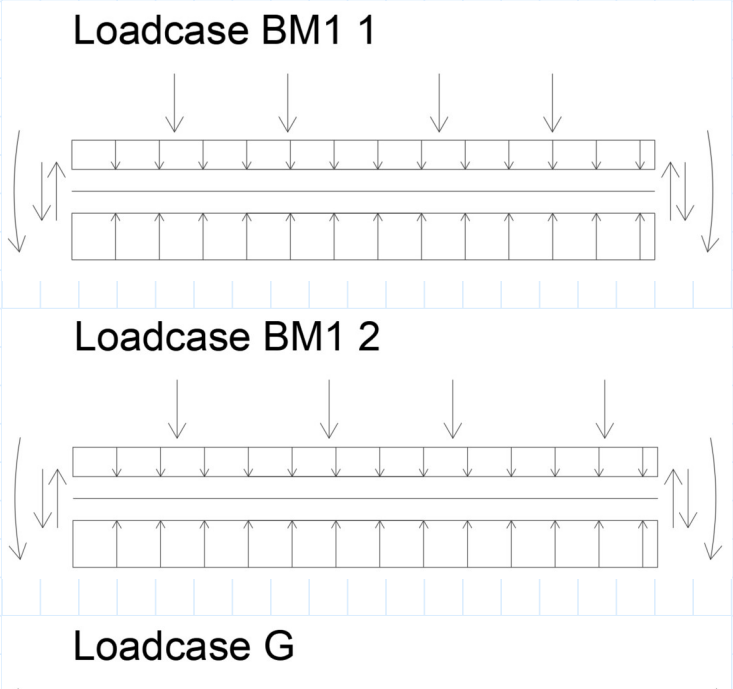

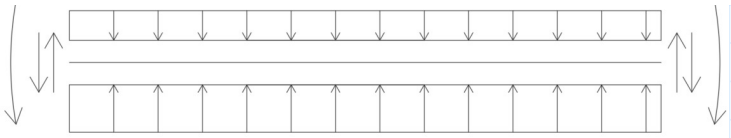

Shear force in deck at midspan

Values from matrix frame

$V_{rd\_BM1\_1\_mid} := 187.97\ kN$

$V_{rd\_BM1\_2\_mid} := 163.01\ kN$

$V_{rd\_G\_BM1\_1\_mid} := 3.78\ kN$ *Shear force due to self weight, at point of maximal shear force from BM1 1*

$V_{rd\_G\_BM1\_2\_mid} := 3.78\ kN$ *Shear force due to self weight, at point of maximal shear force from BM1 2*

Shear force in deck at supports

Values from matrix frame

$V_{rd\_BM1\_1\_end} := 164.84\ kN$

$V_{rd\_BM1\_2\_end} := 150.10\ kN$

$V_{rd\_G\_BM1\_1\_end} := 3.36\ kN$ *Shear force due to self weight, at point of maximal shear force from BM1 1*

$V_{rd\_G\_BM1\_2\_end} := 3.36\ kN$ *Shear force due to self weight, at point of maximal shear force from BM1 2*

Bending moments at midspan

Values from matrix frame

$M_{rd\_BM1\_1\_mid} := 305.39\ kN \cdot m$

$M_{rd\_BM1\_2\_mid} := 222.20\ kN \cdot m$

$M_{rd\_G\_BM1\_1\_mid} := 5.95\ kN \cdot m$ *Bending moments due to self weight, at point of maximal shear force from BM1 1*

$M_{rd\_G\_BM1\_2\_mid} := 5.95\ kN \cdot m$ *Bending moments due to self weight, at point of maximal shear force from BM1 2*

Bending moments at supports

Values from matrix frame

$M_{rd\_BM1\_1\_end} := 272.96\ kN \cdot m$

$M_{rd\_BM1\_2\_end} := 222.92\ kN \cdot m$

$M_{rd\_G\_BM1\_1\_end} := 7.65\ kN \cdot m$ *Bending moments due to self weight, at point of maximal shear force from BM1 1*

$M_{rd\_G\_BM1\_2\_end} := 7.65\ kN \cdot m$ *Bending moments due to self weight, at point of maximal shear force from BM1 2*

Combinations

$$V_{rd\_mid} := \max\begin{pmatrix} 1.5 \cdot V_{rd\_BM1\_1\_mid} & , 1.5 \cdot V_{rd\_BM1\_2\_mid} \\ +1.2 \cdot V_{rd\_G\_BM1\_1\_mid} & +1.2 \cdot V_{rd\_G\_BM1\_2\_mid} \end{pmatrix}$$

$$V_{rd\_end} := \max\begin{pmatrix} 1.5 \cdot V_{rd\_BM1\_1\_end} & , 1.5 \cdot V_{rd\_BM1\_2\_end} \\ +1.2 \cdot V_{rd\_G\_BM1\_1\_end} & +1.2 \cdot V_{rd\_G\_BM1\_2\_end} \end{pmatrix}$$

$V_{Ed\_rd} := \max\left(V_{rd\_mid}, V_{rd\_end}\right) = 286.5\ kN$

$$M_{rd\_mid} := \max\begin{pmatrix} 1.5 \cdot M_{rd\_BM1\_1\_mid} & , 1.5 \cdot M_{rd\_BM1\_2\_mid} \\ +1.2 \cdot M_{rd\_G\_BM1\_1\_mid} & +1.2 \cdot M_{rd\_G\_BM1\_2\_mid} \end{pmatrix}$$

$$M_{rd\_end} := \max\begin{pmatrix} 1.5 \cdot M_{rd\_BM1\_1\_end} & , 1.5 \cdot M_{rd\_BM1\_2\_end} \\ +1.2 \cdot M_{rd\_G\_BM1\_1\_end} & +1.2 \cdot M_{rd\_G\_BM1\_2\_end} \end{pmatrix}$$

$M_{Ed\_rd} := \max\left(M_{rd\_mid}, M_{rd\_end}\right) = 465.2\ kN \cdot m$

$V_{Ed\_rd\_s} := 1.5 \cdot \left(2 \cdot 0.6 \cdot Q_{bm1} + 0.1 \cdot q_{bm1} \cdot b_{supp} \cdot \frac{b_{rd}}{2}\right) = 591\ kN$

Resultant stresses

$\tau_{c\_rd} := \frac{V_{Ed\_rd}}{A_{rd}} = 0.6\ MPa$

$\sigma_{l\_rd} := \frac{M_{Ed\_rd}}{EI_{rd}} \cdot \frac{t_{d\_rd}}{2} \cdot E_{1\_l\_rd} = 36\ MPa$

$\tau_{l\_rd} := \frac{V_{Ed\_rd\_s}}{t_{l\_rd} \cdot b_{supp}} = 4\ MPa$

Unity checks

$u.c._{c\_rd} := \frac{\tau_{c\_rd}}{\quad} = 0.67$

$f_{c\_xz\_d}$

$$u.c._{\sigma\_rd} := \frac{\sigma_{l\_rd}}{f_{rd\_x\_d}} = 0.316$$

$$u.c._{\tau\_l\_rd} := \frac{\tau_{l\_rd}}{f_{rd\_xy\_d}} = 0.056$$

$$u.c._{rd\_\sigma\_\tau\_loc} := u.c._{\sigma\_rd} + u.c._{\tau\_l\_rd} = 0.372$$

Calculations for mainbeam

Loads

Load q mb

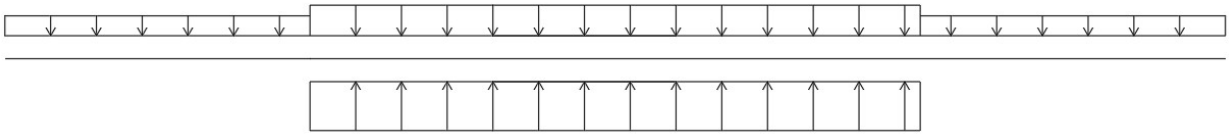

Load Q mb

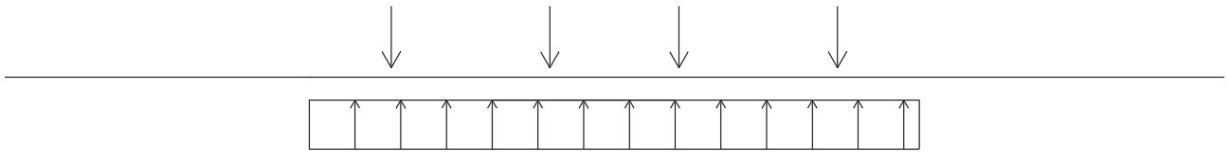

$$q_{mb} := 2 \cdot b_{fcp} \cdot q_{fcp} + b_{rd} \cdot q_{bm1} = 114.8 \ \frac{kN}{m}$$

$$Q_{mb} := 4 \cdot Q_{bm1} = 1200 \ kN$$

Load cases

Loadcase V MB

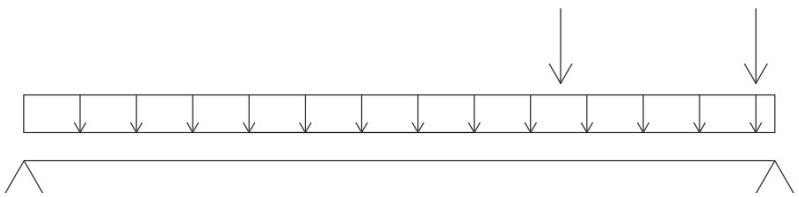

Loadcase M MB

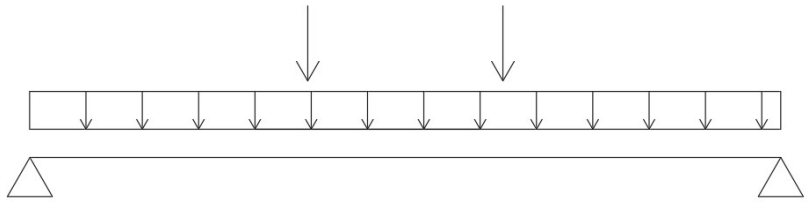

Loadcase G

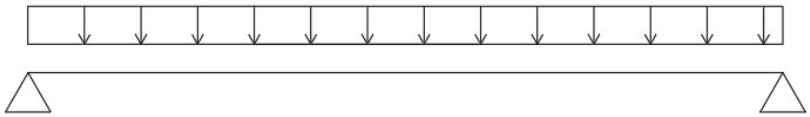

Shear force

Loadcases V MB was used

$$V_{bm1\_mb} := \frac{\frac{1}{2} \cdot q_{mb} \cdot l + 2 \cdot Q_{mb}}{n_{main\_webs}} = 641.6 \ kN$$

Bending moment

Loadcases M MB was used

$$M_{bm1\_mb} := \frac{\frac{1}{8} \cdot q_{mb} \cdot l^2 + 2 \cdot \frac{1}{4} \cdot Q_{mb} \cdot l}{n_{main\_webs}} = \left(4.05 \cdot 10^3\right) \ kN \cdot m$$

Self weight

$$Mass_{fcp} := 16.02 \ tonne$$

$$Mass_{dist} := \left(b_{supp} \cdot t_{mb\_f} + \left(h_{mb} - t_{mb\_f}\right) \cdot t_{mb\_w} \cdot n_{main\_webs}\right) \cdot \rho_{l\_mb} + t_{c\_rd} \cdot b_{supp} \cdot \rho_{balsa} + 2 \cdot t_{l\_rd} \cdot b_{supp} \cdot \rho_{l\_rd} + 2 \cdot \frac{Mass_{fcp}}{l} = 3811 \ \frac{kg}{m}$$

$$G_{mb} := Mass_{dist} \cdot 9.81 \ \frac{m}{s^2} = 37.39 \ \frac{kN}{m}$$

Forces as a result of self weight

Loadcase G was used

$$V_{G\_mb} := \frac{1}{2} \cdot G_{mb} \cdot l = 472 \ \textbf{kN}$$

$$M_{G\_mb} := \frac{1}{8} \cdot G_{mb} \cdot l^2 = 2980 \ \textbf{kN} \cdot \textbf{m}$$

Combined forces with 6.10 B

$$V_{Ed\_mb} := 1.2 \cdot V_{G\_mb} + 1.5 \cdot V_{bm1\_mb} = \left(1.529 \cdot 10^3\right) \ \textbf{kN}$$

$$M_{Ed\_mb} := 1.2 \cdot M_{G\_mb} + 1.5 \cdot M_{bm1\_mb} = \left(9.651 \cdot 10^3\right) \ \textbf{kN} \cdot \textbf{m}$$

$$N_{Ed\_mb} := \frac{2 \cdot 0.6 \cdot Q_{mb}}{2} + \frac{0.1 \cdot q_{bm1} \cdot b_{rd} \cdot l + 2 \cdot 0.1 \cdot q_{fcp} \cdot b_{fcp} \cdot l}{4} = 792.5 \ \textbf{kN}$$

Resultant stresses

$$\tau_{Ed\_mb} := \frac{V_{Ed\_mb}}{A_{mb\_v}} = 37.8 \ \textbf{MPa}$$

$$\sigma_{Ed\_M\_mb} := \frac{M_{Ed\_mb}}{EI_{mb}} \cdot E_{f\_mb} \cdot y_{hb} = 29.9 \ \textbf{MPa}$$

$$\sigma_{Ed\_N\_mb} := \frac{N_{Ed\_mb} \cdot \left(2 \cdot \left(h_{rd} - h_{under\_side}\right) - t_{mb\_f}\right)}{2 \cdot t_{mb\_f} \cdot b_{supp} \cdot \left(h_{rd} - h_{under\_side} - t_{mb\_f}\right)} = 3.5 \ \textbf{MPa}$$

$$\sigma_{Ed\_rd\_add} := \frac{M_{Ed\_mb}}{EI_{mb}} \cdot E_{2\_l\_rd} \cdot \left(h_{rd} - h_{under\_side} - y_{hb}\right) = 34.9 \ \textbf{MPa}$$

Unity checks

$$u.c._{\tau\_mb} := \frac{\tau_{Ed\_mb}}{f_{mb\_xz\_d}} = 0.44$$

$$u.c._{\sigma\_mb} := \frac{\sigma_{Ed\_M\_mb} + \sigma_{Ed\_N\_mb}}{f_{mb\_x\_d}} = 0.19$$

$$u.c._{comb\_rd} := \frac{\sigma_{Ed\_rd\_add}}{f_{rd\_y\_d}} + u.c._{rd\_\sigma\_\tau\_loc} = 0.6$$

Auxiliary calculations

Calculations for ship impact forces

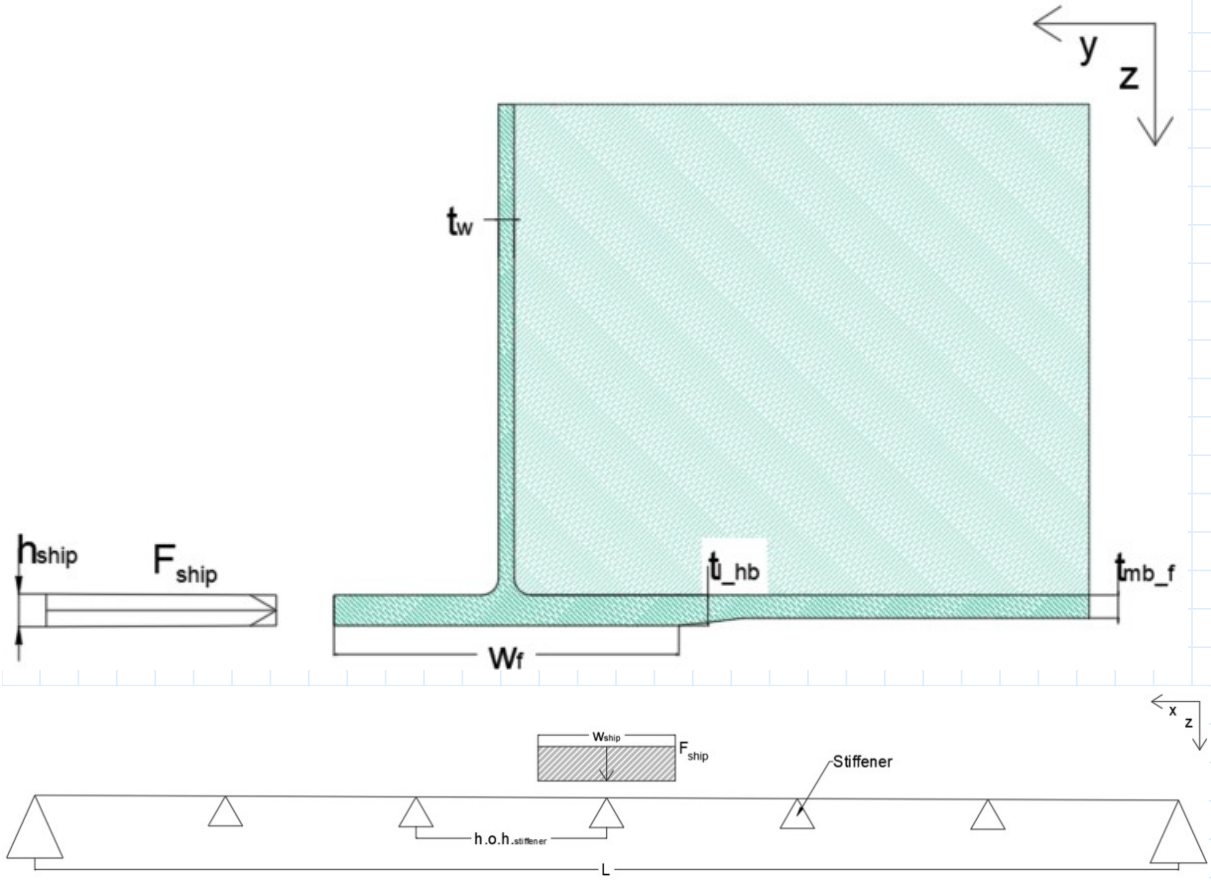

$d_{ship} := h.o.h._{main\_webs}$ $b_{ship\_load} := d_{ship} = 1.89\ m$ $b_{ship\_r} := b_{ship\_load} = 1.89\ m$

Normal force

$N_{ship} := F_{ship} = 0.81\ MN$

Critical buckling force

$D_{11} := 4.69 \cdot 10^7\ N \cdot mm$ $D_{22} := 8.28 \cdot 10^7\ N \cdot mm$

$D_{12} := 1.38 \cdot 10^7\ N \cdot mm$ $D_{66} := 1.67 \cdot 10^7\ N \cdot mm$

$$f_{y\_cr\_k} := \frac{\pi^2}{t_{mb\_f} \cdot b_{ship\_r}^2} \cdot \left(2 \cdot \sqrt{D_{11} \cdot D_{22}} + 2 \cdot \left(D_{12} + 2 \cdot D_{66}\right)\right) = 25.2\ MPa$$

$$f_{ship\_y} := min\left(f_{mb\_y\_d}, \frac{f_{y\_cr\_k}}{\ldots}\right) = 15.7\ MPa$$

f_{ship_y} $\left(\frac{f_{mb\_y\_d}}{\gamma_{m\_mb} \cdot \gamma_{rd\_mb}}\right)$

Resultant stresses

$$\sigma_{n\_sc} := \frac{N_{ship}}{t_{mb\_f} \cdot b_{ship\_load}} = 17.9 \ \textbf{MPa}$$

Unity checks

$$u.c._{\sigma\_sc\_f} := \frac{\sigma_{n\_sc}}{f_{ship\_y}} = 1.138$$

Calculations for opened structure

Wind loads

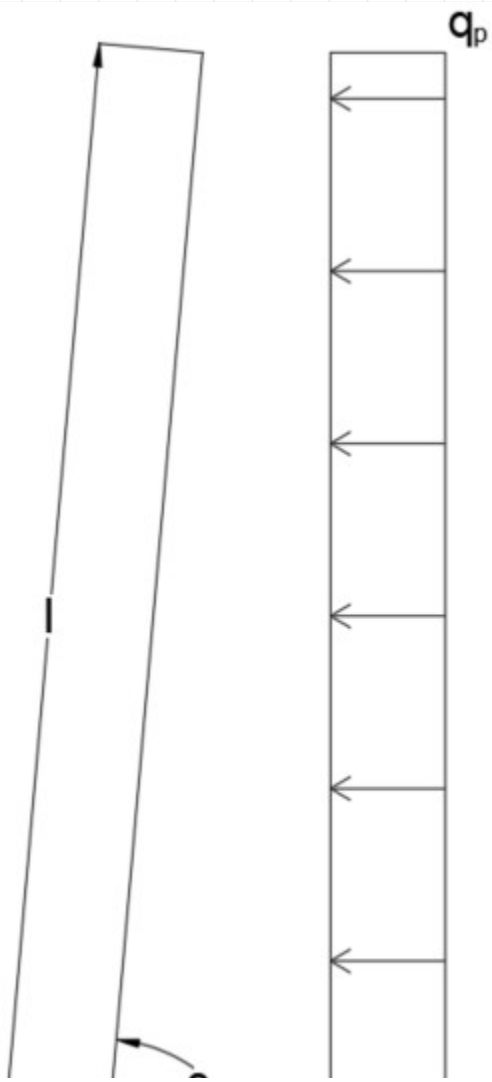

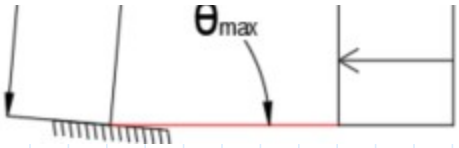

$z_e := h_{under\_side} + \sin(\theta_{max}) \cdot l = 29.2\ m$ $q_{p\_0} := 1.94\ \frac{kN}{m^2}$

$h_{bridge} := h_{rd} - h_{under\_side} = 1.6\ m$ $slenderness := \frac{b_{supp} + 2 \cdot b_{edge}}{h_{bridge}} = 12$

$\rho := 1.25\ \frac{kg}{m^3}$ $v_b := 29.5\ \frac{m}{s}$

$c_{fx\_0} := \begin{cases} \text{if } slenderness \le 4 \\ \quad 2.4 - 0.275 \cdot slenderness \\ \text{else} \\ \quad 1.3 \end{cases} = 1.3$ $c_e := \frac{q_{p\_0}}{\frac{1}{2} \cdot \rho \cdot v_b^2} = 3.6$ $C_t := c_{fx\_0} \cdot c_e = 4.6$

$q_p := \frac{1}{2} \cdot \rho \cdot v_b^2 \cdot C_t = 2.5\ \frac{kN}{m^2}$ $A_{mb} := 2 \cdot t_{mb\_w} \cdot h_{mb} = 0.034\ m^2$

$t_{open} := 15$ $\psi_t := 1 + \frac{\ln\left(\frac{t_{open}}{50}\right)}{9} = 0.9$

Principle resultant forces

$N_{mb\_G\_open} := \frac{G_{mb} \cdot l}{2 \cdot \sin(\theta_{max})} = 479.3\ kN$

$M_{mb\_G\_open} := \frac{1}{2} \cdot G_{mb} \cdot \cos(\theta_{max}) \cdot l^2 = (2.07 \cdot 10^3)\ kN \cdot m$

$N_{mb\_wind} := \frac{\frac{1}{2} \cdot q_p \cdot h_{mb} \cdot (\sin(\theta_{max}) \cdot l)^2}{b_{supp}} = 88.121\ kN$

$M_{mb\_wind\_y} := \frac{1}{2} \cdot \frac{1}{2} \cdot q_p \cdot (2 \cdot b_{edge} + b_{supp}) \cdot (\sin(\theta_{max}) \cdot l)^2 = (7.583 \cdot 10^3)\ kN \cdot m$

Resultant stresses

$\sigma_{mb\_G\_open} := \frac{M_{mb\_G\_open}}{2 \cdot EI_{ca}} \cdot E_{f\_mb} \cdot \frac{1}{2} \cdot h_{mb} + \frac{N_{mb\_G\_open}}{A_{N\_main\_beam}} = 23.4\ MPa$

$$\sigma_{mb\_wind\_1} := \frac{M_{mb\_wind\_y}}{2 \cdot EI_{ca}} \cdot E_{f\_mb} \cdot \frac{1}{2} \cdot h_{mb} + 0.4 \cdot \frac{N_{mb\_wind}}{A_{N\_main\_beam}} = 60.6\ \textit{MPa}$$

$$\sigma_{mb\_wind\_2} := 0.4 \cdot \frac{M_{mb\_wind\_y}}{2 \cdot EI_{ca}} \cdot E_{f\_mb} \cdot \frac{1}{2} \cdot h_{mb} + \frac{N_{mb\_wind}}{A_{N\_main\_beam}} = 25.3\ \textit{MPa}$$

$$\sigma_{mb\_wind} := \max\left(\sigma_{mb\_wind\_1}, \sigma_{mb\_wind\_2}\right) = 60.6\ \textit{MPa}$$

Unity checks

$$u.c._{\sigma\_open} := \frac{1.2 \cdot \sigma_{mb\_G\_open} + 1.8 \cdot \psi_t \cdot \sigma_{mb\_wind}}{f_{ca\_x\_d}} = 0.65$$

Results

Unity checks

Unity checks traffic loads

deflection

$u.c._{deflection\_midspan} = 0.78$ $u.c._{deflection\_threshold} = 0.85$

Road deck strength

$u.c._{\tau\_c\_rd} = 0.67$ $u.c._{comb\_rd} = 0.58$

Main beam strength

$u.c._{\tau\_mb} = 0.44$ $u.c._{\sigma\_mb} = 0.19$

Unity checks ship colision

Main beam

$u.c._{\sigma\_sc\_f} = 1.14$

Unity checks opened position

$u.c._{\sigma\_open} = 0.65$ 1

MKI

€ := 1 ¤

$$Mass_{E\_glass} := 2 \cdot t_{l\_rd} \cdot b_{supp} \cdot l \cdot \rho_{l\_rd} + \left(b_{supp} \cdot t_{mb\_f} + t_{mb\_w} \cdot h_{mb} \cdot \left(n_{main\_webs} - 2\right)\right) \cdot l \cdot \rho_{l\_mb} + 2 \cdot \left(t_{ca\_f} \cdot 0.45\ \textit{m} + t_{ca\_w} \cdot h_{mb}\right)\ l \cdot \rho_{l\_mb} = 32.4\ \textit{tonne}$$

$Mass_{Balsa} := t_{c\_rd} \cdot b_{supp} \cdot l \cdot \rho_{balsa} = 34\ tonne$

$A_{E\_glass} := 4 \cdot \left(b_{edge}\right) \cdot l + 2 \cdot \left(b_{supp} + t_{d\_rd}\right) \cdot l + 2 \cdot h_{mb} \cdot l = \left(1.063 \cdot 10^{3}\right)\ m^2$

$MKI_{E\_glass} := 0.265\ \frac{€}{kg}$ $\quad MKI_{score\_E\_glass} := MKI_{E\_glass} \cdot Mass_{E\_glass} = 8580.6\ €$

$MKI_{Balsa} := -0.129\ \frac{€}{kg}$ $\quad MKI_{score\_Balsa} := MKI_{Balsa} \cdot Mass_{Balsa} = -4386.3\ €$

$MKI_{E\_glass\_cons} := 1.173\ \frac{€}{m^2}$ $\quad MKI_{score\_E\_glass\_cons} := MKI_{E\_glass\_cons} \cdot A_{E\_glass} = 1246.9\ €$

$MKI_{score\_Total} := MKI_{score\_E\_glass} + MKI_{score\_Balsa} + MKI_{score\_E\_glass\_cons} = 5441\ €$

Mass

$Mass_{total} := Mass_{E\_glass} + Mass_{Balsa} = 66\ tonne$

$64 + 2 \cdot 18.4 = 100.8$